UNIVERSIDAD COMPLUTENSE DE MADRID
FACULTAD DE CIENCIAS QUÍMICAS

TESIS DOCTORAL

Stereoselective synthesis on fullerenes:properties and photoelectrochemical applications

Síntesis estereoselectiva en fullerenos: propiedades y aplicaciones fotoelectroquímicas

MEMORIA PARA OPTAR AL GRADO DE DOCTOR

PRESENTADA POR

Rosa María Girón Rubio

Directores

Nazario Martín León
Salvatore Filippone

Madrid
Ed. electrónica 2019

UNIVERSIDAD COMPLUTENSE DE MADRID

FACULTAD DE CIENCIAS QUÍMICAS

Departamento de Química Orgánica

STEREOSELECTIVE SYNTHESIS ON FULLERENES: PROPERTIES AND PHOTOELECTROCHEMICAL APPLICATIONS

SÍNTESIS ESTEREOSELECTIVA EN FULLERENOS: PROPIEDADES Y APLICACIONES FOTOELECTROQUÍMICAS

TESIS DOCTORAL

Rosa M. Girón Rubio

Madrid, 2019

STEREOSELECTIVE SYNTHESIS ON FULLERENES: PROPERTIES AND PHOTOELECTROCHEMICAL APPLICATIONS

SÍNTESIS ESTEREOSELECTIVA EN FULLERENOS: PROPIEDADES Y APLICACIONES FOTOELECTROQUÍMICAS

Directores:

Dr. Nazario Martín León

Dr. Salvatore Filippone

Memoria que para optar al grado de

DOCTOR EN CIENCIAS QUÍMICAS

presenta

Rosa M. Girón Rubio

MADRID

Abril, 2019

D. Nazario Martín León, Catedrático del Departamento de Química Orgánica de la Universidad Complutense de Madrid y D. Salvatore Filippone, Profesor titular del Departamento de Química Orgánica de la Universidad Complutense de Madrid.

CERTIFICAN:

Que la presente Memoria titulada "Stereoselective Synthesis on Fullerenes: Properties and Photoelectrochemical Applications" se ha realizado bajo su dirección en el Departamento de Química Orgánica de la Universidad Complutense de Madrid, por la licenciada en Química Dña. Rosa María Girón Rubio y autorizan su presentación para ser calificada como tesis doctoral.

Y para que conste firmo el presente certificado en Madrid a 5 de marzo de 2019.

Fdo. Dr. Nazario Martín

Fdo. Dr. Salvatore Filippone

The results presented in this thesis have been published and listed below:

R. M. Girón, S. Reboredo, J. Marco-Martínez, S. Fillipone and N. Martín, "Organocatalysis for new chiral fullerene-based materials" *Faraday Discuss*. **2014**, 173, 311-322.

R. M. Girón, J. Marco-Martínez, S. Bellani, A. Insuasty, H. Comas, G. Tullii, M. R. Antognazza, S. Filippone and N. Marín, "Synthesis of modified fullerenes for oxygen reduction reactions" *J. Mat. Chem. A.* **2016**, *4*, 14284-14290.

S. Reboredo, R. M. Girón, S. Filippone, T. Mikie, T. Sakurai, S. Seki and N. Martín, "Cyclobuteno[60]fullerenes as Efficient n-Type Organic Semiconductors" *Chem. Eur. J*. **2016**, *22*, 13627-13631.

O. El Bakouri, M. Garcia-Borràs, R. M. Girón, S. Filippone, N. Martín and M. Solà, "On the regioselectivity of the Diels–Alder cycloaddition to C_{60} in high spin states" *Phys. Chem. Chem. Phys.* **2018**, *20*, 11577-11585.

R. M. Girón, J. Ouyang, L. Favereau, N. Vanthuyne, J. Crassous, S. Filippone and N. Martín, "Reversible Stereodivergent Cycloaddition of Racemic Helicenes to [60]Fullerene: A Chiral Resolution Strategy" *Org. Lett*. **2018**, *20* (7), 1764-1767.

A mi familia

Acknowledgments

El presente trabajo ha sido realizado en el Departamento de Química Orgánica de la Universidad Complutense de Madrid bajo la dirección del Profesor Nazario Martín y el Dr. Salvatore Filippone.

Puesto que la felicidad no es tener si no agradecer, me gustaría dar las gracias a todas las personas que han hecho más agradable esta etapa de mi vida.

En primer lugar me gustaría dar las gracias a mis directores,

Nazario, muchas gracias por haberme brindado la oportunidad de formar parte de tu grupo de investigación y haber confiado en mí. Eres el espejo en el que reflejarse porque es admirable tu pasión por la ciencia y las ganas insaciables de trabajar y aprender cosas nuevas.

Salvo, maestro de vida. Nada hubiese sido igual sin ti. Muchas gracias por tu ayuda, tus consejos y todas las carcajadas que has sido capaz de sacarme. Eres una de las personas más cultas que conozco, he aprendido mucho de ti. Como diría tu coetáneo Miguel de Cervantes "en un lugar de La Mancha…" siempre tendrás una amiga. Me siento muy afortunada por haber podido trabajar con vosotros.

También me gustaría agradecer especialmente a los miembros del grupo que han contribuido en parte del trabajo descrito en esta memoria: Silvia y Juan.

Silvia, muchas gracias por tu paciencia en esos primeros meses, cuando era tu sombra, donde tanto me enseñaste. Gracias en gran parte a ti, soy la química que soy. Hemos compartido muy buenos momentos. Eres una bellísima persona. Me llevo una amiga.

Juan, tu humor hacía los días más amenos y agradables. He aprendido mucho de ti. Formábamos la "U" más molona del labo. Ha sido un placer trabajar con vosotros.

En la realización de esta tesis han contribuido otros grupos de investigación, sin los que no hubiera sido posible este trabajo:

Al grupo de investigación del profesor Shu Seki, Kyoto University, por las medidas de movilidad electrónica de los derivados carbocíclicos de fullereno.

Al grupo de investigación de la profesora Jeanne Crassous, Université Rennes por el suministro del 2-formil[6]heliceno.

Al profesor Israel Fernández de la Universidad Complutense de Madrid, por los estudios teóricos sobre los híbridos quirales metal/fullereno.

A la profesora María Rosa Antognazza (CNST@PoliMi Milano) y al Dr. Sebastiano Bellani (IIT Central Research Lab Genova), por el trabajo realizado en la preparación y medida de los dispositivos para la ORR.

Así mismo, quiero agradecer al personal de los diferentes CAIs de la Facultad de Ciencias Químicas de la UCM, al CAI de Masas y, en especial, al CAI de RMN, a Lola, Elena y Ángel, muchas gracias por ofréceme vuestra ayuda desinteresada siempre que la he necesitado.

Al CAI de Difracción de Rayos X de Monocristal de la Facultad de Ciencias de la Universidad Autónoma de Madrid, en especial a Josefina, por su disposición y su amabilidad.

A continuación me gustaría dar las gracias a todos mis compañeros del departamento y, en especial a los de mi laboratorio, porque habéis hecho que me sienta muy a gusto y me habéis alegrado cada mañana con vuestras sonrisas.

Me gustaría hacer una mención especial a Javi, Sonia, Alberto (Muchachito), Alfonso y Miki.

Javi, gracias por estar siempre dispuesto a ayudarme. Has llegado poco a poco pero te has convertido en mi confidente y en un gran amigo. Pero sin duda, si sólo tuviese que destacar una cosa me quedaría con todo lo que me has hecho reír, esto no hubiese sido lo mismo sin ti. Te mereces todas las cosas buenas que te pasen.

Sonia, gracias por tu predisposición y entrega a los demás. Por tus chistes improvisados, y las canciones que hemos “cantado”. Sé que siempre te tendré para lo que necesite.

Alberto, nunca voy a olvidar tantos ratos que hemos compartido con las chicas fuera y dentro del labo. No puedo evitar que se me dibuje una sonrisa en la cara cada vez que escucho alguna de las canciones con las que nos alegrabas las horas en el laboratorio. Aunque estés lejos, te siento cerca.

Alfonso, gracias por hacer que el labo vibre con esa buena energía que irradias. Admiro tu sentido del humor que te permite aguantar todas nuestras bromas y estar alegre la mayor parte del tiempo. Porque eres capaz de hacer que todo el mundo diga tu frase del momento y porque eres mi influencer favorito.

Miki, no tengo palabras para expresar todo lo que siento. Eres mi pequeña gran revolución. Somos el ying y el yang y eso hace que a tu lado sea tal y como soy, sin necesidad de ocultar mis locuras. Porque eres muy fácil de querer y muy difícil de olvidar, no puedo imaginar esto sin ti. Te quiero un poco mi flor, sé que tengo una hermana al otro lado del charco.

Mª Ángeles, Beti, Carmencita, Ángel, Andreas, Luis, David, Margarita, muchas gracias por demostrarme siempre vuestro cariño y ofrecerme vuestra ayuda en cualquier momento. Virginia, gracias por tu amabilidad y por endulzarnos los días. Ana y Helena, gracias por estar siempre dispuestas a ayudar.

Al resto de mis compañeros, Inés, Rafa, Javi U., José, Agus, Laura (por tus beauty-consejos), Marina, Sara (por tu entrañable dulzura), Antonio (por ser tan atento), Valentina, Paul, Ali, Andrés, Ester (eres encantadora), Chus, y los que ya se fueron, Raúl, Helena, María, Toni, Andreíta, Enrique, André, Jaime, Carmen, Luismo, Javi L., Simona, Javi M. (), Marta I., Marta R. Me llevo muy buenos recuerdos de estos años a vuestro lado. Si tuviese que elegir a mis compañeros de trabajo os elegiría a todos y cada uno de vosotros porque me habéis hecho sentir una más de esta estupenda familia.

A los técnicos del departamento, Javis y Laura, muchas gracias por vuestra agradable colaboración.

A los vecinos de otros laboratorios (Ana, Nora, Julia, Fátimas, Jorge, Yeray, Elisa, Mercedes, Paula, Alberto…siento no poder mencionar a todos), que raro se me haría atravesar el pasillo sin ver vuestras caras. Muchas gracias por vuestra amabilidad.

Finalmente, me gustaría agradecer a las personas que forman parte de mi vida fuera de la universidad y que son importantes para mí.

A mis amigos de toda la vida, en especial a ti, Elena, que después de tantos años eres parte de mí y a mis niñas del insti, Mari, Carmen y Sara (y el pequeño Telmo) porque siempre que os recuerdo, y con ellos alguna de nuestras anécdotas, me sale una sonrisa.

A los que me iniciaron en la investigación, José Ramón y Gonzalo, y los que tuvieron que soportar mis primeros coleteos en un laboratorio, en especial Marc, muchas gracias por vuestra paciencia y por haber hecho despertar en mí la curiosidad por la investigación.

Por último, quiero dar las gracias a las personas más importantes de mi vida, a toda mi familia, mis padres y mi hermano, mis abuelos, mis tíos y mis primos por intentar entender lo que hacía y darme tanto cariño.

A mi segunda familia, Pedro, Feli, Edu y Tati, gracias por tratarme y quererme como una hija y una hermana y hacerme sentir como en mi casa. Porque gracias a vosotros tengo mi lado a la persona más maravillosa.

Papis, muchas gracias por confiar siempre en mí, por habernos dado todo lo que hemos necesitado, guiarnos y aconsejarnos tan bien durante toda nuestra vida. No sé si en algún momento seré capaz de devolveros ni una pequeña parte de todo lo que habéis hecho por nosotros. Sin vuestra ayuda nada de esto hubiese sido posible. Porque gracias a vosotros soy la persona que soy. Os quiero muchísimo.

Alfon, muchas gracias por todos los momentos que hemos compartido y porque sé que siempre puedo contar contigo. Porque no hay un día que no piense en ti. Nunca cambies, me siento muy afortunada de tenerte como hermano. Te quiero.

Alberto, qué decir que no sepas. Eres el mejor compañero de vida que podría tener. Gracias por tu apoyo incondicional, por aguantar mis manías y mis malos días, por estar siempre que te necesito, por tus ánimos tan necesarios cuando veo el vaso medio lleno, por tu amor, por nuestra complicidad, porque eres mi mejor plan y por hacerme sentir especial. Te admiro porque sabes lo que quieres y eres capaz de conseguirlo, dando lo mejor de ti mismo y haciendo que los demás brillen. Te amo.

ABBREVIATIONS AND ACRONYMS

References, abbreviations and acronyms

Bibliographic citations have been placed as footnotes in the pages where they were first cited in the section and at the end of this manuscript.

In addition to the standard abbreviations and acronyms in organic chemistry (as defined by the *J. Org. Chem.* Author Guidelines) the following terms have been used in this manuscript:

Anh	Anhydrous
APFO-3	poly[2,7-(9,9-dioctylfluorene)-alt-5,5-(4,7′-di-2-thienyl- 2′,1′,-3-benzothiadiazole
BHJ	Bulk Heterojunction
***R*-Binaphane**	(R,R)-1,2-Bis[(R)-4,5-dihydro-3H-binaphtho(1,2-c:2′,1′-e)phosphepino]benzene
(S,S)-f-Binaphane	1,1′-Bis[(11bs)-3,5-dihydro-4H-dinaphtho[2,1-c:1′,2′-e]phosphenpin-4yl]ferrocene
Bn	Benzyl
BPE	1,2-Bis(2,5-dimethylphospholano)ethane
Boc	*tert*-butyloxicarbonyl
ca.	circa
CD	Circular Dichroism
CNT	Carbon Nanotube
Conv.	Conversion
Cp*	Pentamethylcyclopentadienyl
CV	Cyclic Voltammetry
DABCO	1,4-Diazabicyclo[2.2.2]octane
DBU	1,8-Diazabicyclo[5.4.0]undec-7-ene
DMAP	4-(Dimethylamino)pyridine
DMF	*N*,*N*-Dimethylformamide
DPM	Diphenylmethanofullerene
DPPE	1,2-Bis(diphenylphosphino)ethane

(*R*)-DTBM-SegPhos	(*R*)-5,5′-Bis[di(3,5-di-*tert*-butil-4-metoxifenil)fosfino]-4,4′-bi-1,3-benzodioxol, [(4*R*)-(4,4′-bi-1,3-benzodioxol)-5,5′-diil]bis[bis(3,5-di-*tert*-butil-4-metoxyfenil)fosfina]
EDC·HCl	N-(3-Dimethylaminopropyl)-N′-ethylcarbodiimide hydrochloride
ee	Enantiomeric excess
E_{red}	Reduction Potential
ESI	Electrospray Ionization
EWD	Electron Withdrawing
DO	Dissolved Oxygen
Fc	Ferrocene
FP-TRMC	Flash-photolysis time-resolved microwave conductivity
(*R*)-FeSulPhos	(*R*)-2-(*tert*-Butylthio)-1-(diphenylphosphino)ferrocene
FTIR	Fourier Transform Infrared Spectroscopy
FTO	Fluorine-doped Tin Oxide
GCE	Glassy Carbon Electrode
HAT	Hydrogen Atom Transfer
HOMO	Highest Occupied Molecular Orbital
HPLC	High Performance Liquid Chromatography
HRMS	High Resolution Mass Spectrometry
IPA	Isopropyl alcohol
IPR	Isolated Pentagon Rule
IUPAC	International Union of Pure and Applied Chemistry
ITO	Indium Tin Oxide
LSV	Linear Scan Voltammetry
LUMO	Lowest Unoccupied Molecular Orbital
MALDI	Matrix Assisted Laser Desorption/Ionization
(*S*)-Me-f-KetalPhos	1,1-Bis[(2*S*,3*S*,4*S*,5*S*)-2,5-dimethyl-3,4-O-isopropylidene-3,4-dihydroxyphospholanyl]ferrocene

Mes	Mesityl
Ms	Mesyl
NHC	N-Heterocyclic Carbene
NLO	Non-Linear Optical
NMR	Nuclear Magnetic Resonance
NOE	Nuclear Overhauser Effect
OFET	Organic Field Effect Transistors
OLED	Organic Light-Emitting Diodes
OP	Onset Potential
OPT	Organic Phototransitors
OPV	Organic Photovoltaic
ORR	Oxygen reduction reaction
P3HT	Poly-3-hexylthiophene
PBS	Phosphate Buffered Saline (Sodium Phosphate Buffer)
PCBM	[6,6]-phenyl-C_{61}-butyric acid methyl ester
PCE	Power Conversion Efficiency
PCET	Proton Coupled Electron Transfer
PDOF	Poly(dioctylfluorene)
PEC	Photoelectrochemical Cell
PEDOT	Poly-3,4-ethylenedioxythiophene
PET	Transfer of the Photo-generated Electron
Piv	Pivaloyl
PV	Photovoltaic
RE	Reference Electrode
RRM	Reactions on racemic mixtures
rr-P3HT	Regioregular poly(3-hexylthiophene)
RT	Room temperature
SEM	Scanning Electron Microscopy
S_N	Nucleophilic Substitution

TGA	Thermogravimetric analyses
TFA	Trifluoroacetic acid
TLC	Thin Layer Chromatography
TMS	Trimethylsilane
TTF	Tetrathiafulvalene
TRMC	Time-resolved microwave conductivity
Py	Pyridine
UV-vis	Ultraviolet Visible Spectroscopy

Table of Contents

SUMMARY

"Stereoselective Synthesis on Fullerenes: Properties and Photoelectrochemical Applications"

Introduction

After the discovery of fullerenes, carbon nanotubes and graphene, the classical allotropes of carbon were enriched with new structures and new potential applications. C_{60}, with its singular spherical shape, its size (~1nm) and its remarkable electronic and photophysical properties, has emerged as a promising material for many potential applications in materials, nanotechnology and biomedical sciences.

Objectives

1. Synthesis and electronic properties of fullerenes-fused unsaturated carbocycles

We will extend the scope of asymmetric phosphine-catalysed cycloaddition of allenoates onto fullerenes through the variation of all the elements involved in the reaction. In addition, the intrinsic electronic mobility of these fullerenic derivatives will be measured with the objective of evaluating the influence of the optical purity on this property.

2. Reversible stereodivergent cycloaddition of a helicene derivative onto [60]fullerene: a chiral resolution strategy

We will try to take advantage of the stereoselective and reversible covalent fullerene chemistry as a tool for the resolution of racemates. For this purpose, enantioselective pyrrolidino[60]fullerenes will be prepared from a racemic iminoester derived from [6]helicene.

3. Metallofurene hybrids

In order to prepare other stereoisomers of the iridium-fulleropyrrolidine hybrids, we will try to control the configuration of the iridium atom, maintaining the chirality of the other three stereocenters. For that purpose, we will synthesize several fulleropyrrolidines with electron withdrawing groups in the phenyl substituent.

Furthermore, we will carry out the synthesis of a gold(I) pyrrolidine[60]fullerene derivative by complexing a phosphine-fulleropyrrolidine with [Au(SMe_2)].

4. Fullerene derivatives for photoelectrocatalytic devices

We will prepare fullerenes able to work simultaneously as acceptors and catalysts for their use in devices such as photoelectrochemical cells. Therefore, we will provide fullerene with catalytic sites where reduction processes can be carried out.

Results and Discussion

1. Synthesis and electronic properties of fullerenes-fused unsaturated carbocycles

Firstly, we have studied the dipolar species in the chiral phosphines-catalyzed [3+2] cycloaddition reaction of allenoates onto [60]fullerene. Thus, 3-alkynoates have been used as direct and easily accessible allenoates precursors, giving rise to the reaction with good yields and enantiomeric excesses.

Considering that the differently substituted allenoates are chiral species, we considered the importance to study the effect of the chirality of allenoates on the enantioselectivity of the cycloaddition on C_{60}. The result of this study has led us to the conclusion that the [3+2] cycloaddition reaction of allenoates on C_{60} is stereoconvergent since the enantiopurity of the allenoates does not influence the enantiomeric excess of cyclopenteno[4,5:1,2][60]fullerene.

On the other hand, we considered the preparation of a chiral phosphine with a phosphethane ring, but unfortunately the conversion and enantioselectivity results were worse than those obtained with the seven-membered ring phosphine.

As far as dipolarophile is concerned, the methodology was carried out on C_{70}. The results of site-, regio- and enantioselectivity obtained, in the studied conditions, are moderately good.

On the other hand, *N*-heterocyclic carbenes (NHCs) have been used as catalysts for this reaction in the presence of large base amounts. The result was a new C_{60} monoadduct whose structure presents a ring of cyclobutene fused to [60]fullerene. The conditions were studied to optimize the results and in one of the tests without NHC, the reaction took place but with a lower conversion.

Then, different bases were tested being tetrabutylammonium hydroxide the one that provided the best conversions.

Finally, a study of the electronic properties of both families of compounds was carried out.

2. Reversible stereodivergent cycloaddition of a helicene derivative onto [60]fullerene: a chiral resolution strategy

The enantioselective cycloaddition of a chiral iminoster derived from 2-formylhexahelicene on C_{60} has been carried out using the methodology previously described in our research group for obtaining chiral fulleropyrrolidines. This reaction gave rise to two diastereomeric fulleropyrrolidines that were separated by "no chiral" conventional chromatographic column. Finally, these diastereoisomers, separately, were submitted for retro-cycloaddition, by optimizing mild conditions, to afford enantiomerically pure starting aldehyde.

3. Metallofullerene hybrids

Iridium-fulleropyrrolidine hybrids have four stereogenic centres, one of them at iridium. Fulleropyrrolidines, which present a cyano or nitro group or different number of fluorine atoms in the aromatic ring, have been synthesized. After the formation of the iridium-fullerene complexes, by reaction of the pyrrolidino[60]fullerenes with the dimer $[IrCp^*Cl_2]_2$, the corresponding complexes are analysed by NMR, observing a desymmetrization of the signals corresponding to the aromatic protons, which indicates that the rotation of the aromatic ring is restricted.

Regarding other metallofullerenes, the stereoselective synthesis of a gold(I) and fulleropyrrolidine hybrid has been addressed by the complexing of a phosphine-pyrrolidino[60]fullerene derivative with $[(Me_2S)AuCl]$. Finally, a diastereomeric *cis-trans* control for the gold(I)-fullerene hybrid was obtained since 9:91 ratio is achieved using $Cu(OAc)_2$ without ligand at room temperature and >99:1, by using the catalytic system $Cu(OAc)_2$/(R_P)-FeSulPhos at -55ºC.

4. Fullerene derivatives for photoelectrocatalytic devices

Two main approaches have been undertaken in parallel to obtain new fullerene derivatives with catalytic active sites avoiding the use of typical and expensive bulky noble metals electrodes:

i) Synthesis of new fullerene hybrid derivatives endowed with noble metals active in redox processes, such as Ir, Rh or Pt. Here the use of noble metals is just limited to catalytic amounts while the bulk of the electrode result to be organic.

ii) Synthesis of metal-free fullerene catalysts, based on the presence of active C_{60}-H bonds.

Finally, these new fullerene derivatives were tested as photo-electrocatalysts for ORR in polymer-based devices, in collaboration with the group of Prof. Antognazza in Milan. All tested new catalysts show photocurrent density values larger than one order of magnitude with respect to reference PCBM. Furthermore, photocurrent generation is clearly related to the presence of dissolved oxygen. Importantly, recorded photocurrent densities for organic derivatives with C_{60}-H show values comparable to the ones obtained for the metalofullerene hybrid catalysts.

Conclusions

We have developed an extended methodology by studying all the elements involved in the synthesis of fullerocyclopentenes by allenoate/alkynoate cycloaddition on C_{60} catalysed by phosphines.

In addition, a new derivative based on cyclobutene has been obtained by carrying out the cycloaddition reaction of allenoate/alkynoate onto C_{60} in a basic medium.

The electronic mobility of these cyclobuteno[60]fullerenes is three times higher than that for the reference PCBM. In the case of cyclopenteno[60]fullerene, the influence of chirality on electronic mobility has been studied, and the obtained values for enantiopure compounds are twofold higher in comparison to the corresponding racemic compound.

We report for the first time the use of the less-explored "reversible" covalent chemistry of [60]fullerene as a useful alternative to carry out the resolution of racemic species.

New chiral fullerenes derivatives endowed with metal centers have been prepared and we have achieved the first stereoselective synthesis of gold(I)-fullerene hybrids.

The electrocatalytic activity on the oxygen reduction reactions of new organic and metallic fullerene derivatives has been tested in bulk heterojunction photo-electrochemical cells, affording current values up to ten fold higher than widely used PCBM. Remarkably, metal-free fullerene derivatives, based on C_{60}-H bond, proved to give photocurrents comparable to related metal hybrids.

RESUMEN

"Síntesis Estereoselectiva en Fullerenos: Propiedades y Aplicaciones fotoelectroquímicas"

Introducción

Con el descubrimiento de los fullerenos por H. W. Kroto, R. F. Curl y R. E. Smalley en 1985, se enriqueció la variedad de alótropos del carbono. El C_{60}, con su singular forma esférica, su tamaño (~1nm) y sus destacables propiedades electrónicas y fotofísicas, surgió como un material prometedor para muchas aplicaciones, tanto en materiales y nanotecnología como en ciencias biomédicas.

Objetivos

1. Síntesis y propiedades electrónicas de derivados carbocíclicos insaturados fusionados a fullerenos

Extenderemos la metodología de la reacción de cicloadición asimétrica de alenoatos sobre fullerenos catalizada por fosfinas mediante la variación de todos los elementos que intervienen en la reacción. Además, se llevará a cabo la medida de la movilidad electrónica intrínseca de estos derivados fullerénicos y se evaluará cómo afecta la pureza óptica a dicha propiedad.

2. Cicloadición estereodivergente reversible de un derivado de heliceno sobre el [60]fullereno: una estrategia de resolución quiral

Realizaremos el estudio de la reversibilidad en la química covalente del fullereno como herramienta para la resolución de racematos. Para ello, se prepararán fulleropirrolidinas enantioselectivas a partir de un iminoéster racémico derivado de [6]heliceno.

3. Híbridos metalofullereno

Con el objetivo de preparar otros estereoisómeros de los híbridos iridio-fulleropirrolidina, intentaremos controlar la configuración del átomo de iridio, manteniendo la quiralidad de los otros tres estereocentros. Para ello, sintetizaremos varias fulleropirrolidinas con grupos electroatractores en el sustituyente fenilo.

Por otro lado, llevaremos a cabo la síntesis de un derivado de oro(I) y pirrolidino[60]fullereno mediante la complejación de una fosfina-fulleropirrolidina con [Au(SMe_2)].

4. Derivados fullerénicos para dispositivos fotoelectrocatalíticos

Prepararemos derivados de fullereno para su empleo en dispositivos como células fotoelectroquímicas. Por lo tanto, dotaremos al fullereno de sitios catalíticos donde se puedan llevar a cabo procesos de reducción.

Resultados y Discusión

1. Síntesis y propiedades electrónicas de derivados carbocíclicos insaturados fusionados a fullerenos

En primer lugar, hemos desarrollado un estudio de la reacción de cicloadición [3+2] de alenoatos sobre el [60]fullereno catalizada por fosfinas quirales. Así, se han empleado 3-alquinoatos como precursores directos y de fácil acceso de los alenoatos, dando lugar a la reacción con buenos rendimientos y excesos enantioméricos.

Teniendo en cuenta que los alenoatos diferentemente sustituidos son especies quirales, hemos pretendido estudiar el efecto de la quiralidad de los alenoatos sobre la enantioselectividad de la cicloadición sobre el C_{60}. El resultado de este estudio nos ha llevado a la conclusión de que la reacción de cicloadición [3+2] de alenoatos sobre el C_{60} es estereoconvergente ya que la enantiopureza de los alenoatos no influye en el exceso enantiomérico del ciclopenteno[4,5:1,2][60]fullereno.

Por otro lado, nos planteamos la preparación de una fosfina quiral con un anillo de fosfetano, pero desafortunadamente los resultados de conversión y de enantioselectividad fueron peores que los obtenidos con la fosfina que presenta un anillo de siete miembros.

En cuanto al dipolarófilo, la metodología se llevó a cabo sobre el C_{70}. Los resultados obtenidos con las condiciones estudiadas tanto de loco-, regio- y enantioselectividad son moderadamente buenos.

Por otro lado, se han empleado carbenos *N*-heterocíclicos como catalizadores de esta reacción, en presencia de grandes cantidades de base. El resultado fue un

nuevo monoaducto de C_{60} cuya estructura presenta un anillo de ciclobuteno fusionado al [60]fullereno. Se estudiaron las condiciones para optimizar los resultados y, en una de las pruebas sin carbeno, la reacción tuvo lugar con una menor conversión. Por ello, se probaron diferentes bases hasta encontrar que el hidróxido de tetrabutilamonio daba lugar a las mejores conversiones.

Finalmente, se estudió la movilidad electrónica de ambas familias de compuestos.

2. Cicloadición reversible estereodivergente de un derivado de heliceno sobre el [60]fullereno: una estrategia para la resolución quiral

Se ha llevado a cabo la cicloadición enantioselectiva de un iminoéster quiral derivado del 2-formilhexaheliceno sobre el C_{60} mediante la metodología, descrita previamente por nuestro grupo de investigación, para la síntesis de pirrolidino[60]fullerenos quirales. Esta reacción dio lugar a dos fulleropirrolidinas diastereoisoméricas que fueron separadas mediante columna cromatográfica convencional. Por último, estos diastereoisómeros, por separado, se sometieron a retro-cicloadición, optimizando unas condiciones suaves, para proporcionar el aldehído de partida enantioméricamente puro.

3. Híbridos metalofullerénicos

Los híbridos de iridio-fulleropirrolidina presentan cuatro centros estereogénicos, uno de ellos en el átomo de iridio. Las fulleropirrolidinas sintetizadas presentan en el anillo aromático un grupo ciano, nitro o diferente número de átomos de flúor. Tras la formación de los complejos iridio-fullereno, mediante la reacción de los pirrolidino[60]fullerenos con el dímero $[IrCp^*Cl_2]_2$, se analizan los correspondientes complejos mediante RMN observándose una desimetrización de las señales correspondientes a los protones aromáticos, lo que indica que el giro del anillo aromático se encuentra restringido.

Por otro lado, se ha abordado la síntesis enantioselectiva de un híbrido de oro(I) y fulleropirrolidina mediante la complejación de un derivado fosfina-pirrolidino[60]fullereno y $[(Me_2S)AuCl]$. Finalmente, se ha conseguido una relación diastereomérica *cis-trans* para el híbrido oro(I)-fullereno de 9:91, utilizando $Cu(OAc)_2$ sin ligando a temperatura ambiente y >99:1, usando el sistema catalítico $Cu(OAc)_2$/(R_P)-FeSulPhos a -55ºC.

4. Derivados fullerénicos para dispositivos fotoelectrocatalíticos

Se han llevado a cabo dos estrategias simultáneamente para la obtención de nuevos derivados fullerénicos funcionalizados adecuadamente con sitios catalíticos activos para la reacción de reducción de oxígeno (RRO), evitando el uso de los electrodos típicos basados en metales nobles:

i) Síntesis de híbridos de [60]fullereno y metales nobles activos en procesos de reducción, como Ir, Rh o Pt. En este caso, el uso de metales nobles se reduce a una cantidad catalítica ya que la mayoría del electrodo es material orgánico.

ii) Síntesis de catalizadores fullerénicos no metálicos basados en la presencia de enlaces activos C_{60}-H.

Finalmente, se probaron estos nuevos derivados fullerénicos como foto-electrocatalizadores para la RRO en dispositivos basados en polímeros. Todos los nuevos catalizadores probados muestran valores de densidad de fotocorriente superiores a un orden de magnitud con respecto al PCBM de referencia. Además, la generación de fotocorriente está claramente relacionada con la presencia de oxígeno disuelto. Es importante destacar que las densidades de fotocorriente registradas para los derivados orgánicos con C_{60}-H muestran valores comparables a los obtenidos para los catalizadores híbridos metalofullerénicos.

Conclusiones

Hemos desarrollado una metodología extendida, mediante el estudio de todos los elementos que intervienen en la síntesis de fullerociclopentenos mediante cicloadición de alenoato/alquinoato sobre el C_{60} catalizada por fosfinas.

Además, se ha obtenido un nuevo derivado basado en ciclobuteno al llevar a cabo la reacción de cicloadición de alenoatos/alquinoatos sobre el C_{60} en medio básico.

Se ha medido la movilidad electrónica de estas dos familias de compuestos con anillos carbonados fusionados al fullereno. Para los ciclobuteno[60]fullerenos se han obtenido valores hasta tres veces superiores con respecto al PCBM de referencia. En el caso de los ciclopenteno[60]fullerenos, se ha estudiado la influencia de la quiralidad en la movilidad electrónica, y se han observado

valores para los compuestos enantiopuros dos veces mayores que para el correspondiente racémico.

Por otro lado, hemos presentado, por primera vez, el uso de la química covalente "reversible" menos explorada del [60]fullereno como una alternativa útil para llevar a cabo la resolución de especies racémicas.

Se han preparado nuevos derivados de fullereno quirales dotados de centros metálicos y se ha conseguido la primera síntesis estereoselectiva de híbridos de oro(I)-fullereno.

La actividad electrocatalítica sobre las reacciones de reducción de oxígeno de los nuevos derivados orgánicos y metálicos de fullereno ha sido medida en celdas fotoelectroquímicas, proporcionando valores de corriente hasta diez veces superiores a los del PCBM, lo que confirma una actividad fotocatalítica mejorada de los nuevos compuestos. Sorprendentemente, los derivados de fullereno orgánicos, basados en el enlace C_{60}-H, demostraron dar corrientes fotoeléctricas comparables a las de los híbridos metálicos relacionados.

INTRODUCTION

1. INTRODUCTION

Carbon is a common element present in living organism. It is the 15th most abundant element in the Earth's crust, the 4th most abundant element in the universe (H, He, O) and the 2nd most abundant element in the human body (≈ 18.5%) after oxygen. Furthermore, it is considered a singular element because of its rather unique ability to form long chains whose central core is constituted exclusively by carbon atoms.[1]

Over thirty years ago, the classical allotropes of carbon, diamond and graphite, were enriched with the discovery of fullerenes by H. W. Kroto, R. F. Curl and R. E. Smalley in 1985,[2] who were awarded with the Nobel Prize in Chemistry in 1996. But it was in 1990 when W. Krätschmer and D. Huffman designed a method for obtaining fullerenes in multigram amounts what allowed the chemical functionalization of these carbon spheres.[3]

In contrast to the former known reticular carbon allotropes, fullerenes present a structure with a defined number of carbon atoms shaped like symmetrical carbon cages. Afterwards, S. Iijima discovered carbon nanotubes (CNTs) in 1991[4] and, more recently, graphene was found by A. K. Geim and K. S. Novoselov in 2004[5] who were also awarded with the Nobel Prize in Physics in 2010 (Figure 1).

[1] a) Levi, P. *The Periodic Table*, Schocken Books, New York, **1995**, b) Carey, F. A. *Organic Chemistry*, McGraw-Hill Companies, New York, **1996**

[2] Kroto, H. W.; Heath, J. R.; O'Brien, S. C.; Curl, R. F.; Smalley, R. E. *Nature* **1985**, *318*, 162-163

[3] Kraetschmer, W.; Lamb, L. D.; Fostiropoulos, K.; Huffman, D. R. *Nature* **1990**, *347*, 354-358

[4] a) Iijima, S. *Nature* **1991**, *354*, 56-58, b) Iijima, S.; Ichihashi, T. *Nature* **1993**, *363*, 603-605, c) Bethune, D. S.; Kiang, C. H.; de Vries, M. S.; Gorman, G.; Savoy, R.; Vazquez, J.; Beyers, R. *Nature* **1993**, *363*, 605-607

[5] a) Novoselov, K. S.; Geim, A. K.; Morozov, S. V.; Jiang, D.; Zhang, Y.; Dubonos, S. V.; Grigorieva, I. V.; Firsov, A. A. *Science* **2004**, *306*, 666-669, b) Geim, A. K.; Novoselov, K. S. *Nat. Mater.* **2007**, *6*, 183-191

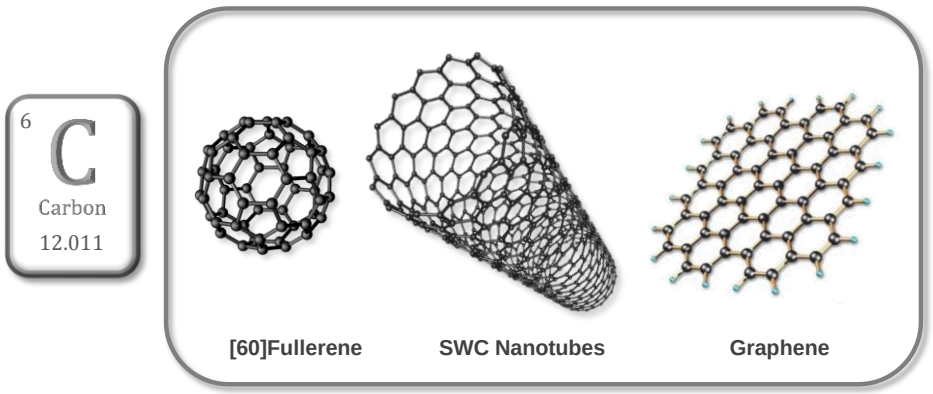

Figure 1. Chemical structures of the main carbon nanoforms.

Along with other molecular forms of carbon, namely endohedral fullerenes,[6] carbon nanohorns,[7] carbon nanoonions,[8] etc, C_{60} with its singular spherical shape, its size in the nanometre scale (~1nm) and its remarkable electronic and photophysical properties, has prompted a great excitement in the scientific community and has emerged as a promising material for many potential applications in materials, nanotechnology and biomedical sciences.[9]

[6] a) Akasaka, T.; Nagase, S. *Endofullerenes: A New Family of Carbon Clusters*, Kluver Academic Publishers, Dordrecht (The Netherlands), **2002**, b) Dunsch, L.; Yang, S. *Small* **2007**, *3*, 1298-1320, c) Chaur, M.; Melin, F.; Ortiz, A.; Echegoyen, L. *Angew. Chem. Int. Ed.* **2009**, *48*, 7514-7538

[7] Iijima, S.; Yudasaka, M.; Yamada, R.; Bandow, S.; Suenaga, K.; Kokai, F.; Takahashi, K. *Chem. Phys. Lett.* **1999**, *309*, 165-170

[8] Ugarte, D. *Nature* **1992**, *359*, 707-709

[9] a) Delgado, J. L.; Herranz, M. Á; Martín, N. *J. Mater. Chem.* **2008**, *18*, 1417-1426, b) Pinzón, R.; Villalta-Cerdas, A.; Echegoyen, L. *Unimolecular and Supramolecular Electronics I: Chemistry and Physics Meet at Metal-Molecule Interfaces*, Springer Berlin Heidelberg, Berlín, **2012**, c) Choudhary, N.; Hwang, S.; Choi, W. *Handbook of Nanomaterials Properties*, Springer Berlin Heidelberg, Berlín, **2014**, d) Marcaccio, M.; Paolucci, F. *Making and Exploiting Fullerenes, Graphene, and Carbon Nanotubes*, Topics in current chemistry, Springer, Berlin, **2014**, e) Martín, N. *Adv. Energy Mater.* **2017**, *7*, 1601102

1.1. Fullerenes Features, Structure and Properties

Fullerenes are highly symmetrical molecules in the form of closed cages consisting only of carbon atoms. Unlike other carbon allotropic forms, diamond and graphite, which present reticular structures of carbon atoms with hybridizations sp^3 and sp^2, respectively, fullerenes, with hybridization $sp^{2,3}$, are discrete molecules.

The most stable and abundant is C_{60}. The 60 carbon atoms in C_{60} are known to be located at the vertices of a truncated icosahedron where all carbon sites are equivalent (Figure 2). A regular truncated icosahedron has 90 edges of equal length, 60 equivalent vertices, 20 hexagonal faces, and 12 additional pentagonal faces to form a closed shell, consistent with Euler's theorem. The 12 pentagonal rings are surrounded by 20 hexagonal rings, which makes its structure remind us of a football.

Figure 2. Truncated icosahedron structure.

Given the icosahedral symmetry of C_{60}, this presents six five-fold rotation axes that pass through the centres of opposite pairs of pentagonal faces. There are therefore two types of bonds in its structure: bonds at the junction between two hexagons ([6,6]) and bonds at the junction between a hexagon and a pentagon ([5,6]). Although initially considered to be a "superaromatic" molecule, it was later found to have a polyenic structure, with all double bonds located between the six-membered rings. These bond lengths between two hexagons, [6,6] bonds are shorter (1.37 Å) than the bonds at the junctions of a hexagon and a pentagon [5,6] bonds (1.45 Å). The structure can be described as a sphere composed by fused subunits of [5]radialene and 1,3,5-cyclohexatriene or what is the same,

subunits of corannulene (Figure 3a). On the other hand, pentagons are responsible for curvature which is the driving force of its reactivity, based on the release of energy produced by saturating a double bond. Therefore, the most reactive bonds will be the double bonds [6,6].

The [60]fullerene stability is justified by the Isolated Pentagon Rule (IPR), puts forward by H. W. Kroto in 1987.[10] This rule stablishes that those structures in which pentagons are surrounded by hexagons will be more stable than those ones having fused pentagons. Adjacent pentagons provide a higher stress on the binding angle with the consequent reduction of orbital overlap, as well as a destabilisation of the π electron cloud for the system (pentalene structures with 8 π electrons doesn't satisfy the Hückel Rule (Figure 3b)).

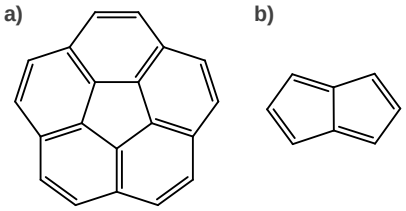

Figure 3. (a) Corannulene structure. (b) Pentalene structure.

The next more stable fullerene is [70]fullerene. It is a cage formed by 12 pentagonal rings and 25 hexagonal rings. These extra 5 hexagons go around an equatorial plane that defines, perpendicular to it, a unique five-fold axis. This leaves the buckyball resembling a rugby ball in shape more than a soccer ball (Figure 4), and leaving it with D_{5h} symmetry which makes that C_{70} is constituted by four non-equivalent double bonds, namely: α, β, γ and δ.[11]

The geometry at the poles (highest curvature) of [70]fullerene is very similar to that of [60]fullerene. The corannulene subunits have the same type of bond length alternation. In contrast to C_{60}, the equatorial belt in [70]fullerene, consisting of fused hexagons, has different reactivity compared with the more reactive polar region.

[10] a) Schmalz, T. G.; Seitz, W. A.; Klein, D. J.; Hite, G. E. *Chem. Phys. Lett.* **1986**, *130*, 203-207, b) Kroto, H. W. *Nature* **1987**, *329*, 529-531

[11] Taylor, R.; Hare, J. P.; Abdul-Sada, A.; Kroto, H. W. *J. Chem. Soc., Chem. Commun.* **1990**, 1423-1425

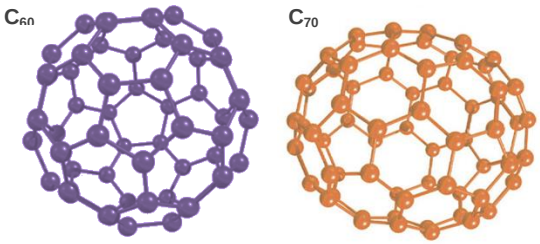

Figure 4. [60]fullerene and [70]fullerene structures.

Fullerenes are soluble in some common organic solvents such as 1,2-dichlorobenzene, carbon disulfide, chlorobenzene or toluene but not in polar solvents or in those ones that present hydrogen bonds like water.

Fullerenes are electron acceptor molecules with singular optoelectronic properties.[12] [60]fullerene presents a relatively low and triply degenerate LUMO, which allows it, in solution, to accept up to six electrons as can be measured by cyclic voltammetry (CV).[12b] CV confirms that the reduction is an easy reversible process by steps in which each of them involves the transfer of an electron giving rise species with low reorganization energy (Figure 5).[13] If these properties are taken into account, fullerenes can be functionalized[14] to obtain materials that can act as acceptors in photovoltaic.[15]

[12] a) Echegoyen, L.; Echegoyen, L. E. *Acc. Chem. Res.* **1998**, *31*, 593-601, b) Guldi, D. M. *Chem. Commun.* **2000**, 321-327
[13] Xie, Q.; Perez-Cordero, E.; Echegoyen, L. *J. Am. Chem. Soc.* **1992**, *114*, 3978-3980
[14] Martín, N.; Sánchez, L.; Illescas, B.; Pérez, I. *Chem. Rev.* **1998**, *98*, 2527-2547
[15] Delgado, J. L.; Bouit, P.; Filippone, S.; Herranz, M. A.; Martín, N. *Chem. Commun.* **2010**, *46*, 4853-4865

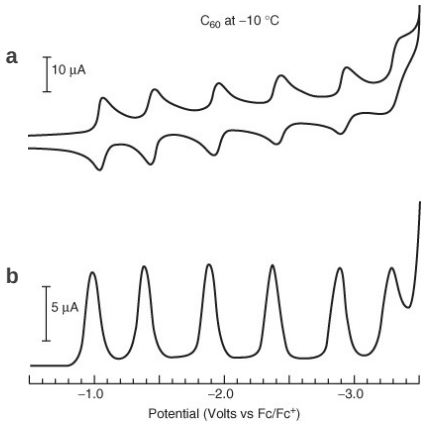

Figure 5. (a) Cyclic voltammogram and (b) Squarewave voltammetry of C_{60} molecule at –10ºC.

Properties that make [60]fullerene an ideal candidate for photoinduced charge transfer processes are:

a) A moderate value for the first reduction potential and the possibility to form stable multianions.

b) A rigid structure and high stability in both, the ground state and the excited one.

c) Low reorganization energy of the [60]fullerene radical-anion since the charge is delocalized along all the carbon sphere.[12a]

Fullerenes are moderate chromophores. [60]fullerene has a high absorption in the UV spectrum and low in the visible. Although fullerenes present some forbidden transitions with low absorption coefficients, which provide them of a purple colour in solution. However, higher fullerenes present an absorption in a wider region of the UV-vis spectrum (Figure 6).[16]

[16] a) Hare, J. P.; Kroto, H. W.; Taylor, R. *Chem. Phys. Lett.* **1991**, *177*, 394-398, b) Harigaya, K.; Abe, S. *J. Phys.: Condens. Matter*. **1996**, *8*, 8057-8066

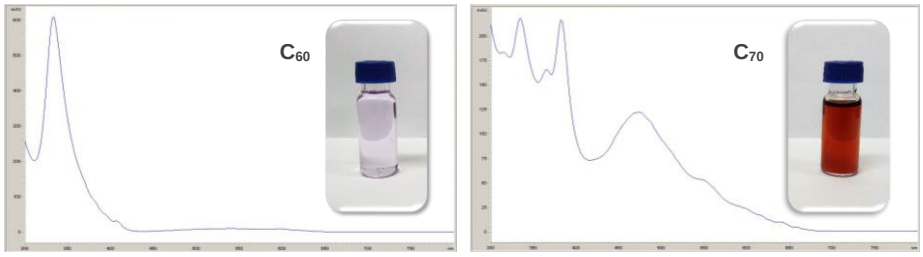

Figure 6. UV-vis spectrum of C_{60} and C_{70} molecules solution (toluene).

Fullerenes are efficient n-type semiconductors.[17] The most commonly used fullerene derivative in organic electronics is the methanofullerene Phenyl-C_{61}-Butyric-Acid-Methyl-Ester ([60]PCBM).[18] The use in organic photovoltaics, photodetectors and organic field effect transistors (OFETs) among other applications, has been investigated and is under active development.

Moreover, [60]fullerene has mechanic and electronic properties suitable for being employed as molecular wire. Indeed, our research group, in collaboration with N. Agrait group (IMDEA-Nanociencia), has proved the usefulness of fullerenes as beacon in STM experiments.[19]

1.2. Chirality in Nanoscience

Chirality is a property of asymmetry with high importance in several fields of science, which manifests across multiple length scales, from elemental particles, to molecules and even macroscopic objects, such as human hands. An object or a system is chiral if it is distinguishable from its mirror image; that is, it cannot be superposed onto it.

Chirality in biological processes and pharmaceutical chemistry is well known and its relevance in these fields does not need to be accounted for. Thus, when

[17] a) Kronholm, D.; Hummelen, J. C. *Material Matters* **2007**, *2*, 16, b) Anthony, J. E.; Facchetti, A.; Heeney, M.; Marder, S. R.; Zhan, X. *Adv. Mater.* **2010**, *22*, 3876-3892
[18] a) Hummelen, J. C.; Knight, B. W.; LePeq, F.; Wudl, F.; Yao, J.; Wilkins, C. L. *J. Org. Chem.* **1995**, *60*, 532-538, b) Yu, G.; Gao, J.; Hummelen, J. C.; Wudl, F.; Heeger, A. J. *Science* **1995**, *270*, 1789-1791
[19] Leary, E.; Gonzalez, M. T.; van der Pol, C.; Bryce, M. R.; Filippone, S.; Martín, N.; Rubio-Bollinger, G.; Agrait, N. *Nano Lett.* **2011**, *11*, 2236-2241

designing a ligand (for example, a drug) for a biological receptor (for instance, a drug target), chirality is an important factor to be considered.

However, chirality role and relevance in nanoscience is not readily evident since this field is still in its infancy and relatively few examples of chiral materials have been reported.[20] Furthermore, given the predominant molecular nature of chirality, its implementation at the nanoscale relies upon successful transfer of chirality of templating materials into nano-building blocks (e.g. ligand chirality in the case of nanoparticles).[21]

Thus chiral nanostructures, such as chiral springs, gears and propellers, could potentially create a new dimension of mechanical applications in nanodevices.[20]

Moreover, it is necessary to highlight the importance to relate the well-understood characteristics of an isolated molecule (molecular properties such as the highest occupied and lowest unoccupied molecular orbital energy levels, and molecular structure) to the behaviour of multiple molecules in the bulk (material properties such as charge transport and morphology).[22]

Therefore, in order to answer fundamental questions such as how chirality influences the electronic and photochemical properties of the nanostructures, the development of methodologies to obtain chiral nanostructures is an important field of research.

[20] Wang, Y.; Xu, J.; Wang, Y.; Chen, H. *Chem. Soc. Rev.* **2013**, *42*, 2930-2962
[21] Kitaev, V. *J. Mater. Chem.* **2008**, *18*, 4745-4749
[22] Henson, Z. B.; Müllen, K.; Bazan, G. C. *Nat. Chem.* **2012**, *4*, 699-704

BACKGROUND

2. BACKGROUND

2.1. Fullerenes Chemical Reactivity

Due to the poor electronic delocalization along the cage structure, [60]fullerene is much more reactive than originally expected, behaving like a polyolefin deficient in electrons. Thus, the highly reactive fullerenes double bonds usually experience a wide variety of addition reactions, being the nucleophilic addition the typical reaction undergone by them (Scheme 1).[23] Nowadays, the exohedric functionalization of fullerenes has reached a great development, in particular, the cycloaddition reactions have been undoubtedly the most studied and those that have led to a greater number of derivatives. These kind of reactions are very useful to introduce functional groups to the fullerenes. Hereunder, the most representative cycloadditions are shown.[24]

2.1.1. Nucleophilic addition

A nucleophile Nu^- initially attacks the double bond and a reactive intermediate $C_{60}Nu^-$ is generated. This one can be stabilized in several ways. The product $C_{60}NuE$ results from the reaction with an electrophile E^+ or EX such as H^+ or alkylhalogenides. Furthermore, an intramolecular reaction is possible that yields bridging functional groups and $C_{60}Nu_2$ is accessible by oxidative work-up of $C_{60}Nu^-$. The most preferred addition pattern is 1,2 but depending on the addend size 1,4 or even 1,6 additions can take place. Furthermore, polyadducts are obtained as isomeric mixtures due to the many double bonds present. Addition can be categorized into cycloadditions, addition involving bridging and addition of separate groups.

[23] a) Taylor, R.; Walton, D. R. *Nature* **1993**, *363*, 685-693, b) Hirsch, A.; Brettreich, M. *Fullerenes: Chemistry and Reactions*, Wiley-VCH, Weinheim (Germany), **2005**

[24] Maroto, E. E.; Izquierdo, M.; Reboredo, S.; Marco-Martínez, J.; Filippone, S.; Martín, N. *Acc. Chem. Res.* **2014**, *47*, 2660-2670

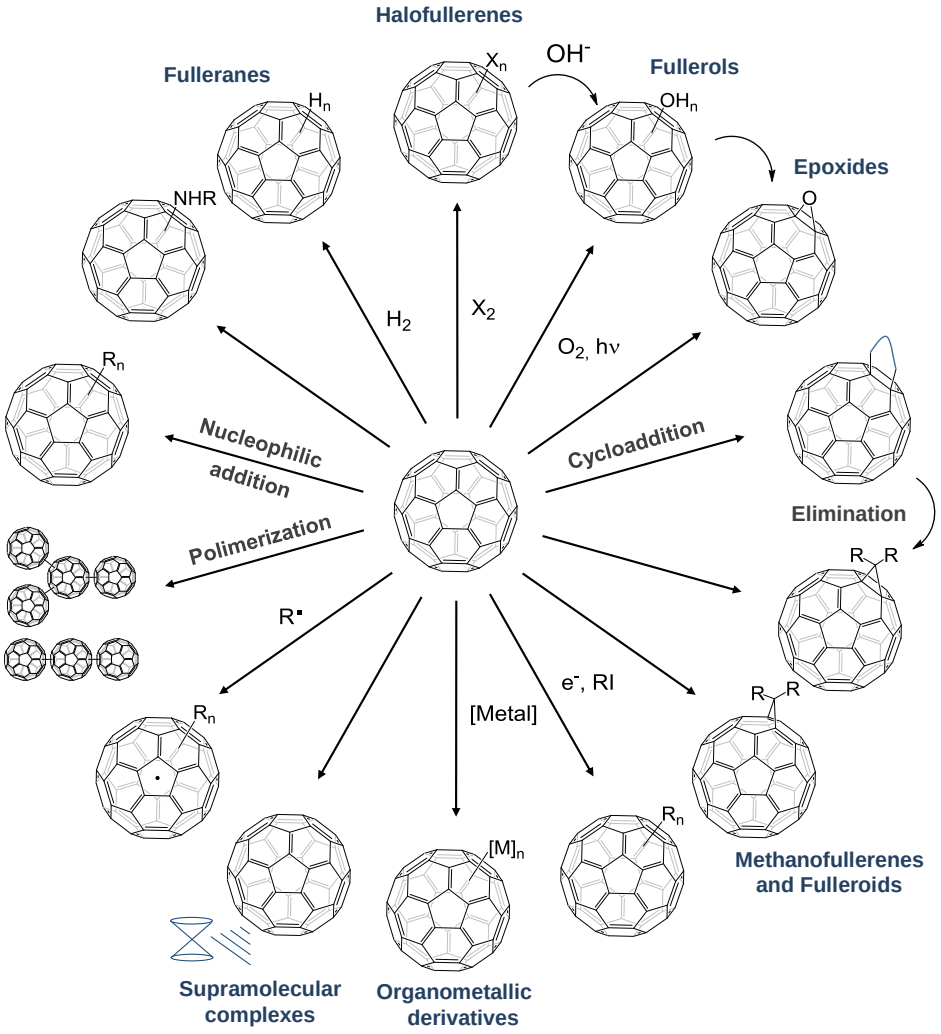

Scheme 1. Representative reactivity in fullerenes.

2.1.1.1. Cycloadditions

As a result of a cycloaddition reaction, a three-, four-, five-, or six-membered ring is fused to the outside of the fullerene shell in such a way that one side of the ring is also part of the cage depending on the kind of cycloaddition: [2+1], [2+2], [3+2], [4+2] and [8+2] (Scheme 2). In these reactions, C=C double bonds

are broken and new bonds form, depending on the number of π electrons involved in these bonds.

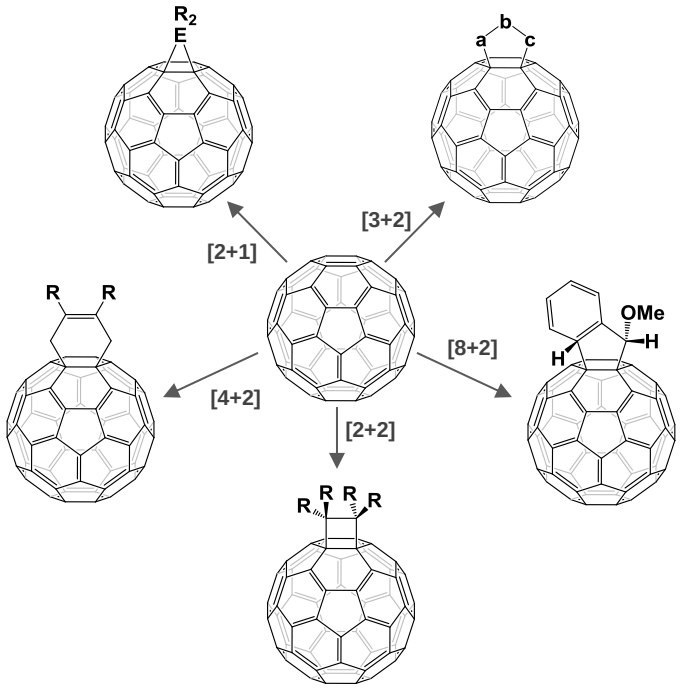

Scheme 2. Cycloaddition reactions carried out on C_{60}.

[3+2] Cycloadditions

The 1,3-dipolar cycloaddition reaction between an azomethine ylide, generated in situ from an aldehyde or ketone, an amino acid or aminoester and one of the double bonds of fullerene, to form a pyrrolidine ring on the surface of fullerene is considered one of the most straightforward procedures for fullerene functionalization. This cycloaddition is commonly known as Prato Reaction (Scheme 3).[25]

[25] a) Maggini, M.; Scorrano, G.; Prato, M. *J. Am. Chem. Soc.* **1993**, *115*, 9798-9799, b) Prato, M.; Maggini, M. *Acc. Chem. Res.* **1998**, *31*, 519-526, c) Tagmatarchis, N.; Prato, M. *Synlett* **2003**, 768-779

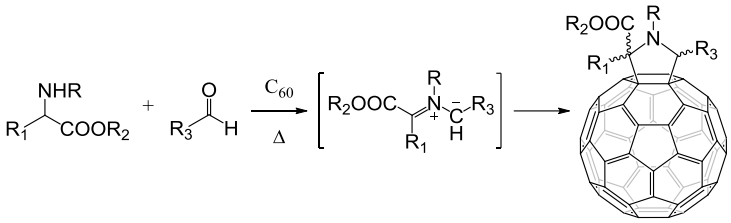

Scheme 3. 1,3-Dipolar cycloaddition of azomethine ylides to C_{60}.

The broad acceptance of this method is explained by the good selectivity (only the [6,6] bond is attacked) and by the versatility of this reaction resulting from the possibility of introducing different substituents into three different positions of the pyrrolidine ring depending on the used aldehyde/ketone and respective amino acid.

Studies carried out in our group have shown that, despite pyrrolidinofullerenes are enough stable compounds, they undergo a retro-cycloaddition reaction in a quantitative way (Scheme 4). This finding increases the versatility of this reaction, since it can be used as a protection-deprotection protocol.[26]

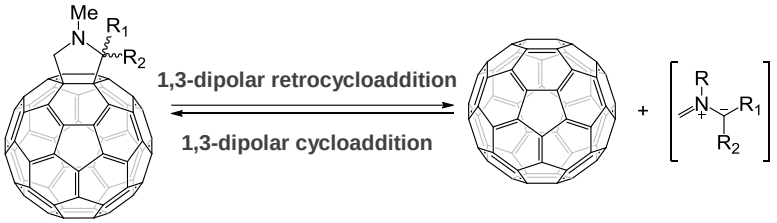

Scheme 4. Reversibility of the 1,3-dipolar cycloaddition of azomethine ylides.

The best results for the thermal retro-cycloaddition reaction were obtained by heating the pyrrolidinofullerene in the presence of a dipolarophile such as maleic

[26] a) Martín, N.; Altable, M.; Filippone, S.; Martín-Domenech, A.; Echegoyen, L.; Cardona, C. M. *Angew. Chem. Int. Ed.* **2006**, *45*, 110-114, b) Lukoyanova, O.; Cardona, C. M.; Altable, M.; Filippone, S.; Martín-Domenech, Á; Martín, N.; Echegoyen, L. *Angew. Chem. Int. Ed.* **2006**, *45*, 7430-7433, c) Filippone, S.; Izquierdo, M.; Martín-Domenech, A.; Osuna, S.; Solà, M.; Martín, N. *Chem. Eur. J.* **2008**, *14*, 5198-5206

anhydride and copper (II) triflate. This methodology was also effective for the deprotection of [70]fullerene and also for carbon nanotubes.[27]

On the other hand, in 2009, Guryanov *et al*. reported an alternative methodology to get the retrocycloaddition of pyrrolidinofullerenes under microwave irradiation in an ionic liquid (1-methyl-3-n-octyl-imidazolium tetrafluorborate) that would stabilize the ionic intermediates.[28]

[4+2] Cycloadditions

The Diels-Alder reaction is undoubtedly one of the most versatile reactions in organic chemistry, being the most elegant method of creating six-member rings due to its remarkable chemo-, regio- and diastereoselectivity. Its application in the chemistry of fullerenes has allowed a wide variety of derivatives to be obtained.[29] However, the main problem found in the reaction of C_{60} with dienes is that the resulting cycloadduct undergoes an easy cycloreversion to the starting materials as a result of its thermal instability.

However, when cycloaddition leads to stable products, this retrocycloaddition does not occur. An example is shown in Scheme 5, where the reaction of C_{60} with *o*-quinodimethane (*o*QDM, a highly reactive transient species) results in a very stable product due to the formation of an aromatic system, and cycloreversion, therefore, does not occur.[30]

[27] Brunetti, F. G.; Herrero, M. A.; Muñoz, J. M.; Giordani, S.; Díaz-Ortiz, A.; Filippone, S.; Ruaro, G.; Meneghetti, M.; Prato, M.; Vázquez, E. *J. Am. Chem. Soc.* **2007**, *129*, 14580-14581

[28] Guryanov, I.; Montellano Lopez, A.; Carraro, M.; Da Ros, T.; Scorrano, G.; Maggini, M.; Prato, M.; Bonchio, M. *Chem. Commun.* **2009**, 3940-3942

[29] Martín, N.; Segura, J. L.; Wudl, F. In *New Concepts in Diels-Alder Cycloadditions to Fullerenes;* Guldi, D. M., Martin, N., Eds.; Fullerenes: From Synthesis to Optoelectronic Properties; Springer: Dordrecht (Netherlands), 2002; pp 81-120

[30] Segura, J. L.; Martín, N. *Chem. Rev.* **1999**, *99*, 3199-3246

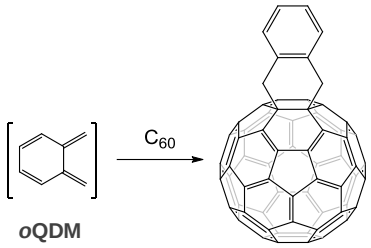

Scheme 5. [4+2] cycloaddition of *o*QDM onto [60]fullerene.

In order to get a better understanding of the Diels-Alder cycloaddition reaction on fullerenes, the addition of butadiene to [60]fullerene has been theoretically studied and demonstrated to be almost completely localized on a [6,6] bond, being the activation energy for the [5,6] addition 45.6 kcal/mol higher than the addition to a [6,6] bond of C_{60}.[31]

[2+2] Cycloadditions

Despite benzyne is an excellent dienophile, in the presence of [60]fullerene, the [2+2] cycloaddition takes place instead of Diels-Alder reaction (Scheme 7). Indeed, an hypothetical [4+2] cycloadduct would require the formation of a double bond at a [5,6] position.[32]

On the other hand, the photochemical [2+2] cycloaddition of enones to C_{60} is possible by irradiation of benzene solutions of the components with a high-pressure mercury lamp or with a XeCl excimer laser, giving rise to *cis* and *trans*-fused stereoisomers arising from the [2+2] cycloaddition to a [6,6] bond of C_{60} (Scheme 6).

[31] Chikama, A.; Fueno, H.; Fujimoto, H. *J. Phys. Chem.* **1995**, *99*, 8541-8549
[32] a) Hoke II, S. H.; Molstad, J.; Dilettato, D.; Jay, M. J.; Carlson, D.; Kahr, B.; Cooks, R. G. *J. Org. Chem.* **1992**, *57*, 5069-5071, b) Tsuda, M.; Ishida, T.; Nogami, T.; Kurono, S.; Ohashi, M. *Chem. Lett.* **1992**, 2333-2334

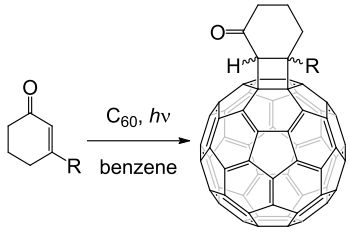

Scheme 6. Photochemical [2+2] cycloaddition of enones to C_{60}.

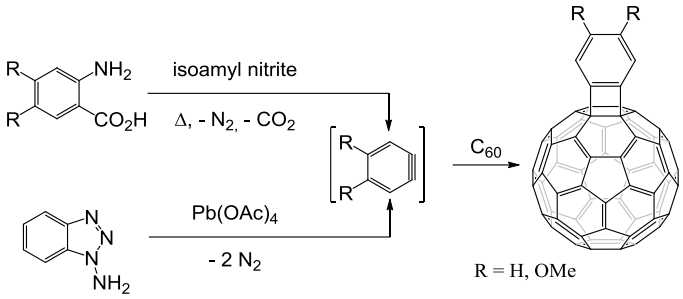

Scheme 7. Addition of generated in situ benzyne to C_{60}.

In the case that two enones are present in the molecule, the photocycloaddition on [60]fullerene occurs on the more substituted double bond, giving rise regiospecifically to one of two possible isomers (Scheme 8). This aspect can be explained by the higher stability of the generated intermediate biradicals.[33]

Regarding the retrocycloaddition, cyclobutane-fused fullerenes derived from acyclic enones are less stable than their bycyclic homologues.

[33] Vassilikogiannakis, G.; Orfanopoulos, M. *J. Org. Chem.* **1999**, *64*, 3392-3393

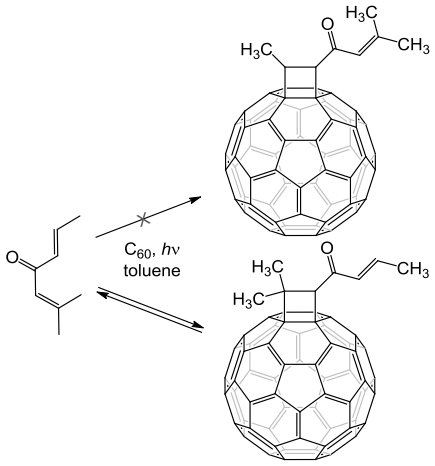

Scheme 8. Regiospecific [2+2] cycloaddition of dienones on C_{60}.

On the other hand, the formation of cyclobutenes fused on the fullerene sphere is considerably less-known in the literature. Only a few examples describe the synthesis of these singular cycloadducts, by using alkynes as 2π-partner of fullerene in phosphine catalyzed processes.

Thus, the cycloaddition of electron-rich alkynes and alkenes has been carried out. *N*,*N*-diethylpropynylamine has been cycloadded to C_{60} upon irradiation of oxygen-free toluene solution at room temperature (Scheme 9). The resulting cycloadduct is not stable, and upon exposure to air and room light for 2h, it cleanly produces the oxoamide via a 1,2-dioxetane intermediate. It can be converted into the fullerene anhydride by heating in toluene at 100 °C in the presence of *p*-TsOH.[34]

According to the proposed mechanism, the addition of electron-rich alkynes to C_{60} involves the triplet excited state of C_{60} in the first step, generated by irradiation.

[34] Zhang, X.; Romero, A.; Foote, C. S. *J. Am. Chem. Soc.* **1993**, *115*, 11024-11025

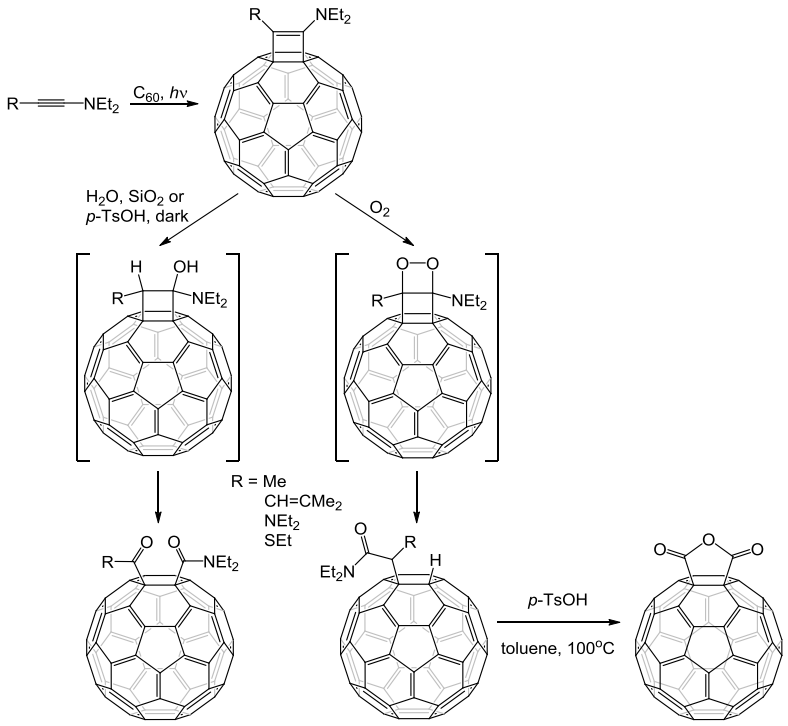

Scheme 9. [2+2] Photocycloaddition of electron-rich alkynes on C_{60}.

On the other hand, thermal or photochemical conditions are able to trigger the cycloaddition of allenamides, electron-rich alkynes or in situ generated ketenes.[35] It must be taken into account that the resultant structure is dependent on the employed method or substrate, being the obtained cycloadduct a cyclobutane with an exocyclic double bond[35c-d] or a cyclobutene.[34,35a-b,36]

[35] a) Zhang, X.; Foote, C. S. *J. Am. Chem. Soc.* **1995**, *117*, 4271-4275, b) Zhang, X.; Fan, A.; Foote, C. S. *J. Org. Chem.* **1996**, *61*, 5456-5461, c) Matsui, S.; Kinbara, K.; Saigo, K. *Tetrahedron Lett.* **1999**, *40*, 899-902, d) Nair, V.; Sethumadhavan, D.; Nair, S. M.; Shanmugam, P.; Treesa, P. M.; Eigendorf, G. K. *Synthesis* **2002**, *2002*, 1655-1657

[36] Other example of [2+2] addition to [60]fullerene: a) Martín, N.; Altable, M.; Filippone, S.; Martín-Domenech, A.; Güell, M.; Solà, M. *Angew. Chem. Int. Ed.* **2006**, *45*, 1439-1442, b) Xiao, Z.; Matsuo, Y.; Maruyama, M.; Nakamura, E. *Org. Lett.* **2013**, *15*, 2176-2178

The reaction of C_{60} with some aryloxy- and alkoxy-ketenes led to the successful characterization of cycloaddition-products (Scheme 10). The reaction proceeds via a formal [2+2] cycloaddition, followed by enolization and acylation.[35c]

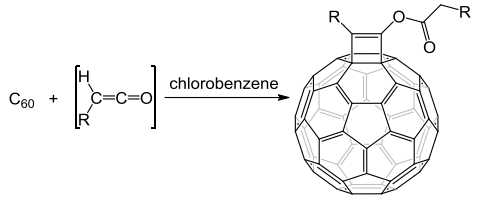

Scheme 10. [2+2] Cycloaddition of ketenes to C_{60}.

[2+1] Cycloadditions

The [2+1] cycloaddition reactions allow synthesizing compounds wherein fullerene is fused to three membered rings, among which the following stand out methanofullerenes.

These methanofullerenes can be synthesized by different methods, which can be conveniently divided into three categories. The most studied route is the thermal addition of diazocompounds, the addition of free carbenes, as well as cyclopropanation reactions which proceed by an addition/elimination mechanism, also known as Bingel reaction.

As far as the addition of diazocompounds, it was in 1991 when Wudl and co-workers reported the synthesis of the first methanofullerene by using diphenyldiazomethane.[37] The first step in this mechanism is the cycloaddition of the diazocompound as a 1,3-dipole onto a [6,6] bond of C_{60}, resulting in a pyrazoline derivative which is thermally unstable.

Photolysis of this intermediate under N_2-extrusion provides an isomeric mixture of methanofullerenes, namely [6,6]-closed ones and [5,6]-open ones.[38] In

[37] Wudl, F. *Acc. Chem. Res.* **1992**, *25*, 157-161

[38] a) Smith, A. B.; Strongin, R. M.; Brard, L.; Furst, G. T.; Romanow, W. J.; Owens, K. G.; King, R. C. *J. Am. Chem. Soc.* **1993**, *115*, 5829-5830, b) Smith, A. B.; Strongin, R. M.; Brard, L.; Furst, G. T.; Romanow, W. J.; Owens, K. G.; Goldschmidt, R. J. *J. Chem. Soc., Chem. Commun.* **1994**, 2187-2188, c) Smith, A. B.; Strongin, R. M.; Brard, L.; Furst, G. T.; Romanow, W. J.; Owens, K. G.; Goldschmidt, R. J.; King, R. C. *J. Am.*

contrast, thermolysis of the pyrazoline proceeds with high regioselectivity and yields [5,6]-open adducts almost exclusively (Scheme 11).[39,38a,c-d]

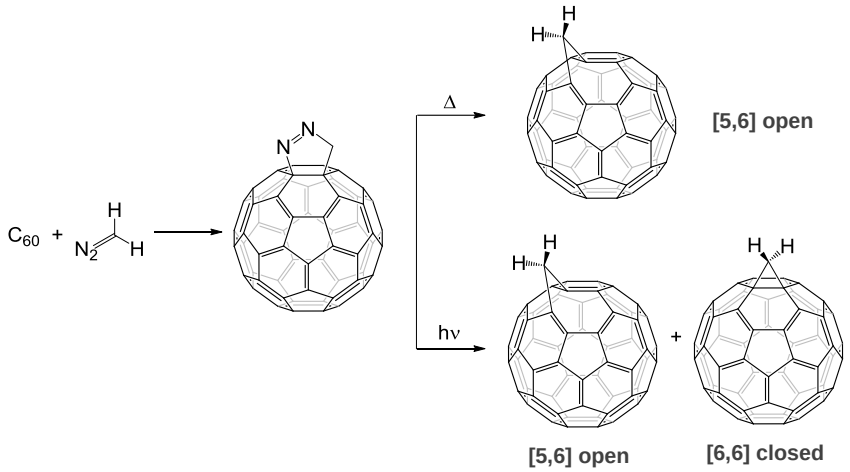

Scheme 11. Addition of diazocompounds onto C_{60}.

Concerning Bingel reaction, it occurs through the generation of a carbon nucleophile by deprotonation of α-halo esters or α-halo ketones which attack to the fullerene where an α-halocarbanion is generated. Then this anion displaces the halogen giving rise to the cyclopropane ring (Scheme 12).[40]

No doubt, Bingel reaction is among the most successful reactions in fullerenes chemistry and a wide variety of derivatives have been prepared for applications both in materials science[41] as well as in bio-medicine, particularly involving hexakis-cycloadducts.[42]

Chem. Soc. **1995**, *117*, 5492-5502, d) Haldimann, R.,F.; Klarner, F.; Diederich, F. *Chem.Commun.* **1997**, 237-238

[39] Suzuki, T.; Li, Q.; Khemani, K. C.; Wudl, F. *J. Am. Chem. Soc.* **1992**, *114*, 7301-7302

[40] Bingel, C. *Chem. Ber.* **1993**, *126*, 1957-1959

[41] a) Figueira-Duarte, T.; Clifford, J.; Amendola, V.; Gégout, A.; Olivier, J.; Cardinali, F.; Meneghetti, M.; Armaroli, N.; Nierengarten, J. *Chem. Commun.* **2006**, *0*, 2054-2056, b) Yan, W.; Seifermann, S. M.; Pierrat, P.; Bräse, S. *Org. Biomol. Chem.* **2015**, *13*, 25-54

[42] Muñoz, A.; Sigwalt, D.; Illescas, B. M.; Luczkowiak, J.; Rodríguez-Pérez, L.; Nierengarten, I.; Holler, M.; Remy, J.; Buffet, K.; Vincent, S. P.; Rojo, J.; Delgado, R.; Nierengarten, J.; Martín, N. *Nat. Chem.* **2016**, *8*, 50-57

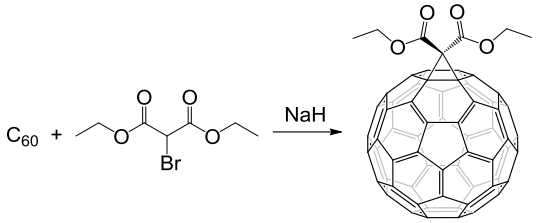

Scheme 12. Bingel reaction.

2.1.2. Hydrogenation

Fullerenes with their 30 (for C_{60}) or more strained C=C double bonds have been envisaged as very useful molecular species for hydrogen storage, being the storage capacity of, for example $C_{60}H_{36}$ 4.8%. Therefore, fullerene hydrides (or fulleranes) have been deeply studied.[43] In all the hydrogenations, mixtures of fullerene hydrides are obtained and the main product is usually $C_{60}H_{36}$, the most stable according to theoretical calculations.[44] These hydrogenated C_{60} and C_{70} derivatives have been synthesized by chemical, electrochemical and catalytic methods. Thus, $C_{60}H_{18}$ and $C_{60}H_{36}$ have been prepared by a Birch reduction,[45] which refers to a chemical process in which Li metal and liquid NH_3 in the presence of t-butanol is used to reduce the C_{60} (or C_{70}) to the monoanion C_{60}^- (or C_{70}^-), which then leads to hydrogen attachment. High levels of hydrogen attachment ($C_{60}H_{36}$ and $C_{70}H_{46}$) have also been obtained by gas-phase catalytic reactions.[46] Furthermore, these species easily undergo dehydrogenation in the presence of even very low amount of molecular oxygen.[47]

[43] a) Nossal, J.; Saini, R. K.; Alemany, L.; Meier, M.; Billups, W. E. *Eur. J. Org. Chem.* **2001**, *2001*, 4167-4180, b) Cataldo, F.; Iglesias-Grothh, S. *Fulleranes: the Hydrogenated Fullerenes*, Springer, Dordrecht, **2010**

[44] Taylor, R. *J. Chem. Soc., Perkin Trans. 2* **1994**, 2497-2498

[45] Haufler, R. E.; Conceicao, J.; Chibante, L. P. F.; Chai, Y.; Byrne, N. E.; Flanagan, S.; Haley, M. M.; O'Brien, S. C.; Pan, C.; et al *J. Phys. Chem.* **1990**, *94*, 8634-8636

[46] Talyzin, A. V.; Tsybin, Y. O.; Purcell, J. M.; Schaub, T. M.; Shulga, Y. M.; Noreus, D.; Sato, T.; Dzwilewski, A.; Sundqvist, B.; Marshall, A. G. *J. Phys. Chem. A* **2006**, *110*, 8528-8534

[47] Wang, G. W.; Li, Y. J.; Li, F. B.; Liu, Y. C. *Lett. Org. Chem.* **2005**, *2*, 595-598

2.2. Chirality in Fullerenes

In fullerenes can be distinguished different chirality classes according the origin of the chiral elements in their structures.

2.2.1. Inherently Chiral Fullerenes

Some fullerenes, despite their Csp^2 structure can present a singular form of chirality by themselves due to the particular arrangement of the carbon atoms which constitute the closed curved cage (*Inherent Chirality*). [48]

Thus, certain higher fullerenes, like D_2-C_{76} (Figure 7a) isolated and characterized in 1991, presents inherent chirality.[49] This one is the smallest all-carbon cage that satisfies both the inherent chirality and the Isolated Pentagon Rule (IPR).[10b] The chirality of D_2-C_{76} is based on the helical arrangement of the sp^2 atoms in space (Figure 7b). Moreover, other higher fullerenes such as D_3-C_{78}, D_2-C_{80}, C_2-C_{82} and D_2-C_{84} are chiral as well (Figure 8).[48a]

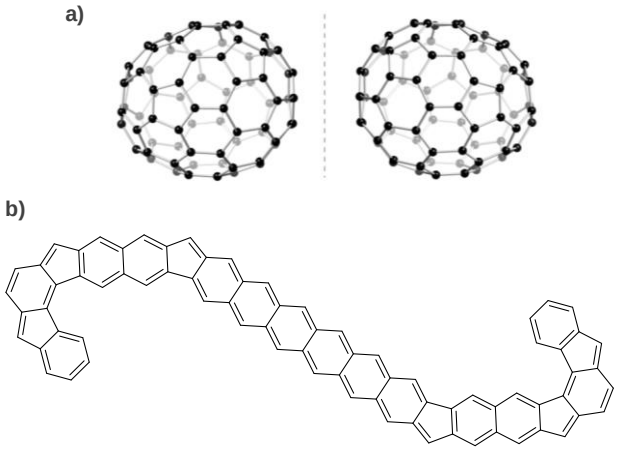

Figure 7. a) Structure of two enantiomers of the inherently chiral fullerene D_2-C_{76}. b) Helix motif of double-helical D_2-C_{76}.

[48] a) Thilgen, C.; Gosse, I.; Diederich, F. *Topics in Stereochemistry*, Chirality in Fullerene Chemistry, **2003**, b) Thilgen, C.; Diederich, F. *Chem. Rev.* **2006**, *106*, 5049-5135

[49] Ettl, R.; Chao, I.; Diederich, F.; Whetten, R. L. *Nature* **1991**, *353*, 149-153

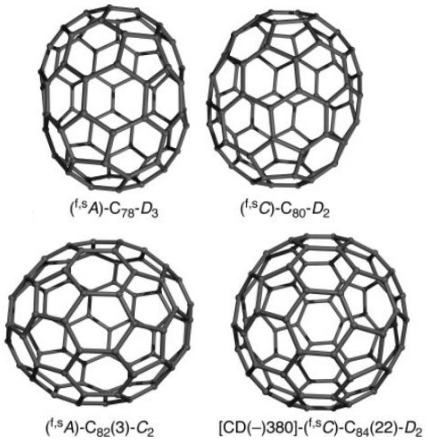

Figure 8. A selection of inherently chiral fullerenes for which certain or confident structural assignments have been possible.

2.2.2. Fullerene Derivatives with Chiral Elements in the Addends

Fullerene chirality is not limited, however, to the allotropes themselves, because it exists the possibility to prepare fullerene derivatives with residues containing chiral elements (Scheme 13).[50]

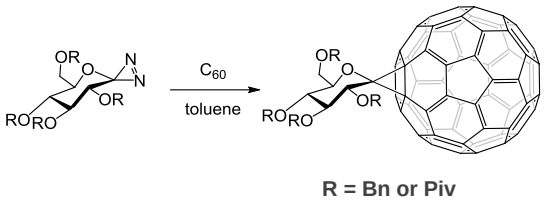

Scheme 13. Preparation of enantiomerically pure, spiro-linked *C*-Glycosides of C_{60}.

[50] Vasella, A.; Uhlmann, P.; Waldraff, C. A. A.; Diederich, F.; Thilgen, C. *Angew. Chem. Int. Ed. Engl.* **1992**, *31*, 1388-1390

2.2.3. Different Addition Patterns on Fullerene Monoadducts

As aforementioned, fullerene chirality is not limited to the allotropes themselves. Actually, the possibility to functionalize them with the suitable distribution of achiral substituents on the fullerene surface has also been accomplished.

Most common monofunctionalization pattern of [60]fullerene is the 1,2-addition in a [6,6] bond as it has already been mentioned. However, some derivatives as fullerene-fused pyrazolines and triazolines can rearrange to a [5,6] isomer, which due to the high symmetry lead to achiral molecules with C_{2v} or C_s symmetry, respectively (Figure 9a,b).

Nevertheless, many radical reactions, such as halogenations or some nucleofilic additions that involve bulky groups followed by the quenching with an electrophile occur as intrahexagonal 1,4-addition (Figure 9c). If introduced groups (*Y* and *Z*) have the same constitution and are achiral, the resulting adduct presents a C_s symmetry. However, if both groups are different, there is not any mirror plane and, therefore, the symmetry is C_1 and the derivative is termed *non-inherently chiral*.[51]

Very bulky groups can lead to a 1,6-addition pattern with occupation of positions C(1) and C(16) of C_{60}, giving rise to a C_2 symmetric derivative, which corresponds to an *inherently chiral mono-addition pattern* (Figure 9d).

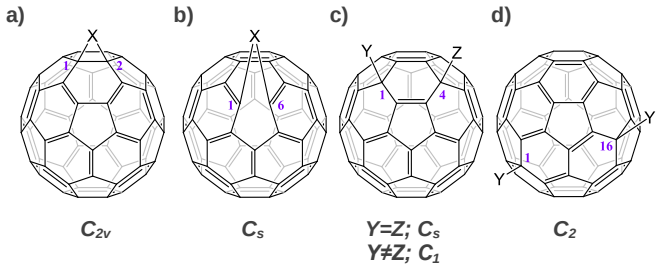

Figure 9. The most characteristic patterns of mono-addition to C_{60}. The symmetry indications are made under the assumption that the bridging addend *X* is C_{2v}-symmetric and that *Y* and *Z* are achiral.

[51] Kusukawa, T.; Ando, W. *J. Organomet. Chem.* **1998**, *561*, 109-120

On the other hand, [70]fullerene presents the same behaviour, but the symmetry decreases with increasing fullerene size. C_{70} has carbons with different degrees of pyramidalization corresponding to different degrees of the local curvature of the sphere. [6,6] Bonds are more reactive as larger is the number of pentagons around them due to the highest degree of pyramidalization (Figure 10). Nevertheless, C_{70} presents a remarkable siteselectivity in the formation of monoadducts, occurring the first addition with preference at α and after at β positions.[52]

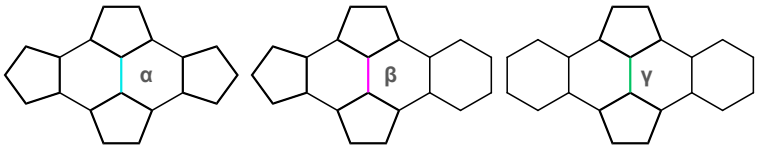

Figure 10. Different reactivity of the double bonds in higher fullerenes.

Respecting C_{70}, a *non-inherently chiral addition pattern* occurs with C_s-symmetric addends bridging the carbon atoms in β position (Figure 11).[53]

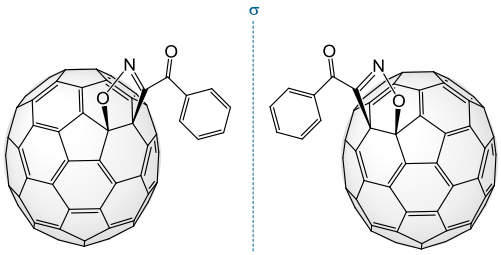

Figure 11. C_{70}-adducts with a non-inherently chiral addition pattern in β-position.

The most common α addition pattern, on the other hand, is achiral with both types of addends, C_{2v}- or C_s-symmetric, but it can give rise to constitutional isomers (regioisomers) with C_s-symmetric addends (Figure 12).

[52] Hawkins, J. M.; Meyer, A.; Solow, M. A. *J. Am. Chem. Soc.* **1993**, *115*, 7499-7500
[53] Kraszewska, A.; Rivera-Fuentes, P.; Thilgen, C.; Diederich, F. *New J. Chem.* **2009**, *33*, 386-396

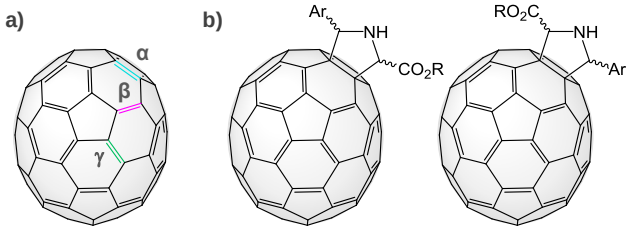

Figure 12. Site- and regioselectivity in C_{70}.

2.2.4. Inherently Chiral Addition Patterns on [60]Fullerene Bisadducts

Considering only C_{2v}-symmetrical addends linked to [6,6] bonds by 1,2-addition, eight possible relative arrangements of addends can be formed for bisadducts derivatives. The different addition patterns are described as *cis*-1, *cis*-2, or *cis*-3, when the second addend is located in the same hemisphere, and as *trans*-1, *trans*-2, *trans*-3, or *trans*-4, when they are located in opposite hemispheres. If the second addend resides at the equator with respect to the first, the addition pattern is termed *e* (Figure 13).[54]

If both addends are identical, among these regioisomers, *cis*-3, *trans*-2, and *trans*-3 will present C_2 symmetry and therefore they will be inherently chiral. If, on the other hand, both addends are different, the symmetry of the bisadducts will be lowered to C_1, being non-inherently chiral, except for *trans*-1 whose symmetry will be C_{2v}, and for the *e* adduct which will keep its C_s symmetry.

In case of trisadducts which present the three addends in (*e*,*e*,*e*) and (*trans*-3,*trans*-3,*trans*-3) positions with C_3 and D_3 symmetry, respectively, also present an *inherently chiral addition pattern* (Figure 14).[55]

[54] a) Hirsch, A.; Lamparth, I.; Karfunkel, H. R. *Angew. Chem. Int. Ed. Engl.* **1994**, *33*, 437-438, b) Nishimura, T.; Tsuchiya, K.; Ohsawa, S.; Maeda, K.; Yashima, E.; Nakamura, Y.; Nishimura, J. *J. Am. Chem. Soc.* **2004**, *126*, 11711-11717

[55] Gross, B.; Schurig, V.; Lamparth, I.; Herzog, A.; Djojo, F.; Hirsch, A. *Chem. Commun.* **1997**, *0*, 1117-1118

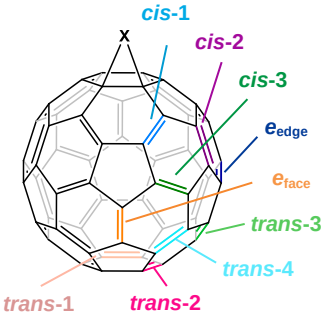

Regio-isomer	Locants	Symmetry (identical addends)	Symmetry (different addends)
cis-**1**	1,2:3,4	C_S	C_1
cis-**2**	1,2:7:21	C_S	C_1
cis-**3**	1,2:16,17	C_2	C_1
e	1,2:18,36	C_S	C_S
trans-**4**	1,2:34,35	C_S	C_1
trans-**3**	1,2:33,50	C_2	C_1
trans-**2**	1,2:51,52	C_2	C_1
trans-**1**	1,2:55,60	D_{2h}	C_{2v}

Figure 13. The possible bisadduct regioisomers resulting from twofold addition of identical, C_{2v}-symmetric addends to C_{60}.

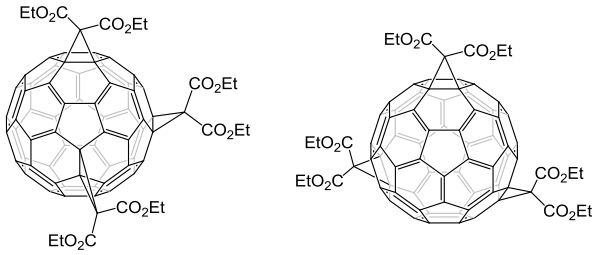

***C*3 (*e*,*e*,*e*)** ***D*3 (*trans*-3,*trans*-3,*trans*-3)**

Figure 14. [60]fullerene trisadducts derivatives with inherently chiral addition pattern.

2.2.5. Asymmetric induction by addition of chiral addends onto fullerenes

A most interesting topic in fullerenes chirality is the functionalization with generation of new stereogenic elements in the addends. There are some types of addition reactions onto [60]fullerene that proceed with the creation of new stereogenic centers. Depending on the addends and their stereochemistry, they can influence the stereoselectivity of these reactions. Thus, the control of stereoselectivity is an issue of paramount importance.

Actually, only relatively few examples based on the use of chiral starting materials have been reported.[56]

In 1996, Maggini, Prato, Bianco and coworkers described the diastereoselective cycloaddition of bulky chiral azomethine ylides derived from (+)-2,3-*O*-isopropylidene-D-glyceraldehyde (Scheme 14).[57]

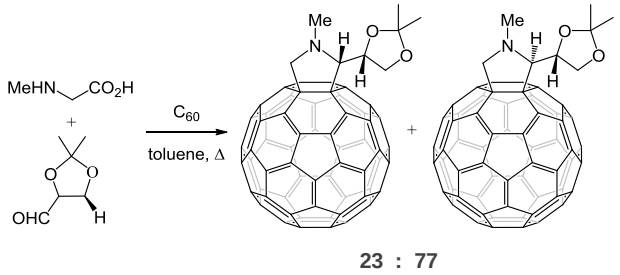

Scheme 14. Diastereoselective addition reaction of bulky chiral reagents onto C_{60}.[56c]

Also, these authors have prompted reaction morpholin-2-one with paraformaldehyde in toluene at reflux in the presence of C_{60}. The reaction proceeded affording a mixture of two products in a 6:94 ratio (Scheme 15).[56a]

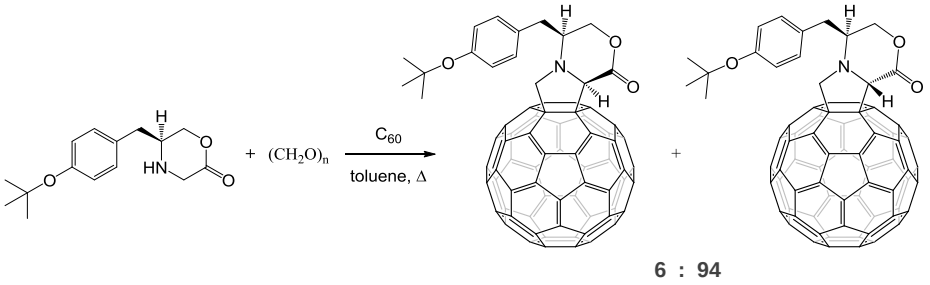

Scheme 15. Diastereoselective synthesis of pyrrolidino[60]fullerene by cycloaddition of morpholine derivative.

[56] a) Bianco, A.; Maggini, M.; Scorrano, G.; Toniolo, C.; Marconi, G.; Villani, C.; Prato, M. *J. Am. Chem. Soc.* **1996**, *118*, 4072-4080, b) Nierengarten, J. F.; Gramlich, V.; Cardullo, F.; Diederich, F. *Angew. Chem. Int. Ed. Engl.* **1996**, *35*, 2101-2103, c) Guerra, S.; Schillinger, F.; Sigwalt, D.; Holler, M.; Nierengarten, J. *Chem. Commun.* **2013**, *49*, 4752-4754

[57] Novello, F.; Prato, M.; Da Ros, T.; De Amici, M.; Bianco, A.; Toniolo, C.; Maggini, M. *Chem. Commun.* **1996**, *0*, 903-904

Our research group reports the first high diastereoselective synthesis of fulleropyrrolidines endowed with diastereomerically pure substituted cyclobutanes. They found that the high stereoselectivity achieved in this reaction was due to energy barrier differences of about 4 kcal mol^{-1}, due to the steric hindrance caused by the bulky organic addend attached to the 1,3-dipole (Scheme 16).[58]

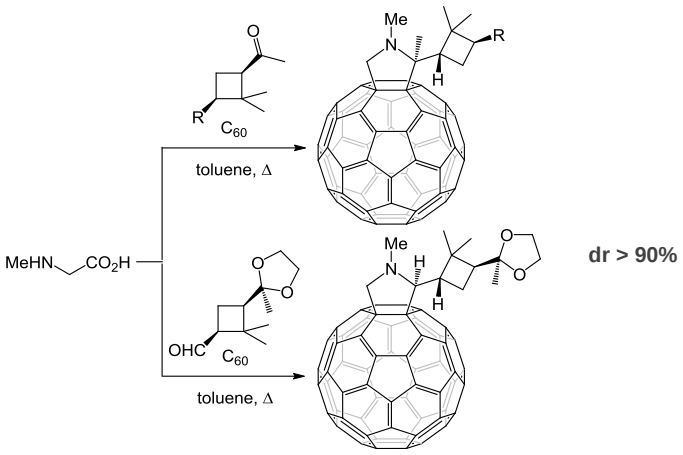

Scheme 16. High diastereoselectivity in cycloaddition reactions of enantiopure azomethine ylides onto C_{60}.

2.2.6. Asymmetric catalysis onto fullerenes

The non-coordinating nature of fullerenes has made difficult the use of asymmetric metal catalysis and, therefore, the synthesis of enantiopure fullerene derivatives has been limited to a few examples or expensive and highly time-consuming HPLC separations.[59]

In this respect, our research group introduced in a pioneering manner the chiral activation of a 1,3-dipole in the cycloaddition of *N*-metalated azomethine ylides onto C_{60} by the introduction of asymmetric metal catalysis. Thus pyrrolidinofullerenes with control of the absolute configuration of the created stereogenic centers were obtained, which represented a first and significant breakthrough.

[58] Illescas, B. M.; Martín, N.; Poater, J.; Solà, M.; Aguado, G. P.; Ortuno, R. M. *J. Org. Chem.* **2005**, *70*, 6929-6932
[59] Djojo, F.; Hirsch, A. *Chem. Eur. J.* **1998**, *4*, 344-356

The employ of transition metals and the suitable ligand makes that the cycloaddition of α-iminoesters take place under very mild conditions, affording pyrrolidinofullerenes with a complete control of diastereo- and enantioselectivity, with enantiomeric excesses from 70 to 97% (Scheme 17).

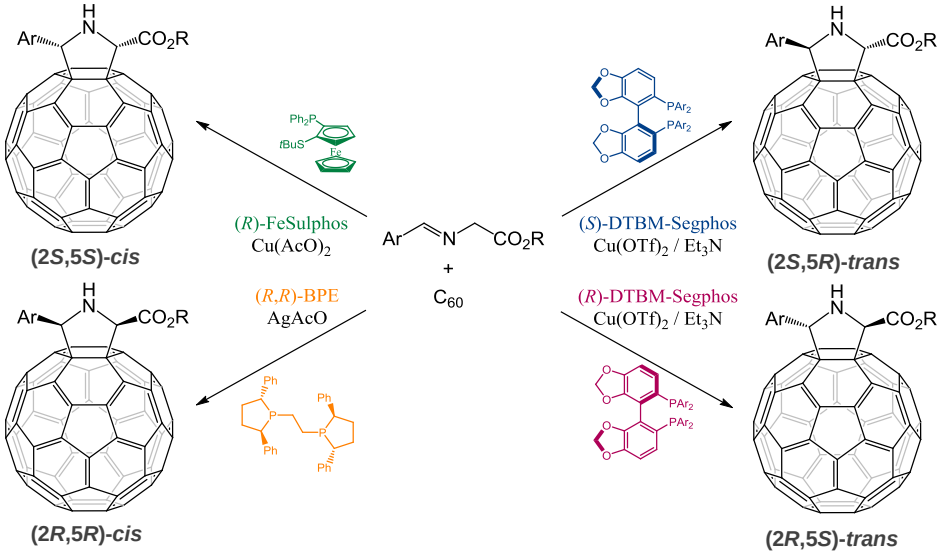

Scheme 17. Complete stereocontrol in the cycloaddition of α-iminoesters onto [60]fullerene

The authors reported that chiral complex formed by copper(II) acetate and (*R*)-FeSulPhos led to the formation of (2*S*,5*S*)-*cis* pyrrolidinofullerenes, whereas the use of silver acetate and chiral (*R*,*R*)-BPE ligand reverses the enantioselectivity toward (2*R*,5*R*)-*cis* pyrrolidinofullerene enantiomers.[60]

Soon after, a fully stereodivergent synthesis of all the possible stereoisomers by using of the complex Cu(II) triflate/(*R*)- or (*S*)-DTBM-Segphos, that addreses the cycloaddition towards both enantiomers of the *trans* pyrrolidino[60]fullerenes with high enantiomeric excess, was achieved.[61]

[60] Filippone, S.; Maroto, E. E.; Martín-Domenech, Á; Suárez, M.; Martín, N. *Nat. Chem.* **2009**, *1*, 578-582
[61] Maroto, E. E.; Filippone, S.; Martín-Domenech, Á; Suárez, M.; Martín, N. *J. Am. Chem. Soc.* **2012**, *134*, 12936-12938

This methodology was extended to C_{70} providing the corresponding pyrrolidino[70]fullerenes with an almost complete siteselectivity toward the most reactive [6,6] bonds, α position, and good levels of regioselectivity since the dipoles are unsymmetrical. The latter is due to the fact that the complexes used afforded the pyrrolidines bearing methoxycarbonyl group in the polar region of C_{70} as major product (Scheme 18). Finally, for this regioisomer all four possible stereoisomers were obtained depending on the used metal chiral complex with high values of diastereo- and enantioselectivity.

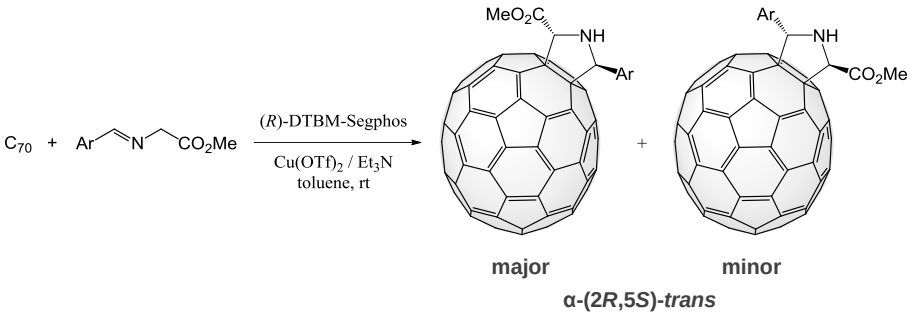

Scheme 18. High stereocontrol on the synthesis of pyrrolidino[70]fullerenes.

Furthermore, asymmetric catalysis were also employed for obtaining chiral endohedral fullerenes such as La@C_{72}($C_6H_3Cl_2$),[62] H_2@C_{60},[63] H_2O@C_{60}[64] and HF@C_{60}.[65]

Other 1,3-dipoles studied in our group have been the azlactones (oxazol-5-(4H)-ones) whose cycloaddition onto C_{60} provides pyrrolino[60]fullerenes. This reaction can be developed stereoselectively by using two different asymmetric activations of azlactones.[66]

[62] Sawai, K.; Takano, Y.; Izquierdo, M.; Filippone, S.; Martín, N.; Slanina, Z.; Mizorogi, N.; Waelchli, M.; Tsuchiya, T.; Akasaka, T.; Nagase, S. *J. Am. Chem. Soc.* **2011**, *133*, 17746-17752
[63] Maroto, E. E.; Izquierdo, M.; Murata, M.; Filippone, S.; Komatsu, K.; Murata, Y.; Martín, N. *Chem. Commun.* **2014**, *50*, 740-742
[64] Maroto, E. E.; Mateos, J.; García-Borràs, M.; Osuna, S.; Filippone, S.; Herranz, M. Á; Murata, Y.; Solà, M.; Martín, N. *J. Am. Chem. Soc.* **2015**, *137*, 1190-1197
[65] Vidal, S.; Izquierdo, M.; Alom, S.; Garcia-Borràs, M.; Filippone, S.; Osuna, S.; Solà, M.; Whitby, R. J.; Martín, N. *Chem. Commun.* **2017**, *53*, 10993-10996
[66] Marco-Martínez, J.; Reboredo, S.; Izquierdo, M.; Marcos, V.; López, J. L.; Filippone, S.; Martín, N. *J. Am. Chem. Soc.* **2014**, *136*, 2897-2904

This work describes the employ of catalysts based on the combination of nonprecious metals with easily available chiral phosphines (Scheme 19) and on an organocatalytic methodology in the reaction onto fullerenes as well as conventional double bonds (Scheme 20).

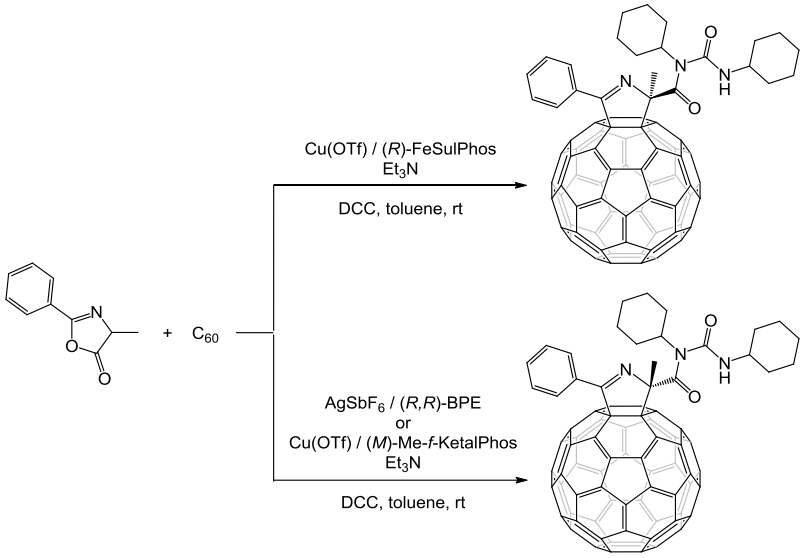

Scheme 19. Metal-catalyzed enantioselective [3+2] cycloaddition of azlactones onto C_{60}.

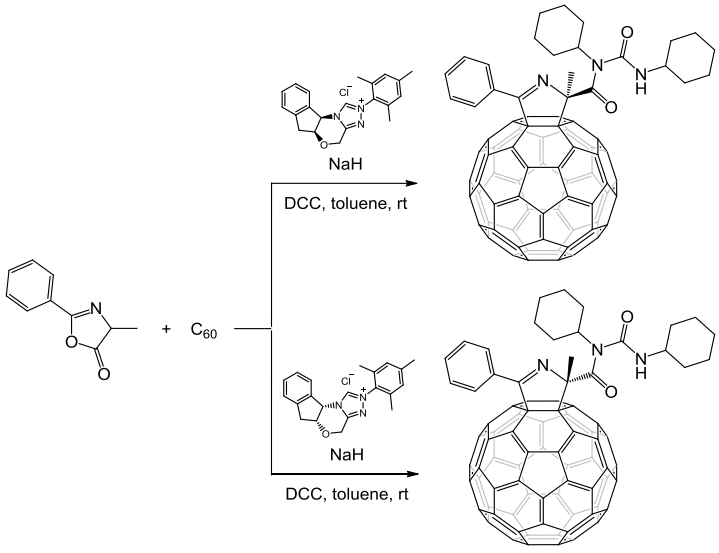

Scheme 20. Organocatalytic enantioselective [3+2] cycloaddition of azlactones onto C_{60}

In this case, since azlactones are monodentate ligand, unlike the α-iminosteres that are bidentate. Therefore, it is necessary to change the acetate counterion for other less-coordinating nonbasic such as hexafluoroantimonate or triflate to promote a tighter interaction between the metal and the monodentate azlactone.

In this organocatalytic methodology, *N*-heterocyclic carbenes (NHC´s) are employed as Brønsted base catalysts to obtain pyrrolino[60]fullerene derivatives with good enantiomeric excesses.[66]

In this regard, another organocatalytic protocol has also been studied in our group by using nucleophilic phosphines as covalent organocatalysts in the

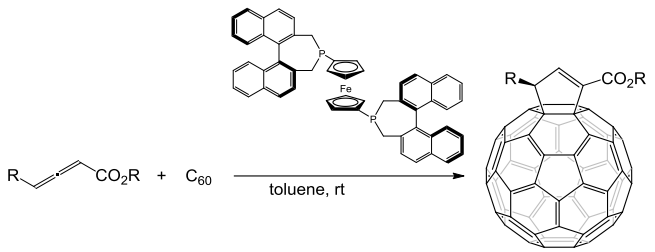

Scheme 21. Chiral phosphine-catalyzed [3+2] cycloaddition of allenoates to [60]fullerene.

cycloaddition of 2,3-butadienoates (allenoates) onto [60]fullerene (Scheme 21).[67] Previously, Kroto and co-workers had reported the racemic cycloaddition reaction of 2,3-butadienoates (allenoates) or 2-butynoates (alkynoates) to C_{60}.[68]

Phosphines are Lewis bases and highly versatile reagents as a consequence of the ability to vary their nucleophilic nature by modifying the steric and electronic features of their substituents as well as their commercial availability and efficiency in the synthesis of a wide range of cyclic and acyclic compounds.

This reaction is based on Lu's cycloaddition[69] that is an efficient synthesis of cyclopentene rings from electron-deficient olefins and simple 2,3-butadienoates or 2-butynoates as the three-carbon moiety under the catalysis of a phosphine. When these allenoates are activated by nucleophilic attack by phosphine on the

[67] Marco-Martínez, J.; Marcos, V.; Reboredo, S.; Filippone, S.; Martín, N. *Angew. Chem. Int. Ed.* **2013**, *52*, 5115-5119
[68] O'Donovan, B. F.; Hitchcock, P. B.; Meidine, M. F.; Kroto, H. W.; Taylor, R.; Walton, D. R. M. *Chem. Commun.* **1997**, *0*, 81-82
[69] Zhang, C.; Lu, X. *J. Org. Chem.* **1995**, *60*, 2906-2908

central sp-hybridized carbon atom, they are able to react with electron-deficient olefins.

The absolute configuration of many of these derivatives could be assigned by a "Sector Rule" that was proposed for chiral fullerenes, for the first time, by Wilson *et al*[70] and corrected by our group.[24] It is based on the circular dichroism

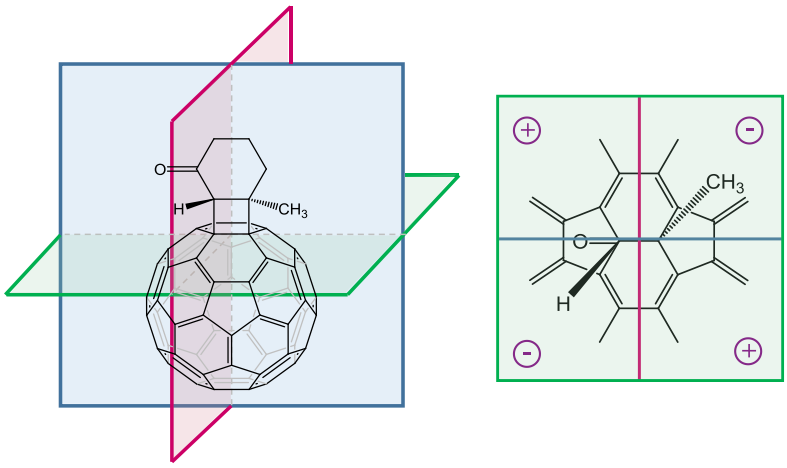

Figure 15. Sector rule for C_{60} derivatives.

(CD) spectra of optically active fullerene where the achiral fullerene chromophore is perturbated by the chiral elements in the addend. This rule relates the CD contribution associated with the ~430 nm absorption band, fingerprint for [6-6] monosubstitution, with a model entailing three orthogonal planes intersecting at the center of the [6,6] bond (Figure 15). Location of atoms in + or - sectors defines the sign of the Cotton effect at 430 nm which is used to determine the absolute configuration of attached groups.

2.3. Chirality and optoelectronic properties

In the case of small-molecules, the influence of chirality in properties has been studied. For instance, different enantiomeric excesses (for example, racemic versus enantiopure) of a chiral organic electronic material will have exactly the same molecular properties but very different material properties. Hence,

[70] Wilson, S. R.; Lu, Q.; Cao, J.; Wu, Y.; Welch, C. J.; Schuster, D. I. *Tetrahedron* **1996**, *52*, 5131-5142

modifying the efficiency of chiral organic materials could be carried out through alteration of the chiral composition without making changes to their molecular structure.

In 2006, Pu and co-workers studied, for the first time, the conductivity of oligo(arylene-ethynylene) containing a chiral 1,1´-binaphthyl unit (Figure 16).

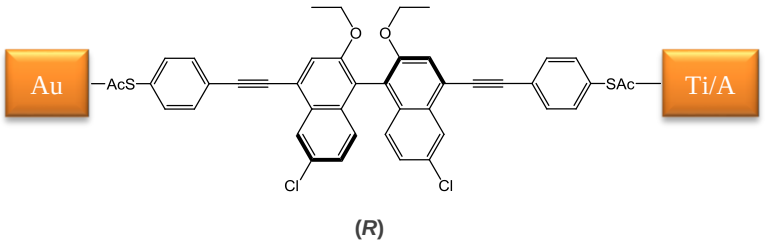

Figure 16. Optically active molecular electronic wire in the device.

They found that devices assembled from enantiopure materials exhibited currents up to ≈80-fold larger than those assembled from racemic.[71]

In this regard, enantiopure and racemic form of the same compounds may have different properties in the solid state, in particular electronic conductivity. This fact has been reported for tetrathiafulvalene (TTF) derivatives and, recently, on azaboradibenzo-[6]helicenes.

In the case of TTF derivatives,[72] the studied compounds are obtained by electrocrystallization experiments, mixing equimolar amounts of TTF compounds (racemic or pure enantiomers), in chloroform solutions with $[(n\text{-}Bu)_4N]AsF_6$ or $[(n\text{-}Bu)_4N]PF_6$, which resulted in salts formulated as or (TTF derivative)$_2AsF_6$ or (TTF derivative)$_2PF_6$, respectively. In the example of the TTF-Oxazoline derivatives (Figure 17a)[72a], racemic and enantiopure salts present metallic behaviour, although the pure enantiomer one higher conductivity. However, for the dimethyl-ethylenedithio-TTF derivatives (Figure 17b)[72b], single crystal conductivity measurements indicate semiconducting behaviour for the enantiopure salts, while the racemic one is metallic down to

[71] Zhu, Y.; Gergel, N.; Majumdar, N.; Harriott, L. R.; Bean, J. C.; Pu, L. *Org. Lett.* **2006**, *8*, 355-358

[72] a) Réthoré, C.; Avarvari, N.; Canadell, E.; Auban-Senzier, P.; Fourmigué, M. *J. Am. Chem. Soc.* **2005**, *127*, 5748-5749, b) Pop, F.; Auban-Senzier, P.; Frąckowiak, A.; Ptaszyński, K.; Olejniczak, I.; Wallis, J. D.; Canadell, E.; Avarvari, N. *J. Am. Chem. Soc.* **2013**, *135*, 17176-17186

120 K at ambient. This is the first case where the racemic salt is more conducting than the enantiopure compounds.

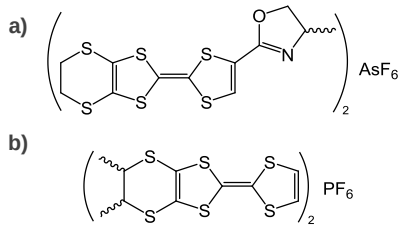

Figure 17. TTF derivatives structures. a) TTF-Oxazoline and b) dimethyl-ethylenedithio-TTF.

For the azaboradibenzo[6]helicene compounds (Figure 18),[73] Nakamura and co-workers have observed that the racemate is a good p-type semiconductor while the enantiopure form is a good n-type semiconductor. This carrier inversion could be accounted for by the different packing structures of the hetero- and homochiral crystals.

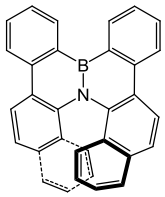

Figure 18. Structure of the azadibenzo[6]helicene.

Furthermore, the chirality effects on the conductive properties has also been studied in aza[6]helicenes (Figure 19).[74] The results agree with the previously mentioned work, observing significant changes in morphology, photophysics, and device performance depending on whether racemic or enantiopure form is used. For these compounds, hole mobility in the freshly prepared devices is over 80-fold greater for the racemic than for the enantiopure compound. After 7 days, these devices show an enhancement in mobility although the effect is more

[73] Hatakeyama, T.; Hashimoto, S.; Oba, T.; Nakamura, M. *J. Am. Chem. Soc.* **2012**, *134*, 19600-19603

[74] Yang, Y.; Rice, B.; Shi, X.; Brandt, J. R.; Correa, d. C.; Hedley, G. J.; Smilgies, D.; Frost, J. M.; Samuel, I. D. W.; Otero-de-la-Roza, A.; Johnson, E. R.; Jelfs, K. E.; Nelson, J.; Campbell, A. J.; Fuchter, M. J. *ACS Nano* **2017**, *11*, 8329-8338

pronounced for the enantiomeric material, a 30-fold increase, while in the racemic one, only a 1.4-fold increase was observed.

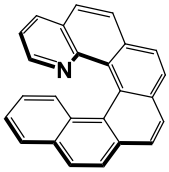

Figure 19. Structure of the aza[6]helicene.

This effect has also been reported in organic photovoltaic devices (OPVs) by Favereau, Blanchard, Cabanetos, Crassous and co-workers. These devices are constituted by polymer poly(3-hexylthiophene) (P3HT) blended with a chiral helicene additive; enantiopure additives showed a fivefold higher power conversion efficiency than racemic additives (Figure 20).[75]

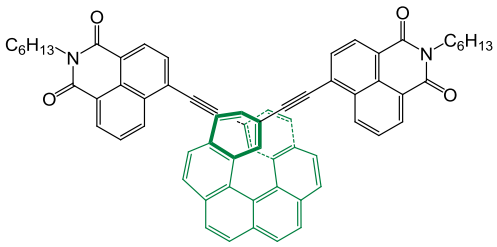

Figure 20. Enentiopure naphthalimide end-capped helicene compounds for OPVs.

Another work that shows the chirality influence on the materials properties was published by Oh and co-workers.[76] They showed that the homochiral nanomaterials exhibit superior charge transport with better electrical performance in organic phototransistors (OPTs) and highly selective detection of circularly polarized light (chiroptical sensing), for the first time, in visible spectral range. However, when the compound was racemic, chiral self-discrimination was observed with the formation of heterochiral nanomaterials leading to completely different optoelectrical properties (Figure 21).

[75] Josse, P.; Favereau, L.; Shen, C.; Dabos-Seignon, S.; Blanchard, P.; Cabanetos, C.; Crassous, J. *Chem. Eur. J.* **2017**, *23*, 6277-6281

[76] Xiaobo, S.; Inho, S.; Hiroyoshi, O.; Lee, Y. H.; Tianming, Z.; Tatsuhiro, K.; Hyung, J. J.; Masaki, K.; Oh, J. H. *Adv. Mater.* **2017**, *29*, 1605828

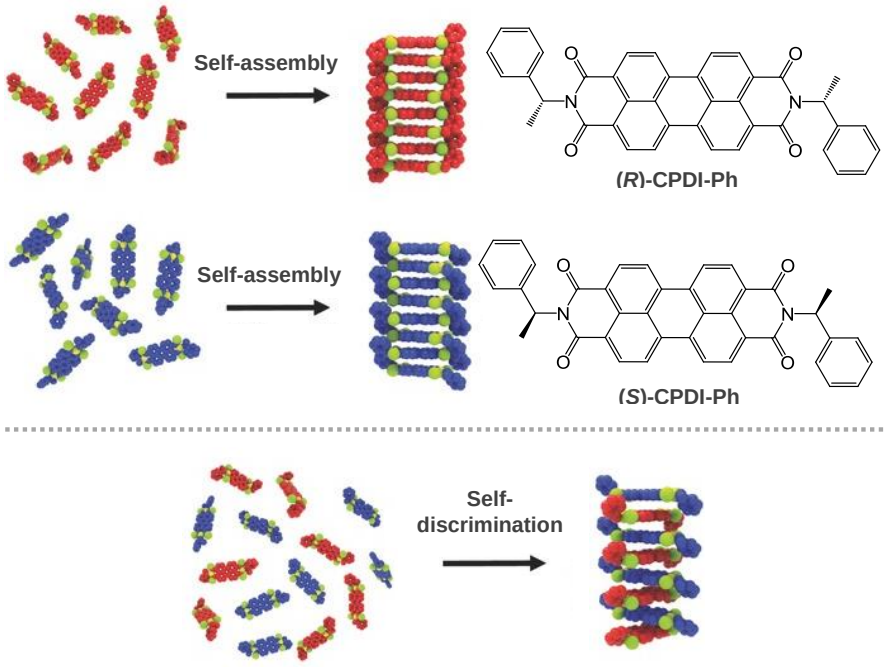

Figure 21. Schematic illustration of self-assembly and chemical structures perylene diimides.

In this respect, how chirality modifies the electronic properties of the carbon-based nanostructures is still an open question. In particular, chiral fullerene derivatives have been shown to be important motifs in materials science,[54b,77] where the solid morphology can be influenced by the presence of stereogenic centers,[78] as well as in biomedicine,[79] where the biologic response can depend on a certain enantiomer. Both aspects represent currently most important challenges in science.

An example, in which an intrinsic property is dependent on the chirality, has been published by Aida et al in 2010.[78]

[77] Ohsawa, S.; Maeda, K.; Yashima, E. *Macromolecules* **2007**, *40*, 9244-9251
[78] Hizume, Y.; Tashiro, K.; Charvet, R.; Yamamoto, Y.; Saeki, A.; Seki, S.; Aida, T. *J. Am. Chem. Soc.* **2010**, *132*, 6628-6629
[79] a) Friedman, S. H.; Ganapathi, P. S.; Rubin, Y.; Kenyon, G. L. *J. Med. Chem.* **1998**, *41*, 2424-2429, b) Zhu, Z.; Schuster, D. I.; Tuckerman, M. E. *Biochemistry* **2003**, *42*, 1326-1333

In this work, they demonstrated that chirality affects the supramolecular structure of a donor-acceptor dyad (D-A dyad) composed by fullerene and porphyrin (Figure 22a) which is able to transport charge carriers. In this case, the racemic dyad shaped sized spheres with an average diameter of 300 nm (Figure 22c) while the enantiopure one was self-assemble, under identical conditions, bundles of very long nanofibers up to 10 μm (Figure 22b). Thus, the intrinsic charge-carrier mobility nanofiber obtained from enantiopure dyad was estimated to be 1 order of magnitude greater than that in the sphere from the racemic one (Figure 22d).

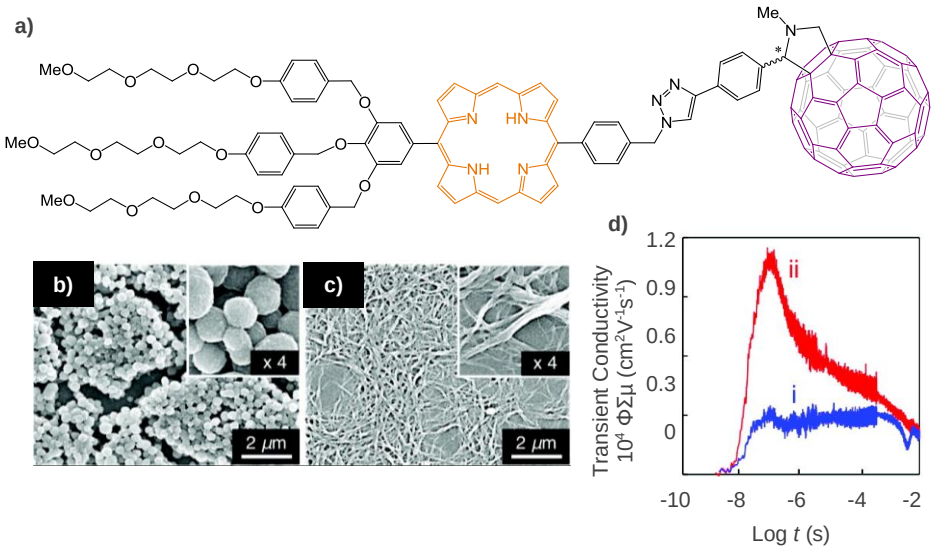

Figure 22. a) Molecular structure of fullerene-porphyrin dyad. SEM micrographs of cast films of assembled (b) racemic dyad and (c) enantiopure dyad. d) FP-TRMC profiles at 16°C upon photoexcitation with a 355-nm laser pulse of (i) racemic dyad and (ii) enantiopure dyad.

2.4. Metal-fullerene hybrids

Within fullerenes chemistry, transition metal-fullerene hybrids represent a broad class of derivatives with potential interesting properties.

Indeed, the presence in the same compound of a fullerene and a transition metal complex can lead to the emergence of new properties or to the modification of

those already known, stemming from the electron-donating character and catalytic activity of transition metals. [80]

There are different kind of complexes consisting of fullerenes with transition metals:

a) Coordination complexes with the metal directly attached to one or more of the fullerene double bonds (Figure 23a). Many examples of these complexes have been described with various metals: platinum,[81] palladium,[82] rhodium,[83] iridium,[84] molybdenum,[85] osmium,[86] ruthenium,[87] iron[88] or tungsten.[89]
b) Compounds in which the metal center is coordinated to a metal binding moiety attached to the fullerene through the formation of covalent bonds (Figure 23b).[90]

[80] Balch, A. L.; Olmstead, M. M. *Chem. Rev.* **1998**, *98*, 2123-2166
[81] a) Fagan, P. J.; Calabrese, J. C.; Malone, B. *Science* **1991**, *252*, 1160-1161, b) Song, L.; Wang, G.; Liu, P.; Hu, Q. *Organometallics* **2003**, *22*, 4593-4598, c) Song, L.; Yu, G.; Su, F.; Hu, Q. *Organometallics* **2004**, *23*, 4192-4198
[82] a) Nagashima, H.; Nakaoka, A.; Saito, Y.; Kato, M.; Kawanishi, T.; Itoh, K. *J. Chem. Soc., Chem. Commun.* **1992**, *0*, 377-379, b) Song, L.; Yu, G.; Wang, H.; Su, F.; Hu, Q.; Song, Y.; Gao, Y. *Eur. J. Inorg. Chem.* **2004**, *2004*, 866-871, c) Song, L.; Su, F.; Hu, Q.; Grigiotti, E.; Zanello, P. *Eur. J. Inorg. Chem.* **2006**, *2006*, 422-429
[83] a) Balch, A. L.; Lee, J. W.; Noll, B. C.; Olmstead, M. M. *Inorg. Chem.* **1993**, *32*, 3577-3578, b) Usatov, A. V.; Kudin, K. N.; Vorontsov, E. V.; Vinogradova, L. E.; Novikov, Y. N. *J. Organomet. Chem* **1996**, *522*, 147-153
[84] a) Balch, A. L.; Catalano, V. J.; Lee, J. W. *Inorg. Chem.* **1991**, *30*, 3980-3981, b) Balch, A. L.; Catalano, V. J.; Lee, J. W.; Olmstead, M. M.; Parkin, S. R. *J. Am. Chem. Soc.* **1991**, *113*, 8953-8955, c) Balch, A. L.; Ginwalla, A. S.; Lee, J. W.; Noll, B. C.; Olmstead, M. M. *J. Am. Chem. Soc.* **1994**, *116*, 2227-2228, d) Usatov, A.; Martynova, E.; Dolgushin, F.; Peregudov, A.; Antipin, M.; Novikov, Y. *Eur. J. Inorg. Chem.* **2002**, *2002*, 2565-2567
[85] Thompson, D.; Jones, M.; Baird, M. *Eur. J. Inorg. Chem.* **2003**, *2003*, 175-180
[86] Song, H.; Lee, K.; Park, J. T.; Choi, M. *Organometallics* **1998**, *17*, 4477-4483
[87] a) Lee, K.; Hsu, H.; Shapley, J. R. *Organometallics* **1997**, *16*, 3876-3877, b) Guldi, D. M.; Rahman, G. M. A.; Marczak, R.; Matsuo, Y.; Yamanaka, M.; Nakamura, E. *J. Am. Chem. Soc.* **2006**, *128*, 9420-9427
[88] Sawamura, M.; Kuninobu, Y.; Toganoh, M.; Matsuo, Y.; Yamanaka, M.; Nakamura, E. *J. Am. Chem. Soc.* **2002**, *124*, 9354-9355
[89] Song, L.; Liu, J.; Hu, Q.; Weng, L. *Organometallics* **2000**, *19*, 1643-1647
[90] a) Maggini, M.; Karlsson, A.; Scorrano, G.; Sandonà, G.; Farnia, G.; Prato, M. *J. Chem. Soc., Chem. Commun.* **1994**, *0*, 589-590, b) Iyoda, M.; Sultana, F.; Sasaki, S.; Butenschön, H. *Tetrahedron Lett.* **1995**, *36*, 579-582, c) Guldi, D. M.; Maggini, M.;

c) Cocrystallates, host−guest inclusion complexes and fulleride salts in which pristine fullerene and metal species are bound by noncovalent interactions such as van der Waals or electrostatic forces (Figure 23c).[91]

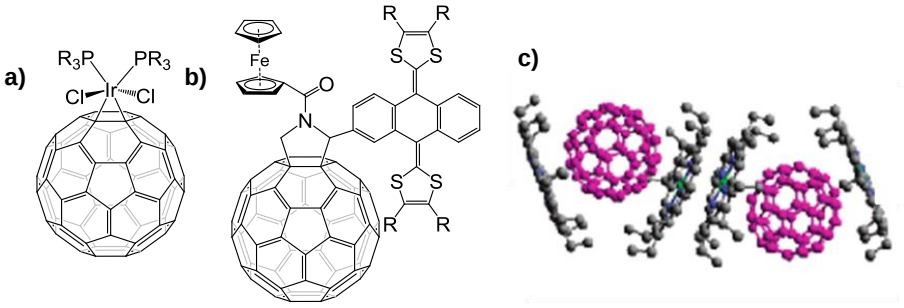

Figure 23. a) Addition of a transition metal complex to a double bond of [60]fullerene; b) addition of metal complex ligands by a binding moiety attached to [60]fullerene and c) cocrystallates of a [60]fullerene-metalloporphyrin.

In a previous work of our group, new chiral fullerene hybrids endowed with different stereogenic metals have been synthesized by asymmetric [3+2] cycloaddition of α-iminoesters onto [60]fullerene, *tert*-butyl ester hydrolysis and subsequent complexation with metal to obtain a half-sandwich complex (Scheme 22).[24,92]

As the result of the complexation of the pyrrolidino[60]fullerene carboxylate with the iridium complex, two additional stereocenters are formed. One of them on the nitrogen atom due to its quaternization in the complexation process and the other one on the metallic center, as it adopts a pseudooctahedral configuration.

Scorrano, G.; Prato, M. *J. Am. Chem. Soc.* **1997**, *119*, 974-980, d) Herranz, M. Á; Illescas, B.; Martín, N.; Luo, C.; Guldi, D. M. *J. Org. Chem.* **2000**, *65*, 5728-5738

[91] a) Crane, J. D.; Hitchcock, P. B.; Kroto, H. W.; Taylor, R.; Walton, D. R. M. *J. Chem. Soc., Chem. Commun.* **1992**, *0*, 1764-1765, b) Crane, J. D.; Hitchcock, P. B. *J. Chem. Soc., Dalton Trans.* **1993**, *0*, 2537-2538, c) Olmstead, M. M.; Costa, D. A.; Maitra, K.; Noll, B. C.; Phillips, S. L.; Van Calcar, P. M.; Balch, A. L. *J. Am. Chem. Soc.* **1999**, *121*, 7090-7097, d) Boyd, P. D. W.; Reed, C. A. *Acc. Chem. Res.* **2005**, *38*, 235-242

[92] Marco-Martínez, J.; Vidal, S.; Fernández, I.; Filippone, S.; Martín, N. *Angew. Chem. Int. Ed.* **2017**, *56*, 2136-2139

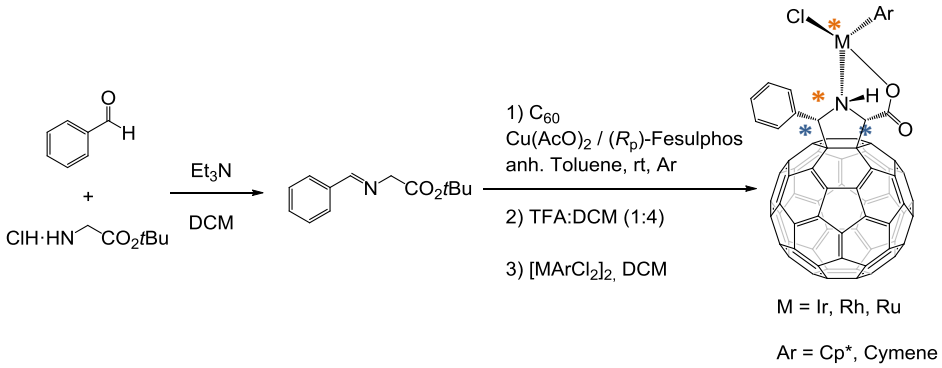

Scheme 22. Synthesis of chiral hybrids metal-fullerenes.

In this special case, in which iridium is coordinated with a fullerene ligand, only one of the epimers of the iridium atom is observed, which is in contrast to that observed for related complexes based on a prolinate ligand (Figure 24).[93]

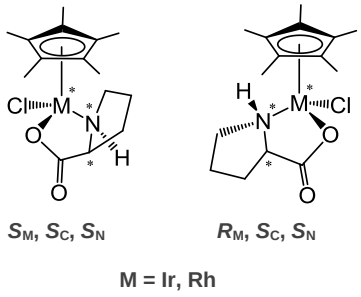

Figure 24. Epimers of the iridium-prolinate complex.

Thus, it has been observed that the configuration of the nitrogen depends on the *C*2-pyrrolidine stereochemistry, what is to say that the iridium atom is located on the same side as the carboxylate due to the formation of the chelate complex. On the other hand, despite the iridium center can adopt two different configurations, only one product has been isolated, that which presents the chlorine atom to the opposite side of the aromatic ring in the pyrrolidine. The stability of this diastereomer is explained by a strong repulsive interaction

[93] a) Carmona, D.; Lamata, M. P.; Viguri, F.; San José, E.; Mendoza, A.; Lahoz, F. J.; García-Orduña, P.; Atencio, R.; Oro, L. A. *J. Organomet. Chem.* **2012**, *717*, 152-163, b) Bauer, W.; Prem, M.; Polborn, K.; Karlheinz, S.; Steglich, W.; Beck, W. *Eur. J. Inorg. Chem.* **1998**, *1998*, 485-493

between the lone-pair of the chloride ligand and the π-electrons of the phenyl substituent. Moreover, there is a stabilizing CH-π interaction between the hydrogen of the pentamethylcyclopentadienyl and the phenyl group known as "β-phenyl effect" (Figure 25).

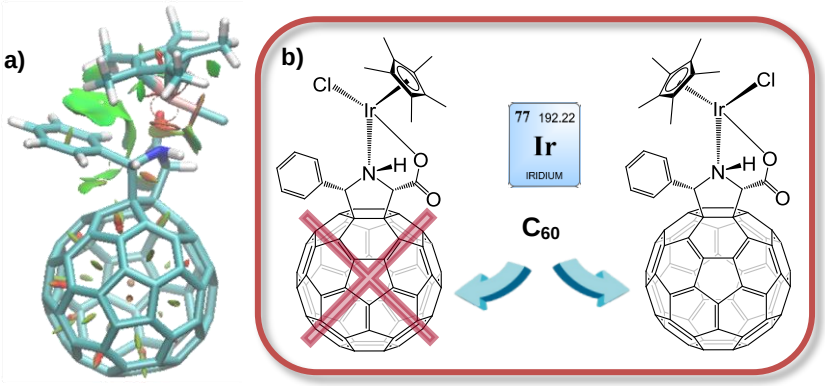

Figure 25. a) Representation of non-covalent attractive interactions in the iridium-fullerene hybrid; b) Structures of the two epimers of the iridium-fullerene hybrids.

2.5. Fullerenes as efficient n-type semiconductors

Nowadays, society is aware of the low-carbon economy and sustainable concept, which greatly promotes the advancement of chemical energy sources such as batteries and fuel cells, as well as the development of inexpensive renewable energy sources.

As far as photovoltaic cells are concerned, inorganic semiconductors have been the first choice on the market. However, research in this field has extended to the development of photosensitive organic materials with suitable electronic properties, due to the disadvantages of inorganic materials such as their complex processing or their rigidity.

In this regard, fullerenes and their derivatives make up the most studied class of n-type semiconductors for use in organic photovoltaic cells (OPVs) and organic field effect transistors (OFETs) among other applications. Especially, $PC_{61}BM$, which has already mentioned in the introduction, and its analogous of [70]fullerene, [6,6]-phenyl-C_{71}-butyric acid methyl ester ($PC_{71}BM$), have been considered as the standard n-type semiconductors in solution processable

organic photovoltaic layers. This is thanks to their well-balanced electronic properties, such us small reorganization energy, high electron affinity, ability to transport charge, their enclosed structure, their high processability and stability. These fundamental properties, coupled with the solubility of fullerene derivatives to pack effectively in crystalline structures suitable to charge transport,[94] have made fullerenes the most important acceptor materials for organic solar cells.

Therefore, the design and synthesis of new fullerene derivatives with better absorption values and electronic properties has become a challenge to be able to compete with efficient PV materials such as silicon or the most recent perovskites.

The general architecture of organic solar cells is sandwich type geometry (Figure 26). The active layer is between two contacts: an indium-tin-oxide (ITO) coated with a hole transport layer poly(ethylene-dioxythiophene) doped with polystyrenesulfonic acid, (PEDOT:PSS) over a transparent electrode (glass) and an aluminum top electrode, acting both as anode and cathode respectively.

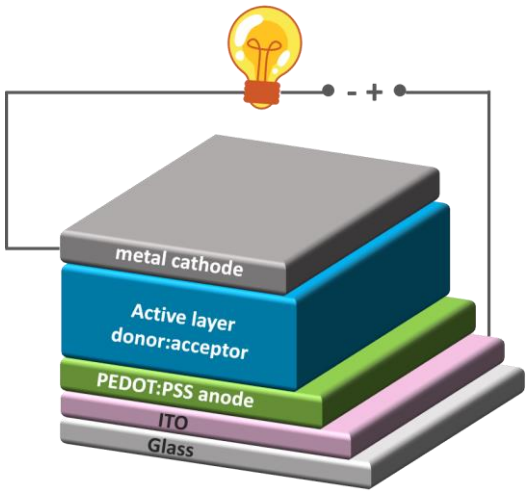

Figure 26. General architecture of organic solar cells.

[94] Rispens, M. T.; Meetsma, A.; Rittberger, R.; Brabec, C. J.; Sariciftci, N. S.; Hummelen, J. C. *Chem. Commun.* **2003**, *0*, 2116-2118

There are some ways to arrange this active layer. The most used are bilayer hetereojunction, where an n-type semiconductor material and a p-type one are disposed in two different layers, and bulk heterojunction (BHJ), in which the electron donor species (a small bandgap polymer) and the electron acceptor one (i.e. a soluble fullerene) are intimately intermixed creating a bi-continous network. Nevertheless, the best arrangement for the active layer is BHJ, since this bi-continuous network increases the interfacial area between the donor and acceptor phases heavily increase, which allows to promote exciton dissociation processes resulting in a high power conversion efficiency.[95]

Thus, bulk heterojunction (BHJ) organic photovoltaic cells (OPV) are a notable application, which consist of p-type conjugated polymers [e.g. poly(3-hexylthiophene-2,5-diyl), P3HT] and n-type fullerene derivatives.

The next frontier in the use of acceptor/donor BHJs, based on PCBM, is the realization of photo-electrochemical cells, able to work in contact with aqueous and/or non-aqueous electrolytes upon visible light illumination. One notable example is the realization of efficient photocathodes for hydrogen production by photo-electrochemical water splitting.[96] Recently, Antognazza *et al*. have reported a high sensitivity, photo-electrochemical oxygen sensor based on an organic BHJ formed by a low band gap polymer (APFO-3) and PCBM, revealing photo-activity towards oxygen reduction reaction (ORR).[97]

In the scheme proposed by the authors (Figure 27), polymer excitation by visible light leads to the efficient generation of bounded charged species (excitons), which are promptly dissociated into free charges (polarons) by highly efficient electron transfer process to the fullerene-based acceptors domain. They have recently reported that this process, typical of solid-state photovoltaic cells,

[95] Hoppe, H.; Sariciftci, N. S. *J. Mater. Res.* **2004**, *19*, 1924-1945

[96] a) Gustafson, M. P.; Clark, N.; Winther-Jensen, B.; MacFarlane, D. R. *Electrochim. Acta* **2014**, *140*, 309-313, b) Bourgeteau, T.; Tondelier, D.; Geffroy, B.; Brisse, R.; Cornut, R.; Artero, V.; Jousselme, B. *ACS Appl. Mater. Interfaces* **2015**, *7*, 16395-16403, c) Haro, M.; Solis, C.; Molina, G.; Otero, L.; Bisquert, J.; Gimenez, S.; Guerrero, A. *J. Phys. Chem. C* **2015**, *119*, 6488-6494, d) Suppes, G. M.; Fortin, P. J.; Holdcroft, S. *J. Electrochem. Soc.* **2015**, *162*, 551-556, e) Fumagalli, F.; Bellani, S.; Schreier, M.; Leonardi, S.; Rojas, H. C.; Ghadirzadeh, A.; Tullii, G.; Savoini, A.; Marra, G.; Meda, L.; Gratzel, M.; Lanzani, G.; Mayer, M. T.; Antognazza, M. R.; Di Fonzo, F. *J. Mater. Chem. A* **2016**, *4*, 2178-2187

[97] Bellani, S.; Ghadirzadeh, A.; Meda, L.; Savoini, A.; Tacca, A.; Marra, G.; Meira, R.; Morgado, J.; Di Fonzo, F.; Antognazza, M. R. *Adv. Funct. Mater.* **2015**, *25*, 4531-4538

occurs in the hybrid system with fully comparable dynamics and efficiency.[98] Photogenerated holes are collected at the underlying fluorine-doped tin oxide (FTO) electrode, while electrons are efficiently transferred at the interface with the aqueous solution, thus giving rise to photoelectrochemical reactions and, in particular, to ORR.

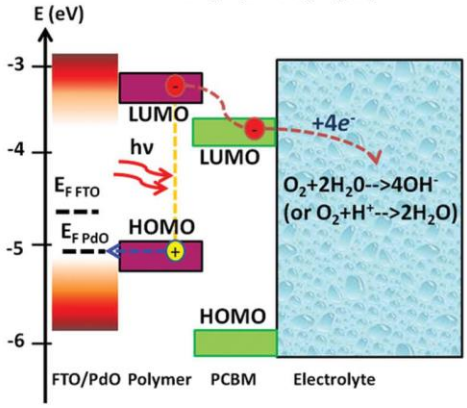

Figure 27. Schematic representation of the energetic levels of the ORR systems and the photocatalytic activity mechanisms

Oxygen reduction reaction (ORR) is a key process in different energy converting systems or electrochemical technologies (fuel cells, metal air batteries, oxygen sensors, etc).[99] Different mechanisms exist for ORR. As a matter of fact, for Pt electrode two-electron reduction of oxygen to H_2O_2 occurs parallel to the four-electron reduction to H_2O (Scheme 23).

In these fields the replacement of the traditional platinum based catalysts with non-precious metals[100] or metal-free electrocatalysts is currently a hot scientific challenge.[101] Particularly, the use of carbon nanomaterials such as nitrogen-

[98] Guerrero, A.; Haro, M.; Bellani, S.; Antognazza, M. R.; Meda, L.; Gimenez, S.; Bisquert, J. *Energy Environ. Sci.* **2014**, *7*, 3666-3673
[99] a) Steele, B. C. H.; Heinzel, A. *Nature* **2001**, *414*, 345-352, b) Cheng, F.; Chen, J. *Chem. Soc. Rev.* **2012**, *41*, 2172-2192
[100] Chen, Z.; Higgins, D.; Yu, A.; Zhang, L.; Zhang, J. *Energy Environ. Sci.* **2011**, *4*, 3167-3192
[101] a) Wang, D.; Su, D. *Energy Environ. Sci.* **2014**, *7*, 576-591, b) Dai, L.; Xue, Y.; Qu, L.; Choi, H.; Baek, J. *Chem. Rev.* **2015**, *115*, 4823-4892

doped carbon nanotubes[102] or graphene,[103] represents an interesting and novel approach.

Alkaline medium:

$O_2 + 2H_2O + 4e^- \rightarrow 4OH^-$ (four electron process)

$O_2 + H_2O + 2e^- \rightarrow HO_2^- + OH^-$ (two electron process)

$H_2O + HO_2^- + 2e^- \rightarrow 3OH^-$

Acidic medium:

$O_2 + 4H^+ + 4e^- \rightarrow 2\ H_2O$ (four electron process)

$O_2 + 2H^+ + 2e^- \rightarrow H_2O_2$ (two electron process)

$H_2O_2 + 2H^+ + 2e^- \rightarrow 2H_2O$

Scheme 23. Four and two electron processes for oxygen reduction reaction (ORR) in both alkaline and acidic media.

[102] Gong, K.; Du, F.; Xia, Z.; Durstock, M.; Dai, L. *Science* **2009**, *323*, 760-763

[103] a) Guan, J.; Chen, X.; Wei, T.; Liu, F.; Wang, S.; Yang, Q.; Lu, Y.; Yang, S. *J. Mater. Chem. A* **2015**, *3*, 4139-4146, b) Higgins, D.; Zamani, P.; Yu, A.; Chen, Z. *Energy Environ. Sci.* **2016**, *9*, 357-390

OBJECTIVES

3. OBJECTIVES

The main objective of this PhD thesis is the development of new methodologies for the stereoselectively preparation of fullerene derivatives as well as the control and study of their electronic and electrochemical properties and their possible practical applications in organic chemistry and devices.

Synthesis and electronic properties of fullerenes-fused unsaturated carbocycles

The aim of this chapter is to extend the scope for the phosphine-catalysed asymmetric cycloaddition of allenoates onto C_{60}[67] by changing all the elements involved in the reaction: dipole, dipolarophile and catalyst.

Regarding to the dipole, we will introduce the alkynoates as easily accessible precursors of the allenoates and a new phosphine screening will be carried out. Furthermore, these precursors will allow us to study the reaction into its two steps: first, the alkynoate isomerization to its corresponding allenoates which could possibly be enantioselective, and then the cycloaddition to fullerene. An acrylate-type dipole is also used to obtain differently substituted cyclopenteno[60]fullerenes.

As far as the dipolarophile is concerned, the cycloaddition reaction will be carried out onto another well known fullerene, C_{70}.

Finally, the effect of the phosphorus-catalyst ring size on the enantioselectivity of the reaction will be studied, as well as other types of catalysts such as *N*-heterocyclic carbenes (NHC's).

The intrinsic electronic properties of these fullerene compounds will be evaluated by measuring the electronic mobility and we will also study how optical purity could affect the electronic mobility.

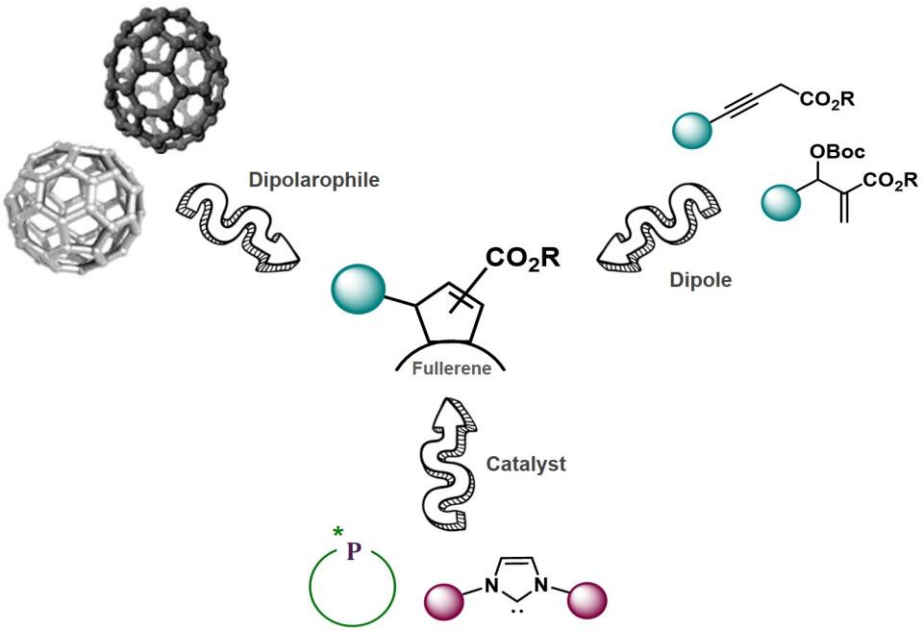

Figure 28. Catalytic cycloaddition onto fullerenes to synthesize fused unsaturated carbocycles derivatives

Reversible stereodivergent cycloaddition of a helicene derivative onto [60]fullerene: a chiral resolution strategy

The enantioselective catalytic methodology for the preparation of chiral fullerene derivatives and the retrocycloaddition reaction of azomethine ylides are two important chemical trasformations, developed in our group, which now belong to the fullerene-chemistry toolkit. In this section, we will demonstrate the usefulness of their joined application as an alternative mean for the resolution of racemates, even those without functional groups such as helicenes. For this purpose, enantioselective pyrrolidino[60]fullerenes will be prepared from a racemic iminoester derived from [6]helicene. The mixture of diastereoisomers of pyrrolidino[60]fullerenes can be separated by conventional chromatographic column and the resulting enantiopure fulleropyrrolidines will be subjected to retrocycloaddition conditions to recover the starting enantiopure helicenes.

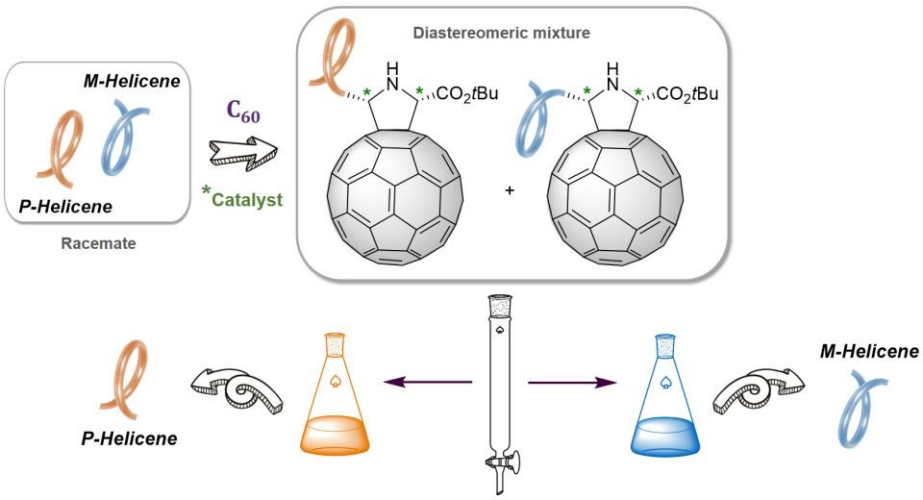

Figure 29.Schematic racemate resolution of helicenes by using [60]fullerene.

Metallofurene hybrids

The combination of fullerene chemistry with that of transition metals can be a source of new properties and perhaps new applications. For this reason, we have been dealing with the (asymmetric) synthesis of metallo-fullerene hybrids that have been applied in catalysis or in organic devices (see further).

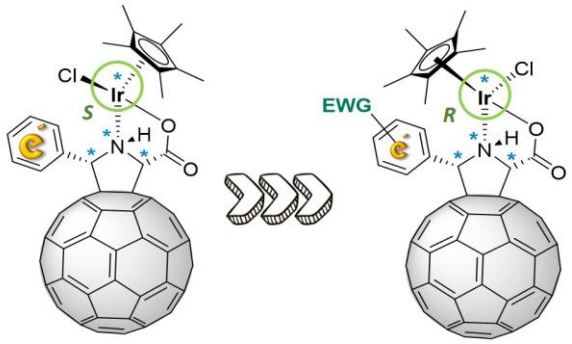

Figure 30. Iridium complexes with electron poor aromatic rings

Some of them are particularly interesting since they feature a stereogenic center at the reactive metal site: an example of these are the iridium-pyrrolidino[60]fullerene hybrids where the iridium center is configurationally stable for a strong C-H-π aromatic interaction between the hydrogen atoms of the group Cp* and the aromatic substituent (see Figure 30). With the objective

to prepare other stereoisomers, we will try to control the iridium configuration, maintaining the chirality of the other three stereocenters by weakening the aforementioned hydrogen bond.

Thus, we will synthesize several pyrrolidino[60]fullerenes with different electronic demand on the phenyl substituent in order to also reduce the repulsive Cl-π interaction and reverse the stereochemistry on the iridium center.

On the other hand, we will undertake the synthesis of a gold(I)-pyrrolidino[60]fullerene by complexation of a phosphine-pyrrolidino[60]fullerene with [$Au(SMe_2)$].

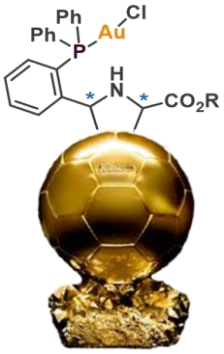

Figure 31. Schematic gold (I)-pyrrolidino[60]fullerene hybrid.

[60]Fullerene derivatives for photoelectro-catalytic devices

The oxygen reduction reaction (ORR) is one of the most important challenges in electro-catalysis because its key role in life processes and in energy converting systems, such as biological respiration and fuel cells, respectively.

In this context, we will orientate the synthesis of [60]fullerene derivatives for their employ in devices such as photoelectrochemical cells. The basic idea is to ensure that the fullerene behaves both as an acceptor, as usual on polymeric solar cells, and as a catalyst. Thus, we will endow the fullerene cage with catalytic sites where reduction processes could take place. Two different classes will be prepared: i) metallo-fullerene hybrids in which fullerene is bound to active

metals and, ii) metal-free fullerene catalysts where an active C_{60}-H bond is expected to catalyse the photo-electrochemical oxygen reduction.

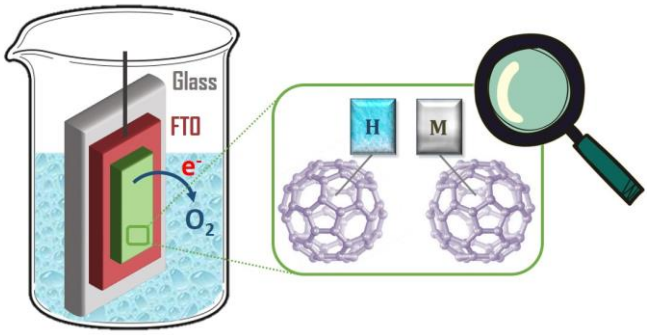

Figure 32. [60]Fullerene with catalytic sites for electrochemical devices.

RESULTS AND DISCUSSION

4. RESULTS AND DISCUSSION

4.1. Synthesis and electronic properties of fullerenes-fused unsaturated carbocycles

As discussed in the background, over the last three decades, chemists have been dealing with the functionalization of fullerenes in order to synthesize derivatives showing a wide variety of specific properties with applications in fields such as bio-medicine, molecular electronics, photovoltaics or materials science.[104] Among the many synthetic approaches developed for the chemical modification of fullerenes, cycloaddition reactions have proven their versatility and efficiency. However, both metal mediated or organocatalytic methods[105] developed for the chiral activation of electron poor olefins in cycloaddition reactions cannot be applied to fullerenes. Indeed, in sharp contrast with coumpounds such as α,β unsaturated esthers or ketones, fullerenes lack of a coordinating group (or other any functional group) able to interact with a chiral Lewis acid (or an organocatalyst) and, consequently, the use of most modern asymmetric methodologies are unusefull for the preparation of chiral fullerenes.

4.1.1. Organocatalysis in the asymmetric synthesis of cyclopentenofullerenes from 3-alkynoates

An important milestone occurred with the application, by our research group, of metal-free catalytic preparation of chiral fullerene derivatives.[67] In the process, easily available chiral phosphines, used as nucleophilic organocatalyst, triggered a HOMO activation of fullerene reagent partners, namely racemic α–allenoates, that lead, through a formal [3+2] stereoconvergent cycloaddition, to cyclopenteno[60]fullerenes with remarkable high enantiomeric excesses. The phosphine-catalyzed [3+2] cycloaddition methodology afforded a novel family of cyclopentenofullerenes with a wide range of allenoates.

As a further step, we envisioned to extend the scope of this organocatalytic method to 3-alkynoates as direct precursors of 2-allenoates. This class of

[104] a) Langa, F.; Nierengarten, J. F. *Fullerenes: Principles and Applications*, RSC: Cambridge, UK, **2007**, b) Martín, N.; Nierengarten, J. F. *Supramolecular Chemistry of Fullerenes and Carbon Nanotubes*, Wiley-VCH, Weinheim (Germany), **2012**
[105] MacMillan, D. W. C. *Nature* **2008**, *455*, 304-308

compounds are, indeed, readily accessible by coupling of terminal alkynes and diazoacetate derivatives under copper catalysis (Scheme 24).[106]

Thus, we carried out the synthesis of alkynoates **1a-f** that have been obtained in moderate to good yields (30 to 63%).

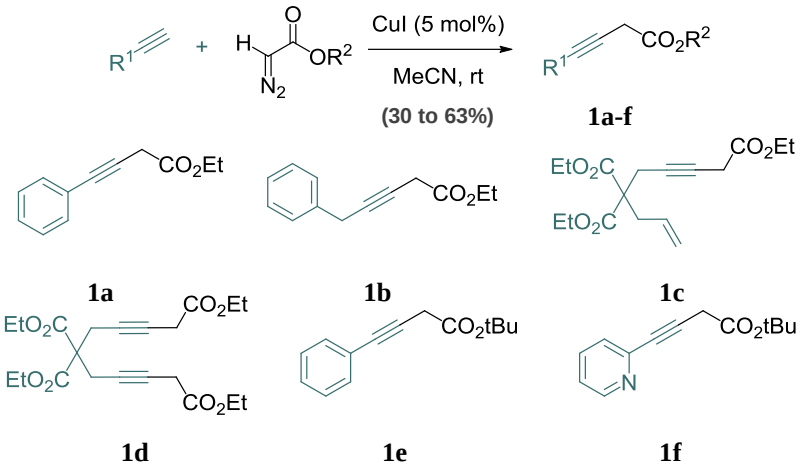

Scheme 24. Synthesis of 3-alkynoates **1a-f**.

The cycloaddition of alkynoates **1a-f** onto C_{60} has been studied in a "*one pot*" methodology (Scheme 25, path A) and also by sequential steps (Scheme 25, path B and C).

Indeed, by decoupling the cycloaddition process onto [60]fullerene in two steps, it is possible to gain more insight into this transformation. Furthermore, we can study the ability of the used catalytic systems to direct enantioselectively the alkynoates isomerization toward the formation of chiral allenoates (Scheme 25, path B).

[106] Suárez, A.; Fu, G. C. *Angew. Chem. Int. Ed.* **2004**, *43*, 3580-3582

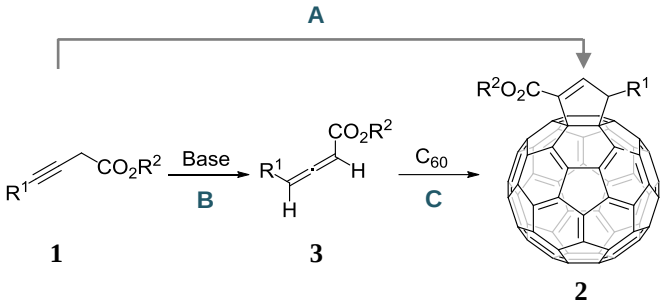

Scheme 25. Cycloaddition of alkynoates onto [60]fullerene "*one pot*" (path A) or by steps by isomerization from alkynoate to allenoate (path B) and further cycloaddition of allenoate on [60]fullerene (path C).

Thereby, we chose as reaction model the cycloaddition of the previously prepared ethyl-4-phenylbut-3-ynoate **1a** onto [60]fullerene that leads to cyclopenteno[60]fullerene **2a** (scheme in Table 1).

When we carried out the reaction in the presence of a sole phosphine, the reaction takes place very slowly and with low yields as the catalyst is not basic enough to carry out a fast isomerization to allenoate. Thus, we added triethylamine as to promote an easier isomerization of the alkynoate to the corresponding allenoate. A wide variety of commercially available chiral phosphines have been tested to control the stereochemical outcome of the cycloaddition (Figure 33).

Aliphatic phosphines, such as **P-I** and **P-II,** afford very low enantiomeric excess values. However, while **P-I** provides a low conversion, **P-II**, which presents aromatic rings in their structure, carries out the reaction with a conversion of 99% (Table 1, entries 1 and 2, respectively). Diphosphines **P-III**, **P-IV**, **P-V** and **PVI** showed modest values of conversion and enantioselectivity (Table 1, entries 3-6). Slightly better results were obtained with **P-VII** and **P-VIII** (Table 1, entries 7 and 8). Phospholane **P-IX**, endowed with an acetalic group, gave excellent yield directing the enantioselectivity toward the enantiomer (*S*)-**2a** with *ee* = 72% (Table 1, entry 9). Once again, (*S*,*S*)-*f*-Binaphane (**P-X**) was the optimal catalyst since it leads to the sole enantiomer (*R*)-**2a** with a complete enantioselectivity and in moderate yield. (Table 1, entry 10). We also tried to figure out if phosphines endowed with an amine group could promote more efficiently the cycloaddition.

Table 1. Phosphine-base-catalyzed [3+2] cycloaddition of alkynoate **1a** to [60]fullerene.[a]

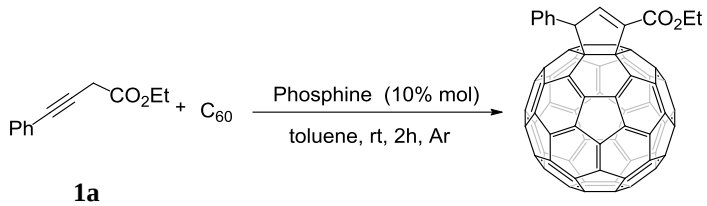

1a **2a**

Entry	Base	Phosphine	Conv.[c] (%)	*ee*[d] (%)
1	Et_3N	**P-I**	21	6 (*S*)
2	Et_3N	**P-II**	99	4 (*R*)
3	Et_3N	**P-III**	12	62 (*S*)
4	Et_3N	**P-IV**	30	20 (*S*)
5	Et_3N	**P-V**	35	24 (*R*)
6	Et_3N	**P-VI**	35	32 (*S*)
7	Et_3N	**P-VII**	49	80 (*R*)
8	Et_3N	**P-VIII**	74	54 (*S*)
9	Et_3N	**P-IX**	99	72 (*S*)
10	Et_3N	**P-X**	57	>99 (*R*)
11	Et_3N	**P-XI**	<5	-
12	Et_3N	**P-XII**	24	72 (*R*)
13	Et_3N	**P-XIII**	60	66 (*S*)
14	Et_3N	**P-XIV**	59	80 (*R*)
15[b]	-	**P-XIV**	31	88 (*R*)

[a] A solution of the base (40 mol%) and alkynoate **1a** (0,016 mmol) in dry toluene (1 mL) was stirred for 15 minutes and then [60]fullerene (0,017 mmol) and the phosphine (10 mol%) were added; the resulting mixture was stirred at rt under Ar atmosphere for 2 h. [b] A solution of the phosphine (10 mol%) and alkynoate **1a** (0,016 mmol) in anh. toluene (1 mL) was stirred for 15 minutes and then [60]fullerene (0,017 mmol) was added; the resulting mixture was stirred at rt under Ar atmosphere for 2 h. [c] Based on consumed [60]fullerene, determined by HPLC analysis (Regis (*R*,*R*)-WhelkO1, hexane:2-propanol 90:10, 3 mL/min). [d] *ee* determined by HPLC analysis (Regis (*R*,*R*)-WhelkO1, hexane:2-propanol 90:10, 3 mL/min); configuration of the chiral center has been determined by analogy with the reported cyclopenteno[60]fullerenes with CD measurements.

Thus, **P-XIV** catalyzed the reaction even in the absence of base, in good *ee* (88%, (*R*)-**2a**), however the conversion was low (Table 1, entry 15). In the presence of Et_3N the yield increased but the enantioselectivity lowered to *ee* = 80% (Table 1, entry 14). Other similar phosphines gave worst results (Table 1, entries 11-13).

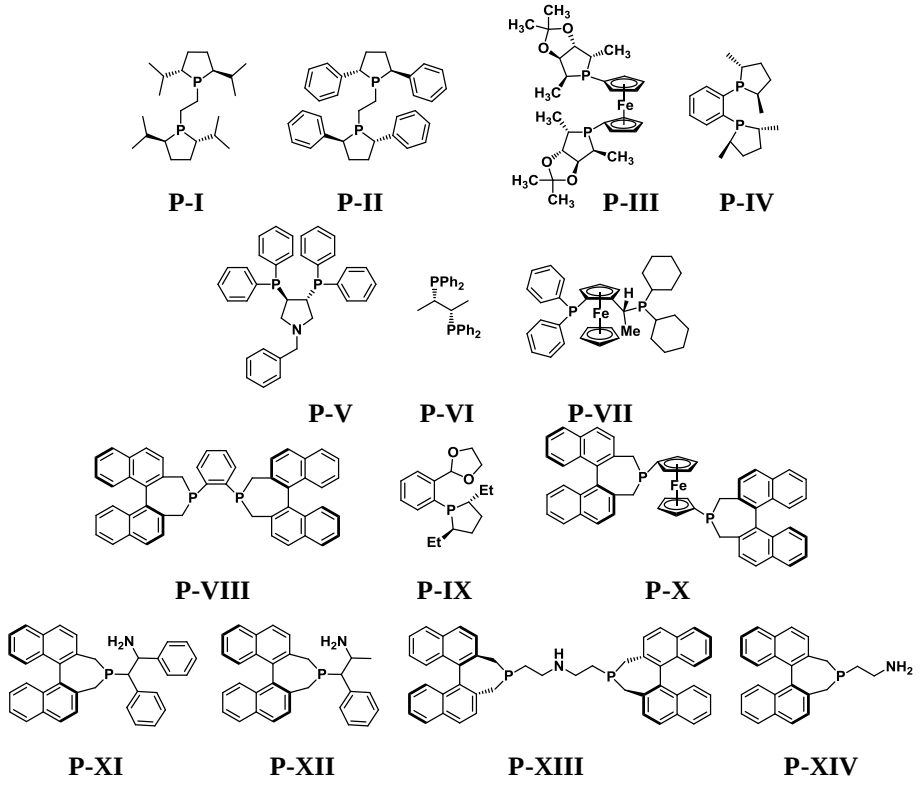

Figure 33. Commercially available chiral phosphines **P-I**-**XIV** used in this study.

Then we point our attention on the first step of the reaction that consists on the base catalyzed isomerization of the alkynoates **1a**. Thus, we carried out the screening of different commercially available chiral bases (Figure 34) to promote the enantioselective synthesis of chiral allenoates,[107] whose enantiomeric excesses were measured by chiral HPLC (Chiralpak IC, hexane:2-propanol (IPA) 98:2, 0.5 mL/min) (Table 2). All the bases carried out the

[107] a) Liu, H.; Leow, D.; Huang, K.; Tan, C. *J. Am. Chem. Soc.* **2009**, *131*, 7212-7213, b) Tang, Y.; Chen, Q.; Liu, X.; Wang, G.; Lin, L.; Feng, X. *Angew. Chem. Int. Ed.* **2015**, *54*, 9512-9516, c) Qian, D.; Wu, L.; Lin, Z.; Sun, J. *Nat. Commun.* **2017**, *8*, 567

reaction in moderate to good yields. Unluckily the enantioselectivity displayed was poor.

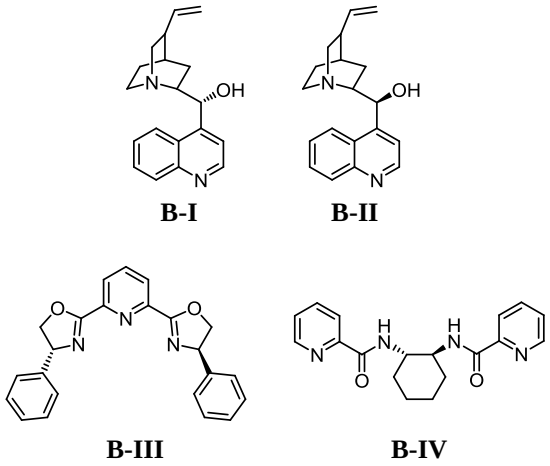

Figure 34. Commercially available chiral bases **B-I-IV** used in this study

Table 2. Isomerization from alkynoate to allenoate by using chiral bases.

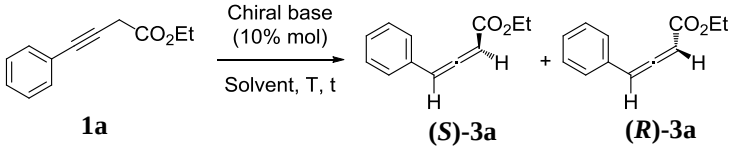

Entry	Chiral base	Solvent	T (ºC)	Time (h)	Conv.[a] (%)	*ee*[a] (%)
1	**B-I**	Hexane	rt	3	63	10
2	**B-III**	Hexane	rt	1,5	62	6
3	**B-IV**	Hexane	rt	1,5	61	4
4	**B-I**	Anh. toluene	rt	2,75	89	54
5	**B-I**	Acetonitrile	rt	1	89	16
6	**B-I**	Anh. toluene	0	4,5	75	39
7	**B-II**	Anh. toluene	rt	1	69	-42[b]
8	**P-XIV**	Anh. toluene	rt	16	50	4
9	**P-VIII**	Anh. toluene	rt	2,75	22	18

[a] Determined by HPLC analysis. [b] A negative value for the enantiomeric excess indicates that the enantiomer obtained in a higher proportion is the second one.

The highest value (*ee* = 54%) was obtained by using cinchonidine **B-I** as chiral base at room temperature (Table 2, entry 4). The pseudo-enantiomer **B-II,** cinchonine, gave the opposite enantiomer but again in low *ee* (Table 2, entry 7). Moreover, the need for the presence of amines as bases is evident since **P-VIII** gave very poor conversion. (Table 2, entry 9).

Although we haven't achieved better *ee* for the enantioselective isomerization than those previously described.[107] We used these results for studying the effect of the allenoates chirality on the enantiomeric excess of the final product by studying possible matching/mismatching effect between the chirality of the intermediates allenoates and the chirality of the phosphine catalysts.

Firstly, we carried out the cycloaddition reaction with the chiral amine cinchonidine, **B-I**, without an additional phosphine and the reaction didn't take place (Table 3, entry 1), so the nitrogenated base itself is not capable of performing the cycloaddition process.

Table 3. Phosphine-base-catalyzed [3+2] cycloaddition of alkynoate **1a** to [60]fullerene.[a]

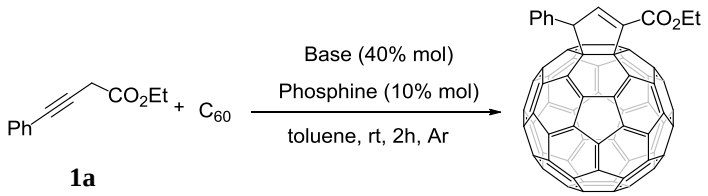

1a **2a**

Entry	Base	Phosphine	Conv.[b] (%)	*ee*[c] (%)
1	**B-I**	-	-	-
2	**B-I**	Bu_3P	77	0
3	**B-I**	**P-XIV**	36	78 (*R*)
4	**B-II**	**P-XIV**	51	82 (*R*)

[a] A solution of the base (40 mol%) and alkynoate **1a** (0,016 mmol) in dry toluene (1 mL) was stirred for 15 minutes and then [60]fullerene (0,017 mmol) and the phosphine (10 mol%) were added; the resulting mixture was stirred at rt under Ar atmosphere for 2 h. [b] Based on consumed [60]fullerene, determined by HPLC analysis (Regis (*R*,*R*)-WhelkO1, hexane:2-propanol 90:10, 3 mL/min). [c] *ee* determined by

HPLC analysis (Regis (*R,R*)-WhelkO1, hexane:2-propanol 90:10, 3 mL/min); configuration of the chiral center has been determined by analogy with the reported cyclopenteno[60]fullerenes with CD measurements.

In presence of cinchonidine **B-I** and Bu_3P, the reaction occurs but without any selectivity since it gives rise to a racemate (Table 3, entry 2). Despite a mismatched effect between the chiralities of amine **B-I** and phosphine **P-XIV** could be found since the *ee* passes from 88% (Table 1, entry 15) to 78%, we have not found a matching with the use of the pseudoenantiomer cinchonine **B-II** since the *ee* increases (82% , entry 4) but remains lower than that obtained using only the phosphine.

Finally, in order to figure out a possible effect of the allenoates chirality on the stereochemical outcome, excluding the effect of nitrogenated base chirality, we proceeded to separate both enantiomers of the starting allenoate **3a** by using semipreparative HPLC (Regis (*R,R*)-WHELK-O1 5/100 25cm x 10.0 mm column, hexane:2-propanol 90:10, flow rate 1.50 mL/min). Both enantiomers reacted, under the same optimised reaction conditions, achieving the corresponding cyclopenteno[60]fullerene **2a** with the same enantiomeric form (*R*) and even in the same *ee* value (78%) (Scheme 26). Therefore, this experimental findings confirm that the cycloaddition process occurs in a stereoconvergent manner being the last step, and the chirality of the phosphine, the responsible for the direction and level of enantioselectivity.

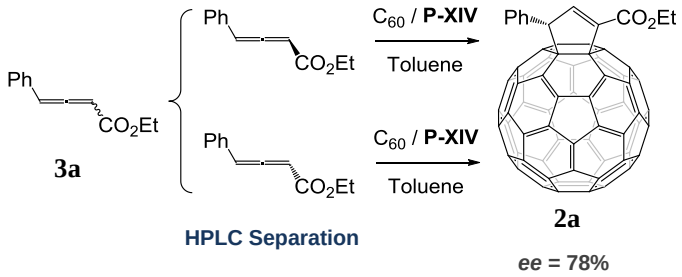

Scheme 26. Chiral HPLC separation of allenoates and cycloaddition onto C_{60}.

These optimized conditions were lately applied to the series of synthetized 3-alkynoates **1a-f** and allenoates **3a-h** (Table 4). Allenoates were synthesized following previously described methods in literature by coupling of α-phosphoranylidene esters and acid chlorides in the presence of Et_3N (Scheme 27).

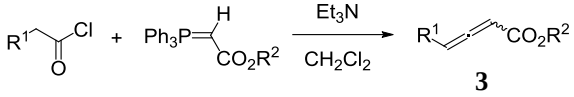

3

Scheme 27. Synthesis of allenoates **3**.

Alkynoate **1b** endowed with a benzyl group at position 4 was unable to cycloadd to C_{60} (Table 4, entry 1). We postulated an uneasay isomerization to allenoate due to the existence of two acidic protons (in α to the ester and the benzilic one) in the dipole which trigger the formation of a complex mixture of compounds that we were unable to purify. Indeed, the corresponding allenoate **3b**, prepared from the chloride and phosphorous ylide (Scheme 27), does cycloadd to C_{60} with 67% conversion and 84% *ee* (Table 4, entry 7). The 1,6-enyne **1c**, gave access to a cyclopentene derivative with an additional double bond in its structure (Table 4, entry 2). However, since we are not able to separate the two enantiomers of **2c**, we were unable to determine the enantiomeric excess of the derivative. The variation of the enyne to an 1,6-diyne (Table 4, entry 3), did not afford positive results because a complex mixture was obtained. By varying the ethyl ester group to a *tert*-butyl group, it was observed a sligth increase in the conversion albeit with a decrease of the enantioselectivity (88% *ee vs* 60%) (Table 4, entry 4). When a pyridinyl group was present as substituent in position 4, the starting materials were recovered unaltered (Table 4, entry 5). Those allenoates that had been previously evaluated under (*S,S*)-*f*-Binaphane catalysis,[67] were tested in the presence of **P-XIV** catalyst (Table 4, entries 6, 8-10, 13). Conversions as well as enantioselectivities were similar. The substitution of the phenyl group by a benzyl one (Table 4, entry 6 *vs* 7), yielded the cycloadduct in very similar results (conv: 42% *vs* 67% and 86% *vs* 84% *ee*). It was also tolerated the modification of the ethyl ester group by a *tert*-butyl ester (Table 4, entry 12). The additional functionalization of the cyclopentene ring was achieved by the use of an allenoate with a formyl group present in the aromatic ring with a moderate conversion (Table 4, entry 12). The additional functionalization of the cyclopentene ring was achieved by the use of an allenoate with a formyl group present in the aromatic ring affording a moderate conversion (Table 4, entry 11). The *ee* was not determined as a consequence of the impossibility of finding HPLC separation conditions.

Table 4. Phosphine-base-catalyzed [3+2] cycloaddition of alkynoates/allenoates **1a-f**/**3a-h** to [60]fullerene.

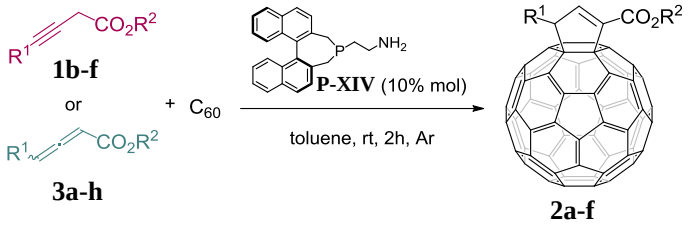

Entry	Addend	R^1	R^2	Conv.[b,c] (%)	*ee*[b] (%)	Product
1	**1b**	Bn	Et	-	-	-
2	**1c**	enyne		19	n.d.	**2c**
3	**1d**	diyne		-	-	-
4	**1e**	Ph	*t*Bu	49	60	**2d** (*R*)
5	**1f**	py	*t*Bu	-	-	-
6	**3a**	Ph	Et	42	86	**2a** (*R*)
7	**3b**	Bn	Et	67	84	**2b** (*S*)
8	**3c**	Me	Et	20	93	**2e** (*S*)
9	**3d**	Et	Et	70	92	**2f** (*S*)
10	**3e**	*i*Pr	Et	42	80	**2g** (*S*)
11	**3f**	4-CHOPh	Et	31	n.d.	**2h**
12	**3g**	Bn	tBu	28	80	**2i** (*S*)
13	**3h**	Ph	Bn	37	99	**2j** (*R*)

[a] A solution of 2-[(11b*S*)-3*H*-binaphtho[2,1-c:1′,2′-e]phosphepin-4(5*H*)-yl]ethanamine (10 mol%) and alkynoate **1a-f**/allenoate **3a-h** (0,016 mmol) in dry toluene (1 mL) was stirred for 15 minutes; then [60]fullerene (0,017 mmol) was added and the resulting mixture was stirred at rt under Ar atmosphere for 2 h. Configuration of the chiral center has been detremined by analogy with the reported cyclopenteno[60]fullerenes with CD measurements. [b] Determined by HPLC analysis (Regis (*R*,*R*)-WhelkO1, hexane:2-propanol 90:10, 3 mL/min). [c] Based on consumed [60]fullerene. n.d.: not determined.

The aforementioned results and those related to the previous work of allenoates demonstrated that the most successful phosphines are those bearing at least two alkyl substituents (Figure 33), which turned to be more nucleophilic than the

related aryl-substituted phosphines and, resulting particularly efficient, the seven-membered phosphacycles. Taking into account the importance of the cyclic structure of these phosphorous-containing heterocycles, we focused on the synthesis of a new four ring derivatives that are more rigid although not commercially available. This catalyst would allow a deeper evaluation of the cycloaddition process as well as the possible switching of the enantioselectivity by the use of the opposite chiral starting phosphine. Phosphines were prepared according to a modified previously reported procedure as it can be seen in Scheme 28.[108]

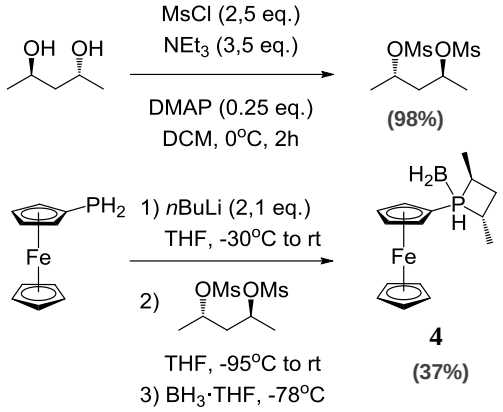

Scheme 28. Synthesis of four-membered phosphacycle **4**.

The commercial ferrocene phosphine was treated with *n*-butyllithium at -30ºC in THF and then a mesylated diol (obtained in a quantitative yield treating the 2,4-pentanediol with mesyl chloride and trimethylamine catalysed by DMAP) is added while the temperature is reduced to -95ºC. The obtained species was stabilized with BH_3 isolating the corresponding final four membered cyclic phosphine **4** in a moderate yield (37%). Despite this type of phosphines had previously been employed with no further modifications, when it was evaluated in the [3+2] cycloaddition reaction between several allenoates or alkynoates and [60]fullerene, no reaction was observed. Afterwards, we tried the "*in situ*" activation of the phosphine **4** by DABCO addition, observing that high temperatures were needed for a complete deprotection (Scheme 29).

[108] a) Marinetti, A.; Kruger, V.; Buzin, F. *Tetrahedron Lett.* **1997**, *38*, 2947-2950, b) Ostermeier, M.; Prieß, J.; Helmchen, G. *Angew. Chem. Int. Ed.* **2002**, *41*, 612-614

Unfortunately, the obtained results in terms of conversion and enantioselectivity values resulted to be significantly lower than those obtained by using the seven-membered ring phosphine. Remarkably, this phosphine gave access to the opposite enantiomer when compared to that obtained from phosphine **P-XIV**.

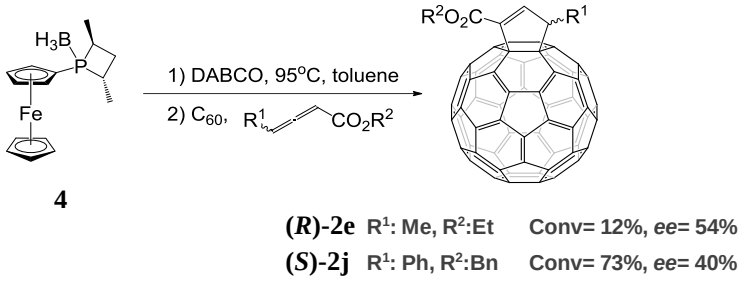

Scheme 29. One-pot deprotection of the four-membered phosphine followed by cycloaddition of allenoate **3c**, **3h** to [60]fullerene.

Following Lu´s initial proposal, we postulate a plausible mechanism (Scheme 30).

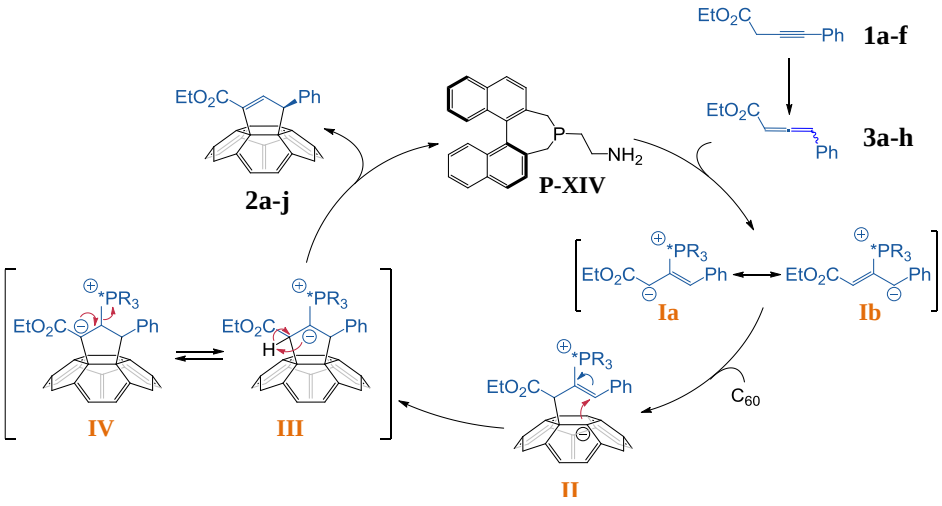

Scheme 30. Mechanism for the phosphine-catalyzed [3+2] cycloaddition of alkynoates/allenoates **1a-f**/**3a-h** to [60]fullerene.

The process starts with a nucleophilic attack from the phosphine onto the central electrophilic atom of the allenoate derived from the isomerization of the starting

alkynoate. Then, the (6,6) double bond of the fullerene would suffer from an attack of the zwitterionic intermediate (**Ia-Ib**). The formed fullerene intermediate (**II**) undergoes a ring closure, followed by a proton transfer of the stabilized ylide (**III-IV**), giving raise to the catalyst recovery and the desired cycloadduct formation.Furthermore, we applied our catalytic asymmetric systems to a previously reported cycloaddition of Boc-protected Morita-Baylis-Hillman adduct that lead to the analogous cyclopenteno[3,4:1,2][60]fullerenes (Scheme 31).[109] To this aim, we prepared the acrylate **5** by Morita-Baylis-Hillman reaction in the presence of Boc anhydride (di-*tert*-butyl dicarbonate) with a 76% yield.

Then, 1,2-bis(diphenylphosphine)ethane (dppe) was used as catalyst for the preparation of the racemic derivative so that its corresponding enantiomers can be localized by chiral HPLC. The characterization of the product **5** confirmed the different substitution of the five-membered ring.

To control the stereochemistry of the new chiral center, we used the phosphepine catalyst **P-XIV**. The reaction proceeded with a 36% conversion and 57% *ee*.

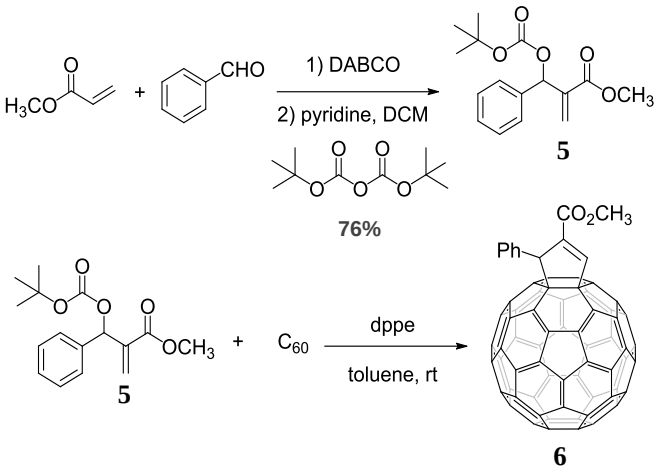

Scheme 31. Synthesis of a *tert*-butyloxycarbonyl-modified Morita-Baylis-Hillman adduct and phosphine-catalyzed [3+2] cycloaddition onto C_{60}.

[109] Yang, H.; Ren, W.; Miao, C.; Dong, C.; Yang, Y.; Xi, H.; Meng, Q.; Jiang, Y.; Sun, X. *J. Org. Chem.* **2013**, *78*, 1163-1170

Taking into account that proposed in the previous work, we postulated the following plausible mechanism (Scheme 32). The intermediate **I** is formed through an allylic nucleophilic sustitution initiated by the nucleophilic attack from the phosphine to the acrylate **5** and the subsequent elimination of the leaving group, *O*-Boc. The next step consists on the deprotonation by the base, giving rise to a *P*-ylide intermediate (**II**) which is able to add to the (6,6) double bond of the C_{60}. Finally, the fullerene intermediate (**III**) undergoes to a ring closure with the catalyst regeneration, what provides the desired product **6**.

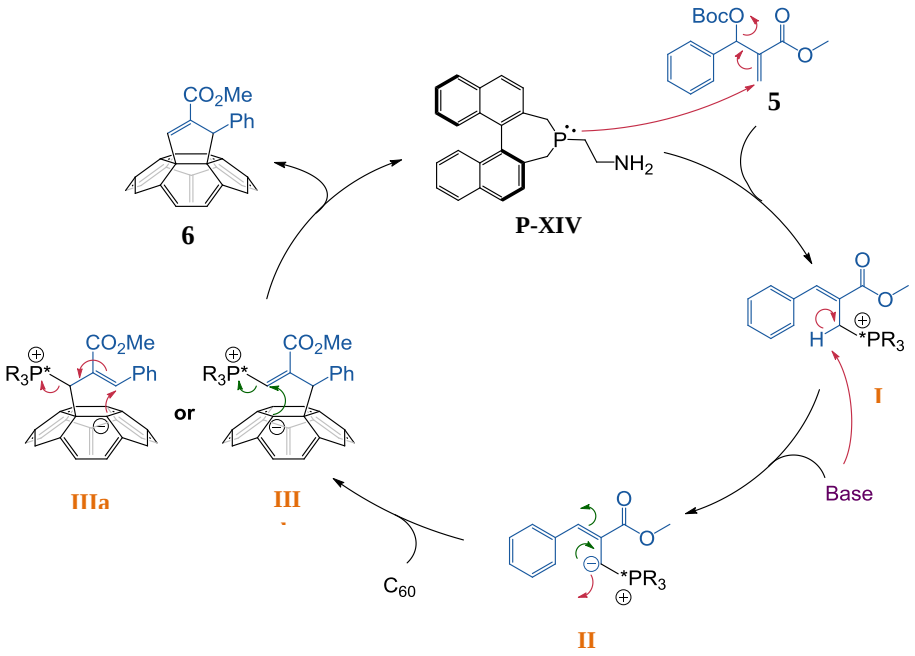

Scheme 32. Mechanism for the phosphine-catalyzed [3+2] cycloaddition of Morita-Baylis-Hillman adduct **4** to [60]fullerene.

Once the reaction has been well-stablished with [60]fullerene as dipolarophile, we turned our attention to higher fullerenes. In contrast to [60]fullerene, [70]fullerene has no spherical symmetry and, therefore, four differently reactive double bonds can be found on the cage giving rise to different site-isomers. In this regard, additions occur preferentially on those double bonds located at the polar zone (the most strained fullerene double bonds), in fact, α site followed by

β and γ sites. On the other hand, the flatter equatorial region is less reactive and the addition only rarely takes place at the δ site.[110]

Keeping this in mind, [70]fullerene was subjected to react in the presence of a racemic phosphine (dppe, 20 mol%) giving rise to the desired cyclopenteno[70]fullerenes in a mixture of site-isomers α and β (Scheme 33). As expected, when the reaction took place under optimized conditions, excellent site-selectivities were afforded. Thus, in the case of **7a**, the yielded α:β ratio was 98:2; and it was even better for **7b**, in which the α site isomer is the unique isomer observed. Moreover, good regioselectivities were also obtained for both cases. Thus, regioisomers with the ester moiety on the polar region and the methyl group (**7a**) or the aromatic ring (**7b**) on the equatorial region were formed preferentially in 89:11 and 85:15 ratios, respectively. The preference of the ester moiety for the polar region has previously been observed in the [3+2] cycloaddition reaction of α-iminoesters onto [70]fullerene.[111] The enantioselective synthesis of the α-regioisomer cyclopenteno[70]fullerene **7b** that is preferently formed was achieved under phosphine **P-XIV** catalysis with 88:12 enantiomeric ratio.

[110] Meier, M. S.; Wang, G.; Haddon, R. C.; Brock, C. P.; Lloyd, M. A.; Selegue, J. P. *J. Am. Chem. Soc.* **1998**, *120*, 2337-2342

[111] Maroto, E. E.; de Cózar, A.; Filippone, S.; Martín-Domenech, Á; Suarez, M.; Cossío, F. P.; Martín, N. *Angew. Chem. Int. Ed.* **2011**, *50*, 6060-6064

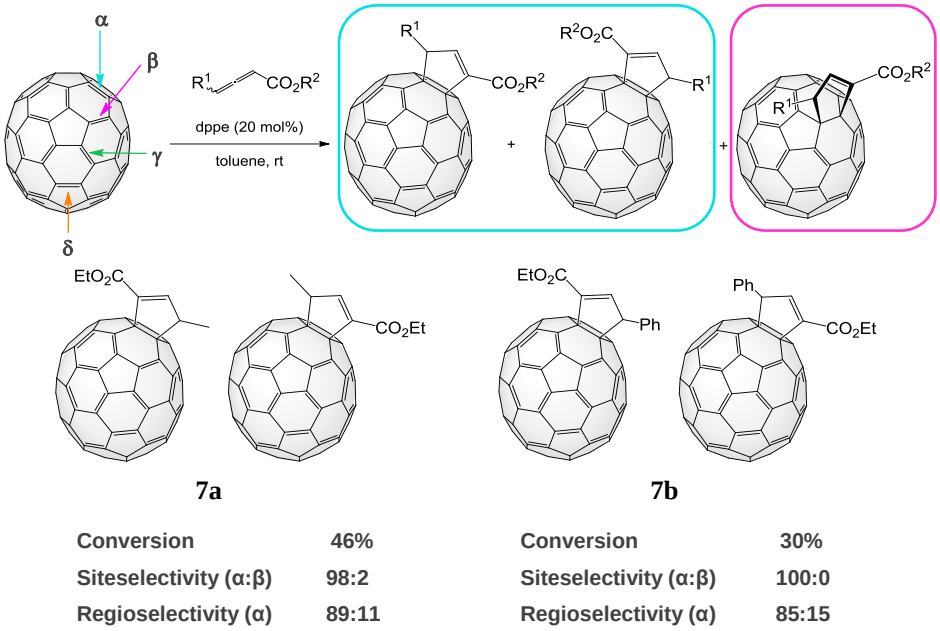

7a

Conversion	**46%**
Siteselectivity (α:β)	**98:2**
Regioselectivity (α)	**89:11**

7b

Conversion	**30%**
Siteselectivity (α:β)	**100:0**
Regioselectivity (α)	**85:15**

Scheme 33. Phosphine-base-catalyzed [3+2] cycloaddition of allenoates **3a** and **3c** to [70]fullerene.

4.1.2. Cyclobuteno[60]fullerenes

During the study of the cyclopenteno[60]fullerenes, we consider the use of the cycloaddition of 3-alkynoates/allenoates onto [60]fullerene, employing *N*-heterocycle carbenes (NHCs) as catalysts. Indeed, previous works in literature,[112] revealed that NHCs reacts with C_{60} yielding an unexpected C-C bonded product that can be described as a Lewis acid/Lewis base adduct and that is characterized by a strong zwitterionic character. Thus, we wondered if a NHC

[112] a) Li, H.; Risko, C.; Seo, J. H.; Campbell, C.; Wu, G.; Brédas, J.; Bazan, G. C. *J. Am. Chem. Soc.* **2011**, *133*, 12410-12413, b) Yamada, M.; Akasaka, T.; Nagase, S. *Chem. Rev.* **2013**, *113*, 7209-7264, c) Lorbach, A.; Maverick, E.; Carreras, A.; Alemany, P.; Wu, G.; García-Garibay, M.; Bazán, G. C. *Phys. Chem. Chem. Phys.* **2014**, *16*, 12980-12986

could catalyse the reaction by the activation of the 3-alkynoates/allenoates or, more interestingly, we could take advantage of a fullerene activation.

Firstly, we prepared the imidazoles **NHC-I** and **NHC-II** shown in Scheme 34 to be used as catalysts.[113] The glyoxal suffers a double nucleophilic attack from the 2,4,6-trimethylaniline to give rise to the diimine compound. One of imine group attacks to the paraformaldehyde and after a subsequent attack from the other imine and water elimination, **NHC-I** is obtained. To form **NHC-II** it is necessary and additional anion metathesis step with HBF_4.

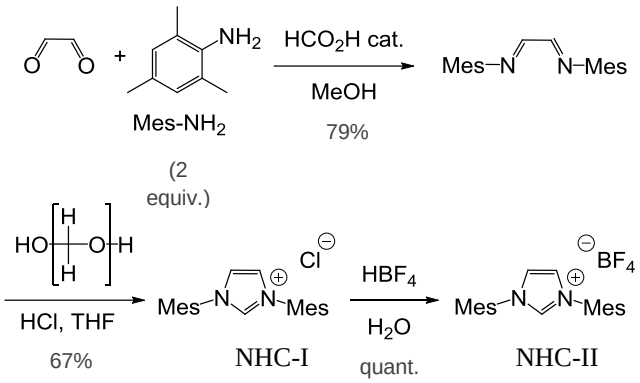

Scheme 34. Synthesis of **NHC-I** and **NHC-II**.

Thus, by stirring overnight 2 equivalents of allenoate **3a**, 1 equivalent of C_{60}, 10 equivalents of NaH[114] and 0.5 equivalents of imidazole **NHC-I**, we gratifyingly discovered the formation of the monoadduct **8a** in 21% conversion which structure did not correspond to the expected cyclopentene **2a**.

Once the spectroscopic techniques [^{1}H-NMR (Figure 35), ^{13}C-NMR, UV-Vis] and mass spectrometry (HRMS) allowed the fully characterization of the product, we found out that the monoadduct **8a** (representative UV-vis spectrum of [60]fullerene monoadducts with a little pick at 434 nm, Figure 36) presented a cyclobutene ring fused to [60]fullerene.

[113] Bantreil, X.; Nolan, S. P. *Nature Protocols* **2011**, *6*, 69-77

[114] 10 equivalents of NaH have been used to deprotonate the NHC salts and therefore to generate the active species. These amounts have been previously optimized in our group.[66]

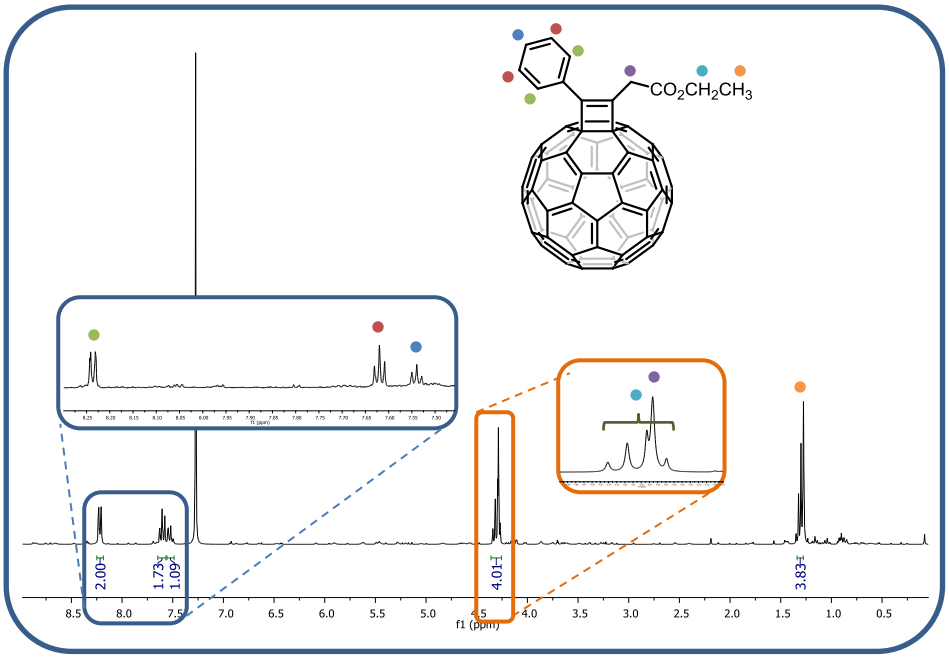

Figure 35. ^{1}H-NMR of cyclobueno[60]fullerene **8a**.

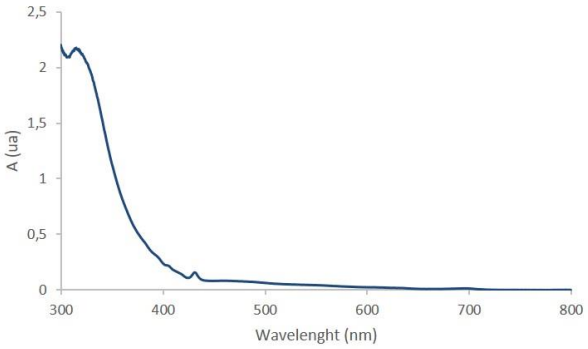

Figure 36. UV-vis spectrum of cyclobuteno[60]fullerene **8a** in clorobencene ($5\cdot10^{-5}$ M, l=10mm)

The ^{1}H-NMR spectrum of the compound **8a** shows the signals of the aromatic ring (one doublet and two triplets between 7,50 and 8,23 ppm), the ethyl group of the ester (a quadruplet and a triplet at 4,31 and 1,30 ppm, respectively) and the signal that led us to make the decision of the structure. This signal is a singlet

at 4,49 ppm overlapping with the quadruplet of the ethyl group which integrates two protons, and these ones belong to the same carbon (CH_2, 35,3 ppm) as it is shown in the HMQC spectrum (Figure 37). Therefore, the only viable structure corresponds to the cyclobutene ring fused to [60]fullerene and not to a cyclopentene fused-ring or a cyclobutane fused-ring with an exocyclic double bond.

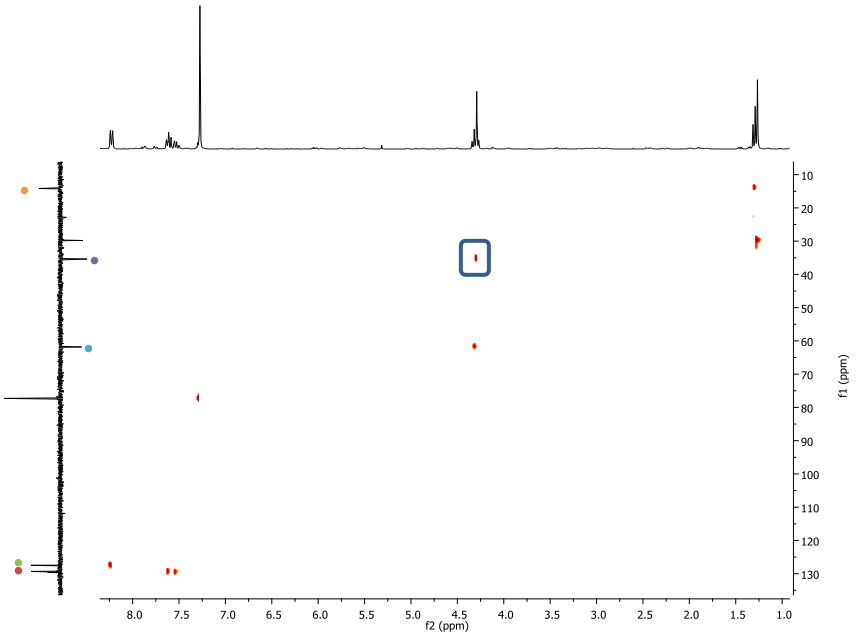

Figure 37. HMQC spectrum of compound **8a**. ^{1}H-NMR *vs* DEPT-135 ($CDCl_3$).

The mass spectrum shows a pick at m/z 908,0831 and the calculated for the corresponding molecular formula ($C_{72}H_{12}O_2$) is 908,0837.

This new cycloadduct resulted to be quite stable and no special storage conditions were needed. The conversion was even higher (up to 30%) when the chloride used as the imidazolium counterion was changed to BF_4 anion (**NHC-II**) (Scheme 35).

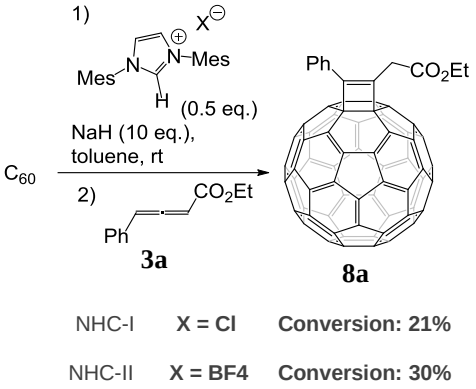

Scheme 35. Synthesis of cyclobuteno[3,4:1,2][60]fullerene.

Since alkynoates behave in some cases similarly to allenoates,[115] as we have demonstrated in phosphine-catalyzed cycloadditions, we carried out the reaction under the same conditions with the alkynoate **1a**. The reaction works with a conversion of 63%, significantly higher than for allenoate **3a** (from 30 to 63%) (Scheme 36).

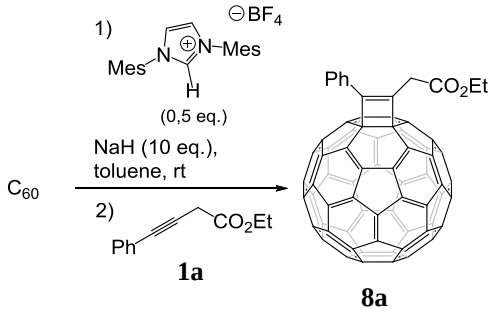

Scheme 36. NHC-catalyzed formal [2+2] cycloaddition of alkynoate **1a** with [60]fullerene

Furthermore, in our attempt to explain the role of each reagent, we carried out the reaction of the alkynoate **1a** and C_{60} in the absence of NHC to check if the base alone was capable of giving the same reaction. For our surprise, the reaction led to the formation of cyclobuteno[60]fullerene, although with a lower conversion, 15% (Scheme 37).

[115] Sampath, M.; Loh, T. *Chem. Sci.* **2010**, *1*, 739-742

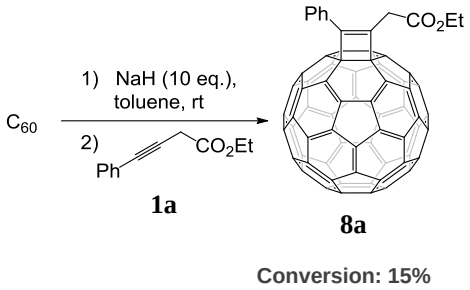

Scheme 37. Reaction of alkynoate **1a** in basic medium and absence of NHC.

Thus, we planned to develop a screening of bases and conditions in the cycloaddition of alkynoate **1a** onto C_{60} without using of NHC (Table 5).

In a first attempt, we started by reducing the base amount to 1 and 5 equivalents of NaH for 18 hours, then the conversion dropped to 7% and 11%, respectively (Table 5, entries 1,2). We then turned our attention to a series of bases; NaOH, Et_3N or DABCO among others (Table 5, entries 3-8). Only tetrabutylammonium hydroxide (Bu_4NOH) (Table 5, entry 8) gave rise to the cyclobuteno[60]fullerene, and surprisingly, not only the reaction selectively took place, but also in a high conversion, 58% measured by HPLC. Assuming that the solubility of the bases in toluene as the selected reaction solvent could play a key role in the formation of the cycle, we evaluated tetrabutylammonium hydroxide, a quaternary amine that has a remarkably higher solubility in organic solvents when compared with traditional bases.

Then, the amount of base was modified but it did not improve the previously obtained results (Table 5, entries 10-13). When the number of equivalents of alkynoate **1a** was reduced so did the conversion (Table 5, entry 14). An increasing of the temperature up to 50ºC allowed the reduction of the reaction time to 3 hours maintaining the conversion (Table 5, entries 15-16). During the optimization, we figured out that a freshly opened base was able to afford the desired cycloadduct in the same time but in a reduced temperature, at rt (Table 5, entry 17).

Table 5. Conditions screening for the synthesis of cyclobuteno[3,4:1,2][60]fullerene **8a**[a]

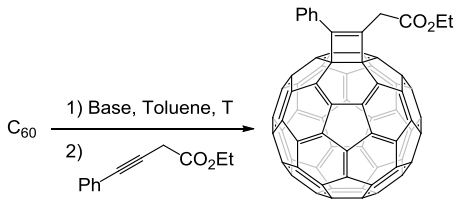

1a **8a**

Entry[a]	Base (Loading, eq.)	T (ºC)	Time (h)	Conversion (%)[b,c]
1	NaH (1)[d]	rt	18	7
2	NaH (5)	rt	18	11
3	NaOH (1)	rt	18	5
4	Et_3N (1)	rt	18	n. r.[e]
5	DABCO (1)	rt	18	n. r.
6	$NaHCO_3$ (1)	rt	18	n. r.
7	$NaCO_3$ (1)	rt	18	n. r.
8	$Bu_4NOH{\cdot}30H_2O$ (1)	rt	18	58
9	Bu_4NOH 1M MeOH (1)	rt	18	n. r.
10	$Bu_4NOH{\cdot}30H_2O$ (0,2)	rt	18	n. r.
11	$Bu_4NOH{\cdot}30H_2O$ (0,5)	rt	18	<5
12	$Bu_4NOH{\cdot}30H_2O$ (2)	rt	18	57
13	$Bu_4NOH{\cdot}30H_2O$ (5)	rt	18	only bisadducts
14[f]	$Bu_4NOH{\cdot}30H_2O$ (1)	rt	18	43
15	$Bu_4NOH{\cdot}30H_2O$ (1)	50ºC	1	35
16	$Bu_4NOH{\cdot}30H_2O$ (1)	50ºC	3	55
17[g]	$Bu_4NOH{\cdot}30H_2O$ (1)	rt	3	57

[a] To a solution of [60]fullerene (1 equiv.), the base (indicated equiv.) in 3 mL of toluene, the alkynoate **1a** (2 equiv.) was added and the resulting mixture was stirred for the indicated time at the indicated temperature. [b] Determined by HPLC analysis (Buckyprep, toluene:acetonitrile 9:1, 1 mL/min). [c] Based on consumed [60]fullerene. [d] NaH 60% in mineral oil. [e] No reaction. [f] 1 eq. alkynoate. [g] A freshly opened base is used.

With the optimized conditions in hands, we explored the scope of the reaction with a series of alkynoates (Table 6). The reaction takes place with different aromatic alkynoates and also with *tert*-buthoxycarbonyl group that allows eventual further modifications.

Table 6. Formal [2+2] cycloaddition of alkynoates **1a, 1g-j** with [60]fullerene.[a]

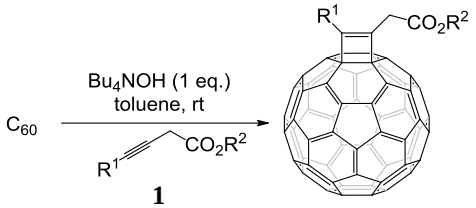

1 **8**

Entry	Alkynoate	R^1, R^2	Product	Conversion (%)
1	**1a**	Ph, Et	**8a**	57
2	**1g**	*p*ClC_6H_4, Et	**8f**	52
3	**1h**	*p*BrC_6H_4, *t*Bu	**8g**	34
4	**1i**	3,4-$Cl_2C_6H_3$, *t*Bu	**8h**	41
5	**1j**	*p*(*t*Bu)-C_6H_4, *t*Bu	**8i**	31

[a] A mixture of 0.01 mmol [60]fullerene, Bu_4NOH (1 equiv.) and the alkynoate **1a, 1g-j** (2 equiv.) in 3 mL of toluene is stirred at room temperature for 3 h. [b] Conversion has been determined by HPLC analysis (Buckyprep, toluene:acetonitrile 9:1, 1 mL/min).

Gratifyingly, one of the derivatives (**8i**) made possible the unambiguous determination of the chemical structure of the compound, thanks to the X-ray diffraction analysis. The slow evaporation of a mixture of Et_2O/toluene allowed us the successful formation of a suitable high quality single crystal (brown and shiny crystals). As expected, the X-ray analysis reveals the formation of a (6,6) fused cyclobutene ring with a C=C bond length of 1,345 Å (Figure 38).

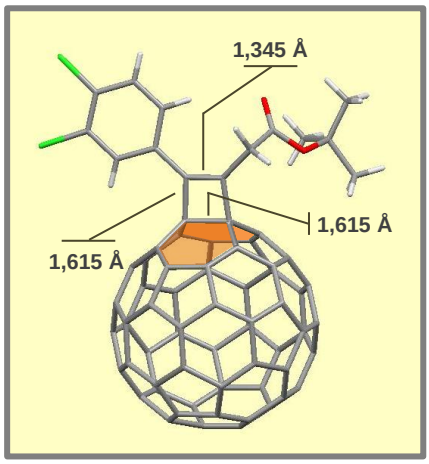

Figure 38. X-ray diffraction analysis of a single crystal of **8i** showing the (6,6) fused cyclobutene ring.

On the other hand, we decided to evaluate the same reaction under the same experimental conditions but using allenoates instead of alkynoates. However, with these substrates the reaction proceeded slower than in the case of the alkynoates. Therefore, we decided to increase the reaction temperature up to 50ºC, reaching in this manner conversion values similar to those derived from the use of alkynoates (Table 7).

Starting with the allenoate **3a**, it has been demonstrated that the reaction works under the aforementioned optimized conditions, thus allowing the formation of the same cycloadduct in a similar conversion value (55 *vs* 40%). As it can be seen in Table 7, the reaction tolerates a series of allenoates with alkyl or aromatic chains and also different esters.

Table 7. Formal [2+2] cycloaddition of allenoates **3a-d**, **3h-k** with [60]fullerene.[a]

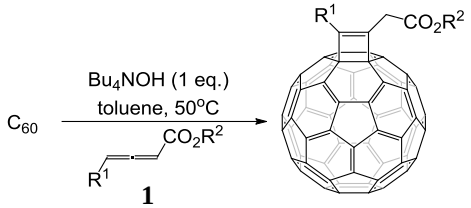

1 **8**

Entry	Allenoate	R^1, R^2	Product	Conversion[b] (%)
1	**3a**	Ph, Et	**8a**	44
2	**3b**	Bn, Et	**8d**	33
3	**3c**	Me, Et	**8c**	18
4	**3d**	Et, Et	**8b**	23
5	**3h**	Ph, Bn	**8e**	52
6	**3i**	*p*ClC_6H_4, Et	**8f**	22
7	**3j**	Ph, Me	**8j**	48
8	**3k**	Bn, Me	**8k**	31

[a] A mixture of 0.01 mmol [60]fullerene, Bu_4NOH (1 equiv.) and the allenoate **3a-d, 3h-k** (2 equiv.) in 3 mL of toluene is stirred at 50°C for 3 h. [b] Conversion has been determined by HPLC analysis (Buckyprep, toluene:acetonitrile 9:1, 1 mL/min).

The scarce literature related to the synthesis of these fullerene cycloadducts and these new results encourage us to postulate another plausible mechanism as it is displayed in Scheme 38. Similarly to that reported in literature,[116] both alkynoates and allenoates afford alkynylenolate intermediates (**I**) after deprotonation in the presence of a strong enough base. While alkynylenolate anions displayed different α and γ regioselectivity depending on the experimental conditions and on the electrophiles used,[116] all the alkynylenolates used led to a γ regioselective nucleophilic addition to [6,6] C_{60} double bond (**II**). Furthermore, in sharp contrast to the analogous Michael acceptors,[116b] the

[116] a) Xu, B.; Hammond, G. *Angew. Chem. Int. Ed.* **2008**, *47*, 689-692, b) Liu, L.; Xu, B.; Hammond, G. B. *Org. Lett.* **2008**, *10*, 3887-3890, c) Wang, W.; Xu, B.; Hammond, G. B. *Org. Lett.* **2008**, *10*, 3713-3716

formed fullerene anion, instead of being protonated, it gives rise to the cyclobutene ring closing (**III**). Finally, the reaction product is obtained after quenching and protonation of the formed anion in α position with respect to the ester group.

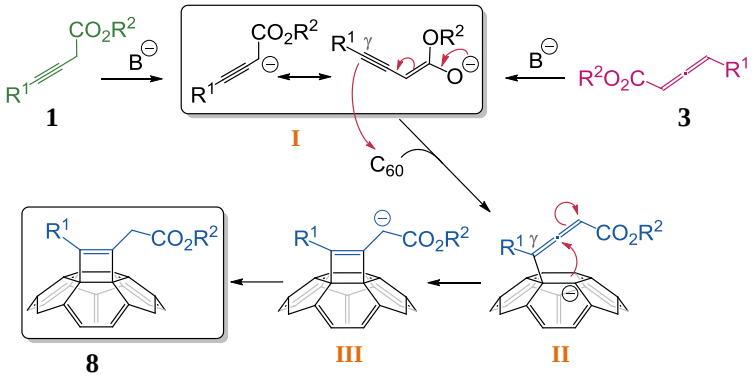

Scheme 38. Plausible mechanism for the formation of cyclobuteno[60]fullerenes.

4.1.3. Electronic properties and electron mobility in fullerene fused-carbocycles

The great interest of fullerenes for electronic/solar devices[15,17a,117] stems both from the appropriate energy values of their LUMO orbitals but also from the fairly good properties as n-type semiconductors.[17a]

Thus, in order to ensure that a fullerene derivative is suitable for such kind of application, both cyclic voltammetry and electron mobility studies are required in order to compare them with the widely used [60]**PCBM**, that is considered as a the fullerene benchmark in organic devices.

[117] a) Liang, P. - W.; Chueh, C. - C.; Williams, S. T.; Jen, A. K. Y. *Adv. Energy Mater.* **2015**, *5*, 1402321, b) Stranks, S. D.; Nayak, P. K.; Wei, Z.; Thomas, S.; Snaith, H. J. *Angew. Chem. Int. Ed.* **2015**, *54*, 3240-3248

4.1.3.1. Cyclobuteno[60]fullerenes

For this study, we pointed out our attention on the cyclobuteno[60]fullerenes **8j,k** since they have exactly the same number of atoms as **PCBM** and identical functional groups. In addition, considering that cyclopropane has been considered as a small ring with "double bond character",[118] cyclobuteno[60]fullerenes seemed to us very similar in their structure as **PCBM** and, therefore, an interesting candidate as n-type semiconductors (Figure 39).

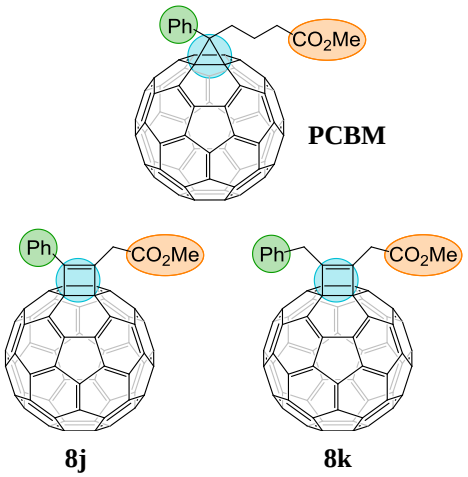

Figure 39. Cyclobutene adducts (**8j** and **8k**) as **PCBM** analogues.

Firstly, we have carried out the electrochemical study of the new prepared compounds **8a**, **8b** and **8f-j**. The electrochemical behavior results to be similar to other fullerene monoadducts and, therefore, to **PCBM**, with three quasireversible waves between 0 and -2 V. A first reduction wave is observed at around -1.080 V for all the compounds featuring an electron rich aromatic ring linked directly to the cyclobutene moiety (**8a**, **8i** and **8j**), (Table 8, entries 2, 6-7). While the monosubstitution on the aromatic group with a chlorine or a bromine atom (**8f-g**) does not affect the first half-wave reduction potential (Table 8, entries 3,4), the reduction peaks of **8h**, endowed with two chlorine atoms is catodically shifted by 30 mV at -1.053 V (Table 8, entry 5). On the other hand,

[118] a) de Meijere, A. *Angew. Chem. Int. Ed Engl.* **1979**, *18*, 809-826, b) La Rosa, A.; Gillemot, K.; Leary, E.; Evangeli, C.; González, M. T.; Filippone, S.; Rubio-Bollinger, G.; Agraït, N.; Lambert, C. J.; Martín, N. *J. Org. Chem.* **2014**, *79*, 4871-4877

the substitution of the cyclobutene moiety with an ethyl group gives rise to an anodic shift up to -1.103 V (**8b**, Table 8, entry 1).

Table 8. Cyclic voltammetry of compounds **8a**, **8c** and **8f-j**.[a]

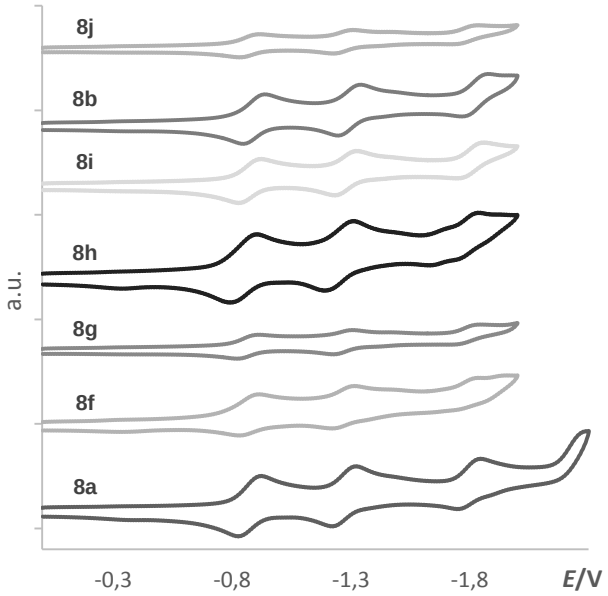

Entry	Product	$E_{1/2}^{red1}$/V	$E_{1/2}^{red2}$/V	$E_{1/2}^{red3}$/V
1	**8a**	-1.081	-1.485	-2.006
2	**8b**	-1.103	-1.501	-2.032
3	**8f**	-1.079	-1.483	-2.005
4	**8g**	-1.079	-1.476	-1.994
5	**8h**	-1.053	-1.467	-2.009
6	**8i**	-1.079	-1.487	-2.017
7	**8j**	-1.081	-1.479	-1.994

[a] Potential in Volts *vs* ferrocene/ferrocenium measured with cyclic voltammetry in *o*-DCB/MeCN (4:1) containing $Bu_4N^+PF_6^-$ (0.1M) as a supporting electrolyte. Glassy carbon (GCE), platinum wire, and Ag/Ag^+ electrodes were used as working, counter, and reference electrodes, respectively; scan rate: 0,1V/s.

Apart from the small differences (20-30 mV) showed in the aforementioned reduction potentials, the cyclobutene fullerene functionalization features the typical electrochemical properties of the fullerene monoadduct and, therefore, of the **PCBM**.

The next step was to determine the behaviour of cyclobuteno[60]fullerenes as n-type semiconductor by measuring their electron mobility.

Electron mobility, but in general, charge carrier mobility, is an important property for materials of application in organic electronics. Molecular structures of the materials, disorder, defects, electron density strongly affect this propriety.[119] Despite mobility values could be extracted from devices such as solar cells or organic field-effect transistors, many of these techniques are affected by the contacts, morphology etc.

In order to determine the intrinsic charge carrier transport property of the new cyclobutene-containing cycloadducts, we have carried out, in collaboration with the group of Prof. Seki in Kyoto, a comparative study with **PCBM** by using a new technique: flash-photolysis time-resolved microwave conductivity[120] (FP-TRMC).[121] TRMC is able to provide the "intrinsic charge carrier mobility" of the material excluding other effect that stems from the contacts with the electrodes or from the morphology.

Interestingly, these results revealed that the cyclobutene derivatives **8a**, **8j-k** showed an electron mobility significantly larger than that observed for **PCBM** (Table 9). The estimated value of electron mobility (μ^-) for **8j** was three fold

[119] a) Honsho, Y.; Miyakai, T.; Sakurai, T.; Saeki, A.; Seki, S. *Sci. Rep.* **2013**, *3*, 3182, b) Mitsui, C.; Okamoto, T.; Yamagishi, M.; Tsurumi, J.; Yoshimoto, K.; Nakahara, K.; Soeda, J.; Hirose, Y.; Sato, H.; Yamano, A.; Uemura, T.; Takeya, J. *Adv. Mater.* **2014**, *26*, 4546-4551

[120] A technique allowing the quantitative and qualitative detection of radiation-induced charge separation by time-resolved measurement of the changes in microwave absorption resulting from the production and decay of charged and dipolar molecular entities. In a typical TRMC experiment, separated charge carriers, which are generated by a laser pulse, lead to a perturbation of the initial microwave absorbance. The temporal decay of the conductivity signal (i.e. microwave absorbance) reflects the lifetime of the photogenerated carriers (definition by Royal Society of Chemistry).

[121] a) Seki, S.; Saeki, A.; Sakurai, T.; Sakamaki, D. *Phys. Chem. Chem. Phys.* **2014**, *16*, 11093-11113, b) Saeki, A.; Koizumi, Y.; Aida, T.; Seki, S. *Acc. Chem. Res.* **2012**, *45*, 1193-1202

higher than the value of **PCBM** and two than that for **8a** and **8k**. Compound **8b** bearing two ethyl groups in the cyclobutene moiety exhibited only a slight increase in the electron mobility, which confirms the importance of the phenyl group as substituent in these compounds. Besides the potential high electron-conducting nature of the new fullerene compounds with characteristic photo-carrier generation processes, they are excellent candidates as new n-type materials for application in the fabrication of photovoltaic (PV) devices since the new fullerene derivatives **8a**, **8j** and **8k** are thermally stable compounds as revealed by their thermogravimetric analyses (TGA).

Table 9. Intrinsic mobility of charge carriers in **8a**, **8b**, **8j-k** and **PCBM** observed by FP-TRMC measurements.

Entry	Compound	$\phi\Sigma\mu/10^{-5}$ $cm^2V^{-1}s^{-1}$	$\phi^a/10^{-4}$	$\mu^b/cm^2V^{-1}s^{-1}$
1	**8a**	2.3	3.5	0.066
2	**8b**	1.3	2.8	0.044
3	**8j**	3.3	3.5	0.095
4	**8k**	2.1	2.9	0.072
5	**PCBM**	1.9	6.0	0.035

[a] Determined by photocurrent measurements for the compounds casted onto an interdigitated comb-type Au electrode with poly(dioctylfluorene) (PDOF) standard (Figure 80, Experimental Section). [b] Estimated as electron mobility in the compounds.

4.1.3.2. Chirality effect in charge-carrier mobility of cyclopenteno[60]fullerenes

All new cyclopenteno[60]fullerenes have been also characterized by cyclic voltammetry (CV) studies in *o*-DCB/MeCN (4:1) containing $Bu_4N^+PF_6^-$ (0,1M) as supporting electrolyte at room temperature, along with pristine C_{60} as a reference. Moreover, glassy carbon, platinum wire, and Ag/Ag^+ electrodes were used as working, counter and reference electrodes, respectively (Table 10).

As it was expected, three reversible reduction waves were observed at similar potential values, with the usual cathodic shift (80-100 mV for the first reduction wave), when compared with pristine [60]fullerene, as a result of the saturation of a double bond. Indeed, this technique could be considered as another

"spectroscopic" analysis that enable to determine unambiguously the number of saturated double bonds in the fullerene sphere. Therefore, taking into account the reduction potential values obtained for these compounds, we can easily confirm the sole presence of mono-adducts in our samples. Indeed, only the saturation of one of the double bonds of the carbon cage takes place, which produces a rising in the energy of the LUMO.

Table 10. Reduction potentials for the cyclopenteno[60]fullerenes **2b**-**d**, **2h**-**i**, and pristine[60]fullerene.[a]

Product	$E_{1/2}^{red1}$ (V)	$E_{1/2}^{red2}$ (V)	$E_{1/2}^{red3}$ (V)
C_{60}	-1.027	-1.421	-1.877
2b	-1.107	-1.505	-2.019
2c	-1.118	-1.500	-2.025
2d	-1.133	-1.525	-2.050
2h	-1.081	-1.476	-2.003
2i	-1.114	-1.512	-2.039

[a] Potential in volts *vs* ferrocene/ferrocenium. Cyclic voltammogram recorded in o-DCB/ACN 4:1 using a GCE (glassy carbon electrode) as the working electrode, Ag/AgNO3 as the reference electrode and Bu4N·PF6 (0.1M) as the supporting electrolyte at 100 mVs-1.

While, as expected, the enantiomeric excess does not affect the reduction potential of the fullerene derivative, we wonder if, analogously to the examples reported in chapter 2.3, the difference in the enantiomeric excess of chiral materials could influence some electronic properties.

Thus, once cyclopenteno[60]fullerenes have been prepared both in racemic and enantiopure form (chapter 4.1.1) we carried out measurements by using time-resolved microwave conductivity (TRMC) to determine if and how charge carrier transport property is affected by the enantiomeric excess.

Compounds **2a** and **2j** have been selected since their structures are similar to the cyclobuteno[60]fullerene **8j** that showed the higher values of electronic mobility.

Compound **2a**, featuring an ethyl ester and a phenyl group in the stereogenic center, presents the same charge carrier generation yield (ϕ) both in his racemate and in each enantiomeric form. However, when we measured the transient mobility, the $\phi\Sigma\mu$ value of the enantiomer (*R*)-**2a** is higher, and double, than that of racemic **2a** (Table 11, entry 1 and 2). It is worthy to note that the other enantiomer (*S*)-**2a** still present a similar behaviour although, due to the minor *ee*, the value is slightly lower with respect to optically pure enantiomer (*R*)-**2a** (Table 11, entries 2 and 3).

Table 11. Conductivity Transient ($\phi\Sigma\mu$), Charge-Carrier Generation Yield (ϕ) and Charge-Carrier Mobility (μ) of the film of the compound **2a**[a]

Entry	Compound	*ee*	$\phi\Sigma\mu/10^{-5}$ $cm^2V^{-1}s^{-1}$	$\phi/10^{-4}$	$\mu/cm^2V^{-1}s^{-1}$
1	Rac-**2a**	-	1.5	1.1	0.14
2	(*R*)-**2a**	99	3.0	1.1	0.27
3	(*S*)-**2a**	94	2.5	1.1	0.23

[a] The enantiomers separation has been carried out by semipreparative HPLC using the column (*R,R*)-WHELKO1 5/100 (25 cm x 10.0 mm), hexane:IPA 85:15, 3mL/min.

On the other hand, compound (*R*)-**2j** with an *ee* = 99% gives rise to a Charge-Carrier Generation Yield (ϕ) arround four-fold higher and a mobility more than twice than racemic **2j**. Enantiomer (*S*)-**2j** could not be separated in its optically pure form, however the mobility recorded was higher than the racemic one. (Table 12).

Table 12. Conductivity Transient ($\phi\Sigma\mu$), Charge-Carrier Generation Yield (ϕ) and Charge-Carrier Mobility (μ) of the film of the compound **2j**

Entry	Compound	*ee*	$\phi\Sigma\mu/10^{-5}$ $cm^2V^{-1}s^{-1}$	$\phi/10^{-4}$	$\mu/cm^2V^{-1}s^{-1}$
1	Rac-**2j**	-	1.2	2.5	0.05
2	(*R*)-**2j**	99	5.3	9.6	0.12
3	(*S*)-**2j**	80	2.1	2.4	0.09

[a] The enantiomers separation has been carried out by semipreparative HPLC using the column (*R*,*R*)-WHELKO1 5/100 (25 cm x 10.0 mm), hexane:IPA 85:15, 4mL/min.

By comparing the results of both products (**2a** and **2j**), we can realize that derivative **2a**, which presents an ethyl ester, provides higher charge-carrier mobility than the film of **2j**.

These results disclose the relevance of chirality in an important electronic property of fullerenes such as charge carrier mobility and it complements a previous results.[78] Moreover, it demonstrates the importance of asymmetric synthesis for the preparation of chiral carbon nanostructures.

4.2. Reversible stereodivergent cycloaddition of a helicene derivative onto [60]fullerene: a chiral resolution strategy

The importance of optically active compounds in many fields of science is more than evident. Therefore, their direct preparation with the highest possible optical purity has become a major challenge. The main methodologies to reach optically pure compounds are asymmetric (chemical or enzymatic) synthesis, chiral chromatographic separation, kinetic resolution or crystallization methods. Far from being out of interest, each one of these strategies are still developing new alternative tools in order to face new challenging chemical problems as well as the constantly high demand of enantiopure chiral compounds.

In this respect, the use of divergent reactions on racemic mixtures (RRM) is presented as a suitable alternative to the large number of processes in which both kinetic resolution and asymmetric synthesis failed.[122] This strategy is based on the reaction of both enantiomers of a racemate with a chiral substrate (reagent, catalyst or solvent) giving rise to non-enantiomeric products that could eventually be diastereoisomers (stereodivergent), constitutional isomers (regiodivergent) or different chemical compounds (chemodivergent). Although no difference in reaction rates for both enantiomers, such as kinetic resolution, or stoichiometric amount of chiral reagents are required, high selectivity and ease of products separation are a prerequisite to develop an efficient divergent RRM.

On the other hand, chiral carbon-based nanostructures, such as helicenes,[123] fullerenes[48b,78] or curved polyaromatics hydrocarbons,[124] feature new optoelectronic properties as charge-carrier mobility or chiroptical properties, stemming from their chiral arrangement. Actually, for these types of compounds, often lacking functional groups, the enantiomeric chromatographic separation is

[122] a) Russell, T. A.; Vedejs, E. *Enantiodivergent Reactions: Divergent Reactions on a Racemic Mixture and Parallel Kinetic Resolution,* Wiley-VCH Verlag GmbH & Co. KGaA, Weinheim, Germany, **2014**, b) Miller, L. C.; Sarpong, R. *Chem. Soc. Rev.* **2011**, *40*, 4550-4562
[123] Gingras, M. *Chem. Soc. Rev.* **2013**, *42*, 1051-1095
[124] a) Rickhaus, M.; Mayor, M.; Juricek, M. *Chem. Soc. Rev.* **2017**, *46*, 1643-1660, b) Rickhaus, M.; Mayor, M.; Juricek, M. *Chem. Soc. Rev.* **2016**, *45*, 1542-1556

the only available pathway to obtain optically pure compounds, which entails long times and high costs.[125]

For this reason, we focused our attention on the search for alternative racemate resolutions by using the [60]fullerene covalent chemistry and, in particular, its less-exploited reversible character. Actually, stereoselective cycloadditions on [60]fullerene by the use of chiral reagents (asymmetric induction) have been reported[50,56a,b,59,68,126] In this regard, RRM have previously been used, followed by retro-functionalization reactions, to separate chiral fullerenes such as, for instance, those already mentioned D_2-C_{76} and D_2-C_{84}.[127] However, as far as we are concerned, fullerenes have never been previously used for racemates resolution. Furthermore, from one hand, the introduction of new catalytic methods for the enantioselective functionalization of fullerenes (asymmetric catalysis) allows their application in RRM by using only minor amounts of chiral materials.[11124,60,61,66,111,128] On the other hand, the availability of new synthetic tools to carry out retro-cycloaddition processes[26a,b,126c,129] would enable the recovery of the former racemic starting materials in an enantioenriched form.

Thus, in order to probe the usefulness of this approach, we decided to carry out, the enantiodivergent resolution of racemic helicenes, followed by a subsequent retro-cycloaddition reaction, affording the respective isolated enantiomers in an efficient manner. We have considered the helicenes as useful racemic benchmark in which to test efficiency of stereodivergent reversible reactions by means of

[125] Gingras, M.; Felix, G.; Peresutti, R. *Chem. Soc. Rev.* **2013**, *42*, 1007-1050
[126] a) Giacalone, F.; Segura, J. L.; Martín, N. *J. Org. Chem.* **2002**, *67*, 3529-3532, b) Illescas, B.; Rifé, J.; Ortuño, R. M.; Martín, N. *J. Org. Chem.* **2000**, *65*, 6246-6248, c) Maggini, M.; Scorrano, G.; Bianco, A.; Toniolo, C.; Prato, M. *Tetrahedron Lett.* **1995**, *36*, 2845-2846
[127] a) Crassous, J.; Rivera, J.; Fender, N. S.; Lianhe, S.; Echegoyen, L.; Thilgen, C.; Herrmann, A.; Diederich, F. *Angew. Chem. Int. Ed.* **1999**, *38*, 1613-1617, b) Kessinger, R.; Crassous, J.; Herrmann, A.; Rüttimann, M.; Echegoyen, L.; Diederich, F. *Angew. Chem. Int. Ed.* **1998**, *37*, 1919-1922
[128] Maroto, E. E.; Filippone, S.; Suárez, M.; Martínez-Álvarez, R.; de Cózar, A.; Cossío, F. P.; Martín, N. *J. Am. Chem. Soc.* **2014**, *136*, 705-712
[129] a) Martín, N.; Altable, M.; Filippone, S.; Martín-Domenech, Á *Synlett* **2007**, *2007*, 3077-3095, b) Martín, N.; Altable, M.; Filippone, S.; Martín-Domenech, Á; Martínez-Álvarez, R.; Suárez, M.; Plonska-Brzezinska, M.; Lukoyanova, O.; Echegoyen, L. *J. Org. Chem.* **2007**, *72*, 3840-3846

[60]fullerene, due to the aromatic sp^2 carbon structure without functional groups of the helicenes.

Helicenes are non-planar polycyclic aromatic compounds whose helical backbone is formed of *ortho*-fused aromatic rings. Their extended π-conjugation combined with their helical topology provide them with high chiroptical properties (huge optical rotations, strong circular dichroic responses and substantial circularly polarized luminescence) and good electronic properties (conductivity and redox properties).[123,130,131,132] For these reasons, they are of great interest for many optoelectronic applications such as chiral organic light-emitting diodes (OLEDs),[133,134] transistors,[135] photovoltaic devices, chiroptical switches,[136,137] or non-linear optical (NLO) materials[138] and conductive materials.[73,139]

In particular, we used 2-formylhexahelicene racemate **9** as starting material, which has been provided by the group of Prof. Crassous in Rennes, to carry out the synthesis of the respective helicene-iminoester racemate **10**.

In a first step, racemic 2-hexahelicene-iminoesters **10** (*tert*-butyl (*E*)-2-((hexahelicen-11-ylmethylene)amino)acetate) underwent an enantioselective azomethine ylide 1,3-dipolar cycloaddition reaction to [60]fullerene, which results in a mixture of enantioenriched diastereomers (*M*-**11** and *P*-**12**). This two

[130] Saleh, N.; Shen, C.; Crassous, J. *Chem. Sci.* **2014**, *5*, 3680-3694
[131] Isla, H.; Crassous, J. *Compt. Rend. Chim.* **2016**, *19*, 39-49
[132] Shen, Y.; Chen, C. F. *Helicenes Chemistry: From Synthesis to Applications*, Springer, Berlin, **2017**
[133] Ying, Y.; da Costa, R. C.; Smilgies Detlef-M.; Campbell, A. J.; Fuchter, M. J. *Adv. Mater.* **2013**, *25*, 2624-2628
[134] Brandt, J. R.; Wang, X.; Yang, Y.; Campbell, A. J.; Fuchter, M. J. *J.Am.Chem.Soc.* **2016**, *138*, 9743-9746
[135] Yang, Y.; da Costa, R. C.; Fuchter, M. J.; Campbell, A. J. *Nat. Photon.* **2013**, *7*, 634-638
[136] Schweinfurth, D.; Zalibera, M.; Kathan, M.; Shen, C.; Mazzolini, M.; Trapp, N.; Crassous, J.; Gescheidt, G.; Diederich, F. *J. Am. Chem. Soc.* **2014**, *136*, 13045-13052
[137] Shen, C.; Loas, G.; Srebro-Hooper, M.; Vanthuyne, N.; Toupet, L.; Cador, O.; Paul, F.; López Navarrete, J. T.; Ramírez, F. J.; Nieto-Ortega, B.; Casado, J.; Autschbach, J.; Vallet, M.; Crassous, J. *Angew. Chem. Int. Ed.* **2016**, *55*, 8062-8066
[138] Verbiest, T.; Elshocht, S. V.; Kauranen, M.; Hellemans, L.; Snauwaert, J.; Nuckolls, C.; Katz, T. J.; Persoons, A. *Science* **1998**, *282*, 913-915
[139] Kiran, V.; Mathew, S. P.; Cohen, S. R.; Hernández Delgado, I.; Lacour, J.; Naaman, R. *Adv. Mater.* **2016**, *28*, 1957-1962

diastereoisomers were easily separated by conventional silica-gel chromatography. Finally, the use of a metal-catalyzed retro-cycloaddition reaction under mild conditions[26a,c] afforded both starting 1,3-dipoles which, after *in-situ* hydrolysis, yielded both 2-formylhexahelicene enantiomers **9** (Scheme 39).

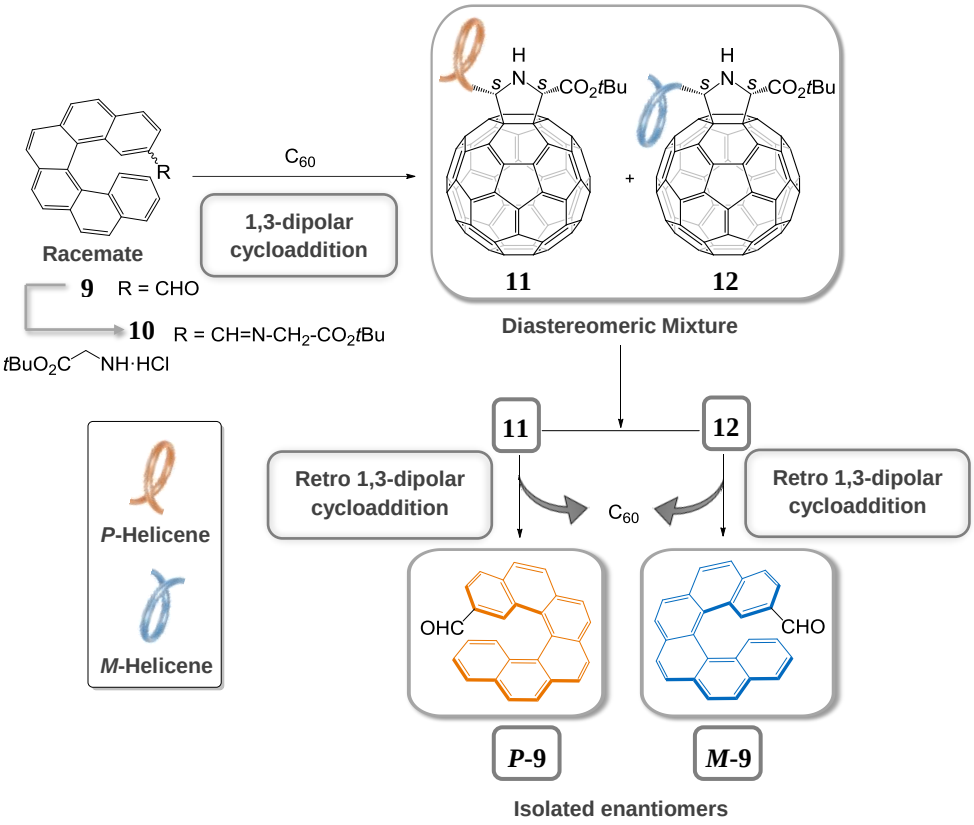

Scheme 39. Resolution strategy carried out for 2-formylhexahelicene racemate **9**.

In the first instance, the racemic iminoester rac-**10** is synthesized by coupling of glycine *tert*-butyl ester hydrochloride, previously deprotonated by Et_3N, and racemic 2-formylhexahelicene **9** in a 99% yield. The next step is the [3+2] cycloaddition of this iminoester rac-**10** onto [60]fullerene. Among the available catalytic systems, we chose the pair Cu(II) acetate/(R_p)-Fesulphos **P-XV** which revealed its efficiency in previous studies directed to the formation of the (*2S,5S*) pyrrolidino[3,4:1,2][60]fullerene with *ee* values up to 92%.[60]

It is important to note that the use of only 10% of chiral catalyst [Cu(II) acetate/(R_P)-Fesulphos **P-XV**] directed efficiently the cycloaddition of the racemic helicene-iminoester **10** onto [60]fullerene affording two diastereoisomers, **11** and **12** (Scheme 40), which are obtained in a 1:1 ratio and in 80% yield (with respect to helicene-iminoester **10**) (Figure 40, Buckyprep (Waters) (4.6 x 250 mm, 5µm), toluene:acetonitrile:hexane 50:10:40, flow rate 1.00 mL/min.)

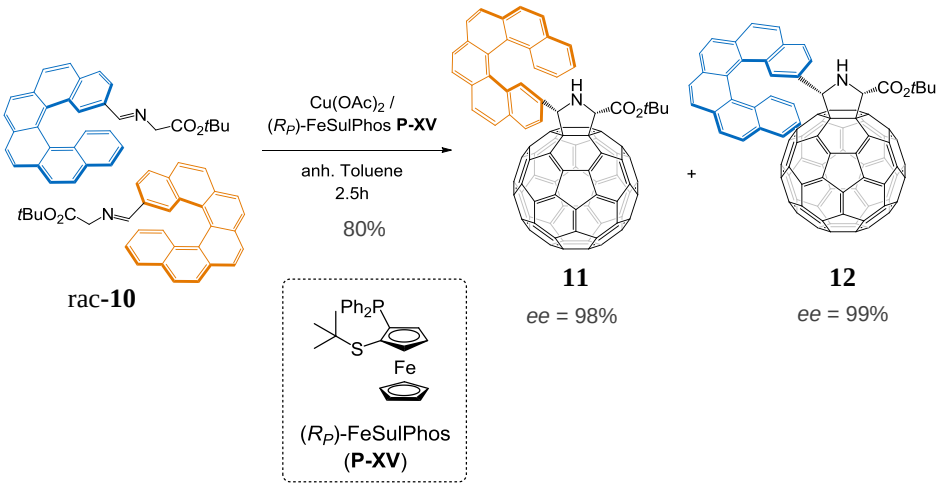

Scheme 40. [3+2] cycloaddition of racemic helicene-iminoester **10** onto [60]fullerene.

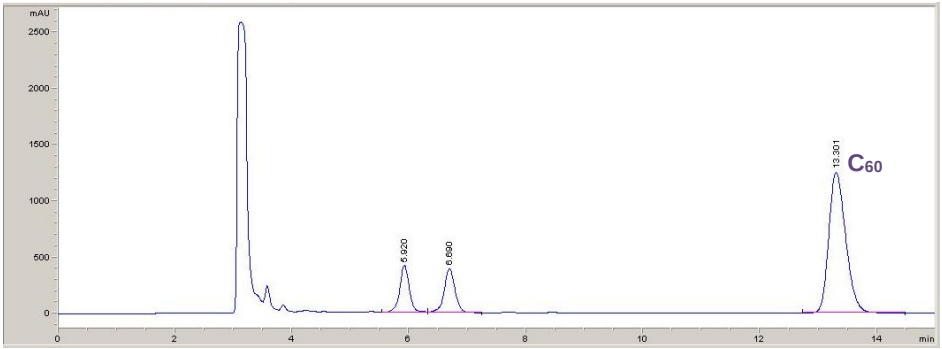

#	Time	Area	Height	Width	Area%	Symmetry
1	5.92	4786.9	416.1	0.1742	13.689	0.943
2	6.69	5051.5	393.5	0.1958	14.446	0.943
3	13.301	25129.2	1251.1	0.3123	71.864	0.726

Figure 40. Diastereomeric ratio of racemic iminoester **10** cycloaddition onto [60]fullerene.

As result of the high enantiocontrol in the new formed asymmetric carbons of pyrrolidine, the two diastereoisomers differ in the helicenes moiety configuration, while both *C*-2 and *C*-5 feature the same configuration (almost completely a *S,S* configuration). Indeed, by observing CD spectra, diastereoisomer **11** (Figure 41, blue line) presents a positive peak at 330 nm consistent with the *P* configuration of helicene moiety, while the same peak for **12** is negative and consistent with the *M* configuration. The signals at 427 nm, diagnostic for the fullerene monoaddition, are not mirror images and both are positive (despite for diastereomer **11** the peak is partially covered by the bigger helicene signal) as we could expect from sector rule for pyrrolidino[60]fullerene with *S,S* configuration at *C*-2 and *C*-5 (Figure 41). It is important to note that diastereoisomers **11** and **12**, could be easily separated by conventional silica-gel chromatography, thus fulfilling the key requirement for the separation of racemates by stereodivergent RRM.

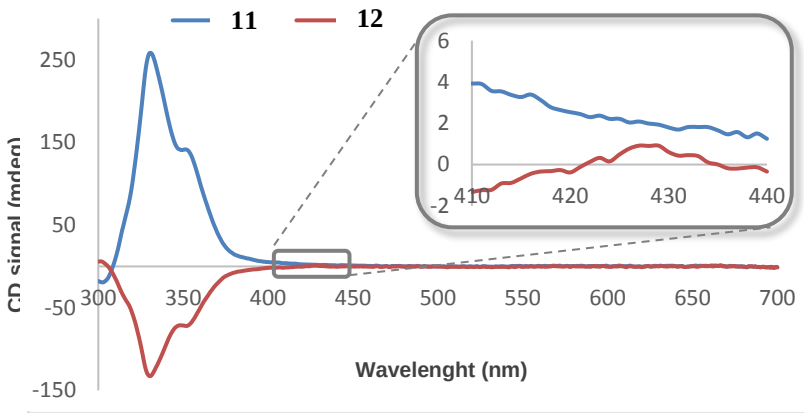

Figure 41. Circular Dichroism (CD) spectra of diastereisomers **11** and **12** (2 x 10^{-4} M in CH_2Cl_2, 25 °C, l = 1mm). Inset peak corresponding to [60]fullerene chirality.

Thus, each separated diastereoisomer, analysed by chiral HPLC and circular dichroism (CD), showed a very high optical purity: diastereoisomer **12** was obtained in a high enantioenriched form, being *ee* > 99% between (*M,S,S*)-**12** and (*P,R,R*)-**12**, (Figure 42, Chiralpak IC (4.6 x 250 mm, 5µm), hexane:isopropanol 97:3, flow rate 2.00 mL/min.) while for diastereoisomer **11** the enantiomeric ratio, (*P,S,S*)-**11** to (*M,R,R*)-**11**, was 99:1 (Figure 43, Chiralpak IC (4.6 x 250 mm, 5µm), hexane:isopropanol 97:3, flow rate 2.00 mL/min.).

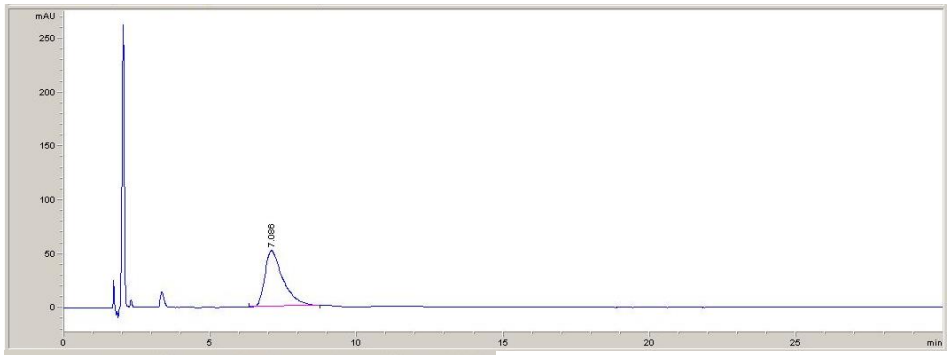

#	Time	Area	Height	Width	Area%	Symmetry
1	7.086	2235.7	52	0.6214	100.000	0.541

Figure 42. Enantiomeric excess of diastereoisomer (*M*,*S*,*S*)-**12**/(*P*,*R*,*R*)-**12**. The main enantiomer is (*M*,*S*,*S*)-**12** (t_R = 7.1 min) while the enantiomer (*P*,*R*,*R*)-**12**, that usually is eluted at 15 min. is not detected.

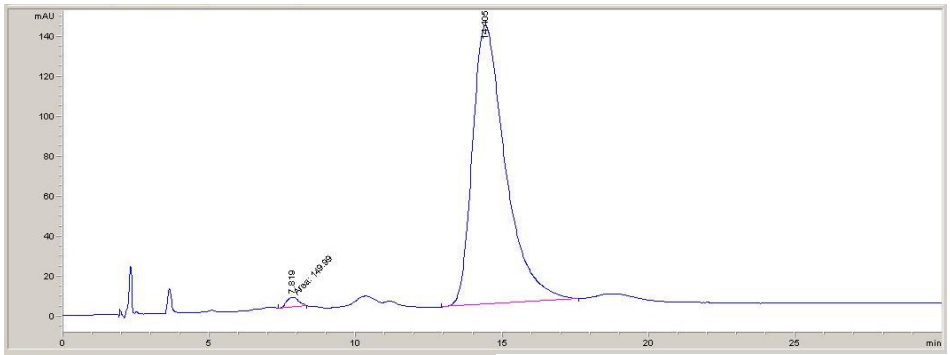

#	Time	Area	Height	Width	Area%	Symmetry
1	7.819	150	5.2	0.4846	1.353	0.973
2	14.405	10937.7	139.4	1.1313	98.647	0.592

Figure 43. Enantiomeric excess of diastereoisomer, (*M*,*R*,*R*)-**11** (t_R = 14.4 min)/(*P*,*S*,*S*)-**11** (t_R = 7.8 min)

In order to confirm the stereochemical outcome in the racemic series, we carried out the same synthetic study on each of both pure enantiomers (*P* and *M*) of helicene **9**. This study should allow: i) a more easy characterization of the products, and ii) the assessment of the catalytic system to maintain the sign of the asymmetric induction in the presence of another chiral element.

Thus, since **11** is the main product when optically pure *P*-**10** underwent the cycloaddition reaction onto [60]fullerene in the presence of 10% of Cu(II) acetate/(R_p)-Fesulphos, it can be deduced the configuration *(P,S,S)* for this diastereoisomer. Diastereoisomer **12**, formed in a minor amount as result of the

unfavorable *(R,R)* asymmetric induction sense of the catalytic system, features a *(P,R,R)* configuration. On the contrary and consistently, *(M,S,S)*-**12** is the main product and *(M,R,R)*-**11** is the minor one when *M*-**10** is used.

Therefore, the catalytic system proved to maintain a high level of stereoselectivity even in the presence of a helicoidally chiral element. It was also observed a slight different behaviour with each helicene enantiomers. Indeed, the diastereomeric ratio between *(P,S,S)*-**11** and *(P,R,R)*-**12** (92/8), observed in the reaction with iminoester *P*-**10,** (Figure 44, Buckyprep (Waters) (4.6 x 250 mm, 5µm), toluene:acetonitrile:hexane 50:10:40, flow rate 1.00 mL/min.) was higher than *(M,S,S)*-**12**/*(M,R,R)*-**11** (83/17) (Figure 45, Buckyprep (Waters) (4.6 x 250 mm, 5µm), toluene:acetonitrile:hexane 50:10:40, flow rate 1.00 mL/min.). This is a consequence of the matching of chirality *P* and chirality of the catalyst Cu(II) acetate/(R_p)-FeSulphos and a mismatching with the chirality *M* (Scheme 41).

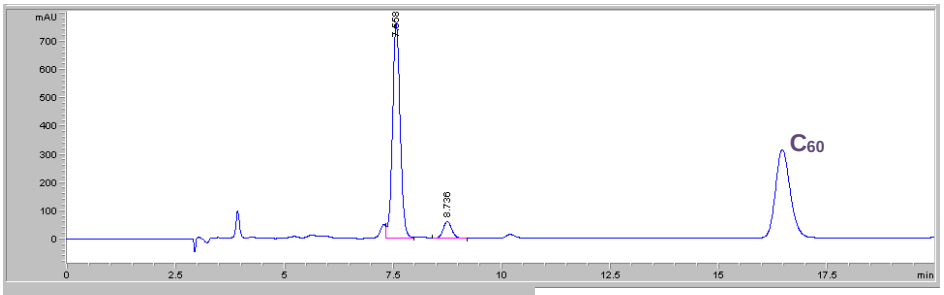

#	Time	Area	Height	Width	Area%	Symmetry
1	7.558	9329.8	764.9	0.1883	91.530	0.889
2	8.736	863.4	60.4	0.2188	8.470	0.917

Figure 44. Diastereomeric ratio between (*P*,*S*,*S*)-**11** (t_R = 7.6 min) and (*P*,*R*,*R*)-**12** (t_R = 8.7 min) of enantioriched iminoester *P*-**10** cycloaddition onto [60]fullerene.

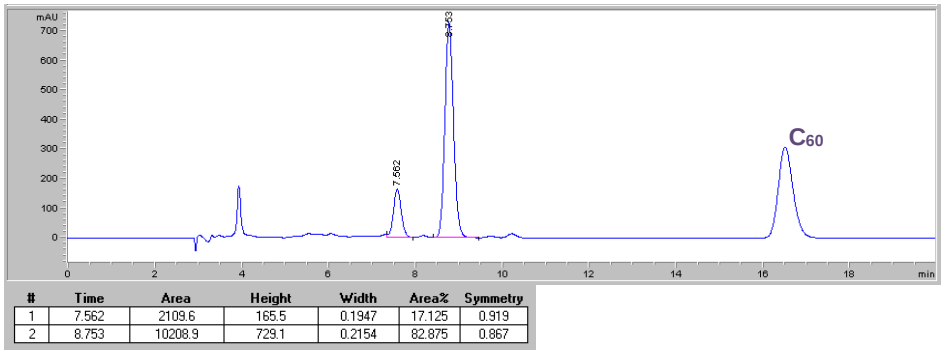

#	Time	Area	Height	Width	Area%	Symmetry
1	7.562	2109.6	165.5	0.1947	17.125	0.919
2	8.753	10208.9	729.1	0.2154	82.875	0.867

Figure 45. Diastereomeric ratio between (*M*,*R*,*R*)-**11** (t_R = 7.6 min) and (*M*,*S*,*S*)-**12** (t_R = 8.7 min) of enantioenriched iminoester *M*-**10** cycloaddition onto [60]fullerene.

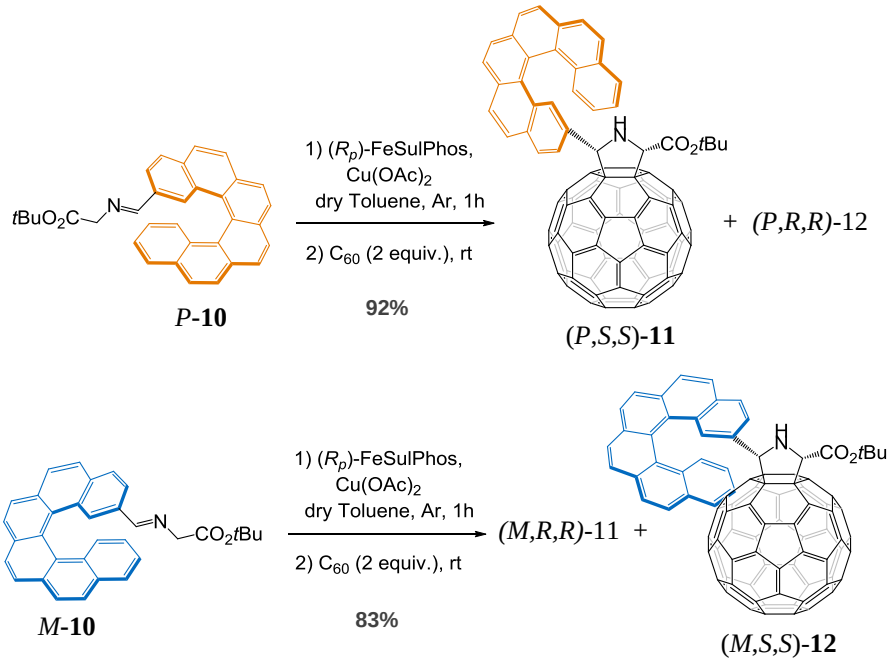

Scheme 41. Cycloaddition reaction of iminoesters *P*-**10** and *M*-**10** to C_{60}.

The CD spectra of the four stereoisomers feature the characteristic peaks of both helicene and [60]fullerene monoadduct, and they also confirm the aforementioned asignment. Thus, at 330 nm the helicene moiety gives rise to an

intense peak in the circular dichroism spectrum (Figure 46),[140] with the positive or negative sign corresponding to the enantiomers *P* or *M*, respectively, while the peak at 427 nm is the fingerprint of the [60]fullerene monoadducts chirality, which appeared to show a lower intensity (Figure 46, inset), and is used to assign the absolute stereochemistry of each stereoisomer.[67]

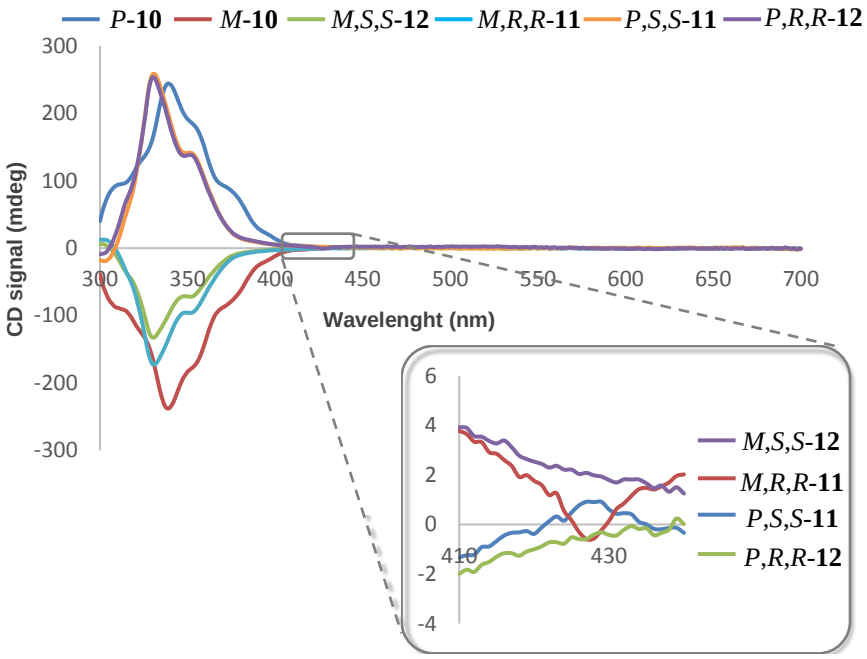

Figure 46. CD spectra (2 x 10^{-4} M in CH_2Cl_2, 25 °C, l = 1mm). Inset peak corresponding to [60]fullerene chirality.

Once proved the efficiency of the chiral catalytic system to carry out the stereodivergent RRM, we extended the scope of such functionalization in order to assess the singular reversible covalent chemistry of fullerenes as a useful platform to carry out the racemate resolution. In particular, we have focused our interest on the retro-cycloaddition reaction of pyrrolidino[3,4:1,2][60]fullerenes developed by our research group (retro-Prato reaction).[26a,c] However, despite this reaction gives rise –in a quantitative manner– to pristine [60]fullerene and

[140] Bouvier, R.; Durand, R.; Favereau, L.; Srebro-Hooper, M.; Dorcet, V.; Roisnel, T.; Vanthuyne, N.; Vesga, Y.; Donnelly, J.; Hernandez, F.; Autschbach, J.; Trolez, Y.; Crassous, J. *Chem. Eur. J.* **2018**, *24*, 14484-14494

aldehyde starting materials in refluxing toluene, we had to change the experimental conditions in order to avoid racemization of chiral aldehydes **9**.

We eventually found in the pair $Cu(ClO_4)_2$/dppe in refluxing THF (70ºC) the suitable conditions to reverse the cycloaddition reaction in good yields and maintaining the enantiomeric excess (Scheme 42). Thus, helicene starting material *P*-**9** was obtained in a 78% yield and *ee* = 99 % from the separated diastereoisomer **11** [99% *ee*, (*P*,*S*,*S*)-**11**], thus maintaining unchanged the optical purity (Figure 47). Analogously, the retro-cycloaddition of **12** [92% *ee*, (*M*,*S*,*S*)-**12**] affords the helicene *M* with 82% yield although the *ee* was slightly lower, 80% *ee* (Figure 48).

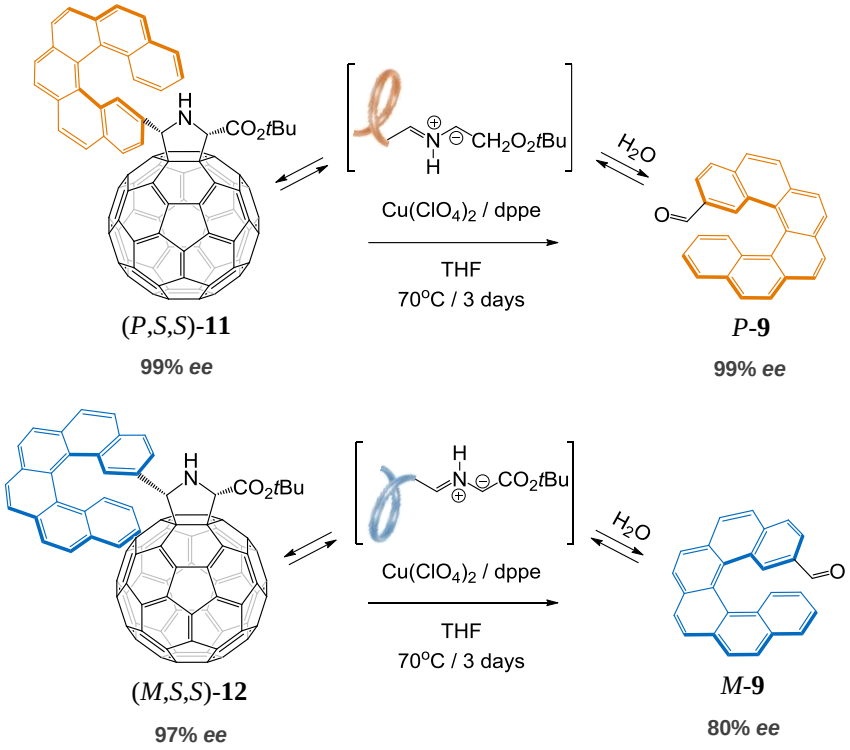

Scheme 42. Enantiospecific retrocycloaddition reaction affording the resolved enantiomer of 2-formyl-helicene **9** with high optical purity.

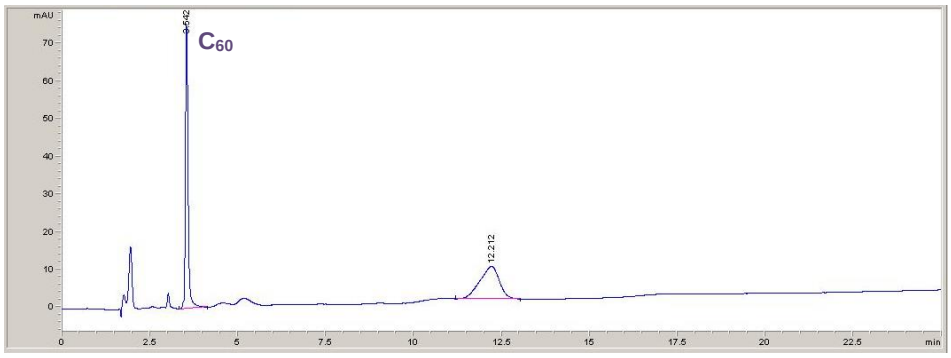

Figure 47. Crude of retrocycloaddition of (*P*,*S*,*S*)-**11**.

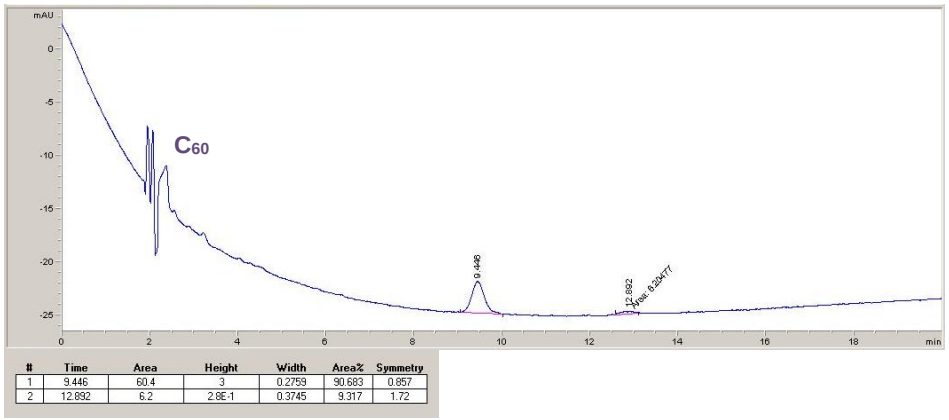

#	Time	Area	Height	Width	Area%	Symmetry
1	9.446	60.4	3	0.2759	90.683	0.857
2	12.892	6.2	2.8E-1	0.3745	9.317	1.72

Figure 48. Crude of retrocycloaddition of (*M*,*S*,*S*)-**12**.

Thus, the efficiency of this resolution and the optical purity obtained reveal the catalytic enantioselective reversible chemistry of fullerene as very useful and alternative tool to carry out a racemate resolution.

4.3. Metallofullerene hybrids

Transition metals are widely recognized as important species for the catalysis of many chemical reactions and continuous efforts are being made to expand their reactivity and to meet new ways of action through suitable ligand choice. In this regard, we wondered if the association of transition metals with fullerenes could give rise to derivatives with new catalytic properties. Actually, the use of fullerenes for catalytic purposes is a topic that has almost been neglected in the literature. In particular, we have been dealing with the synthesis of chiral metallo-fullerenes.[92]

4.3.1. Study of the iridium-fullerene hybrid configuration

In a previous work from our group,[92] the hybrids prepared were endowed with a stereogenic iridium, rhodium or ruthenium metal with a fixed configuration. The uncommon lack of metal racemization was rationalized, by theoretical calculations, with the presence of stabilizing H-bonds between the hydrogens of the pentamethylcyclopentadienyl unit and the phenyl groups and a destabilizing force between the lone pair of the chlorine atom and the π-electrons of the phenyl group for the other opposite metal configuration, which is therefore not observed.

In this regard, we have considered the synthesis of several pyrrolidino[60]fullerenes with different electronic demand on the phenyl substituent to withdraw electron density of the aromatic ring in an attempt to reduce the repulsive Cl-π interaction and to promote the formation of the other epimer, which would feature the opposite metal configuration albeit maintaining the same configuration in the *N*, *C*-2 and *C*-5 atoms of pyrrolidino[60]fullerene.

Thus, we prepared pyrrolidino[60]fullerenes endowed with a cyano group, a nitro group and different number of fluorine atoms in the aromatic ring by the method previously described by our group (Scheme 43).[60]

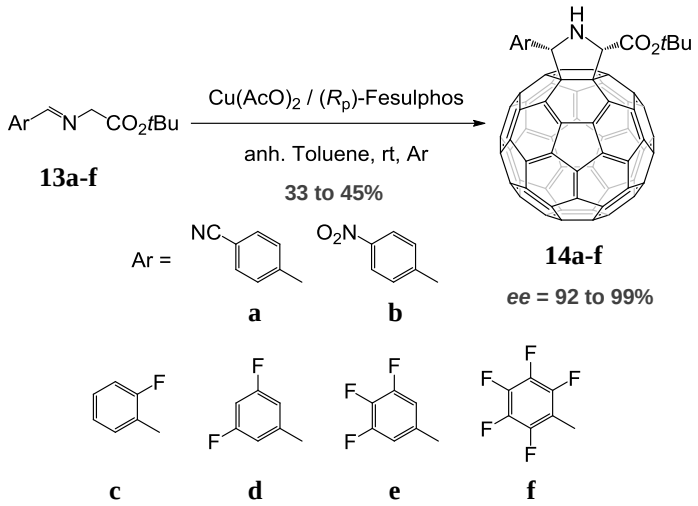

Scheme 43. Synthesis of pyrrolidino[60]fullerenes endowed with electron withdrawing (EWD) groups.

Firstly, iminoesters **13a-f** have been synthesized, by coupling of glycine *tert*-butyl ester hydrochloride and the corresponding substituted benzaldehyde in the presence of triethylamine with 89% to quantitative yields. Then, pyrrolidino[60]fullerenes **14a-f** were synthesized by asymmetric [3+2] cycloaddition of the iminoesters obtained in the previous step onto C_{60} employing the catalytic system Cu(II) acetate/(R_P)-FeSulPhos **P-XV**. Pyrrolidino[60]fullerenes **14** were prepared with 33 to 45% yields and with enantiomeric excesses between 92 and 99%.

Pleasantly, it has been possible to obtain a monocrystal from two of the pyrrolidine derivatives (**14a** and **14b**) which made it possible to confirm the chemical structure and the configuration of its two stereocenters, thanks to the X-ray diffraction analysis. The slow evaporation of a mixture of $CHCl_3/CS_2$ allowed us the successful formation of a suitable high quality single crystal (brown and shiny crystals) (Figure 49). As expected, the X-ray analysis reveals that the configuration of the *C*2 and *C*5 is (2*S*,5*S*) in both cases, which is according to the previously work of our research group for the catalytic system $Cu(OAc)_2$/(R_P)-FeSulPhos **P-XV**.[60]

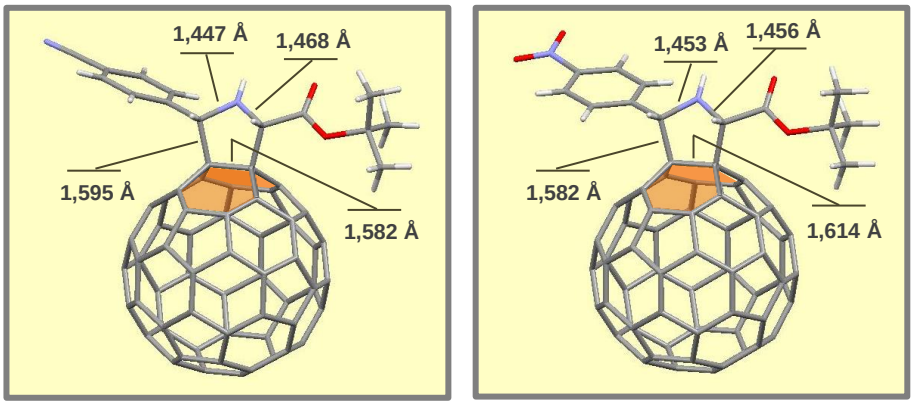

Figure 49. X-ray diffraction analysis of a single crystal of enantiopure pyrrolidino[60]fullerenes (*S*,*S*)-**14a** (left) and (*S*,*S*)-**14b** (right).

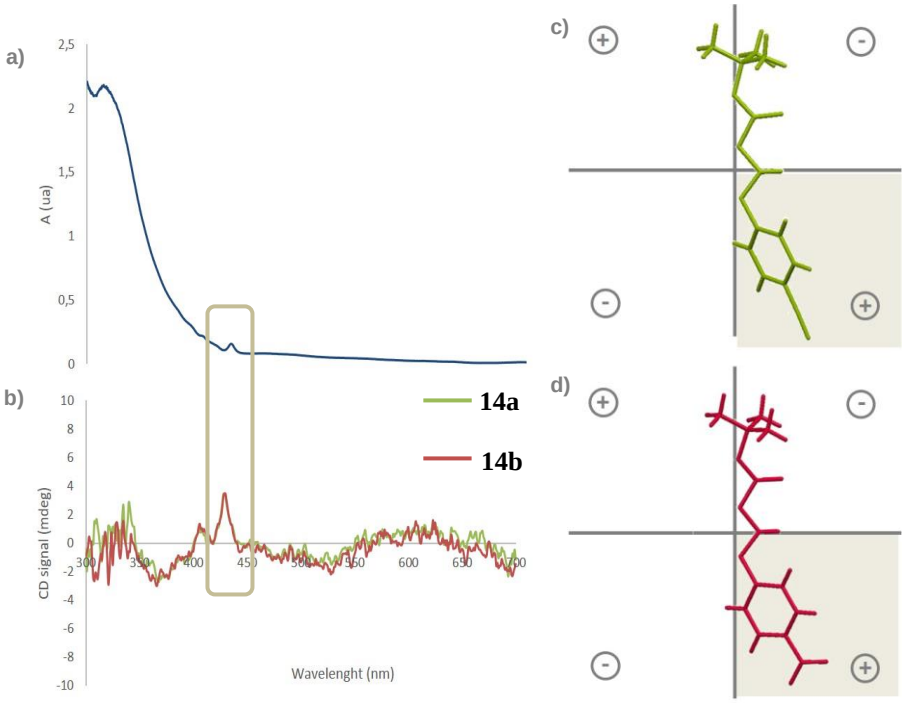

Figure 50. a) UV spectrum of solution $5 \cdot 10^{-5}$ M of **14a** in chlorobenzene (l=10 mm). b) CD spectrum of solutions $5 \cdot 10^{-4}$ M in chlorobenzene of pyrrolidino[60]fullerenes **14a** (green) and **14b** (red). Structure of X ray disposed in the quadrants according to the sector rule of c) **14a** d) **14b**

Moreover, it is important to note that these two crystals and the corresponding CD spectra confirm one more time the validity of the previously reported sector rule (Figure 50).[24,70] Since if the X-ray diffraction elucidated structures of the enantiopure compounds are placed in the quadrants of the sector rule, the bulkiest substitute, the aromatic ring, is placed in a quadrant with a positive sign, which corresponds with the sign of the cotton effect at 429 nm in both compounds, **14a** and **14b**.

After *tert*-butyl ester hydrolysis with TFA (trifluoroacetic acid) of the pyrrolidino[60]fullerenes **14a-f** and iridium complexation by reaction with $[IrCp^*Cl_2]_2$, the corresponding complexes **15a-e** were obtained in good yields, from 67 to 72%, while maintaining the stereochemistry of pyrrolidino[60]fullerenes (Scheme 44). In this step, two new stereocenters appear: the first at the nitrogen atom since it becomes quaternary after the iridium complexation and the second at the metal atom, due to its pseudooctahedral configuration. The nitrogen configuration is determined by the *C*-2 stereochemistry because iridium forms a five member metallacycle fused with the pyrrolidine ring in such a way that the hydrogens in *C*-2 and in the nitrogen atom remain in a cis configuration. However, iridium could adopt two configurations, which would give rise to two epimers (see below). All hybrids have been isolated and characterised with the exception of the pentafluoro derivative which has not been isolated.

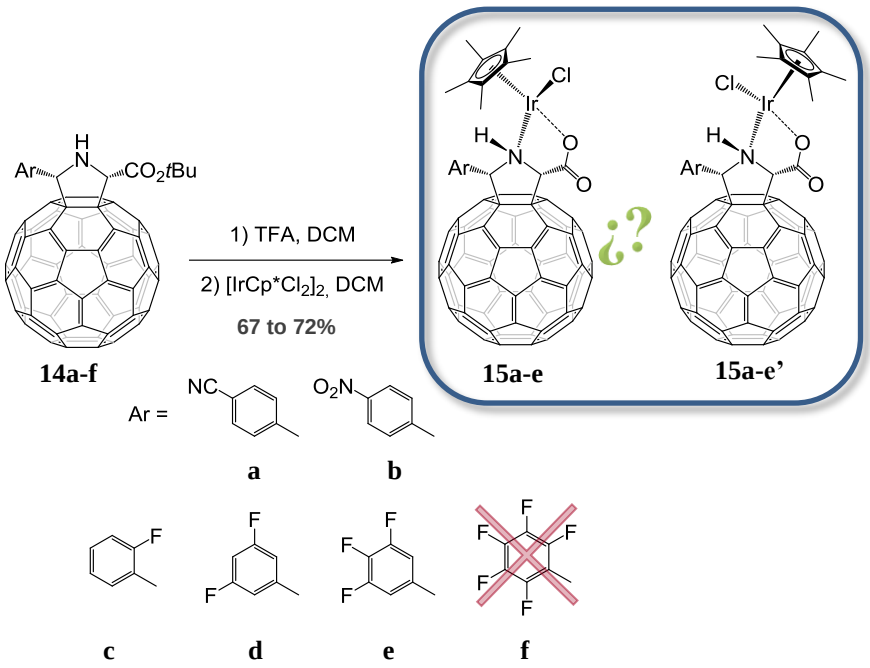

Scheme 44. Synthesis of iridium-fullerene hybrids with electron deficient aromatic rings.

In the case of *p*-cyano and *p*-nitro substituted aromatic rings, the aromatic AB protons system is duplicated after iridium complexation. For *p*-cyano complex **15a**, two aromatic signals should appear in the spectrum, however, there are three signals with an integral ratio of 1:1:2 (Figure 51). For *p*-nitro compound **15b**, the spectrum consists of four aromatic signals with a ratio 1:1:1:1 instead of two signals (Figure 52).

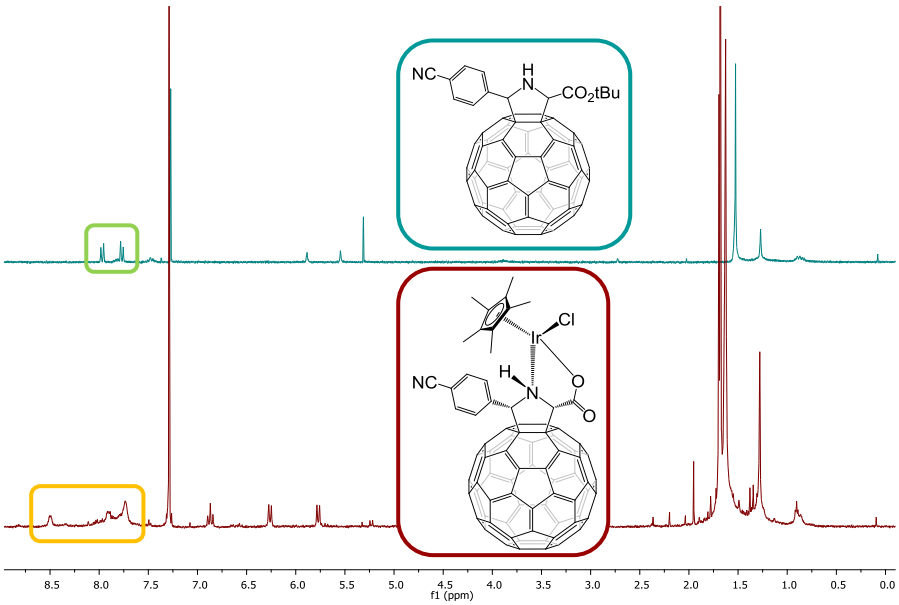

Figure 51. ^{1}H-NMR spectra of pyrrolidino[60]fullerene **14a** (top) and iridium-fullerene hydrid **15a** (down).

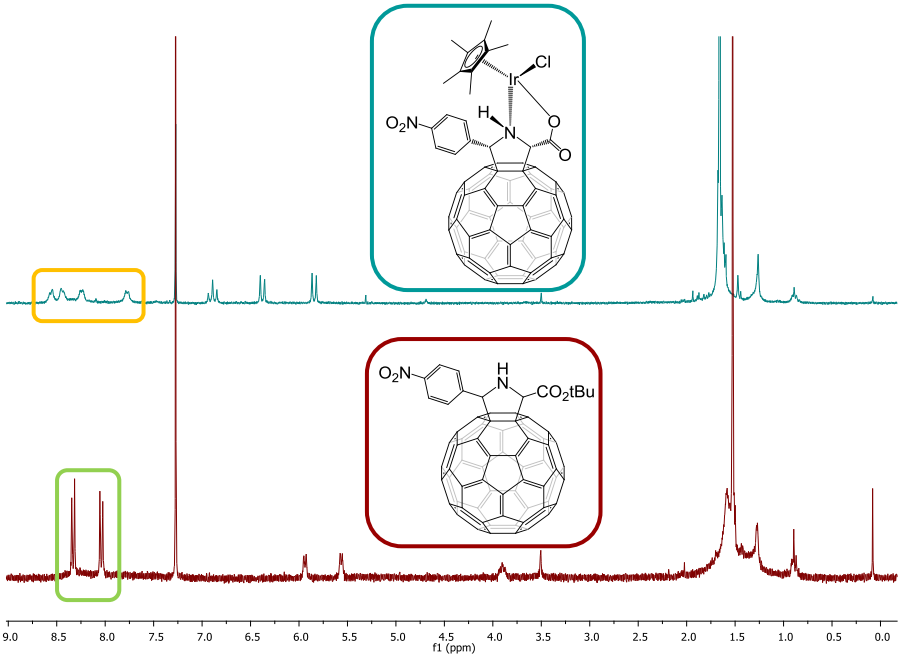

Figure 52. ^{1}H-NMR spectra of pyrrolidino[60]fullerene **14b** (down) and iridium-fullerene hydrid **15b** (top).

The same experimental trend takes place for 3,4,5-trifluorophenyl hybrid **15e** where, instead the expected one aromatic signal, two broad signals appeared in the spectrum (Figure 53).

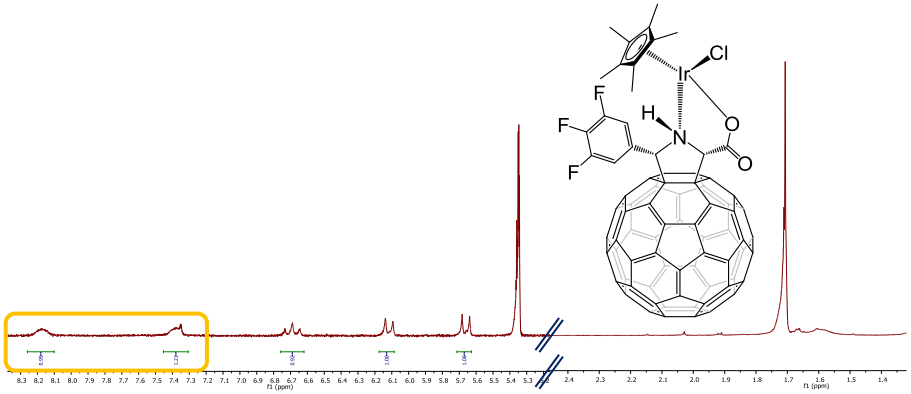

Figure 53. ^{1}H-NMR spectrum of iridium-fullerene hydrid **15e**.

For the *o*-fluorophenyl derivative **15c**, due to the non-symmetric phenyl ring, the number of expected aromatic signals and those appearing in the spectrum are the same (Figure 54).

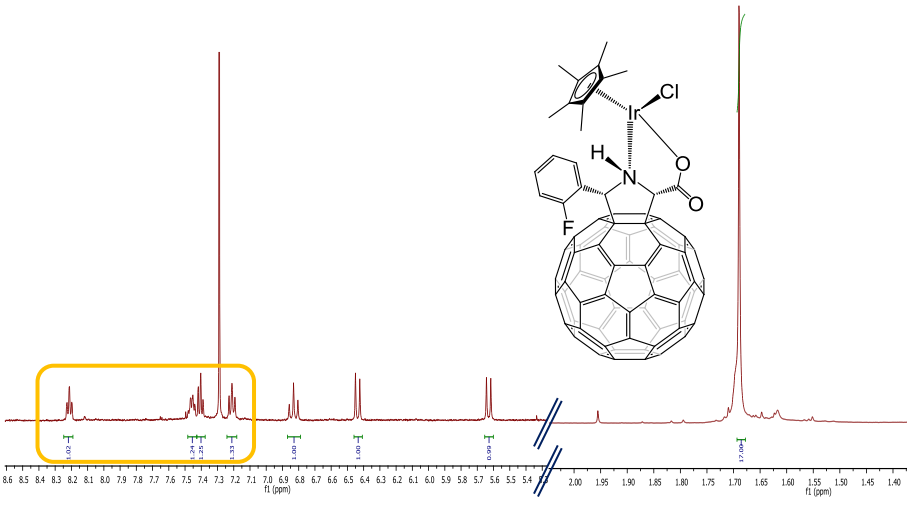

Figure 54. NMR spectrum of iridium-fullerene hydrid **15c**.

However, in the case of the 3,5-difluorophenyl hybrid **15d**, in addition to the loss of aromatic symmetry, also a duplicate of them is appearing in a ratio 1:3, which seems to indicate the presence of two diastereomers (Figure 55).

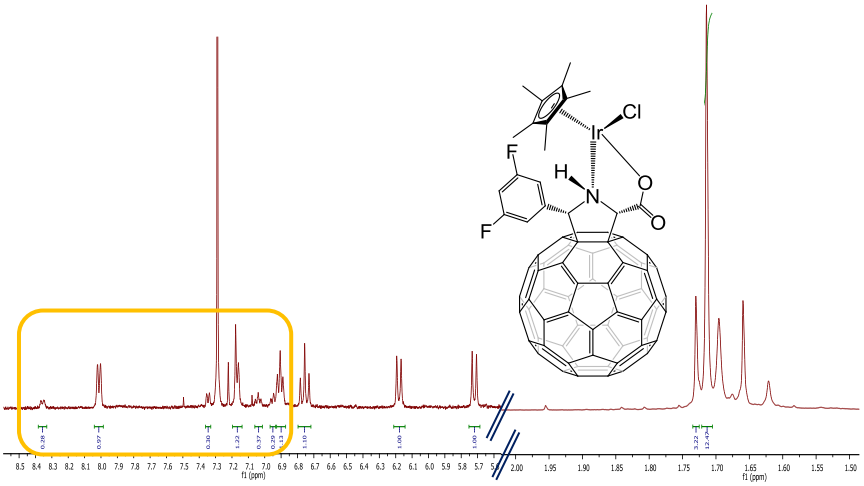

Figure 55. ^{1}H-NMR spectrum of iridium-fullerene hydrid **15d**.

Similar results have been reported by us and other group:[141] A restricted rotation of the aryl ring gives rise to different peaks for the *ortho* and *meta* aromatic protons.

Therefore, in order to confirm this hypotesis, we carried out a temperature ^{1}H-NMR experiment of compound **15b** to analyse the behaviour of these aromatic signals (Figure 56). In this study, the coalescence of the four aromatic signals into a single one from 25ºC to 70ºC is shown.

[141] a) Ajamaa, F.; Figueira Duarte, T. M.; Bourgogne, C.; Holler, M.; Fowler, P. W.; Nierengarten, J. *Eur. J. Org. Chem.* **2005**, *2005*, 3766-3774, b) Suárez, M.; Verdecia, Y.; Illescas, B.; Martínez-Álvarez, R.; Álvarez, A.; Ochoa, E.; Seoane, C.; Kayali, N.; Martín, N. *Tetrahedron* **2003**, *59*, 9179-9186, c) Illescas, B.; Martínez-Grau, M. A.; Torres, M. L.; Fernández-Gadea, J.; Martín, N. *Tetrahedron Lett.* **2002**, *43*, 4133-4136, d) De la Torre, M. D. L.; Marcorin, G. L.; Pirri, G.; Tomé, A. C.; Silva, A. M. S.; Cavaleiro, J. A. S. *Tetrahedron Lett.* **2002**, *43*, 1689-1691, e) Eckert, J.; Nicoud, J.; Nierengarten, J.; Liu, S.; Echegoyen, L.; Barigelletti, F.; Armaroli, N.; Ouali, L.; Krasnikov, V.; Hadziioannou, G. *J. Am. Chem. Soc.* **2000**, *122*, 7467-7479, f) De la Cruz, P.; De la Hoz, A.; Font, L. M.; Langa, F.; Pérez-Rodríguez, M. C. *Tetrahedron Lett.* **1998**, *39*, 6053-6056

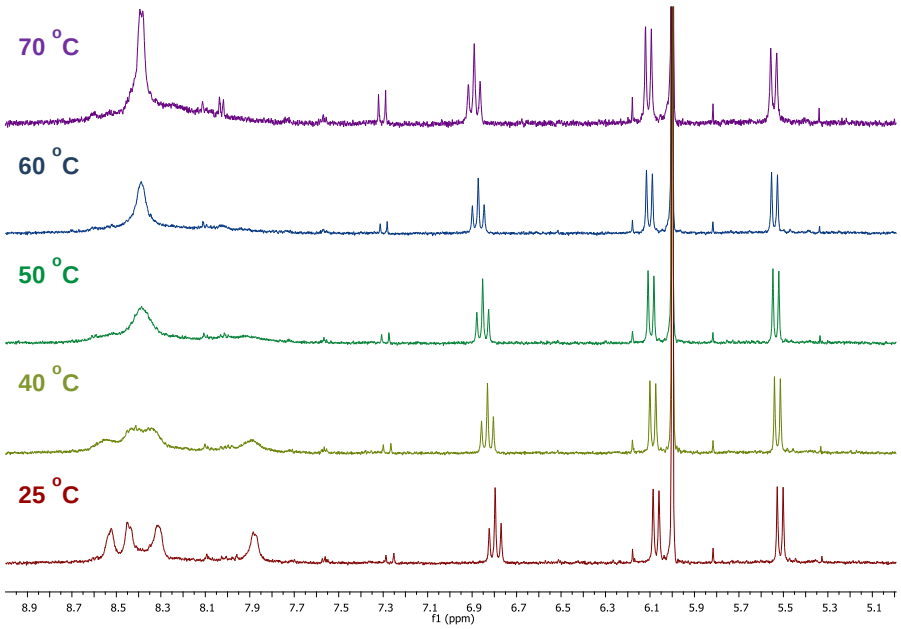

Figure 56. ^{1}H-NMR spectra of **15b** at different temperatures (500 MHz, $C_2D_2Cl_4$).

On the other hand, NOE experiments were registered at 5ºC for the derivative **15b**. When we irradiated at 8.25 ppm, another aromatic signal (8.45 ppm) also appears with the same sign as it also were irradiated (Figure 57). The same effect is observed when we irradiated, in this case at 7.75 ppm, and also the signal at 8.57 ppm is irradiated even though they are very far apart (Figure 58). These findings seem to indicate that the signals that are irradiated together correspond to the same proton but located in different environments.

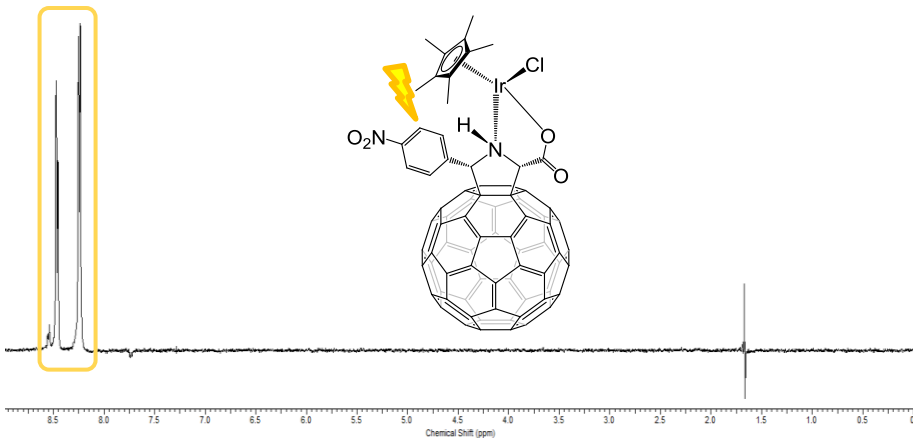

Figure 57. NOE experiment of **15b** irradiating at 8.25ppm.

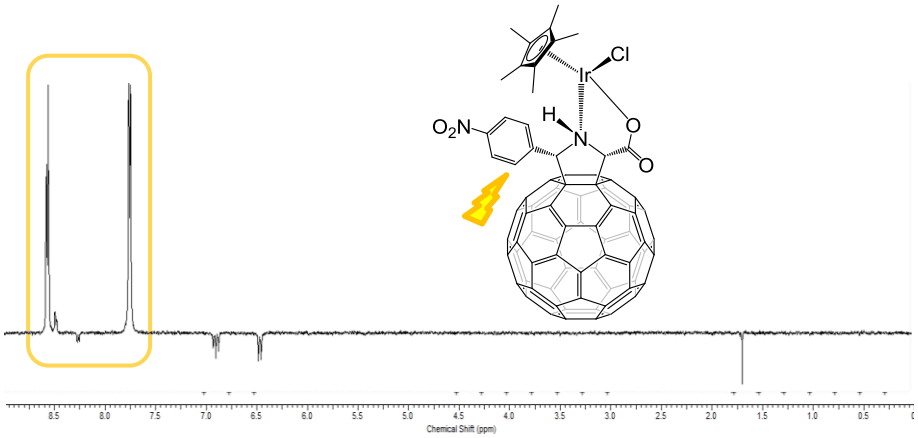

Figure 58. NOE experiment of **15b** irradiating at 7.75ppm.

These ^{1}H-NMR experiments confirm the presence of a restricted rotation of the aromatic ring. It is worthy to note that in sharp contrast with to precedent reported examples,[141] derivatives **15a-e** do not feature bulky substituents (being fluorine atom similar in size to hydrogen atom) in the aromatic ring. Thus, the presence of strong interactions between the Cp* group and aromatic ring (see below) does not only account for the presence of a sole epimer but also for the blockage of the aromatic ring. Actually, no epimerization was observed for any of the aforementioned derivatives **15a-e**. Furthermore, theoretical calculations carried out by Dr. Israel Fernández (Univerisdad Complutense de Madrid), do

not show significant changes of energy when aromatic rings bearing electron withdrawing groups are used (Table 13, entries 2-4, Figure 59-Figure 61). Furthermore, the difference between the two epimers remains similar regardless of the phenyl substituent hybrid (Table 13, entry 1).

Table 13. Energy difference between two epimers of iridium-fullerene hybrids

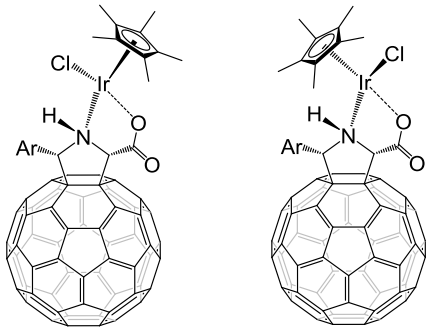

15 **15'**

Entry	Ar (compound)	ΔE / kcal mol^{-1}
1	Ph[92]	8.7
2	*p*-CN-Ph (**15a**, **15a'**)[a]	7.3
3	*p*-NO_2-Ph (**15b**, **15b'**)[b]	7.4
4	3,5-F_2-Ph (**15d**, **15d'**)[c]	8.7

Show the simulated structure of two epimers in: [a] Figure 59; [b] Figure 60; [c] Figure 61.

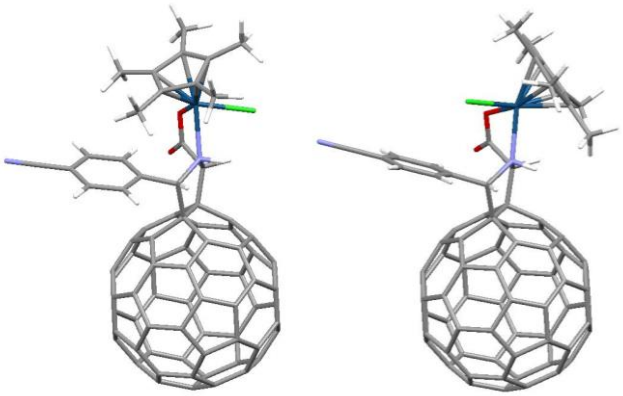

15a **15a'**

Figure 59. Simulated structure of two epimers from iridium atom of iridium-*p*-cyanophenylpyrrolidino[60]fullerene hybrid **15a** and **15a'**.

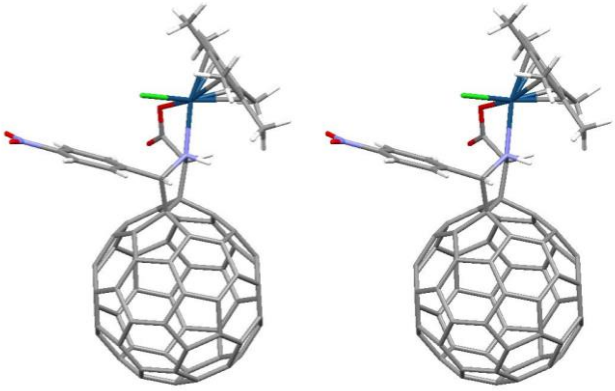

15b **15b'**

Figure 60. Simulated structure of two epimers from iridium atom of iridium-*p*-nitrophenylpyrrolidino[60]fullerene hybrid **15b** and **15b'**.

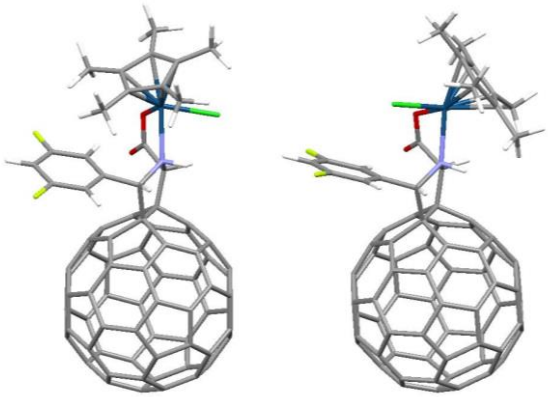

15d **15d'**

Figure 61. Simulated structure of two epimers from iridium atom of iridium-3,5-difluorophenylpyrrolidino[60]fullerene hybrid **15d** and **15d'**.

Thus, contrary to that expected, the employ of electron poor aromatic rings are not able to change the configuration of the metal centers with respect to a pristine phenyl group. Furthermore, the distance between the CH_3 of Cp* and the centroid of the aromatic ring, from 2.497 Å for **15d** to 2.520 Å for **15a** and **15b**, is short enough to hamper the free rotation of this ring (Figure 62).

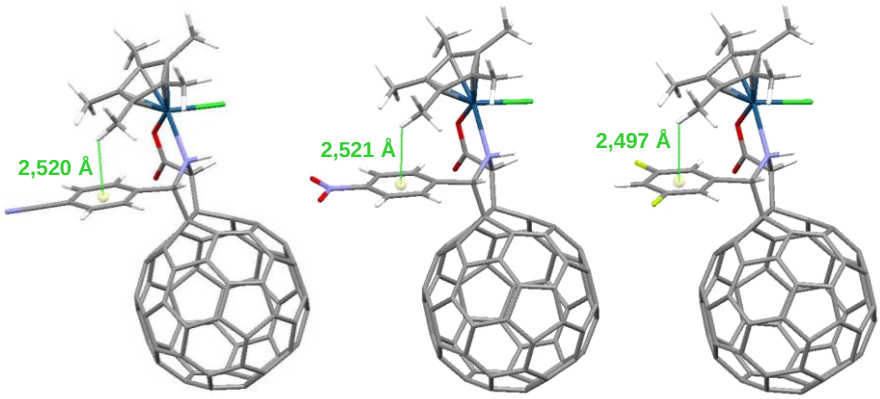

15a **15b** **15d**

Figure 62. Distance (Å) between CH_3 of the Cp* and the centroid of the aromatic ring of iridium-pyrrolidino[60]fullerene hybrids **15a-b** and **15d**.

4.3.2. Synthesis of gold-fullerene hybrid based on pyrrolidino[60]fullerene

Due to the broad use of gold(I) complexes in catalysis, we also considered to extend the family of metallofullerenes to the preparation of gold(I)-fullerene hybrids. A gold fullerene complex had been previously reported using pyrrolidino[60]fullerene endowed with a phosphine due to the good affinity of gold for the phosphorous ligands.[142] However, and taking into account the correlation of some properties of fullerene hybrids with their stereochemistry, we envisaged a more versatile catalyst by the stereoselective preparation of such derivatives.[143]

As a first step, the condensation of the *o*-(diphenylphosphino)benzaldehyde with *tert*-butyl glycinate was carried out under strictly argon atmosphere conditions to avoid the phosphine oxidation (Scheme 45). The α-iminoester **16** was obtained in 83% yield, without further purification.

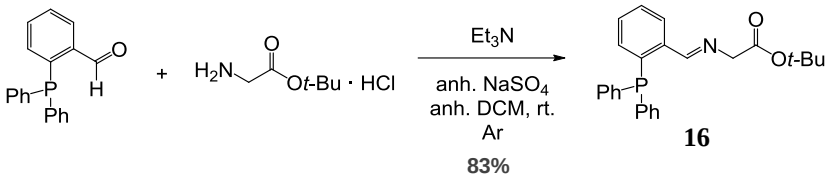

Scheme 45. Synthesis of iminoester bearing a phosphine group (**16**).

As usual, in order to find suitable stereoselective catalysis for the cycloaddition of the α-iminoester **16** to [60]fullerene, we started to evaluate different metals (Ag(I) or Cu(II)), ligands or base (Figure 63). It is important to carry out the reaction and the isolation process under inert conditions, argon atmosphere and anhydrous solvent, in order to avoid oxidation of the phosphine group, easier now due to the presence of the fullerene (scheme in Table 14).

[142] Chen, C.; Yeh, W. *J. Organomet. Chem.* **2015**, *784*, 41-45
[143] Stasyuk, A. J.; Stasyuk, O. A.; Filippone, S.; Martín, N.; Solà, M.; Voityuk, A. A. *Chem. Eur. J.* **2018**, *24*, 13020-13025

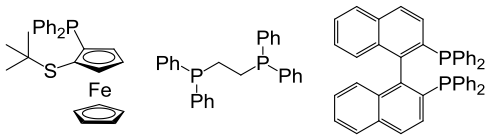

P-XV **P-XVI** **P-XVII**

Figure 63. Commercially available phosphines employed in the cycloaddition of iminoesters onto C_{60}.

Table 14. Cycloaddition of phosphine iminoester **16** onto C_{60}.[a]

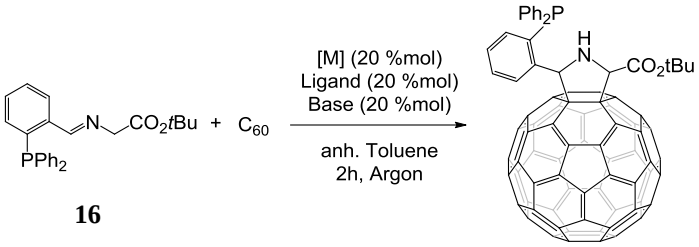

16 **17**

Entry	[M]	Ligand	Base	T (ºC)	Yield[c]	*cis*:*trans* ratio[d]
1	Ag(OAc)	**P-XVI**	-	rt.	80%	35:65
2	$Cu(OAc)_2$	**P-XV**	-	0	68%	39:61
3	$Cu(OTf)_2$[b]	(±)-**P-XVII**	Et_3N (20 %mol)	rt.	76%	8:92

[a] Procedure: The catalytic system (20% mol metallic salt + 20% mol ligand) is preformed for 30 minutes in anhydrous toluene under argon atmosphere at room temperature; then 1.5 equiv. of α-iminoester **16** and 1 equiv. of C_{60} were added. [b] Et_3N is used as a base. [c] Isolated yield; calculated after isolation by column chromatography. [d] Determined by ^{1}H-NMR.

In general, the cycloaddition reaction takes place with high yields (Table 14). However, the presence of a phosphine group seems to affect the diastereoselective direction which tends to be *trans*, even with catalytic systems that had been demonstrated to be *cis*-diastereoselective, such us Ag(OAc)/dppe **P-XVI** and $Cu(OAc)_2$/(R_P)-FeSulPhos **P-XV** (Table 14, entries 1 and 2). On the other hand, the $Cu(OTf)_2$/(±)-BINAP **P-XVII** catalyst, which already directed

the reaction towards the formation of *trans* pyrrolidino[60]fullerenes, provides an increase in diastereoselectivity towards this same diastereoisomer, ratio *cis*:*trans* 8:92 (Table 14, entry 3).

Both diastereoisomers of the pyrrolidino[60]fullerene **17** have been isolated by chromatographic column in silica gel and characterized by NMR. NOE-selective experiments have been carried out irradiating the proton on *C*2 in each diastereoisomer, been observed for one of them an interaction with the *C*5 proton (*cis*-**17**, Figure 64) while the other one interacts with the aromatic protons (*trans*-**17**, Figure 65), thus being able to assign each diastereoisomer.

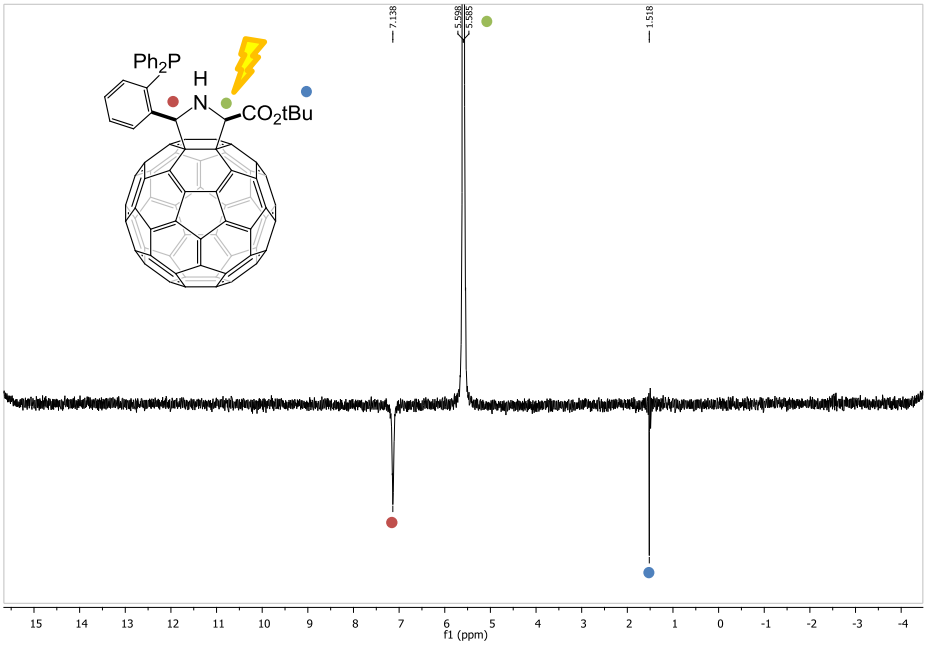

Figure 64. NOE selective spectra of *cis*-phosphinepyrrolidino[60]fullerene (*cis*-**17**) irradiating at 5.69 ppm.

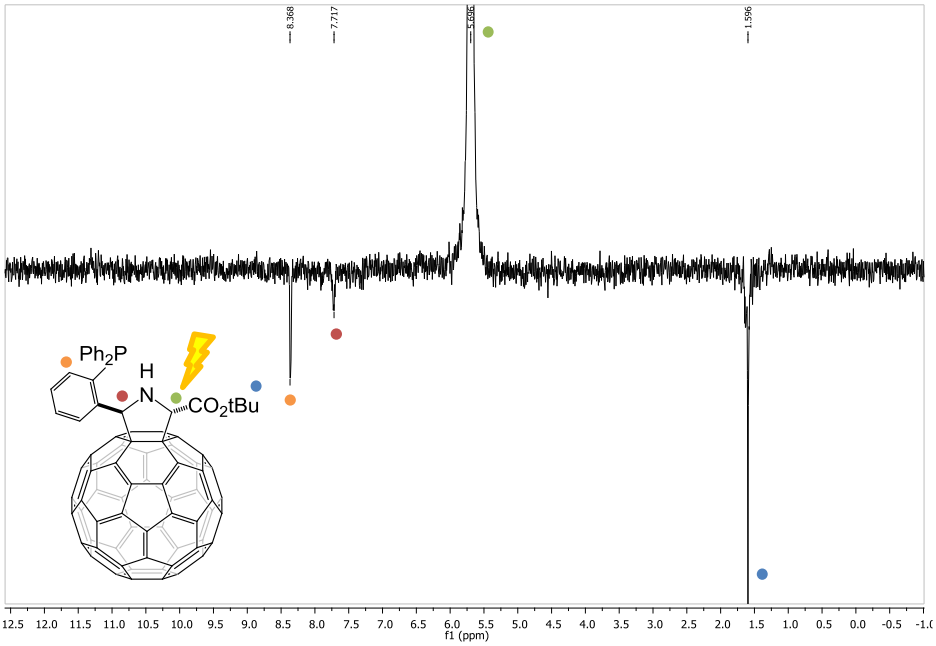

Figure 65. NOE selective spectra of trans-phosphinepyrrolidino[60]fullerene (*trans*-**17**) irradiating at 5.59 ppm.

Given the extreme ease towards oxidation of phosphorous fullerene derivatives **17**, the formation of gold complex **18** was carried out *in situ* on the mixture of pyrrolidino[60]fullerene diastereoisomers. Only later the diastereoisomeric gold complexes were separated by chromatographic column. Quantitative yields have been obtained in the formation of the gold(I)-pyrrolidine[60]fullerene hybrid **18** (Scheme 46).

The complexation of gold complex to phosphine has been confirmed by ^{31}P{1H}-NMR. In *trans*-pyrrolidino[60]fullerene (*trans*-**17**), the signal corresponding to phosphorus appears as a singlet at -20.45 ppm (Figure 66a). The displacement of the same signal at 28.25 ppm corroborates the formation of the gold(I) (*trans*-**18**) hybrid (Figure 66b). The formation of oxidized phosphine from pyrrolidino[60]fullerne (*trans*-**17**-ox) is excluded because the latter exhibits a singlet at 42.66 ppm (Figure 66c).

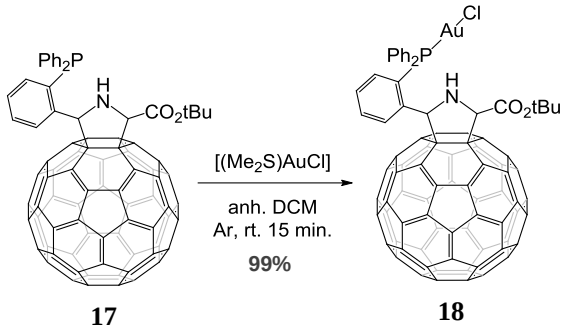

17 **18**

Scheme 46. Synthesis of gold(I)-pyrrolidino[60]fullerene hybrid **18**.

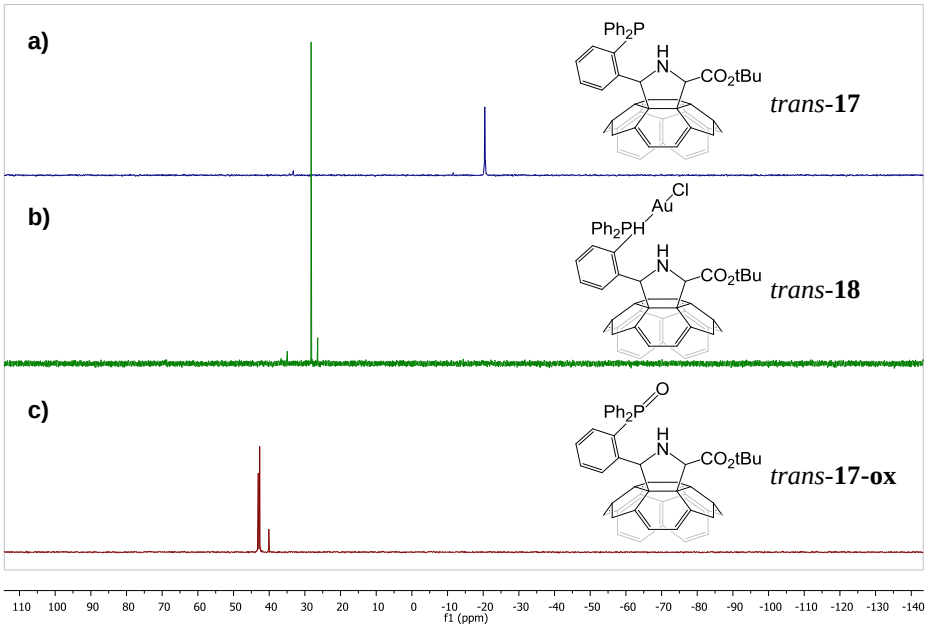

Figure 66. ^{31}P-NMR spectra of a) phosphine pyrrolidino[60]fullerne *trans*-**17**, b) gold(I)-pyrrolidino[60]fullerene hybrid *trans*-**18** and phosphine pyrrolidino[60]fullerne oxide *trans*-**17**-ox.

The two gold(I)-pyrrolidine[60]fullerene diastereoisomers (*cis*-**18** and *trans*-**18**) have been characterized by NMR. Thus, the protons in *C*2 and *C*5 have a chemical displacement of 5.53 and 7.36 ppm, respectively for *cis*-**18**, and 5.63 and 7.65 ppm, for *trans*-**18**. The structures of the two diastereoisomers have been confirmed by NOE-selective irradiating the pyrrolidine *C*2 proton of the two

obtained gold complexes **18**. In the *cis*-**18** isomer, this proton evidences the interaction with the pyrrolidine *C*5 proton and with the *tert*-butyl ester group (Figure 67). On the other hand, these same couplings of the *C*2 proton (hydrogen on *C*5, less intense in this case, and the *tert*-butyl group) together with a spatial interaction with the aromatic protons allow us to confirm the structure of the *trans*-**18** isomer (Figure 68).

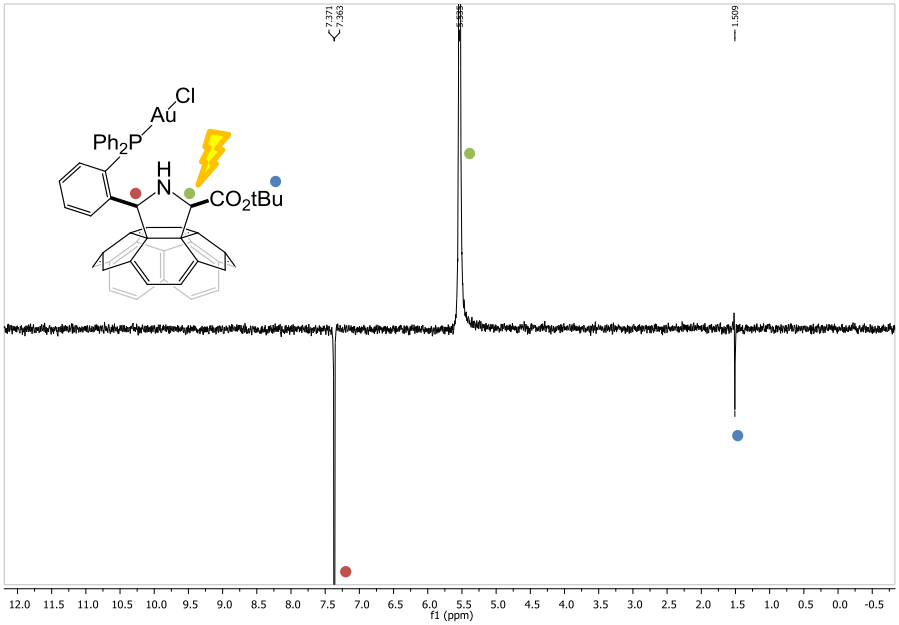

Figure 67. NOE selective spectra of *cis*-gold(I)-fullerene hybrid (*cis*-**18**) irradiating at 5.54 ppm.

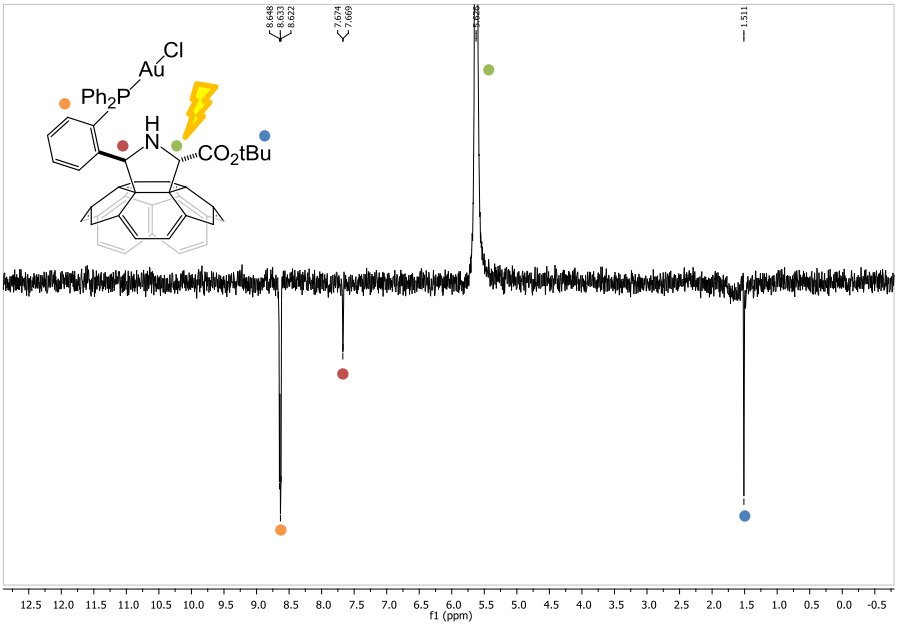

Figure 68. a) NOE selective spectra of *trans*-gold(I)-fullerene hybrid (*trans*-**18**) irradiating at 5.63 ppm

Gold(I)-fullerene hybrids could also be prepared in a "*one pot*" process from α-iminoester **16**, without the need for prior isolation of phosphine-pyrrolidino[60]fullerenes **17** (scheme in Table 15). This new methodology, besides being more direct, avoids the easy oxidation of pyrrolidino[60]fullerenes **17**, since through purification by silica gel chromatography, phosphine-pyrrolidino[60]fullerenes are partially oxidised.

Thus, we studied the effect of different catalytic systems, temperature and amount of reagents on the stereochemical result of [3+2] cycloaddition of azomethine ylide onto C_{60}.

Copper acetate, without the need for phosphine ligand, is capable of carrying out the 1,3-dipolar cycloaddition of azomethine ylide with C_{60} at room temperature. Thus, a conversion of 62% is obtained after half an hour, *trans*-**18** diastereosomer is obtained predominantly (*d.e.* 82 %, Table 15, entry 1). When the temperature decreases to -40ºC the reaction is slower, while the diastereoselectivity is lower, increasing the product *cis*-**18**, with respect to the

same reaction at room temperature, being the ratio *cis*-**18**:*trans*-**18** almost 1:1 (Table 15, entry 2).

Table 15. Stereoselective synthesis "*one pot*" of gold(I)-pyrrolino[60]fullerene **18**.

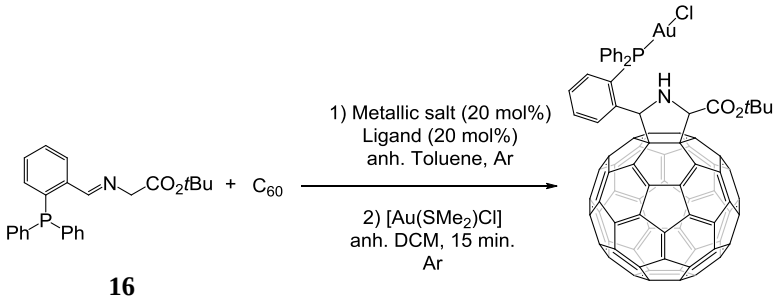

16 **18**

Entry	Metallic salt	Ligand	T (ºC)	Time (min)	Conv.[d] (%)	*cis*-**18** *trans*-**18** ratio[d]
1	$Cu(OAc)_2$	-	rt.	30	62	9:91
2	$Cu(OAc)_2$	-	-40	120	48	49:51
3	$Cu(OAc)_2$	**P-XV**	0	5	45	77:23
4	$Cu(OAc)_2$[b]	**P-XV**	0	5	68	51:49
5	$Cu(OAc)_2$	**P-XV**	-18	180	74	97:3
6	$Cu(OAc)_2$	**P-XV**	-40	120	71	97:3
7	$Cu(OAc)_2$	**P-XV**	-55	390	75	>99:1
8	$Cu(OAc)_2$[c]	**P-XV**	-18	60	71	>99:1
9	$Cu(OAc)_2$[c]	**P-XV**	-40	60	33	>99:1
10	Ag(OAc)	**P-XIV**	-40	120	55	70:30

[a] Procedure: The catalytic system (20% mol metallic salt + 20% mol ligand) is preformed for 30 minutes in anhydrous toluene under argon atmosphere at room temperature; then 1 equiv. of α-iminoester **16** and 1 equiv. of C_{60} are added. After the indicated time, 1 equiv. of [(SMe_2)AuCl] solved in anh. DCM is added. [b] 1.5 equiv. of iminoester **16** is employed. [c] The order of addition is reversed: firstly, the α-iminoéster **16** is complexed with [(SMe_2)AuCl] and, subsequently, it has been mixed with the catalyst and finally with C_{60}. [d] Determined by HPLC (ChiralPack IA. toluene:DCM:hexane:acetonitrile = 45:14:40:1, 0.5 mL/min).

When the ligand (R_P)-FeSulPhos **P-XV** has been used, the reaction becomes faster. In addition, a drastic change in diastereoselectivity is showed, with prevalent formation of *cis*-**18** isomer, according to the results reported in the literature (Table 15, entry 3).[60,61,128] If the number of equivalents of α-iminoester **16** is increased from 1 to 1.5, the conversion raised, nevertheless, the diastereomeric excess decreases, since possibly the iminoester could react without ligand, which favours the *trans* diastereoselective (Table 15, entry 4). Fortunately, it has been possible to completely change the diastereoselectivity by lowing the temperature (Table 15, entries 5-7) and thus, *cis*-**18** isomer is obtained exclusively at -55ºC using $Cu(OAc)_2$/(R_P)-FeSulPhos **P-XV** (Table 15, entries 7).

On the other hand, we wondered if a change in the order of reactive addition would affect stereoselectivity. Thus, firstly, the iminoester **16** was reacted with the complex [(SMe_2)AuCl], and later, the [3+2] cycloaddition of gold(I)-azomethine ylide complex onto C_{60} has been carried out (Table 15, entries 8 and 9). The gold(I)-fullerene hybrid **18** was obtained with good conversion and with the same excellent *cis* diastereoselectivity without the need of extremely low temperature (-18ºC) and in shorter reaction time (Table 15, entry 9).

Finally, we tested the system AgOAc/**P-XIV**, which provided a lower conversion and diastereomeric excess in comparison to $Cu(OAc)_2$/(R_P)-FeSulPhos **P-XV** pair (Table 15, entry 10 *vs* entry 6).

For our pleasure, we have been able to obtain a single crystal of the *cis*-gold(I)-fullerene hybrid **18** with which it has been possible to confirm the complex structure by X-ray diffraction (Figure 69).

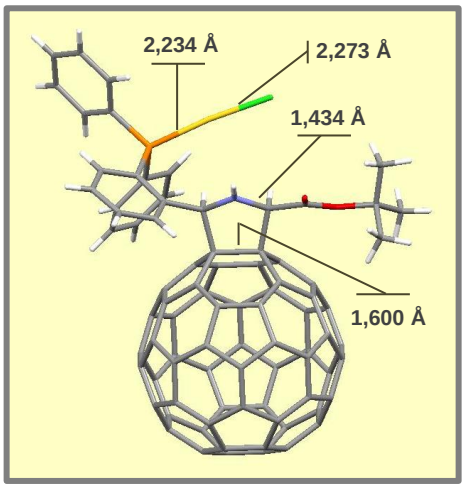

Figure 69. X-ray diffraction of a crystal of *cis*-**18** obtained by slow evaporation in toluene/acetonitrile.

4.4. Fullerenes derivatives for photoelectrocatalytic devices

Based on the electronic properties of fullerene derivatives, bulk heterojunction (BHJ) organic photovoltaic solar cells (OPV) have been the most notable application for these compounds. However, an interesting and challenging extension of acceptor/donor BHJs has been the realization of photo-electrochemical cells, similar to polymeric solar cells but in contact with aqueous and/or non-aqueous electrolytes. These devices are thought, upon visible light illumination, to carry out efficient oxygen reduction reaction (ORR) by the use of suitable redox catalysts.

Thus, we have carried out the synthesis of new fullerene derivatives, suitably functionalized with catalytic active sites towards ORR in order to exploit them with a double purpose. Firstly, fullerene derivatives are expected to act as electron acceptors, along with the donor polymer, like in BHJ solar cells. Secondly, by endowing them with active redox sites, it would be avoided the use of typical and expensive bulky noble metals electrodes, such as platinum, as in classical photoelectrochemical cells. (PECs) (Figure 70).

Therefore, two main approaches have been undertaken in parallel:

i) Synthesis of new fullerene hybrid derivatives endowed with noble metals active in redox processes, such as Ir, Rh or Pt. Here the use of noble metals is just limited to catalytic amounts while the bulk of the electrode results to be organic.

ii) Synthesis of metal-free fullerene catalysts, based on the presence of active C_{60}-H bonds.

To this aim, both metal- and organo-catalytic methodologies have been employed, to obtain fullerene derivatives with tailored electronic and photocatalytic properties characterized by high stereo-selectivity.

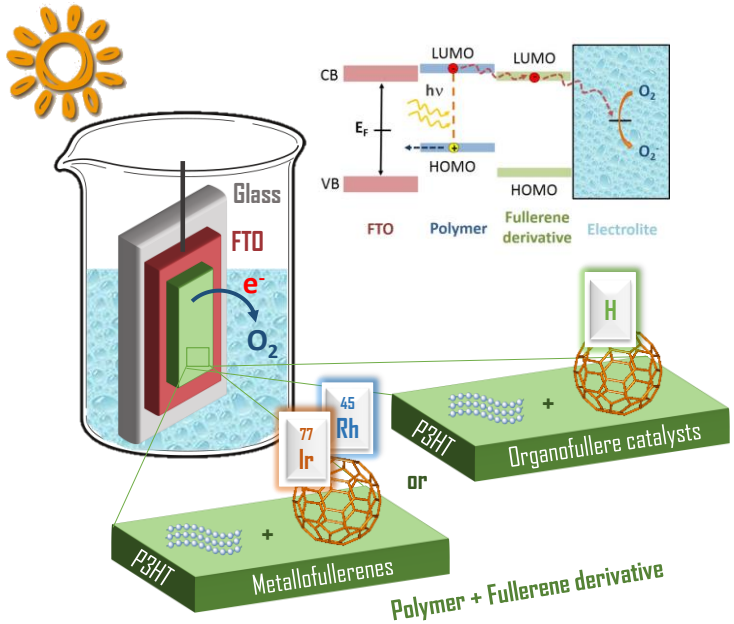

Figure 70. Schematic sketch of an organic-based photo-electrochemical device for ORR, based on P3HT:fullerene BHJ thin films. The working mechanism and the energetic levels schemes are also represented.

4.4.1. Synthesis of metallo- and organo-fullerenes catalysts

4.4.1.1. Pyrrolino-metallo-fullerenes

With the aim of preparing stable metallo-fullerene hybrids, we firstly directed our attention onto iridium (III) complexes due to their wide use in hydrogenation processes and for their ability to form stable and easily isolable complexes. Thus, the design of the iridium-fullerene complexes were based on the preparation of pyrrolino[60]fullerene ligands endowed with a carboxylic group to bind efficiently iridium(III) as well as other active metals. To this purpose, we carried out the 1,3-dipolar cycloaddition reaction of azlactone **19** onto [60]fullerene by using a racemic BINAP (**PXVII**)/silver acetate catalyst, followed by the addition of the iridium dimer $[Cp^*IrCl_2]_2$ (Scheme 47). A unique compound, **20Ir**, was obtained in "one-pot" and in good yield (ca. 40%) as a result of two sequential processes where two chiral centers are formed: in the first step, a pyrrolino[3,4:1,2][60]fullerene carboxylic acid is formed with a stereogenic center in the *C*-5 of the pyrroline ring. In the second process, iridium(III) is

covalently linked diastereoselectively to the [60]fullerene derivative through the formation of two new bonds, one with the nitrogen of the pyrroline ring and the other one with the oxygen of the carboxylate group. The presence of the metal is confirmed by the IR spectrum of the isolated solid, since the ν(CO) of the starting pyrroline shifts from 1700 cm^{-1} to 1660 cm^{-1} in the final product, which is in agreement with the previously observed behaviour of fullerene-iminocarboxylate as (*N*, *O*)-chelating monoanionic ligands.[144] It is worthy to note that, despite iridium(III), with its typical pseudo-tetrahedral geometry, could adopt two possible configurations and, therefore, affording a diastereomeric mixture, the overall process occurs diastereoselectively and no epimerization is observed, as well as iridium complexes derived from phenyl-pyrrolidino[60]fullerene, in sharp contrast to other related examples.[93b]

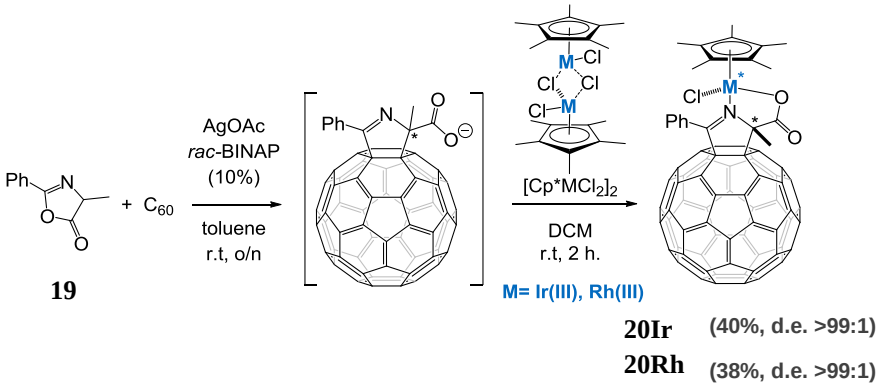

Scheme 47. Diastereomeric synthesis of iridium (**20Ir**) and rhodium (**20Rh**) pyrrolino[3,4:1,2][60]fullerene.

Indeed, this behaviour was observed by ^{1}H-NMR (Figure 71): in particular, a sole signal corresponding to the 15 hydrogen atoms of Cp* group appear at 1.57 ppm sharp and high as a singlet while in the presence of epimerization Cp* gives rise to two signals.

[144] a) Laurie, S. H. *Comprehensive Coordination Chemistry, vol. 2*, Pergamon, Oxford, **1987**, b) Nakamoto, K. *Infrared and Raman Spectra of Inorganic and Coordination Compounds*, Wiley, New York, **1986**

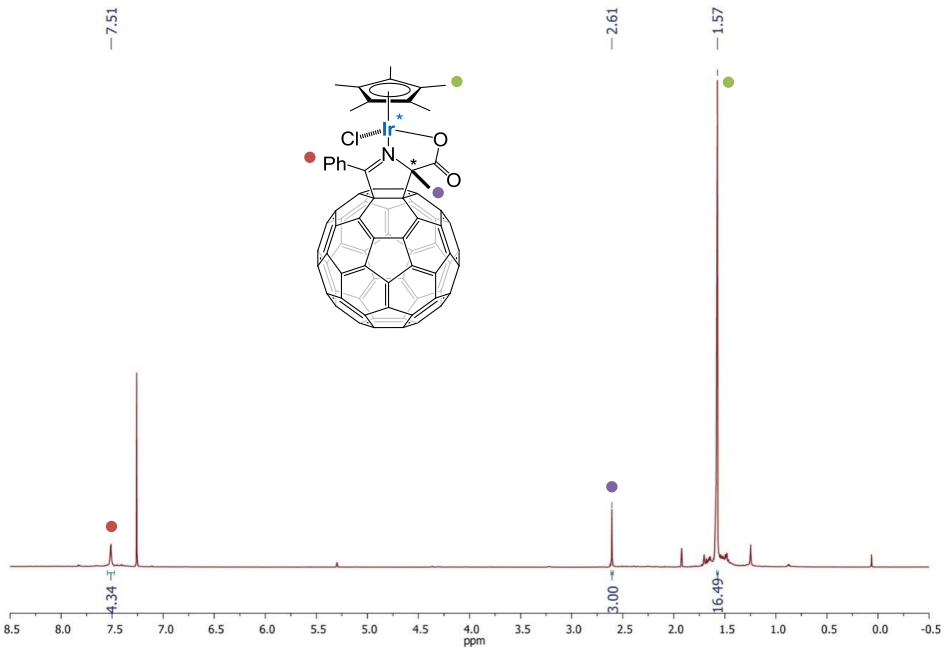

Figure 71. ^{1}H NMR spectrum of **20Ir**.

Luckily, its structure and its relative stereochemistry has been confirmed by X-ray diffraction analysis of a monocrystal obtained by slow evaporation of **20Ir** in CS_2/hexane.

As it is shown in Figure 72, the iridium atom adopts a pseudo octahedral geometry where Cp* group occupies a face of the octahedron, being 1.775 Å the distance between the metal and the ring centroid. Two other octahedron positions involve the chelate pyrrolinofullerene carboxylate featuring an Ir-N, Ir-O bonds of 2.103(4) Å and 2.095(4) Å length, respectively. Finally, the determined Ir-Cl bond distance resulted to be 2.393(2) Å, which is slightly shorter than other related pyrrolidinocarboxylate Iridiun Cp* complexes.[93b] The distance between the two sphere sp^3 carbon atoms is 1.590(8) Å, which is in the typical range for a fullerene monoadduct.

X-Ray analysis confirms the presence of a single diastereomer (with both enantiomers) with the chlorine atom in a *trans* position to the methyl group of the pyrroline cycle.

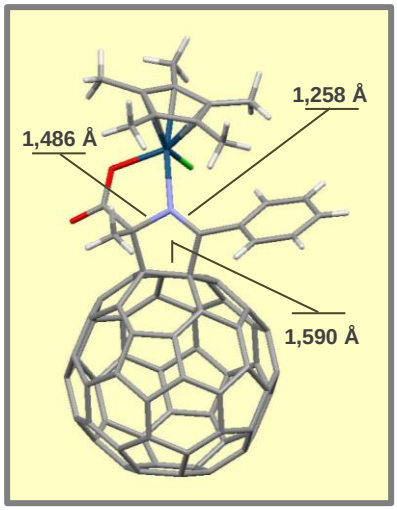

Figure 72. X-ray diffraction of a crystal of **20Ir** obtained by slow evaporation in CS_2/hexane.

Analogously, a rhodium pyrroline[60]fullerene hybrid **20Rh** was prepared in 38% yield, by using $[Cp^*RhCl_2]_2$ after the cycloaddition of the same azlactone **19** (Scheme 47).

4.4.1.2. Organocatalytic synthesis of metal-free fullerene catalyst

Considering that hydrogenated fullerene derivatives are reactive in the presence of low amounts of oxygen, we wondered if the presence of highly active hydrogen directly linked to the carbon cage could replace precious metals but still maintaining a high catalytic activity. Thus, we designed a regioselective double addition on [60]fullerene where a C_{60}-H bond is formed by the use of organocatalytic methodology. To this aim, we extended the scope of our previously described phosphine catalysed cycloaddition of allenoates/alkynoates to [60]fullerene to 5-hydroxy-3-alkynoates (Scheme 48).

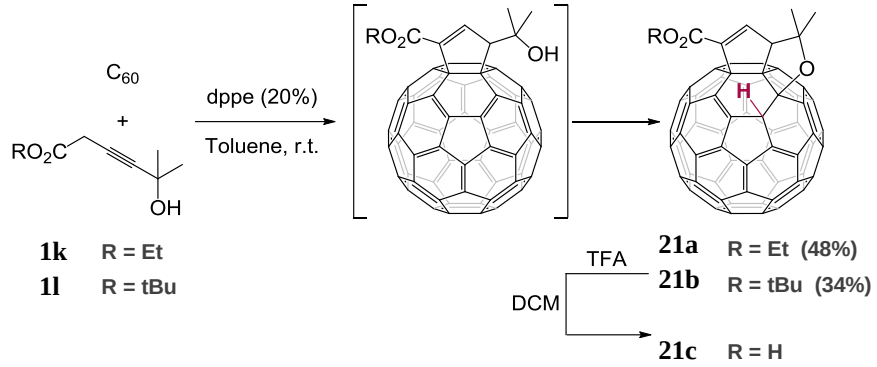

Scheme 48. *Cis*-1 regioselective fullerene bifunctionalization affording fullerene hydrides.

Thus, as described in chapter 4.1.1, after alkynoate/allenoate isomerization, 1,2-diphenylphosphino ethane (dppe, **P-XVI**) catalysed Lu's [3+2] cycloaddition[69] of **1k-l** affording the corresponding cyclopenteno[60]fullerene. These products are not isolated since they underwent an easy regioselective addition of the hydroxyl group to the *cis*-1 double bond of C_{60} giving rise to bisadducts **21a-b** endowed with a C_{60}-H bond in 48% and 34% yields, respectively. Eventually, the corresponding acid **21c** was obtained after acidic removal of *tert*-butyl ester.

4.4.2. Photocatalytic activity of [60]fullerene derivatives toward ORR in photoelectrochemical devices

The new fullerene derivatives were finally tested as photo-electrocatalysts for ORR in polymer-based devices, in collaboration with the group of the Prof. Antognazza in Milan. The overall electrochemical performances were compared to devices employing **PCBM** as a standard reference material. The compounds that have been tested are classified in Figure 73 into three main types: fullerenes without catalytic sites, but with higher-lying LUMO levels compared to **PCBM**, as mere acceptor components (DPM-12 and bisDPM-12, top panel); hybrid fullerenes with metallic catalytic sites (**20Ir**, **20Rh** and **22** compounds, down-left panel) and metal-free fullerenes (**21a-c** compounds, down-right panel).

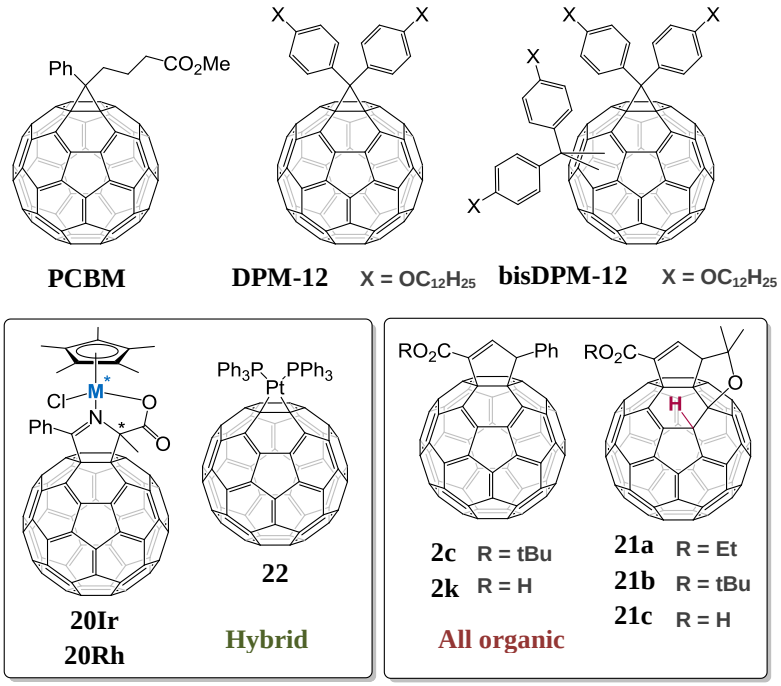

Figure 73. Fullerene derivatives used as acceptors/catalysts in photo-electrochemical devices.

BHJ thin films (~140 nm), based on rr-P3HT as photoactive donor component, were deposited by spin coating on top of FTO-covered glass substrates. In some cases, a second thin film fullerene layer was deposited on top of the photoactive component, in order to directly expose catalytic sites to the electrolyte. Photo-catalytic activity towards oxygen reduction was assessed in sodium phosphate buffer (PBS) at pH 7.4 and controlled dissolved oxygen (DO) concentration (5.8 mg/L). The optical absorption spectra of all prepared thin films showed similar absorption values, which ensured that different current values were not the result of films with different absorptions (Figure 74).

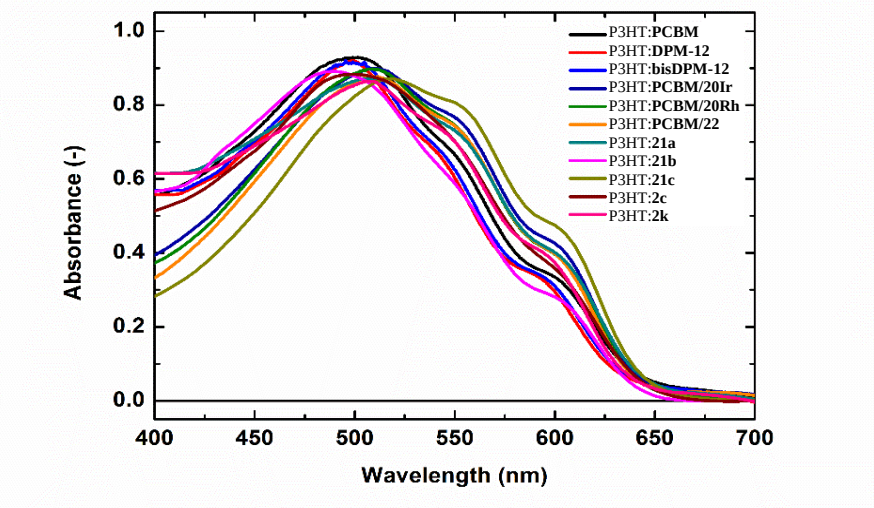

Figure 74. Optical absorption spectra of BHJ (P3HT:**fullerene**) and bilayer (P3HT:**PCBM**/**fullerene**) thin films based on P3HT as electron donor and different fullerene derivatives as electron acceptors/catalysts for promotion of ORR. Fullerene compounds include **PCBM** (here used as benchmark, reference material), bis-adducts fullerenes (**DPM-12** and **bisDPM-12**), fullerenes endowing metallic catalytic centers (**20Ir**; **20Rh**; **22**) and metal-free organo-fullerene catalysts (**21a-c**, **2c, 2k**).

Figure 75 reports Linear Scan Voltammetry (LSV) recorded in dark and upon illumination (1 SUN) in devices based on fullerene acceptors without any catalytic site (**PCBM**, **DPM-12** and **bisDPM-12**). As reported in a previous work,[97] in the absence of light, negligible current values (dashed lines) are generated in the observed window bias (from -0.2 to 0.4 V), thus the recorded current signal can be unambiguously attributed to photo-activated electrochemical reactions occurring at the hybrid organic/electrolyte interface and in particular to ORR. An increase of photocurrent was observed in **DPM-12** based films (red line) with respect to **PCBM** (black line), and even more for the DPM bisadducts **bisDPM-12** (blue line), as a result of a more efficient ORR.

In particular, the use of **DPM-12** and **bisDPM-12** fullerene bisadducts allows to increase the Onset Potential (OP, defined here as the voltage at which the photocurrent density amounts at 100 nA/cm^2) up to 0.15 V *vs*. Ag/AgCl and 0.35 V *vs*. Ag/AgCl, respectively, with respect to the reference **PCBM**, 0.12 V *vs*. Ag/AgCl. Correspondingly, at a fixed voltage the photocurrent density increases: at -0.15 V *vs*. Ag/AgCl, for instance, it amounts at -2.4 μA/cm^2, -5.2

μA/cm^2, -8.2 μA/cm^2 for **PCBM**, **DPM-12** and **bisDPM-12**, respectively. An analogous behavior has also been reported in organic solar cells, where an increase of the open circuit voltage in the case of **DPM-12** and **bisDPM-12** was reported, when compared to **PCBM**.[145] The enhanced performances are possibly attributed to the broader density of states and to the higher-lying LUMO level of the fullerene bisadducts, able to facilitate the electron transfer processes occurring at the organic/electrolyte interfaces (Figure 76).

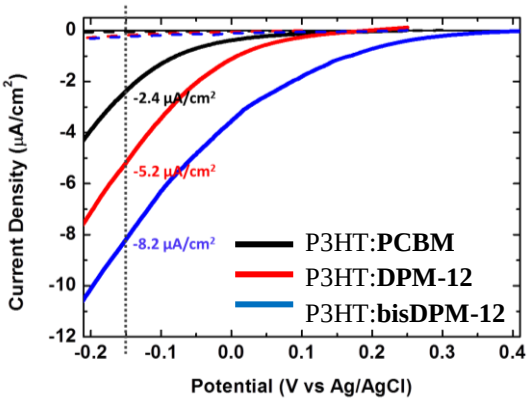

Figure 75. Linear Scan Voltammetry (LSV) measurements under dark (dashed lines) and upon visible light (1 SUN) (solid lines) on FTO/ P3HT:fullerenes (**PCBM**, DPM-12 and bisDPM-12) photo-electrochemical cells (scan rate, 10 mV/s). Measurements were performed in sodium phosphate buffer (PBS) at pH 7.4 and controlled dissolved oxygen (DO) concentration (5.8 mgL/1).

Iridium, rhodium and platinum are known to be efficient catalysts for ORR.[146] Thus hybrid catalysts, **20Ir**, **20Rh** and **22**, are expected to provide catalytic properties typical of the embedded metal component, but with a consistently reduced use of precious metals, and with the advantage of a more localized interaction. In this case photo-electrodes were realized by covering the reference P3HT:**PCBM** BHJ layer with an over-layer of pristine electron acceptor, in order

[145] a) Cheng, Y.; Liao, M.; Chang, C.; Kao, W.; Wu, C.; Hsu, C. *Chem. Mater.* **2011**, *23*, 4056-4062, b) Sánchez-Díaz, A.; Izquierdo, M.; Filippone, S.; Martín, N.; Palomares, E. *Adv. Funct. Mater.* **2010**, *20*, 2695-2700, c) García-Belmonte, G.; Boix, P. P.; Bisquert, J.; Lenes, M.; Bolink, H. J.; La Rosa, A.; Filippone, S.; Martín, N. *J. Phys. Chem. Lett.* **2010**, *1*, 2566-2571

[146] a) Nie, Y.; Li, L.; Wei, Z. *Chem. Soc. Rev.* **2015**, *44*, 2168-2201, b) Qiao, J.; Lin, R.; Li, B.; Ma, J.; Liu, J. *Electrochim. Acta* **2010**, *55*, 8490-8497, c) Cao, D.; Wieckowski, A.; Inukai, J.; Alonso-Vante, N. *J. Electrochem. Soc.* **2006**, *153*, A874

to maximize the localization at the electrolyte interface of the catalytic sites endowed within the functionalized fullerene derivatives (P3HT:**PCBM**/hybrid catalyst configuration).

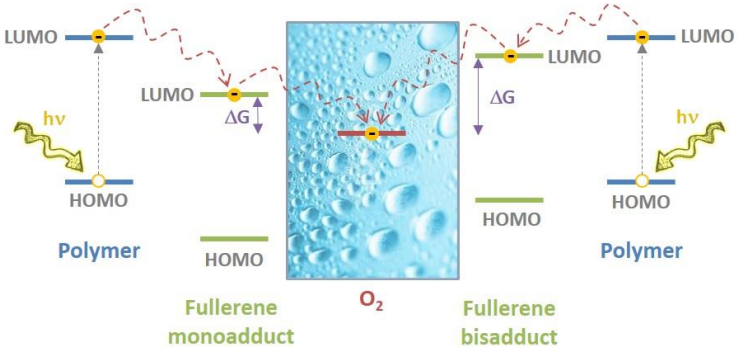

Figure 76. Comparison of energy levels of mono- and bisadduct fullerene derivatives.

The adopted strategy resulted to be successful. All tested hybrid catalysts show photocurrent density values larger of more than one order of magnitude with respect to reference **PCBM**, while dark current values are negligible (Figure 77). Photocurrent generation is clearly related to the presence of dissolved oxygen, and its origin can be safely attributed to the occurrence of ORR. OPs are also considerably increased, shifting from 0.12 V *vs* Ag/AgCl for **PCBM** up to 0.3 V *vs* Ag/AgCl for **20Ir** and **20Rh** and to 0.35V *vs* Ag/AgCl for **22**. Reported data allow to conclude that electrons can be more easily transferred through metallic catalytic centres which, in turn, are highly efficient in reducing the overpotential needed to foster ORR. In other words, the use of hybrid fullerenes endowed with catalytic centres increases both the electron transfer rate (observed as a net photocurrent density increase) and the driving force for electrochemical reactions (observed as OP increase).

On the other hand, following the recent trend for using carbon based materials as catalyst in ORR,[101-103] we planned the preparation of a molecular organocatalyst by replacement of the metallic atoms from the fullerene derivatives, with a fullerene hydride as active site. The choice of using catalysts such as **21a-c** relies on the reported hydrogen transfer from the fullerene

hydrides, namely $C_{60}H_2$, to dioxygen[47] and on the easy deprotonation of fullerene hydrides leading to very stable fullerene anions **21**$^-$.[43a]

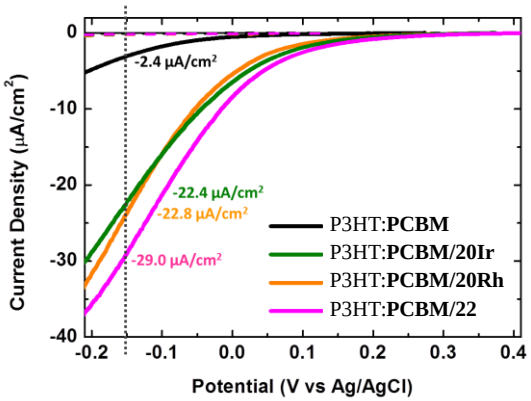

Figure 77. Hybrid fullerenes, bearing metallic catalytic sites, for ORR. Linear Scan Voltammetry (LSV) measurements (scan rate, 10 mV/s) under dark (dashed lines) and upon visible light (1 SUN) (solid lines) on FTO/ P3HT:**PCBM**/hybrid catalyst (**20Ir**, **20Rh** and **22**) photo-electrochemical cells. Measurements were performed in sodium phosphate buffer (PBS) at pH 7.4 and controlled dissolved oxygen (DO) concentration (5.8 mg/L).

In order to evaluate the importance of the hydrogen fullerene bond, devices based on analogous cyclopentenoate functionalization but lacking the C_{60}-H bond (**2c**, **2k**) were also prepared.

Figure 78 summarizes the results obtained in the characterization of photo-electrochemical cells based on **21a-c**, **2c** and **2k** components as hybrid electron acceptor/catalysts components, as compared to the reference device based on **PCBM**.

We notice that **21a** leads to higher catalytic activity, with more than 5-folds increase in photocurrent density at -0.15 V *vs* Ag/AgCl respect to **PCBM**, and a higher OP value (0.3V *vs* Ag/AgCl). Conversely, **2c** and **2k**, despite presenting a similar cyclopentenoate moiety on the C_{60} cage, they do not show a significative increase of the performance due to the lack of C_{60}-H bond. While **2c** exhibits a similar behaviour to **PCBM**, the higher hydrophilicity of **2k**, bearing a carboxylic acid group, leads to a closer interaction with dissolved oxygen molecules, which could explain the higher photocurrent densities observed in **2k**.

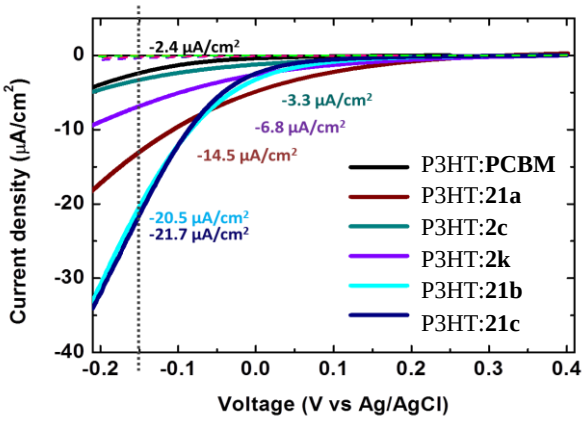

Figure 78. Use of metal-free fullerene catalysts for ORR. Linear Scan Voltammetry (LSV) measurements (scan rate, 10 mV/s) under dark (dashed lines) and upon visible light (1 SUN) (solid lines) on FTO/ P3HT:fullerene catalysts (**21a**, **2c**, **2k**, **21b** and **21c**). Measurements were performed in sodium phosphate buffer (PBS) at pH 7.4 and controlled dissolved oxygen (DO) concentration (5.8 mg/L).

Finally, the importance of a C_{60}-H bond was also confirmed with derivatives **21b** and **21c** that gave rise to current values even higher than **21a**, probably due to the presence of a hydrophilic carboxylic moiety in **21c**. In the case of **21b**, a possible the *tert*-butyl removal during the formation of the films, or by the interaction with electrolytic solution, would lead to derivatives **21b** and could account for the higher current values and for the very similar I-V curves

Once more, photocurrent generation is related to the occurrence of ORR because in the nitrogen flushed solutions negligible currents were recorded.

In more detail, these data have been compared with those based on **PCBM**. Importantly, recorded photocurrent densities for **21b** and **21c** show values comparable to the ones obtained for the hybrid catalysts P3HT:**PCBM**/**20Ir** and P3HT:**PCBM**/**20Rh**, in the order of -20 µA/cm^2 at -0.15 V *vs* Ag/AgCl. OPs resulted 0.28 V in both cases which are still lower respect to the ones of precious metal hybrid samples (0.3 V vs Ag/AgCl for **PCBM**/**20Ir** and 0.35 V *vs* Ag/AgCl for **PCBM**/**20Rh** and **PCBM**/**22**) suggesting future efforts to increment the cell's voltage efficiency with these catalytic materials. Despite of this, metal-free fullerene samples showed higher durability respect to the

precious metal hybrid samples. As figure of merit, the photocurrents recorded at -0.2V *vs* Ag/AgCl for consecutive Cyclic Voltammetry (CV) cycles have been taken (Figure 79). At the fortieth cycle a decrease of the photocurrent of 12.9%, 21.2% and 45.4%, respect to the value recorded at the first cycle, is observed for the case of **PCBM**, **21c** and **22**, respectively. Interestingly, while for **PCBM** and **21c** photocurrent reached stable values after few cycles of stabilization, for the case of **22** a progressively decrease is observed, probably as a consequence of detrimental effects.

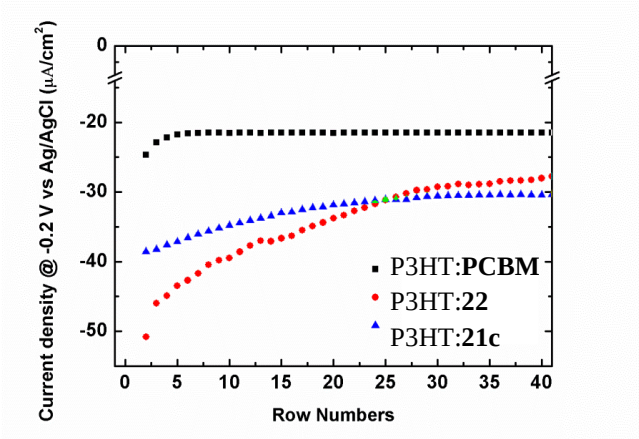

Figure 79. Current density recorded at -0.2V *vs* Ag/AgCl upon white light illumination (1 SUN) and constant 5.8 mg/L dissolved oxygen (DO) concentration for consecutive CV cycles (scan rate 200 mV/s).

Regarding the catalytic activity of the metal-free fullerene derivatives **21a-c**, a plausible mechanism to account for the photocurrent increase and observed stability is based on the initial transfer of the photo-generated electron (PET) from the polymer to catalysts **21a-c** affording the corresponding fullerene radical anion (Scheme 49). Thus, an easier oxygen reduction takes place with the formation of a hydroperoxyl radical, through a hydrogen atom transfer (HAT) or by a proton coupled electron transfer (PCET). The highly stable fullerene anions **21**$^{-}$ (fullerene hydrides feature an unusual acidity for a C_{sp3}-H bond) suppose an

important driving force for the efficiency of the process. Finally the anion **21**$^-$ is protonated by the aqueous medium and the cycle could continue.

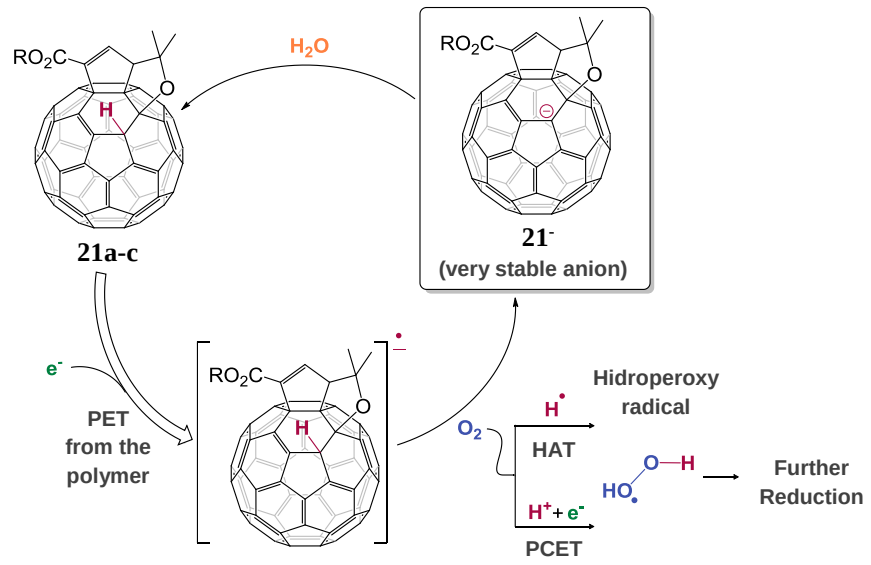

Scheme 49. Plausible ORR mechanism involving fullerene organocatalysts.

These overall results clearly show that it is possible to obtain comparable results to the hybrid catalysts through multiple metal-free functionalization, taking advantage from the positive roles in increasing catalytic activity towards ORR by each organo-modification of the fullerene cage.

EXPERIMENTAL SECTION

5. EXPERIMENTAL SECTION

5.1. General Methods

-***Thin layer chromatography:*** Reactions were monitored by thin-layer chromatography carried out on 0.2 mm TLC-aluminium sheets of silica gel (Merck, TLC Silica gel 60 F_{254}).

-***Purification of Reaction Mixtures****:* Flash column chromatographies were performed using silica gel (Merck, 230-400 mesh).

-***Infrared Spectroscopy***: FTIR spectra were carried out using ATR of the solid compounds. The instrument used was a Bruker TENSOR FTIR. The spectral range was 4000-550 cm^{-1}.

-***Nuclear Magnetic Resonance Spectroscopy:*** ^{1}H NMR and ^{13}C NMR spectra were recorded on a BRUKER DPV-300MHz, BRUKER AV-500MHz or BRUKER AVIII-700MHz using deuterated solvents as reference. Coupling constants (*J*) are reported in Hz and the chemical shifts (δ) in ppm relative to tetramethylsilane (δ=0) at room temperature. Spin multiplicities are reported as a singlet (s), broad singlet (br. s), doublet (d), triplet (t) quartet (q) and multiplet (m).

-***Mass Spectrometry:*** Matrix-assisted laser desorption ionization (MALDI-TOF) mass spectrometry (MS) was performed on a BRUKER-ULTRAFLEX III spectrometer using dithranol as matrix, or on a HP1100EMD with electrospray ionization (ESI).

-***Cyclic Voltammetry****:* Cyclic voltammograms were recorded with a potentiostat/galvanostat AUTOLAB PGSTAT30 equipped with GPES software for Windows version 4.9 in a conventional three-compartment cell by using a GCE (glassy carbon electrode) as the working electrode, $Ag/AgNO_3$ as the reference electrode, platinum wire as counter electrode, $Bu_4N^+PF_6^-$ (0.1M) as the supporting electrolyte, *o*-dichlorobenzene/acetonitrile as the solvent (4:1 v/v), and a scan rate of 100 mVs^{-1}.

-***HPLC***: *Agilent 1100 Series* and *Agilent 1260 Infinity*. The *ee* values were determined by Chiral HPLC. Columns *Pirkle Covalent* (*R,R*) *Whelk-02 10/100 FEC* (4.6 x 250 mm), *Pirkle Covalent (R,R) Whelk-01 5/100* (4.6 x 250 mm) and *Chiralpak IC* (4.6 x 250 mm, 5μm) were used. The relative yield and the isolation of some products was carried out in HPLC, columns: *Buckyprep Waters*

(4.6 x 250 mm) and semipreparative *Pirkle Covalent (R,R) Whelk-01 5/100* (10 x 250 mm). All the HPLC chromatograms were monitored in a 320 nm spectrophotometer detector.

-***UV-Spectroscopy***: The optical properties of the samples in the range of 400–700 nm were measured with a UV/Vis/nIR spectrometer (Perkin Elmer Lambda 1050) in transmission and reflectance mode. Absorbance values of all fabricated devices are fully comparable.

-***Circular Dichroism***: Measurements were carried out on a JASCO J-815 DC spectrometer.

-***X-Ray Difraction***: X-Ray analysis was carried out in an Agilent SuperNova Cu diffractometer, equipped with an Atlas CCD detector, at 100K using a Cryostream 700 de Agilent Cryosystems (liquid N_2).

-***TRMC mesurement.*** Nanosecond laser pulses from a Nd:YAG laser {INDI-HG[full width at half maximum ($\phi\Sigma\mu$) of 5−8 ns], second harmonic generation (SHG) (532 nm) and third harmonic generation (THG)(355); Spectra-Physics} were used as excitation sources. The laser power density was set to 5 mW/cm^2 (0.09−5.1×10^{16} photons/cm^2). For TRMC measurements, the microwave frequency and power were set at approximately 9.1 GHz and 3mW, respectively, so that the charge-carrier motion was not disturbed by the low electric field of the microwave. The TRMC signal picked up by a diode (rise time < 1 ns) is monitored using a digital oscilloscope. All experiments described above were conducted at room temperature.

-***Photo-electrochemical cell preparation and characterization***: SnO_2:F (FTO) TEC 15 covered glass substrates (~200 μm, thickness, 15 Ω/sq resistance) were purchased from Dyesol. rr-P3HT (regio-regularity of 99.5%; average molecular weight 54,000-75,000 g/mol, Sigma-Aldrich), acting as electron donor in a BHJ configuration, was used without any further purification.

Electrochemical characterization of films was carried out in a quartz cell by using an Autolab potentiostat/galvanostat (PGSTAT 302N), in a three electrode configuration. A Pt wire was used as the counter electrode (CE) and an Ag/AgCl electrode filled with saturated KCl solution (0.197 V *vs* the standard hydrogen electrode at 25 °C) was used as the reference electrode (RE). All measurements were performed by employing phosphate buffered saline solution (PBS) at pH 7.4 (obtained by mixing 39 mL of 0.1 M sodium dihydrogen phosphate

(NaH_2PO_4) and 61 mL of 0.1 M sodium hydrogen phosphate (Na_2HPO_4) and adjusting the final volume to 200 mL with deionized water) at room temperature 22 °C. A 300 W Xe light source equipped with AM filters (Lot Quantum Design, model LS0306) calibrated to 1 sun on the electrode surface in the electrolyte was used to illuminate the photocathode.

Linear Scan Voltammetry (LSV) was performed with a scan rate of 10 mV/s while Cyclic Voltammetry has been done using 200 mV/s. DO concentration solution was monitored through a commercial DO sensor (Oxygen meter OXI 45+, Crison). Deoxygenation of the solution was achieved purging N_2 into the solution, while O_2-saturated conditions were obtained purging O_2. All the data were handled by NOVA 1.10.3 package software.

-***Solvents***: The solvents used were purified and dried following the usual methods.[147]

-***Reagents***: Reagents for synthesis were mostly purchased from Sigma-Aldrich, Cymit and Acros.

[147] Perrin, D. D.; Amariego, I. F.; Perrin, D. R. *Purification of laboratory Chemicals,* Pergamon Press, Oxford, **1980**

5.2. Synthesis and characterization of compounds

5.2.1. Synthesis of alkynoates 1a-l

General procedure

Alkynoates **1a-l** were synthesized following the procedure described in the literature by coupling between alkynes and diazoacetate compounds, both commercially available, in the presence of cooper (I) iodide, which showed identical spectroscopic properties.[106]

The diazoacetate compound (1.2 eq.) was added to a solution of the corresponding terminal alkyne (1 eq.) and CuI (5% mmol) in MeCN (1,25 mL/mmol). The resulting mixture was stirred for 12 h at room temperature. Then, the volatiles were removed, the residue was purified by chromatography column (hexane:Et_2O, 10:1 to 3:2)

Ethyl 4-phenylbut-3-ynoate (**1a**)[106]

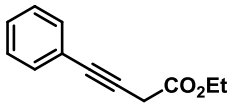

The alkynoate **1a** was prepared according to the general procedure using phenylacetylene (0.4 mL, 3.646 mmol), ethyl diazoacetate (0.5 mL, 4.375 mmol) and CuI (34.8 mg, 0.182 mmol). Pale yellow oil; 95% yield (651.4 mg). ^{1}H NMR (300 MHz, $CDCl_3$) δ 7.49 – 7.41 (m, 2H), 7.33 – 7.27 (m, 3H), 4.22 (q, *J* = 7.1 Hz, 2H), 3.50 (s, 2H), 1.30 (t, *J* = 7.1 Hz, 3H). ^{13}C NMR (75 MHz, $CDCl_3$) δ 168.6, 132.1, 128.6, 128.6, 123.4, 83.8, 81.7, 62.0, 27.1, 14.5.

Ethyl 5-phenylpent-3-ynoate (**1b**)[106]

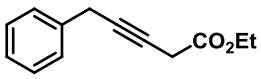

The alkynoate **1b** was prepared according to the general procedure using 3-phenyl-1-propyne (0.3 mL, 2.428 mmol), ethyl diazoacetate (0.3 mL, 2.913 mmol) and CuI (23.1 mg, 0.121 mmol). Pale yellow oil; 97% yield (476.0 mg). ^{1}H NMR (300 MHz, $CDCl_3$) δ 7.54 – 7.14 (m, 5H), 4.24 (q, *J* = 7.1 Hz, 2H), 3.67 (s, 2H), 3.36 (t, *J* = 2.4 Hz, 2H), 1.33 (t, *J* = 7.1 Hz, 3H).

Triethyl oct-7-en-2-yne-1,5,5-tricarboxylate (**1c**)

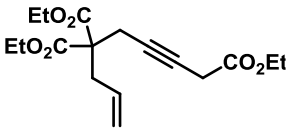

The alkynoate **1c** was prepared according to the general procedure using diethyl 2-allyl-2-(prop-2-yn-1-yl)malonate (100 mg, 0.420 mmol), ethyl diazoacetate (53 μL, 0.504 mmol) and CuI (4.0 mg, 0.021 mmol). Colorless oil; 92% yield (125.0 mg). ^{1}H NMR (300 MHz, $CDCl_3$) δ 5.56 (tdd, *J* = 10.5, 8.1, 5.2 Hz, 1H), 5.17 – 5.08 (m, 1H), 5.08 – 5.02 (m, 1H), 4.18 – 4.06 (m, 6H), 3.15 (t, *J* = 2.4 Hz, 2H), 2.74 (dd, *J* = 4.4, 1.8 Hz, 4H), 1.23 – 1.15 (m, 9H). ^{13}C NMR (75 MHz, $CDCl_3$) δ 170.2, 168.7, 132.3, 120.0, 78.5, 75.3, 61.9, 61.8, 57.2, 36.8, 26.4, 23.2, 14.4. ATR-FTIR ν (C≡C) = 1965 cm^{-1}, ν (C=O) = 1731 cm^{-1}. HRMS (ESI POS): $[M+Na]^+$ Calc. for $C_{17}H_{24}O_6Na$: 347,1465; found: 347,1460.

Tetraethyl nona-2,7-diyne-1,5,5,9-tetracarboxylate (**1d**)

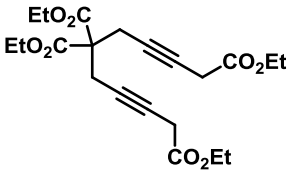

The dialkynoate **1d** was prepared according to the general procedure using diethyl 2,2-di(prop-2-yn-1-yl)malonate (150 mg, 0.635 mmol), ethyl diazoacetate (0.2 mL, 1.905 mmol) and CuI (12.1 mg, 0.063 mmol) Colorless oil; 34% yield (89.6 mg). ^{1}H NMR (300 MHz, $CDCl_3$) δ 4.27 – 4.14 (m, 6H), 3.22 (t, *J* = 2.4 Hz, 2H), 3.00 (t, *J* = 2.4 Hz, 2H), 1.32 – 1.19 (m, 12H). ATR-FTIR ν (C=O) = 1738 cm^{-1}. HRMS (ESI POS): $[M+Na]^+$ Calc. for $C_{21}H_{28}O_8Na$: 431,1676; found: 431,1659.

tert-Butyl 4-phenylbut-3-ynoate (**1e**)[107a]

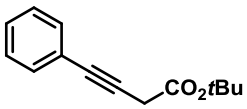

The alkynoate **1e** was prepared according to the general procedure using phenylacetylene (0.4 mL, 3.646 mmol), *tert*-butyl diazoacetate (0.6 mL, 4.375 mmol) and CuI (34.8 mg, 0.182 mmol). Colorless oil; 79% yield (622.7 mg).^{1}H NMR (300 MHz, $CDCl_3$) δ 7.49 – 7.41 (m, 2H), 7.31 (dd, *J* = 6.6, 3.6 Hz, 3H), 3.43 (s, 2H), 1.51 (s, 9H). HRMS (ESI POS): $[M+Na]^+$ Calc. for $C_{14}H_{16}NaO_2$: 239,10425; found: 239,10548.

Ethyl 4-(4-chlorophenyl)but-3-ynoate (**1g**)

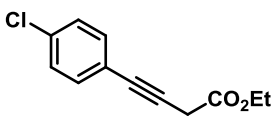

The alkynoate **1g** was prepared according to the general procedure using (4-chlorophenyl)acetylene (0.5 g, 3.661 mmol), ethyl diazoacetate (0.46 mL, 4.393 mmol) and CuI (34.9 mg, 0.183 mmol). Pale yellow oil; 79% yield (643.4 mg). ^{1}H NMR (300 MHz, $CDCl_3$) δ 7.43 – 7.35 (m, 2H), 7.34 – 7.21 (m, 3H), 4.24 (q, *J* = 7.1 Hz, 2H), 3.50 (s, 2H), 1.32 (t, *J* = 7.1 Hz, 3H). ^{13}C NMR (75 MHz, $CDCl_3$) δ 168.48, 134.60, 133.48, 128.96, 121.88, 82.79, 82.70, 62.14, 27.13, 14.53. HRMS (ESI POS): $[M+Na]^+$ Calc. for $C_{12}H_{11}ClNaO_2$: 245,03398; found: 245,03510. ATR-FTIR ν (C=O) = 1737 cm^{-1}.

tert-Butyl 4-(4-bromophenyl)but-3-ynoate (**1h**)

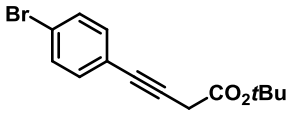

The alkynoate **1h** was prepared according to the general procedure using (4-bromophenyl)acetylene (0.3 g, 1.657 mmol), *tert*-butyl diazoacetate (0.28 mL, 1.989 mmol) and CuI (15.8 mg, 0.083 mmol). Pale yellow oil; 76% yield (370.3 mg). ^{1}H NMR (300 MHz, $CDCl_3$) δ 7.42 (d, *J* = 8.5 Hz, 2H), 7.29 (d, *J* = 8.5 Hz, 2H), 3.41 (s, 2H), 1.49 (s, 9H). ^{13}C NMR (75 MHz, $CDCl_3$) δ 167.6, 133.6, 131.8, 122.7, 122.5, 83.6, 82.8, 82.5, 28.4. ATR-FTIR ν (C=O) = 1742 cm^{-1}. HRMS (ESI POS): $[M+Na]^+$ Calc. for $C_{14}H_{15}BrNaO_2$: 317,01476; found: 317,01790.

tert-Butyl 4-(3,4-dichlorophenyl)but-3-ynoate (**1i**)

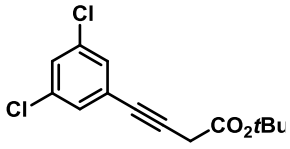

The alkynoate **1i** was prepared according to the general procedure using (3,5-dichlorophenyl)acetylene (0.3 g, 1.754 mmol), *tert*-butyl diazoacetate (0.29 mL, 2.105 mmol) and CuI (16.7 mg, 0.088 mmol). Pale yellow oil; 72% yield (363.7 mg). ^{1}H NMR (300 MHz, $CDCl_3$) δ 7.51 (d, *J* = 1.8 Hz, 1H), 7.35 (d, *J* = 8.3 Hz, 1H), 7.24 (dd, *J* = 8.3, 1.8 Hz, 1H), 3.41 (s, 2H), 1.49 (s, 9H). ^{13}C NMR (75 MHz, $CDCl_3$) δ 167.4, 133.8, 132.9, 132.8, 131.3, 130.6, 123.5, 84.6, 82.6, 81.6, 28.4, 28.2. ATR-FTIR ν (C=O) = 1738 cm^{-1}. HRMS (ESI POS): $[M+Na]^+$ Calc. for $C_{14}H_{14}Cl_2NaO_2$: 307,02631; found: 307,02845.

tert-Butyl 4-(4-(tert-butyl)phenyl)but-3-ynoate (**1j**)

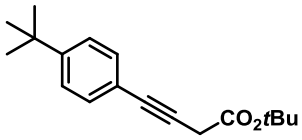

The alkynoate **1j** was prepared according to the general procedure using (4-*tert*-butylphenyl)acetylene (0.4 mL, 2.217 mmol), *tert*-butyl diazoacetate (0.37 mL, 2.660 mmol) and CuI (21 mg, 0.111 mmol). Pale yellow oil; 94% yield (569.6 mg).^{1}H NMR (300 MHz, $CDCl_3$) δ 7.40 (d, J = 8.5 Hz, 3H), 7.32 (d, J = 8.5 Hz, 3H), 3.42 (s, 3H), 1.51 (s, 14H), 1.31 (s, 13H). ^{13}C NMR (75 MHz, $CDCl_3$) δ 167.9, 151.6, 131.9, 125.6, 120.6, 83.8, 82.2, 81.5, 35.1, 31.6, 28.4. HRMS (ESI POS): $[M+Na]^+$ Calc. for $C_{18}H_{24}NaO_2$: 295,16685; found: 295,16992.

Ethyl 5-hydroxy-5-methylhex-3-ynoate (mixture of alkynoate/allenoate) (**1k**)

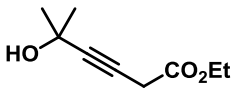

The alkynoate **1k** was prepared according to the general procedure using 2-methyl-3-butyn-2-ol (0.32 mL, 3.301 mmol), ethyl diazoacetate (0.42 mL, 3.962 mmol) and CuI (30.8 mg, 0.165 mmol). Yellow oil; 91% yield (511.1 mg). ^{1}H NMR (300 MHz, $CDCl_3$) δ 5.83 (d, *J* = 6.1 Hz, 0.7H), 5.72 (d, *J* = 6.1 Hz, 0.7H), 4.27 – 4.12 (m, 3.6H), 3.27 (s, 2H), 2.67 (br. s, 0.6H), 2.62 (br. s, 1H), 1.51 (s, 6H), 1.41 (s, 6H), 1.28 (td, *J* = 7.1, 1.0 Hz, 6H). ^{13}C NMR (75 MHz, $CDCl_3$) δ 210.6, 169.0, 166.5, 105.6, 90.9, 88.9, 73.8, 70.1, 65.1, 61.9, 61.4, 31.6, 29.9, 26.2, 14.5, 14.4. ATR-FTIR ν (O-H) = 3419 cm^{-1}, ν (C≡C) = 1960 cm^{-1}, ν (C=O) = 1722 cm^{-1}. HRMS (ESI POS): $[M+Na]^+$ Calc. for $C_9H_{14}NaO_3$: 193,08406; found: 193,0831.

tert-Butyl 5-hydroxy-5-methylhex-3-ynoate (mixture alkynoate/allenoate) (**1l**)

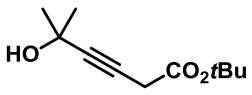

The alkynoate **1l** was prepared according to the general procedure using 2-methyl-3-butyn-2-ol (0.2 mL, 2.270 mmol), *tert*-butyl diazoacetate (0.38 mL, 2.724 mmol) and CuI (22.0 mg, 0.114 mmol). Yellow oil; 96% yield (432.0 mg). ^{1}H NMR (300 MHz, $CDCl_3$) δ 5.79 (d, *J* = 6.1 Hz, 0.5H), 5.64 (d, *J* = 6.1 Hz, 0.5H), 3.19 (s, 2H), 2.64 (br. s, 0.6H), 2.61 (br. s, 1H), 1.52 (s, 7H), 1.48 (s, 6H), 1.46 (s, 9H). ^{13}C NMR (75 MHz, $CDCl_3$) δ 210.2, 168.3, 165.9, 105.5, 92.4, 88.9, 82.2, 81.6, 74.4, 70.1, 65.1, 31.7, 30.0, 29.9, 28.4, 28.3. ATR-FTIR ν (O-H) = 3417 cm^{-1}, ν (C≡C) = 1960 cm^{-1}, ν (C=O) = 1726 cm^{-1}. HRMS (ESI POS): $[M+Na]^+$ Calc. for $C_{11}H_{18}NaO_3$: 221,1148; found: 221,1141.

5.2.2. Synthesis of allenoates 3a-j

General procedure

Allenoates **3a-j** were synthesized following the procedure described in the literature from α–phosphoranylidene esters and acid chlorides, both commercially available, in the presence of triethylamine, which showed identical spectroscopic properties.[148]

A three-necked, round-bottomed flask is equipped with a nitrogen inlet, a pressure-equalizing dropping funnel fitted with a gas outlet, and a teflon-coated magnetic stirring bar. The flask is charged with dichloromethane (3 mL/mmol) and corresponding (triphenylphosphoranylidene)acetate (1 eq.) and flushed with nitrogen. The yellow solution is stirred at 25°C as a solution triethylamine in dichloromethane (1 eq.; 1M) is added dropwise over 5 min. After 10 min, a solution of the appropriate acid chloride in dichloromethane (1 eq.; 1M) is added dropwise to the vigorously stirred solution over 15 min. Stirring is continued for an additional 0.5 hr, after which the clear, yellow-tinted mixture is evaporated on a rotary evaporator at reduced pressure using a water bath maintained at 25°C. Afterthat, pentane is added to the semisolid residue, and the slurry is allowed to stand for 2 hr while it is shaken periodically to facilitate solidification and to complete the extraction of the product. The precipitate is removed by filtration through a Büchner funnel, and the filter cake is washed with pentane. The filtrates are combined and concentrated at reduced pressure to approximately one-fourth of the original volume using a water bath maintained at 25°C. The mixture is filtered again to remove triphenylphosphine oxide, and the remaining solvent is then evaporated. The residue was purified by chromatography column (hexane:Et_2O, 10:1).

Ethyl 4-phenylbuta-2,3-dienoate (**3a**)[149]

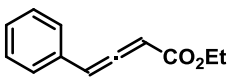

The allenoate **3a** was prepared according to the general procedure using (ethoxycarbonylmethylene)triphenyl phosphorane (2 g, 5.741 mmol), triethylamine (0.80 mL, 5.741 mmol) and phenylacetyl chloride (0.76 mL, 5.741 mmol). Pale yellow oil;

[148] Lang, R. W.; Hansen, H. *Org. Syn.* **1984**, *62*, 202-207
[149] Li, C.; Wang, X.; Sun, X.; Tang, Y.; Zheng, J.; Xu, Z.; Zhou, Y.; Dai, L. *J. Am. Chem. Soc.* **2007**, *129*, 1494-1495

38% yield (412.6 mg). ^{1}H NMR (300 MHz, $CDCl_3$) δ 7.43 – 7.28 (m, 5H), 6.64 (d, *J* = 6.4 Hz, 1H), 6.03 (d, *J* = 6.3 Hz, 1H), 4.24 (q, *J* = 7.2 Hz, 2H), 1.30 (t, *J* = 7.1 Hz, 3H).

Ethyl 5-phenylpenta-2,3-dienoate (**3b**)[150]

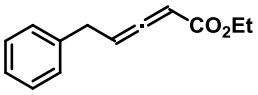

The allenoate **3b** was prepared according to the general procedure using (ethoxycarbonylmethylene)triphenyl phosphorane (200 mg, 0.574 mmol), triethylamine (79.8 μL, 0.574 mmol) and hydrocinnamoyl chloride (85.3 μL, 0.574 mmol). Pale yellow oil; 81% yield (94.6 mg). ^{1}H NMR (300 MHz, $CDCl_3$) δ 7.37 – 7.21 (m, 5H), 5.78 (td, *J* = 7.5, 6.2 Hz, 1H), 5.63 (dt, *J* = 6.1, 2.7 Hz, 1H), 4.31 – 4.14 (m, 2H), 3.58 – 3.41 (m, 2H), 1.32 (t, *J* = 7.1 Hz, 3H).

Ethyl penta-2,3-dienoate (**3c**)[150]

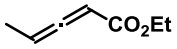

The allenoate **3c** was prepared according to the general procedure using (ethoxycarbonylmethylene)triphenyl phosphorane (500 mg, 1.435 mmol), triethylamine (0.20 mL, 1.435 mmol) and propionyl chloride (0.13 mL, 1.435 mmol). Colourless oil; 89% yield (161.1 mg). ^{1}H NMR (300 MHz, $CDCl_3$) δ 5.67 – 5.53 (m, 2H), 4.26 – 4.16 (m, 2H), 1.81 (ddd, *J* = 10.5, 6.2, 2.8 Hz, 3H), 1.33 – 1.26 (m, 3H).

Ethyl hexa-2,3-dienoate (**3d**)[151]

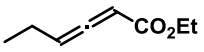

The allenoate **3d** was prepared according to the general procedure using (ethoxycarbonylmethylene)triphenyl phosphorane (2 g, 5.741 mmol), triethylamine (0.80 mL, 5.741 mmol) and butyryl chloride (0.60 mL, 5.741 mmol). Colourless oil; 61% yield (487.9 mg).^{1}H NMR (300 MHz, $CDCl_3$) δ 5.69 (q, *J* = 6.3 Hz, 1H), 5.61 (dt, *J* = 6.3, 3.3 Hz, 1H), 4.20 (q, *J* = 6.8 Hz, 2H), 2.26 – 2.09 (m, 2H), 1.29 (t, *J* = 7.1 Hz, 3H), 1.08 (t, *J* = 7.4 Hz, 3H).

[150] Rout, L.; Harned, A. *Chem. Eur. J.* **2009**, *15*, 12926-12928
[151] Wang, G.; Liu, X.; Chen, Y.; Yang, J.; Li, J.; Lin, L.; Feng, X. *ACS Catal.* **2016**, *6*, 2482-2486

Ethyl 5-methylhexa-2,3-dienoate (**3e**)[152]

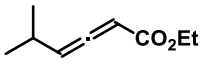

The allenoate **3e** was prepared according to the general procedure using (ethoxycarbonylmethylene)triphenyl phosphorane (2 g, 5.741 mmol), triethylamine (0.80 mL, 5.741 mmol) and isovaleryl chloride (0.92 mL, 5.741 mmol). Colourless oil; 56% yield (495.7 mg).^{1}H NMR (300 MHz, $CDCl_3$) δ 5.67 – 5.55 (m, 2H), 4.26 – 4.07 (m, 2H), 2.55 – 2.36 (m, 1H), 1.26 (t, *J* = 7.1 Hz, 3H), 1.06 (d, *J* = 6.8 Hz, 6H).

Ethyl 4-(4-formylphenyl)buta-2,3-dienoate (**3f**)

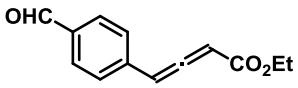

The allenoate **3f** has been obtained by the methodology of alkynoates, according to the general procedure using 4-ethynylbenzaldehyde 214 mg, 1.644 mmol), ethyl diazoacetate (0.21 mL, 1.973 mmol) and CuI (15.7 mg, 0.082 mmol). Yellow oil; 26% yield (90.7 mg). ^{1}H NMR (300 MHz, $CDCl_3$) δ 9.97 (s, 1H), 7.83 (d, *J* = 8.2 Hz, 2H), 7.44 (d, *J* = 8.1 Hz, 2H), 6.66 (d, *J* = 6.3 Hz, 1H), 6.07 (d, *J* = 6.3 Hz, 1H), 4.22 (dd, *J* = 14.2, 7.1 Hz, 3H), 1.27 (t, *J* = 7.1 Hz, 4H).

tert-Butyl 5-phenylpenta-2,3-dienoate (**3g**)[153]

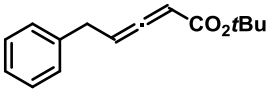

The allenoate **3g** was prepared according to the general procedure using (*tert*-buthoxycarbonyl-methylene)triphenylphosphorane (1 g, 2.657 mmol), triethylamine (0.37 mL, 2.657 mmol) and hydrocinnamoyl chloride (0.40 mL, 2.657 mmol). Yellow oil; 69% yield (424.7 mg). ^{1}H NMR (300 MHz, $CDCl_3$) δ 7.37 – 7.12 (m, 5H), 5.74 (td, *J* = 7.5, 6.2 Hz, 1H), 5.58 – 5.53 (m, 1H), 3.49 (ddd, *J* = 7.3, 4.6, 2.7 Hz, 2H), 1.53 (s, 9H).

[152] Hashmi, A. S.; Döpp, R.; Lothschütz, C.; Rudolph, M.; Riedel, D.; Rominger, F. *Adv. Synth. Catal.* **2010**, *352*, 1307-1314

[153] Hopkinson, M. ; Tessier, A.; Salisbury, A.; Giuffredi, G. T.; Combettes, L. ; Gee, A. D.; Gouverneur, V. *Chem. Eur. J.* **2010**, *16*, 4739-4743

Benzyl 4-phenylbuta-2,3-dienoate (**3h**)

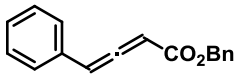

The allenoate **3h** was prepared according to the general procedure using (benzyloxycarbonyl-methylene) triphenylphosphorane (2 g, 4.873 mmol), triethylamine (0.66 mL, 4.873 mmol) and phenylacetyl chloride (0.64 mL, 4.873 mmol).Yellow oil; 43% yield (523.8 mg). ^{1}H NMR (300 MHz, $CDCl_3$) δ 7.56 (dd, *J* = 6.6, 2.9 Hz, 1H), 7.51 – 7.31 (m, 9H), 6.72 (d, *J* = 6.3 Hz, 1H), 6.18 (d, *J* = 6.4 Hz, 1H), 5.32 (s, 2H).

Ethyl 4-(4-chlorophenyl)buta-2,3-dienoate (**3i**)

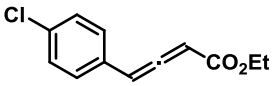

The allenoate **3i** was prepared according to the general procedure using (ethoxycarbonyl-methylene) triphenylphosphorane (2 g, 5.741 mmol), triethylamine (0.80 mL, 5.741 mmol) and (4-chlorophenyl)acetyl chloride (0.84 mL, 5.741 mmol). Pale yellow oil; 36% yield (458.9 mg). ^{1}H NMR (300 MHz, $CDCl_3$) δ 7.34 (d, *J* = 8.7 Hz, 2H), 7.26 (d, *J* = 8.6 Hz, 2H), 6.62 (d, *J* = 6.4 Hz, 1H), 6.06 (d, *J* = 6.4 Hz, 1H), 4.16 (q, *J* = 7.1 Hz, 2H), 0.92 (t, *J* = 7.1 Hz, 3H).

Methyl 4-phenylbuta-2,3-dienoate (**3j**) [154]

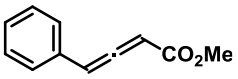

The allenoate **3j** was prepared according to the general procedure using (methoxycarbonyl-methylene) triphenylphosphorane (2 g, 5.982 mmol), triethylamine (0.83 mL, 5.982 mmol) and phenylacetyl chloride (0.73 mL, 5.982 mmol). Yellow oil; 37% yield (380.6 mg). ^{1}H NMR (300 MHz, $CDCl_3$) δ 7.37 – 7.28 (m, 5H), 6.64 (d, *J* = 6.4 Hz, 1H) , 6.04 (d, *J* = 6.3 Hz, 1H), 3.78 (s, 3H).

Methyl 5-phenylpenta-2,3-dienoate (**3k**)[154]

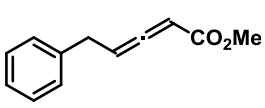

The allenoate **3k** was prepared according to the general procedure using (methoxycarbonyl-methylene)triphenylphosphorane (2 g, 5.982 mmol), triethylamine (0.83 mL, 5.982 mmol) and hydrocinnamoyl chloride (0.89 mL, 5.982 mmol). Pale yellow oil; 92% yield (1.0352 g). 1H NMR (300 MHz, CDCl3) δ 7.31 (tt, J = 6.9, 6.5 Hz, 5H), 5.80 (dd, J = 11.2, 10.0 Hz, 1H), 5.69 –

[154] Sano, S.; Matsumoto, T.; Yano, T.; Toguchi, M.; Nakao, M. *Synlett* **2015**, *26*, 2135-2138

5.62 (m, 1H), 3.77 (s, 3H), 3.50 (d, J = 7.5 Hz, 2H). ^{13}C NMR (75 MHz, $CDCl_3$) δ 213.27, 166.80, 139.00, 128.93, 127.08, 95.29, 88.71, 52.45, 34.53.

5.2.3. Synthesis of cyclopenteno[4,5:1,2][60]fullerenes 2a-k

General procedure for the [3+2] cycloaddition of alkynoates/allenoates **1a-f**/**3a-h** onto [60]fullerene

In an ordinary vial under Ar atmosphere, a suspension of the corresponding alkynoates/allenoates **1a-f**/**3a-h** (1.0 eq.) and 2-[(11b*S*)-3*H*-binaphtho[2,1-c:1′,2′-e]phosphepin-4(5*H*)-yl]ethanamine (**P-XIV**, 0.1 eq.) in 1.0 mL of dry toluene is prepared. After 15 min. of stirring at room temperature, [60]fullerene (1.07 eq., 0.017 mmol) is added and the mixture is stirred at room temperature for two hours. Finally, the solvent is evaporated under vacuum and dark residue is then purified by silica-gel column chromatography using CS_2 as eluent (for recovering unreacted [60]fullerene). Then, mixtures of solvents (indicated in each case) are used affording desired cyclopenteno[4,5:1,2][60]fullerene derivatives **2a-j**. Conversions and *ee* are determined by HPLC analysis using *Pirkle Covalent (R,R) Whelk-02* and *Pirkle Covalent (R,R) Whelk-01* as chiral columns (conditions and enantiomers retention times are indicated in each case). For the synthesis of the racemic compounds (**2a-j**) the same procedure was used replacing the optically pure phosphine **P-XIV** by racemic 1,2-bis(diphenylphosphine)ethane (dppe).

(3*R*)-1-ethoxycarbonyl-3-phenyl-1-cyclopenteno[4,5:1,2][60]fullerene (**2a**)[67]

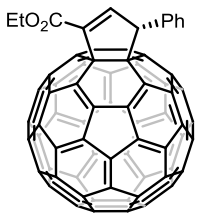

The adduct **2a** was prepared according to the general procedure ethyl 4-phenyl-3-butynoate **1a** (2.9 mg, 0.016 mmol), [60]fullerene (12 mg, 0.017 mmol) and 2-[(11b*S*)-3*H*-binaphtho[2,1-c:1′,2′-e]phosphepin-4(5*H*)-yl]ethanamine (0.6 mg, 0.002 mmol). Conversion: 31% (eluent: hexane:CH_2Cl_2, 3:1); *ee*: 88% (Pirkle Covalent (*R,R*) Whelk-02, hexane/2-propanol 98:2,flow rate 3.00 mL/min). This adduct **2a** was also prepared by using ethyl 4-phenylbuta-2,3-dienoate **3a** ((2.9 mg, 0.016 mmol), [60]fullerene (12 mg, 0.017 mmol) and 2-[(11b*S*)-3*H*-binaphtho[2,1-c:1′,2′-e]phosphepin-4(5*H*)-yl]ethanamine (0.6 mg, 0.002 mmol). Conversion: 42%. *ee*: 86%. ^{1}H NMR (700 MHz, $CDCl_3$) δ 1.46 (t, 3H, J= 7.1 Hz), 4.45-4.53 (m, 2H), 6.06 (d, 1H, J= 2.4 Hz), 7.37-7.41 (m, 1H),

7.47-7.53 (m, 2H), 7.72 (d, 2H, *J*= 7.3 Hz), 7.89 (d, 1H, *J*= 2.4 Hz) ppm. ^{13}C NMR (175 MHz, $CDCl_3$) δ 14.2, 29.7, 61.4, 63.6, 76.0, 128.3, 129.2, 129.7, 134.1, 135.5, 135.8, 134.0, 137.9, 139.1, 139.4, 138.5, 140.3, 141.6, 141.7, 141.8, 141.9, 142.1, 142.2, 142.4, 142.4, 142.6, 142.6, 142.7, 142.7, 143.1, 143.1, 144.4, 144.5, 144.5, 144.5, 144.8, 145.0, 145.0, 145.0, 145.1, 145.1, 145.3, 145.3, 145.4, 145.5, 145.6, 145.7, 1455.9, 145.9, 146.0, 146.0, 146.1, 146.2, 146.2, 146.2, 146.3, 146.4, 147.3, 147.4, 145.0, 148.5, 150.4, 151.0, 153.7, 157.0, 163.8 ppm.

1-ethoxycarbonyl-3-(2,2-diethoxycarbonyl-4-pentenyl)-1-cyclopenteno[4,5:1,2][60]fullerene (**2b**)

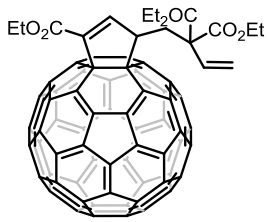

The adduct **2b** was prepared according to the general procedure using triethyl oct-7-en-2-yne-1,5,5-tricarboxylate **1c** (5.1 mg, 0.016 mmol), [60]fullerene (12 mg, 0.017 mmol) and 2-[(11b*S*)-3*H*-binaphtho[2,1-c:1′,2′-e]phosphepin-4(5*H*)-yl]ethanamine (0.6 mg, 0.002 mmol). Conversion: 19% (eluent: hexane:CH_2Cl_2, 1:1). ^{1}H NMR (700 MHz, $CDCl_3$) δ 1.35 (t, *J*= 7.1 Hz, 3H). 1.42 (td, *J*= 7.1, 2.4 Hz, 6H), 2.85 (dd, *J*= 14.3, 12.0 Hz, 1H), 3.04 (qd, *J*= 14.6, 7.4 Hz, 2H), 3.24 (dd, *J*= 14.4, 2.9 Hz, 1H), 4.36-4.28 (m, 2H), 4.45-4.37 (m, 4H), 4.87 (dt, *J*= 11.9, 2.6 Hz, 1H), 5.17 (d, *J*= 10.1 Hz, 1H), 5.25 (d, *J*= 17.0 Hz, 1H), 5.77 (ddt, *J*= 17.1, 10.1, 7.4 Hz, 1H), 7.68 (d, *J*= 2.3 Hz, 1H) ppm. ^{13}C NMR (176 MHz, $CDCl_3$) δ 14.2, 14.2, 14.3, 29.7, 38.0, 38.3, 53.2, 57.0, 61.4, 62.0, 62.0, 74.9, 76.1, 120.3, 131.6, 134.0, 135.7, 135.7, 136.1, 136.2, 139.2, 139.3, 139.8, 140.0, 141.6, 141.7, 141.9, 142.0, 142.0, 142.2, 142.3, 142.4, 142.5, 142.6, 142.7, 142.7, 142.8, 143.1, 143.1, 144.4, 144.5, 144.5, 144.5, 144.8, 145.1, 145.1, 145.4, 145.5, 145.6, 145.9, 146.0, 146.0, 146.0, 146.1, 146.2, 146.3, 146.3, 146.4, 146.4, 146.8, 147.3, 147.4, 148.1, 148.4, 150.8, 151.2, 152.0, 156.7, 163.6, 170.8, 171.4 ppm. HRMS (ESI POS.): [M]+ Calc. for $C_{77}H_{24}NaO_6$: 1067.14706; found: 1067.14442.

(3*R*)-1-*tert*-butoxycarbonyl-3-phenyl-1-cyclopenteno[4,5:1,2][60]fullerene (**2c**)

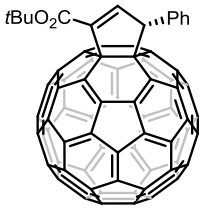

The adduct **2c** was prepared according to the general procedure using *tert*-butyl-4-phenyl-3-butynoate **1e** (3.4 mg, 0.016 mmol), [60]fullerene (12 mg, 0.017 mmol) and 2-[(11b*S*)-3*H*-binaphtho[2,1-c:1′,2′-e]phosphepin-4(5*H*)-yl]ethanamine (0.6 mg, 0.002 mmol). Conversion: 49% (eluent: hexane:CH_2Cl_2, 3:1); *ee*: 60% (Pirkle Covalent (*R*,*R*) Whelk-02, hexane/2-propanol 98:2, flow rate 3.00 mL/min; t_R for the major (3*R*) isomer: 4.29 min, t_R for the minor (3*S*) isomer: 5.07 min). ^{1}H NMR (700 MHz, $CDCl_3$) δ 1.65 (s, 9H), 6.02 (d, *J*= 2.5 Hz, 1H), 7.39 (t, *J*= 7.5 Hz, 1H), 7.50 (t, *J*= 7.8 Hz, 2H), 7.72 (d, *J*= 7.2 Hz, 2H), 7.80 (d, *J*= 2.5 Hz, 1H) ppm. ^{13}C NMR (176 MHz, $CDCl_3$) δ 28.4, 29.7, 63.3, 76.2, 76.4, 82.8, 128.2, 129.1, 129.8, 134.1, 135.5, 135.8, 135.9, 139.0, 139.3, 139.5, 139.5, 139.7, 140.2, 141.6, 141.6, 141.7, 141.8, 141.9, 141.9, 142.0, 142.1, 142.2, 142.2, 142.4, 142.4, 142.6, 142.6, 142.7, 142.7, 143.1, 143.1, 144.4, 144.4, 144.5, 144.8, 145.0, 145.0, 145.1, 145.3, 145.3, 145.3, 145.4, 145.5, 145.6, 145.7, 145.9, 146.0, 146.0, 146.1, 146.2, 146.2, 146.2, 146.3, 146.4, 147.3, 147.4, 148.1, 148.7, 150.6, 151.2, 153.9, 157.2, 163.0 ppm. HRMS (MALDI+): $[M]^+$ Calc. for $C_{74}H_{16}O_2$: 936.1150; found: 936.1165.

(3*S*)-1-ethoxycarbonyl-3-benzyl-1-cyclopenteno[4,5:1,2][60]fullerene (**2d**)

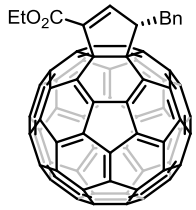

The adduct **2d** was prepared according to the general procedure using ethyl 5-phenylpenta-2,3-dienoate **3b** (3.2 mg, 0.016 mmol), [60]fullerene (12 mg, 0.017 mmol) and 2-[(11b*S*)-3*H*-binaphtho[2,1-c:1′,2′-e]phosphepin-4(5*H*)-yl]ethanamine (0.6 mg, 0.002 mmol). Conversion: 67% (eluent: hexane:CH_2Cl_2, 1:1); *ee*: 84% (Pirkle Covalent (*R*,*R*) Whelk-01, hexane/2-propanol 95:5, flow rate 3.00 mL/min; t_R for the major (3*S*) isomer: 14.46 min, t_R for the minor (3*R*) isomer: 17.95 min).^{1}H NMR (700 MHz, $CDCl_3$) δ 1.38 (t, *J*= 7.1 Hz, 3H), 3.93 (dd, *J*= 13.2, 5.7 Hz, 1H), 4.45-4.36 (m, 2H), 3.47-3.39 (m, 1H), 5.10 (ddd, *J*= 11.7, 5.7, 2.3 Hz, 1H), 7.38 (t, *J*= 7.4 Hz, 1H), 7.48 (t, *J*= 7.6 Hz, 2H), 7.53 (d, *J*= 7.3 Hz, 2H), 7.62 (d, *J*= 2.4 Hz, 1H) ppm. ^{13}C NMR (176 MHz, $CDCl_3$) δ 14.3, 29.7, 31.0, 41.9, 53.5, 59.3, 61.4, 74.0, 127.0, 129.0, 129.2, 134.2, 135.7, 135.9, 136.1, 138.7, 139.2, 139.3, 139.6, 140.2, 141.6, 141.7, 141.9, 142.0, 142.1, 142.2, 142.3, 142.4, 142.7, 142.7, 142.8, 143.1, 143.1, 143.2, 144.4, 144.5, 144.5, 144.5, 144.8,

145.1, 145.2, 145.3, 145.4, 145.4, 145.5, 145.6, 146.0, 146.0, 146.1, 146.2, 146.3, 146.3, 146.3, 146.4, 146.4, 147.3, 147.4, 148.3, 148.3, 50.8, 151.0, 152.7, 156.9, 163.8 ppm. HRMS (ESI POS.): $[M]^+$ Calc. for $C_{73}H_{14}NaO_2$: 945.08860; found: 945.08892.

(3*S*)-1-ethoxycarbonyl-3-methyl-1-cyclopenteno[4,5:1,2][60]fullerene (**2e**)[67] **¡Error! Marcador no definido.**

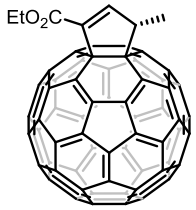

The adduct **2e** was prepared according to the general procedure using ethyl penta-2,3-dienoate **3c** (2.0 mg, 0.016 mmol), [60]fullerene (12 mg, 0.017 mmol) and 2-[(11b*S*)-3*H*-binaphtho[2,1-c:1′,2′-e]phosphepin-4(5*H*)-yl]ethanamine (0.6 mg, 0.002 mmol). Conversion: 20% (eluent: hexane:CH_2Cl_2, 3:1); *ee*: 93% (Pirkle Covalent (*R,R*) Whelk-02, hexane/2-propanol 98:2, flow rate 3.00 mL/min). ^{1}H NMR (700 MHz, $CDCl_3$) δ 1.43 (t, 3H, *J*= 7.1 Hz), 2.01 (d, 3H, *J*= 7.5 Hz), 4.40-4.48 (m, 2H), 4.90 (dq, 1H, *J*= 7.1 Hz), 7.78 (d, 1H, *J*= 2.3 Hz) ppm. ^{13}C NMR (175 MHz, $CDCl_3$) δ 14.3, 20.4, 52.3, 61.4, 74.4, 76.7, 135.3, 135.7, 136.0, 139.1, 139.3, 139.9, 140.2, 141.6, 141.6, 191.4, 192.0, 142.2, 142.2, 142.3, 143.1, 144.5, 144.5, 145.0, 145.0, 145.2, 145.2, 145.3, 145.4, 145.4, 145.5, 145.6, 146.0, 146.0, 146.0, 146.1, 146.2, 146.2, 146.3, 146.3, 146.4, 147.3, 147.4, 148.2, 148.4, 149.7, 150.8, 151.2, 153.2, 157.1, 163.9 ppm.

(3*S*)-1-ethoxycarbonyl-3-ethyl-1-cyclopenteno[4,5:1,2][60]fullerene (**2f**)[67]

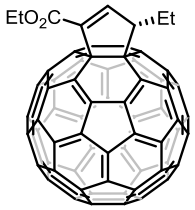

The adduct **2f** was prepared according to the general procedure using ethyl penta-2,3-dienoate **3d** (2.2 mg, 0.016 mmol), [60]fullerene (12 mg, 0.017 mmol) and 2-[(11b*S*)-3*H*-binaphtho[2,1-c:1′,2′-e]phosphepin-4(5*H*)-yl]ethanamine (0.6 mg, 0.002 mmol). Conversion: 70% (eluent: hexane:CH_2Cl_2, 3:1); *ee*: 92% (Pirkle Covalent (*R,R*) Whelk-02, hexane/2-propanol 98:2, flow rate 3.00 mL/min). ^{1}H NMR (700 MHz, $CDCl_3$) δ 1.44 (t, 3H, *J*= 7.1 Hz), 1.51 (t, 3H, *J*= 7.3 Hz), 2.22-2.33 (m, 1H), 2.54-2.70 (m, 1H), 4.35-4.50 (m, 2H), 4.90 (dq, 1H, *J*= 7.1 Hz), 7.93 (d, 1H, *J*= 2.4 Hz) ppm. ^{13}C NMR (175 MHz, $CDCl_3$) δ 13.5, 14.7, 29.6, 30.1, 59.9, 61.7, 74.9, 128.7, 136.1, 136.3, 136.4, 139.7, 140.1, 143.6, 141.2, 140.1, 140.6, 141.2, 142.0, 142.0, 142.4, 142.6, 142.8, 143.2, 143.5, 144.9, 144.9, 145.3, 145.7, 145.9, 145.9, 146.4, 146.4, 146.6, 146.6, 147.7, 148.0, 148.7, 148.8, 151.3, 151.6, 153.5, 157.7, 164.2 ppm.

(3*S*)-1-ethoxycarbonyl-3-isopropyl-1-cyclopenteno[4,5:1,2][60]fullerene (**2g**)[67]

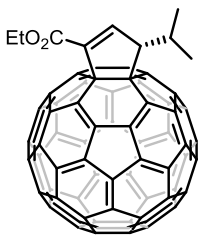

The adduct **2g** was prepared according to the general procedure using ethyl 5-methylhexa-2,3-dienoate **3e** (2.5 mg, 0.016 mmol), [60]fullerene (12 mg, 0.017 mmol) and 2-[(11b*S*)-3*H*-binaphtho[2,1-c:1′,2′-e]phosphepin-4(5*H*)-yl]ethanamine (0.6 mg, 0.002 mmol). Conversion: 42% (eluent: hexane:CH_2Cl_2, 3:1); *ee*: 80% (Pirkle Covalent (*R*,*R*) Whelk-02, hexane/2-propanol 98:2,flow rate 3.00 mL/min). ^{1}H NMR (700 MHz, $CDCl_3$) δ 1.44 (t, 3H, *J*= 7.1 Hz), 1.49 (d, 3H, *J*= 6.7 Hz), 1.55 (d, 3H, *J*= 6.9 Hz), 2.91-3.01(m, 1H), 4.40-4.50 (m, 2H), 4.79 (t, 1H, *J*= 2.6 Hz), 7.87 (d, 1H, *J*= 2.5 Hz) ppm. ^{13}C NMR (175 MHz, $CDCl_3$) δ 14.7, 19.8, 24.5, 30.1, 31.9, 61.7, 64.7, 75.2, 135.7, 136.3, 137.1, 139.6, 140.0, 140.6, 142.0, 142.1, 142.3, 142.3, 142.3, 142.3, 142.7, 142.8, 142.9, 143.0, 143.1, 143.2, 143.5, 143.6, 144.8, 144.9, 144.9, 145.1, 145.4, 145.5, 145.6, 145.7, 145.9, 145.9, 146.3, 146.4, 146.4, 146.5, 146.6, 146.6, 146.7, 146.8, 146.8, 147.0, 147.7, 147.8, 148.6, 151.6, 153.5, 158.3 ppm.

1-ethoxycarbonyl-3-(4-formylphenyl)-1-cyclopenteno[4,5:1,2][60]fullerene (**2h**)

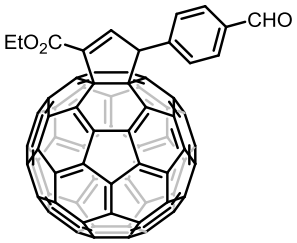

The adduct **2h** was prepared according to the general procedure using ethyl 4-(4-formylphenyl)-2,3-butadienoate **3f** (3.4 mg, 0.016 mmol), [60]fullerene (12 mg, 0.017 mmol) and 2-[(11b*S*)-3*H*-binaphtho[2,1-c:1′,2′-e]phosphepin-4(5*H*)-yl] ethanamine (0.6 mg, 0.002 mmol). Conversion: 31% (eluent: hexane:CH_2Cl_2, 1:1). ^{1}H NMR (700 MHz, $CDCl_3$) δ 1.46 (t, *J*= 7.1 Hz, 3H), 4.50 (dddd, *J*= 18.0, 10.9, 7.1, 3.8 Hz, 2H), 6.14 (d, *J*= 2.4 Hz, 1H), 7.87 (d, *J*= 2.5 Hz, 1H), 7.91 (d, *J*= 8.1 Hz, 2H), 8.02 (d, *J*= 8.1 Hz, 2H), 10.08 (s, 1H) ppm. ^{13}C NMR (176 MHz, $CDCl_3$) δ 14.3, 28.7, 29.7, 61.7, 63.4, 75.6, 76.4, 130.4, 130.5, 134.3, 135.66, 135.71, 135.8, 136.1, 138.9, 138.9, 139.2, 139.4, 139.6, 140.3, 141.6, 141.7, 141.9, 142.0, 142.1, 142.2, 142.4, 142.5, 142.7, 142.7, 142.7, 143.1, 144.5, 144.5, 144.7, 145.1, 145.2, 145.2, 145.4, 145.6, 145.7, 145.8, 145.9, 146.0, 146.1, 146.2, 146.2, 146.2, 146.3, 146.3, 146.4, 146.4, 146.4, 147.3, 147.4, 147.9, 148.3, 150.0, 150.5, 152.8, 156.4, 163.5, 191.8 ppm. HRMS (ESI POS.): $[M]^+$ Calc. for $C_{73}H_{11}O_3$: 935.0714; found: 935.0677.

(3*S*)-1-*tert-but*oxycarbonyl-3-benzyl-1-cyclopenteno[4,5:1,2][60]fullerene (**2i**)

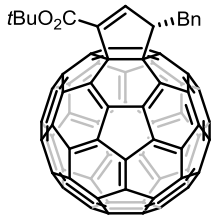

The adduct **2i** was prepared according to the general procedure using *tert*-butyl 5-phenyl-2,3-pentadienoate **3g** (3.6 mg, 0.016 mmol), [60]fullerene (12 mg, 0.017 mmol) and 2-[(11b*S*)-3*H*-binaphtho[2,1-c:1′,2′-e]phosphepin-4(5*H*)-yl]ethanamine (0.6 mg, 0.002 mmol). Conversion: 28% (eluent: hexane:CH_2Cl_2, 3:1); *ee*: 80% (Pirkle Covalent (*R*,*R*) Whelk-01, hexane/2-propanol 98:2, flow rate 2.00 mL/min; t_R for the major (3*S*) isomer: 9.94 min, t_R for the minor (3*R*) isomer: 12.01 min).^{1}H NMR (700 MHz, $CDCl_3$) δ 1.58 (s, 9H), 3.49-3.38 (m, 1H), 3.92 (dd, *J*= 13.3, 5.6 Hz, 1H), 5.06 (ddd, *J*= 11.6, 5.6, 2.3 Hz, 1H), 7.36 (t, *J*= 7.3 Hz, 1H), 7.46 (t, *J*= 7.6 Hz, 2H), 7.52 (d, *J*= 7.2 Hz, 2H), 7.54 (d, *J*= 2.3 Hz, 1H) ppm. ^{13}C NMR (176 MHz, CDCl3) δ 21.6, 28.3, 42.0, 59.1, 74.2, 82.5, 125.4, 127.0, 128.3, 129.0, 129.1, 129.3, 134.2, 135.7, 136.1, 137.5, 137.8, 138.8, 139.1, 139.2, 139.7, 140.3, 141.6, 141.7, 142.0, 142.0, 142.1, 142.1, 142.2, 142.3, 142.3, 142.4, 142.7, 142.7, 142.8, 143.1, 143.2, 144.5, 144.5, 144.5, 144.9, 145.1, 145.2, 145.3, 145.4, 145.4, 145.5, 145.6, 146.0, 146.1, 146.1, 146.2, 146.3, 146.4, 146.4, 146.4, 146.4, 146.5, 147.3, 147.4, 148.4, 148.6, 151.0, 151.2, 152.9, 157.1, 162.9 ppm. HRMS (ESI POS.): $[M]^+$ Calc. for $C_{75}H_{18}O_2$: 950.1312; found: 950.1270.

(3*R*)-1-benzyloxycarbonyl-3-phenyl-1-cyclopenteno[4,5:1,2][60]fullerene (**2j**)[67]

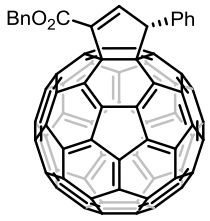

The adduct **2j** was prepared according to the general procedure using benzyl 4-phenylbuta-2,3-dienoate **3h** (4.0 mg, 0.016 mmol), [60]fullerene (12 mg, 0.017 mmol) and 2-[(11b*S*)-3*H*-binaphtho[2,1-c:1′,2′-e]phosphepin-4(5*H*)-yl]ethanamine (0.6 mg, 0.002 mmol). Conversion: 37% (eluent: hexane:CH_2Cl_2, 3:1); *ee*: 99% (Pirkle Covalent (*R*,*R*) Whelk-01, hexane/2-propanol 98:2, flow rate 2.00 mL/min). ^{1}H NMR (700 MHz, $CDCl_3$) δ 5.42 (d, 1H, *J*= 12.2), 5.48 (d, 1H, *J*= 12.2), 6.05 (d, 1H, *J*= 2.5 Hz), 7.35-7.45 (m, 4H), 7.45-7.52 (m, 4H), 7.70 (d, 2H, J= 7.2 Hz), 7.93 (d, 1H, *J*= 2.5 Hz) ppm. ^{13}C NMR (175 MHz, $CDCl_3$) δ 31.3, 64.0, 67.7, 76.3, 128.7, 129.0, 129.1, 129.6, 130.1, 134.5, 135.6, 135.9, 136.2, 136.4, 138.1, 138.1, 139.5, 139.76, 139.8, 140.0, 140.7, 142.0, 142.1, 142.1, 142.2, 142.3, 142.3, 142.5, 142.6, 142.6, 142.9, 142.8, 143.0, 143.0, 143.1, 143.1, 143.5, 144.8,

144.8, 144.8, 144.9, 145.2, 145.4, 145.4, 145.5, 145.7, 145.7, 145.8, 145.9, 146.0, 146.1, 146.2, 146.3, 146.4, 146.38, 146.5, 146.6, 146.6, 146.6, 146.7, 146.8, 147.1, 147.1, 147.7, 147.8, 148.3, 148.8, 150.7, 151.2, 154.0, 157.3, 163.8 ppm.

3-phenyl-1-cyclopenteno[4,5:1,2][60]fullerene-1-carboxylic acid (**2k**)

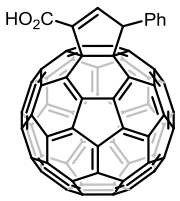

The adduct rac-**2k** was prepared treating rac-**2c** (30 mg, 0.033 mmol) with 0.5 mL of TFA in 2 mL of DCM and stirring for 6h. The crude is evaporated and the residue is centrifuged in DCM (3 x 10 mL, 10 min at 6000 rpm) and dried under vacuum. The resulting residue is a brown solid very insoluble; 96% yield (27.9 mg). ^{1}H NMR (300 MHz, DMSO) δ 7.89 – 7.85 (m, 1H), 7.73 (d, *J* = 8.7 Hz, 2H), 7.50 (t, *J* = 6.2 Hz, 2H), 7.41 – 7.34 (m, 1H), 6.34 – 6.28 (m, 1H).

5.2.4. Synthesis of phosphetane catalyst 4

General procedure for the synthesis of phosphetane catalyst (**4**)

A solution of the phosphinoferrocene (300 mg, 1,376 mmol) in THF (4mL/mmol) is preparred in a dry Schlenk flask and it is degassed (vaccumm-argon). This solution is cooled to -30ºC and then, *n*-BuLi (2,890 mmol) is added dropwise. The solution is maintained at -30ºC for 10 minutes and afterthat, is stirred at rt. for 5 minutes. Hereunder, the reaction is cooled to -95ºC (hexane/N_2 bath) and then, a solution of the (2*R*,4*R*)-pentane-2,4-diol dimesylate (1,376 mmol) in THF (4mL/mmol) is cannulated slowly. After addition, the reaction is allowed to reach rt. for 20h. Then, the reaction is cooled to -78ºC, the borane tetrahydrofuran complex (4,128 mmol) is added drop by drop and the reaction is stirred for 5h at -78ºC. Finally, the excess of BH_3·THF is hydrolyzed by addition of water and the desired compound is extracted with ethyl acetate. Purification by chromatographic column is carried out (hexane, hexane:diethyl ether from 15:1 to 1:1) (37% yield, orange solid)

(*R*,*R*)-2,4-Dimethyl-1-ferrocenylphosphetane Borane Complex (**4**)[155]

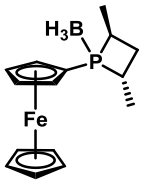

^{1}H NMR (300 MHz, $CDCl_3$) δ 4.54 (dt, *J* = 3.0, 1.3 Hz, 1H), 4.46 (dtd, *J* = 3.5, 2.4, 1.2 Hz, 2H), 4.35 (dd, *J* = 2.4, 1.2 Hz, 1H), 4.20 (s, 5H), 2.78 (qd, *J* = 14.3, 7.2 Hz, 1H), 2.60 – 2.46 (m, 1H), 2.33 – 2.03 (m, 2H), 1.38 (dd, *J* = 18.8, 7.4 Hz, 3H), 0.92 (dd, *J* = 15.6, 7.4 Hz, 3H), 0.58 (br. s, 1H), 0.28 (br. s, 1H). ^{13}C NMR (75 MHz, $CDCl_3$) δ 74.64 (d, J = 14.4 Hz), 72.33 (d, J = 7.9 Hz), 71.95 (d, J = 5.8 Hz), 70.79 (d, J = 3.2 Hz), 69.52 (s), 35.56 (d, J = 15.9 Hz, CH2), 28.91 (d, J = 41.0 Hz), 28.11 (d, J = 43.2 Hz), 15.76 (s), 15.65 (d, J = 6.6 Hz). ^{31}P NMR (121 MHz, CDCl3) δ 50.19 (d, J = 60.3 Hz).

5.2.5. Synthesis of cyclopenteno[4,5:1,2][60]fullerene from tert-butyloxycarbonyl-modified Morita-Baylis-Hillman adduct 6

General procedure for the [3+2] cycloaddition of *tert*-butyl-modified Morita-Baylis-Hillman **5** onto C_{60}

We used the same described procedure (section 5.2.3) for alkynoates and allenoates but replacing these later by *tert*-butyloxycarbonyl-modified Morita-Baylis-Hillman adduct **5**.

Methyl 2-(((tert-butoxycarbonyl)oxy)(phenyl)methyl)acrylate (**5**)[156]

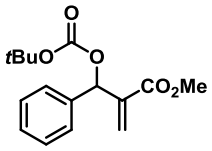

The acrylate **5** was prepared according to the literature by Morita-Baylis-Hillman reaction between methyl acrylate and benzaldehyde catalysed by DABCO and subsequent hydroxyl protection with Boc anhydride and pyridine. ^{1}H NMR (300 MHz, $CDCl_3$) δ 7.43 – 7.39 (m, 3H), 7.36 – 7.32 (m, 2H), 6.49 (s, 1H), 6.42 (s, 1H), 5.93 (s, 1H), 3.73 (s, 3H), 1.47 (s, 9H).

[155] Marinetti, A.; Jus, S.; Labrue, F.; Lemarchand, A.; Genêt, J.; Ricard, L. *Synthesis* **2001**, *14*, 2095-2104
[156] Zhang, T.; Dai, L.; Hou, X. *Tetrahedron: Asymmetry* **2007**, *18*, 1990-1994

(3*S*)-2-methoxycarbonyl-3-phenyl-1-cyclopenteno[4,5:1,2][60]fullerene (**6**)

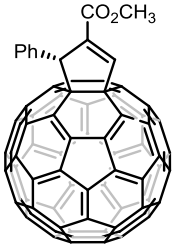

The adduct **6** was prepared according to the general procedure using methyl 2-(((tert-butoxycarbonyl)oxy)(phenyl)methyl) acrylate **5** (4.6 mg, 0.016 mmol), [60]fullerene (12 mg, 0.017 mmol) and 2-[(11b*S*)-3*H*-binaphtho[2,1-c:1′,2′-e]phosphepin-4(5*H*)-yl]ethanamine (0.6 mg, 0.002 mmol). Conversion: 36% (eluent: hexane:CH_2Cl_2, 1:1). *ee*: 57% (Pirkle Covalent (*R*,*R*) Whelk-02, hexane/2-propanol 98:2, flow rate 3.00 mL/min; t_R for the major (3*S*) isomer: 9.33 min, t_R for the minor (3*R*) isomer: 51.48 min). ^{1}H NMR (700 MHz, $CDCl_3$) δ 3.92 (s, 3H), 6.24 (d, *J*= 1.8 Hz, 1H), 7.35 (t, *J*= 7.5 Hz, 1H), 7.41 (s, 1H), 7.54 (s, 1H), 7.66 (s, 1H), 7.79 (s, 1H), 8.12 (d, *J*= 1.8 Hz, 1H) ppm. ^{13}C NMR (176 MHz, $CDCl_3$) δ 29.7, 52.4, 63.1, 74.7, 127.9, 134.2, 135.5, 136.2, 136.9, 138.5, 139.4, 140.2, 140.4, 140.6, 141.0, 141.7, 141.8, 141.8, 141.8, 142.0, 142.0, 142.1, 142.2, 142.3, 142.5, 142.6, 142.6, 142.7, 142.7, 143.1, 143.2, 144.3, 144.4, 144.5, 144.5, 145.0, 145.1, 145.2, 145.4, 145.5, 145.5, 145.5, 145.6, 145.7, 145.7, 145.8, 145.8, 145.9, 146.1, 146.1, 146.1, 146.2, 146.4, 146.5, 147.4, 147.5, 150.9, 151.1, 153.9, 156.4, 164.6 ppm. HRMS (ESI POS.): $[M]^+$ Calc. for $C_{71}H_{10}O_2$: 894.0686; found: 894.0682.

5.2.6. Synthesis of cyclopenteno[4,5:25',8']][70] fullerenes 7a-b

General procedure for the [3+2] cycloaddition of allenoates **3a**, **3c** onto [70]fullerene.

We use the same described procedure for C_{60} (section 5.2.3) but replacing these by [70]fullerene.

1-ethoxycarbonyl-3-methyl-1-cyclopenteno[4,5:25',8']][70]fullerene (**7a**)

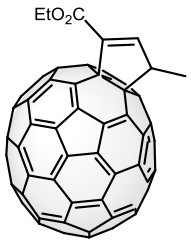

The adduct **7a** was prepared according to the general procedure using ethyl-2,3-pentadienoate **3c** (91.5μL, 0.556 mmol), [70]fullerene (500 mg, 0.595 mmol) and dppe (26 mg, 0.056 mmol). Conversion: 46% (eluent: hexane:CH_2Cl_2, 1:1). ^{1}H NMR (700 MHz, $CDCl_3$) δ 1.59 (t, *J*= 7.2 Hz, 3H), 1.68 (d, *J*= 7.5 Hz, 3H), 4.21 (qd, *J*= 7.5, 2.2 Hz, 1H), 4.57 (q, *J*= 7.1 Hz, 2H), 7.34 (d, *J*= 2.2 Hz, 1H) ppm. ^{13}C NMR (176 MHz, $CDCl_3$) δ 14.6, 20.5, 30.0, 50.3, 61.5, 67.4, 131.4, 131.4, 131.4, 131.5, 133.6, 133.9, 134.0, 135.3, 135.9, 137.5, 140.0, 140.1, 140.2, 140.4, 142.9, 143.2, 143.3, 143.3, 143.3, 143.4, 143.4, 143.7, 145.7, 145.8, 145.8, 146.0, 146.2, 146.9, 147.0, 147.1, 147.2, 147.5, 147.8, 148.8, 148.9, 148.9, 149.1, 149.2, 149.4, 149.4, 149.8, 149.8, 150.0, 150.0, 150.1, 150.4, 150.5, 150.5, 150.6, 150.7, 150.7, 151.2, 151.2, 151.5, 151.6, 156.2, 156.3, 156.9, 161.2, 163.7 ppm. HRMS (ESI POS.): [M]+ Calc. for $C_{79}H_9O_2$: 966.0681; found: 966.0655.

1-ethoxycarbonyl-3-phenyl-1-cyclopenteno[4,5:25',8']][70]fullerene (**7b**)

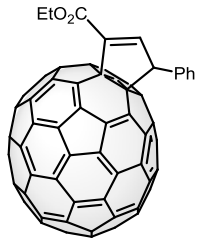

The adduct **7b** was prepared according to the general procedure using ethyl 4-phenyl-2,3-butadienoate **3a** (41.9 mg, 0.223 mmol), [70]fullerene (200 mg, 0.238 mmol) and 2-[(11b*S*)-3*H*-binaphtho[2,1-c:1′,2′-e]phosphepin-4(5*H*)-yl]ethanamine (8 mg, 0.022 mmol). Conversion: 58% (eluent: hexane:CH_2Cl_2, 1:1). *ee*: 76% (Pirkle Covalent (*R*,*R*) Whelk-01, hexane/methanol 98:2, flow rate 2.50 mL/min; t_R for the major (3*S*) isomer: 8.05 min, t_R for the minor (3*R*) isomer: 10.09 min). ^{1}H NMR (700 MHz, $CDCl_3$) δ 1.61 (t, *J* = 7.2 Hz, 3H), 4.62 (qq, *J*= 10.7, 7.2 Hz, 2H), 5.32 (d, *J*= 2.4 Hz, 1H), 7.28–7.26 (m, 1H), 7.38–7.32 (m, 4H), 7.43 (d, *J*= 2.4 Hz, 1H) ppm. ^{13}C NMR (176 MHz, $CDCl_3$) δ 14.6, 61.1, 61.7, 69.0, 69.1, 128.3, 129.0, 129.3, 131.2, 131.4, 131.4, 131.4, 131.5, 131.5, 133.1, 133.8, 133.9, 134.0, 135.4, 136.8, 138.3, 139.4, 139.8, 140.1, 140.3, 140.4, 142.7, 143.2, 143.3, 143.3, 143.3, 143.4, 143.4, 143.5, 143.5, 144.5, 145.3, 145.6, 145.7, 145.9, 146.2, 146.7, 147.0, 147.0, 147.1, 147.5, 147.5, 148.7, 148.8, 148.8, 148.9, 149.1, 149.1, 149.3, 149.3, 149.6, 149.7, 149.9, 149.9, 150.1, 150.5, 150.5, 150.5, 150.6, 150.7, 150.7, 151.0, 151.3, 151.5,

151.5, 151.5, 156.2, 156.4, 157.5, 161.1, 163.7 ppm. HRMS (ESI POS.): [M]+ Calc. for $C_{82}H_{12}O_2$: 1028.0837; found: 1028.0786.

1-ethoxycarbonyl-3-phenyl-1-cyclopenteno[4,5:,8':25'][70]fullerene (**7b´**)

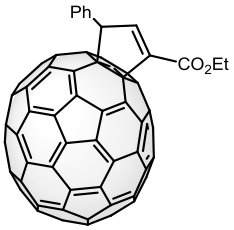

The adduct **7b´** was prepared according to the general procedure using ethyl 4-phenyl-2,3-butadienoate **3a** (41.9 mg, 0.223 mmol), [70]fullerene (200 mg, 0.238 mmol) and 2-[(11b*S*)-3*H*-binaphtho[2,1-c:1′,2′-e]phosphepin-4(5*H*)-yl]ethanamine (8 mg, 0.022 mmol). Conversion: 6% (eluent: hexane:CH_2Cl_2, 1:1). ^{1}H NMR (700 MHz, $CDCl_3$) δ 1.32 (t, *J*= 7.1 Hz, 6H), 4.36–4.26 (m, 2H), 5.60 (d, *J*= 2.4 Hz, 1H), 7.44 (d, *J*= 2.5 Hz, 1H), 7.51 (t, *J*= 7.5 Hz, 1H), 7.62 (t, *J*= 7.7 Hz, 2H), 7.70 (d, *J*= 7.3 Hz, 2H) ppm. ^{13}C NMR (176 MHz, $CDCl_3$) δ 14.2, 29.8, 61.4, 65.0, 128.5, 129.4, 130.0, 131.1, 131.2, 131.6, 131.6, 132.5, 132.8, 133.8, 136.7, 137.2, 137.7, 138.8, 139.1, 139.8, 140.1, 140.3, 143.0, 143.2, 143.2, 143.3, 143.3, 143.4, 143.5, 145.2, 146.0, 146.1, 146.3, 146.4, 146.6, 147.0, 147.0, 147.0, 147.4, 147.5, 147.6, 148.2, 148.6, 148.7, 148.8, 148.8, 149.2, 149.2, 149.3, 149.3, 149.5, 149.7, 149.8, 150.1, 150.7, 150.7, 150.8, 150.9, 150.9, 151.3, 151.4, 151.5, 154.3, 155.2, 155.4, 155.8, 163.2 ppm.

5.2.7. Synthesis of cyclobuteno[4,5:1,2][60]fullerenes 8a-k

General procedure for the formal [2+2] cycloaddition of the alkynoates **1a-e** onto [60]fullerene

In an ordinary vial a suspension of [60]fullerene (1 eq.) and $Bu_4NOH{\cdot}30H_2O$ (1 eq.) in 3.0 mL of toluene is prepared and stirred at room temperature. Then, the corresponding alkynoate **1a-e** (2 eq.) is added and the mixture is stirred 3h at rt. Finally, the solvent is evaporated under vacuum and dark residue is then purified by silica-gel column chromatography using CS_2 as eluent (for recovering unreacted [60]fullerene). Then, mixtures of solvents (indicated in each case) are used affording desired cyclobuteno[4,5:1,2][60]fullerene derivatives **2a-e**. Conversions are determined by HPLC analysis using Buckyprep (Waters) as the chromatographic column.

General procedure for the formal [2+2] cycloaddition of allenoates **3a-h** onto [60]fullerene

In an ordinary vial a suspension of [60]fullerene (1 eq.) and $Bu_4NOH·30H_2O$ (1 eq.) in 3.0 mL of toluene is prepared and stirred at room temperature. Then, the corresponding allenoate **3a-h** (2 eq.) is added and the mixture is stirred 3h at 50ºC. Finally, the solvent is evaporated under vacuum and dark residue is then purified by silica-gel column chromatography using CS_2 as eluent (for recovering unreacted [60]fullerene). Then, mixtures of solvents (indicated in each case) are used affording desired cyclobuteno[4,5:1,2][60]fullerene derivatives **2a-b**, **2f-k**. Conversions are determined by HPLC analysis using Buckyprep (Waters) as the chromatographic column.

1-(ethoxycarbonylmethyl)-2-phenyl-1-cyclobuteno[3,4:1,2][60]fullerene (**8a**)

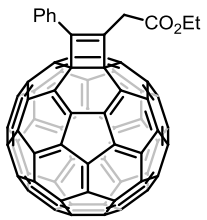

The adduct **8a** was prepared according to the general procedure by using ethyl 4-phenyl-3-butynoate **1a** or ethyl 4-phenylbuta-2,3-dienoate **3a** (3.1 mg, 0.016 mmol), [60]fullerene (6 mg, 0.008 mmol), and tetrabutylammonium hydroxide (6,7 mg, 0.008 mmol). Conversion: 57% with the alkynoate, 44% with the allenoate. Isolated yield (0,069 mmol C_{60}): 25% (15,7 mg) with the alkynoate (eluent CS_2). ^{1}H NMR (700 MHz, $CDCl_3$) δ 1.31 (t, *J* = 7.1 Hz, 3H), 4.30 (s, 2H), 4.32 (q, *J* = 7.1 Hz, 2H), 7.54 (t, *J* = 7.4 Hz, 1H), 7.62 (t, *J* = 7.7 Hz, 2H), 8.24 (d, *J* = 8.4 Hz, 2H) ppm. ^{13}C NMR (175 MHz, $CDCl_3$) δ 14.2, 35.4, 50.9, 127.5, 129.3, 129.6, 132.9, 139.5, 139.8, 140.4, 140.4, 142.0, 142.2, 142.3, 142.6, 142.6, 142.9, 143.1, 143.4, 144.6, 144.6, 145.3, 145.3, 145.4, 145.4, 146.1, 146.1, 146.1, 146.8, 146.9, 147.2, 152.4, 154.7, 155.5, 169.2 ppm. HRMS (MALDI+): $[M]^+$ Calc. for $C_{72}H_{12}O_2$: 908.0832; found: 908.0831.

1-(ethoxycarbonylmethyl)-2-ethyl-1-cyclobuteno[3,4:1,2][60]fullerene (**8b**)

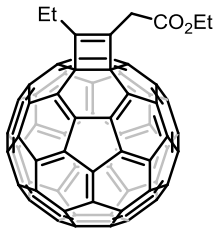

The adduct **8b** was prepared according to the general procedure by using ethyl hexa-2,3-dienoate **3d** (2.3 mg, 0.016 mmol), [60]fullerene (6 mg, 0.008 mmol) and tetrabutylammonium hydroxide (6,7 mg, 0.008 mmol). Conversion: 23%. Isolated yield (0,069 mmol C_{60}): 14% (8,3 mg) (eluent CS_2). ^{1}H NMR (700 MHz, $CDCl_3$) δ 1.31 (t, *J*= 7.1 Hz, 3H), 1.66 (t, *J* = 7.6 Hz, 3H), 3.07 (dd, *J* = 15.3, 7.6 Hz, 2H), 3.99 (s, 2H), 4.29 (q, *J* = 7.1 Hz, 2H) ppm. ^{13}C NMR (175 MHz, $CDCl_3$) δ 13.6, 14.2, 21.9, 34.0, 61.6, 77.3 (Csp^3-adduct), 77.5 (Csp^3-adduct), 139.4, 139.5, 140.2, 140.3, 142.0, 142.1, 142.2, 142.5, 142.8, 143.1, 143.5, 144.5, 144.6, 145.2, 145.2, 145.2, 145.3, 145.3, 146.0, 146.7, 146.9, 147.2, 156.0, 158.6, 169.8 ppm. HRMS (MALDI+): $[M]^+$ Calc. for $C_{68}H_{12}O_2$: 860.0832; found: 860.0832.

1-(ethoxycarbonylmethyl)-2-methyl-1-cyclobuteno[3,4:1,2][60]fullerene (**8c**)

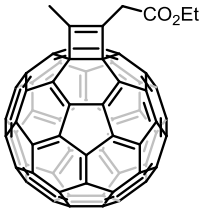

The adduct **8c** was prepared according to the general procedure by using ethyl penta-2,3-dienoate **3c** (2.1 mg, 0.016 mmol), [60]fullerene (6 mg, 0.008 mmol) and tetrabutylammonium hydroxide (6,7 mg, 0.008 mmol). Conversion: 18% (eluent CS_2). ^{1}H NMR (700 MHz, $CDCl_3$) δ 1.32 (t, *J* = 7.1 Hz, 3H), 2.62 (s, 2H), 3.98 (s, 2H), 4.29 (q, *J* = 7.1 Hz, 2H) ppm. ^{13}C NMR (175 MHz, $CDCl_3$) δ 12.5, 14.2, 33.9, 61.6, 76.2 (Csp^3-adduct), 78.4 (Csp^3-adduct), 139.3, 139.8, 140.2, 140.3, 141.9, 142.09, 142.14, 142.2, 142.5, 142.5, 142.8, 142.9, 144.5, 144.6, 144.7, 145.2, 145.3, 145.3, 146.0, 146.1, 146.7, 147.1, 147.2, 153.0, 155.4, 155.8, 169.7 ppm. HRMS (MALDI+): $[M]^+$ Calc. for $C_{67}H_{10}O_2$: 846.0675; found: 846.0657.

1-(ethoxycarbonylmethyl)-2-benzyl-1-cyclobuteno[3,4:1,2][60]fullerene (**8d**)

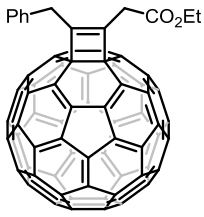

The adduct **8d** was prepared according to the general procedure by using ethyl 5-phenylpenta-2,3-dienoate **3b** (3.4 mg, 0.016 mmol), [60]fullerene (6 mg, 0.008 mmol) and tetrabutylammonium hydroxide (6,7 mg, 0.008 mmol). Conversion: 33% (eluent CS_2, CS_2:CH_2Cl_2 100:1). ^{1}H NMR (700 MHz, $CDCl_3$) δ 1.32 (t, *J* = 7.1 Hz, 3H),

3.88 (s, 2H), 4.28 (q, *J* = 7.1 Hz, 2H), 4.35 (s, 2H), 7.30 (m, 1H), 7.39 (t, *J* = 7.6 Hz, 2H), 7.66 (d, *J* = 7.6 Hz, 2H) ppm. ^{13}C NMR (175 MHz, $CDCl_3$) δ 14.2, 33.8, 34.9, 61.6, 77.5 (Csp^3-adduct), 77.6 (Csp^3-adduct), 127.2, 128.9, 129.9, 137.1, 139.3, 139.4, 140.0, 140.2, 141.9, 142.0, 142.1, 142.2, 142.4, 142.5, 142.8, 144.5, 144.9, 145.1, 145.2, 145.2, 145.3, 146.0, 146.0, 146.7, 146.7, 146.9, 147.1, 155.5, 155.6, 155.7, 169.6 ppm. HRMS (MALDI+) $[M]^+$ Calc. for $C_{73}H_{14}O_2$: 922.0988; found: 922.0970.

1-(benzyloxycarbonylmethyl)-2-phenyl-1-cyclobuteno[3,4:1,2][60]fullerene (**8e**)

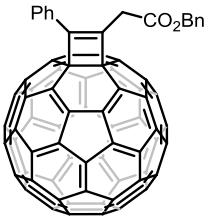

The adduct **8e** was prepared according to the general procedure by using benzyl 4-phenylbuta-2,3-dienoate **3h** (4.2 mg, 0.016 mmol), [60]fullerene (6 mg, 0.008 mmol) and tetrabutylammonium hydroxide (6,7 mg, 0.008 mmol). Conversion: 52% (eluent CS_2, CS_2:CH_2Cl_2 100:1). ^{1}H NMR (700 MHz, $CDCl_3$) δ 4.35 (s, 2H), 5.29 (s, 2H), 7.34 (q, *J* = 6.0 Hz, 3H), 7.38 (d, *J* = 6.3 Hz, 2H), 7.54 (t, *J* = 7.4 Hz, 1H), 7.61 (t, *J* = 7.6 Hz, 2H), 8.23 (d, *J* = 7.2 Hz, 2H) ppm. ^{13}C NMR (175 MHz, $CDCl_3$) δ 35.3, 67.6, 76.6 (Csp^3-adduct), 127.4, 128.6, 128.7, 128.7, 129.3, 129.6, 132.8, 139.5, 139.8, 140.3, 140.4, 142.0, 142.0, 142.2, 142.2, 142.5, 142.6, 142.9, 142.9, 143.0, 144.5, 144.6, 145.2, 145.3, 145.3, 145.3, 145.4, 146.4, 146.1, 146.1, 146.8, 146.8, 146.8, 147.2, 152.6, 154.5, 155.4, 169.2 ppm. HRMS (MALDI+) $[M]^+$ Calc. for $C_{77}H_{14}O_2$: 970.0988; found: 970.0975.

1-(ethoxycarbonylmethyl)-2-(4-chlorophenyl)-1-cyclobuteno[3,4:1,2][60]fullerene (**8f**)

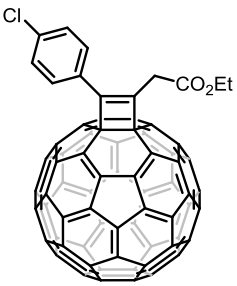

The adduct **8f** was prepared according to the general procedure by using ethyl 4-(4-chlorophenyl)but-3-ynoate **1g** or ethyl 4-(4-chlorophenyl)buta-2,3-dienoate **3i** (3.8 mg, 0.016 mmol), [60]fullerene (6 mg, 0.008 mmol), and tetrabutylammonium hydroxide (6,7 mg, 0.008 mmol). Conversion: 52% with the alkynoate, 22% with the allenoate (eluent CS_2, CS_2:CH_2Cl_2 100:1). ^{1}H NMR (300 MHz, $CDCl_3$) δ 8.16 (d, *J* = 8.5 Hz, 1H), 7.58 (d, *J* = 8.5 Hz, 1H), 4.31 (q, *J* = 7.2 Hz, 1H), 4.26 (s, 1H), 1.30 (d, *J* = 7.1 Hz, 2H). ^{13}C NMR (126 MHz, $CDCl_3$) δ 169.5, 155.5, 154.8, 151.7, 147.5, 147.1, 146.5, 146.5, 146.5, 146.5, 145.8, 145.8, 145.7, 145.6, 145.0, 145.0, 144.4,

143.5, 143.3, 143.0, 143.0, 142.7, 142.6, 142.4, 140.8, 140.8, 140.2, 139.8, 136.0, 131.7, 130.1, 130.1, 130.0, 129.1, 62.3, 35.8, 30.1, 14.5. HRMS (MALDI+): $[M]^+$ Calc. for $C_{72}H_{11}ClO_2$: 942.0448; found: 942.0442.

1-(*tert*-butoxycarbonylmethyl)-2-(4-bromophenyl)-1-cyclobuteno[3,4:1,2][60]fullerene (**8g**)

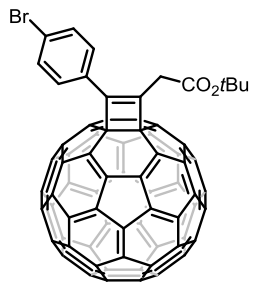

The adduct **8g** was prepared according to the general procedure by using *tert*-butyl 4-(4-bromophenyl)but-3-ynoate **1h** (4.9 mg, 0.016 mmol), [60]fullerene (6 mg, 0.008 mmol) and tetrabutylammonium hydroxide (6,7 mg, 0.008 mmol). Conversion: 34%. Isolated yield (0,069 mmol C_{60}): 22% (15,4 mg) (eluent CS_2, CS_2:CH_2Cl_2 100:1). ^{1}H NMR (500 MHz, Tol) δ 7.99 (d, *J* = 8.5 Hz, 2H), 7.41 (d, *J* = 8.5 Hz, 2H), 3.83 (s, 2H), 1.39 (s, 9H) ppm. ^{13}C NMR (126 MHz, Tol) δ 28.1, 36.9, 82.0, 124.2, 125.5, 127.6, 128.3, 128.4, 129.2, 132.1, 132.7, 137.2, 137.6, 139.8, 140.1, 140.8, 140.8, 142.2, 142.3, 142.5, 142.5, 142.9, 142.9, 143.2, 143.2, 143.2, 144.8, 144.9, 145.3, 145.5, 145.6, 145.7, 145.7, 145.7, 146.4, 146.4, 146.4, 146.4, 146.9, 147.1, 147.6, 154.8, 155.5, 167.6 ppm. HRMS (MALDI+): $[M]^+$ Calc. for $C_{74}H_{15Br}O_2$: 1014.0255; found: 1014.0237.

1-(*tert*-butoxycarbonylmethyl)-2-(3,4-dichlorophenyl)-1-cyclobuteno[3,4:1,2][60]fullerene (**8h**)

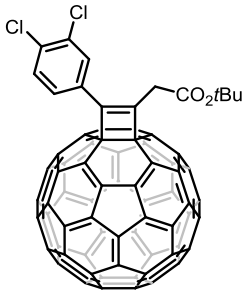

The adduct **8h** was prepared according to the general procedure by using *tert*-butyl 4-(3,4-dichlorophenyl)but-3-ynoate **1i** (4.8 mg, 0.016 mmol), [60]fullerene (6 mg, 0.008 mmol) and tetrabutylammonium hydroxide (6,7 mg, 0.008 mmol). Conversion: 41%. Isolated yield (0,069 mmol C_{60}): 23% (16,2 mg) (eluent CS_2, CS_2:CH_2Cl_2 100:1). ^{1}H NMR (500 MHz, $CDCl_3$) δ 1.52 (s, 9H), 4.14 (s, 2H), 7.65 (d, *J* = 8.3 Hz, 1H), 8.09 (dd, *J* = 2.0, 8.3 Hz, 1H), 8.32 (d, *J* = 2.0 Hz, 1H) ppm. ^{13}C NMR (175 MHz, $CDCl_3$) δ 28.5, 37.4, 83.2, 127.0, 129.5, 131.7, 133.1, 134.0, 134.0, 139.9, 140.2, 140.9, 142.3, 142.4, 142.6, 142.7, 143.0, 143.0, 143.3, 143.5, 144.9, 145.0, 145.6, 145.8, 145.8, 145.8, 146.5, 146.6, 146.9, 147.2, 147.5, 150.2, 154.6, 155.2, 168.4 ppm. HRMS (MALDI+) $[M]^+$ Calc. for $C_{74}H_{14}Cl_2O_2$: 1004.0371; found: 1004,0365.

1-(*tert*-butoxycarbonylmethyl)-2-(4-*tert*-butylphenyl)-1-cyclobuteno[3,4:1,2][60]fullerene (**8i**)

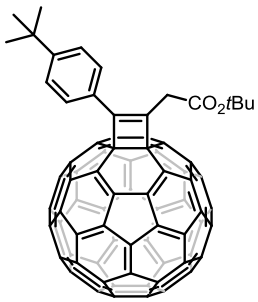

The adduct **8i** was prepared according to the general procedure by using *tert*-butyl 4-(4-(*tert*-butyl)phenyl)but-3-ynoate **1j** (4.4 mg, 0.016 mmol), [60]fullerene (6 mg, 0.008 mmol) and tetrabutylammonium hydroxide (6,7 mg, 0.008 mmol). Conversion: 31% (eluent CS_2). ^{1}H NMR (500 MHz, CDCl3) δ 8.24 (d, *J* = 8.5 Hz, 2H), 7.65 (d, *J* = 8.4 Hz, 2H), 4.19 (s, 2H), 1.53 (s, 9H), 1.43 (s, 9H) ppm. ^{13}C NMR (126 MHz, CDCl3) δ 28.5, 31.7, 35.4, 37.5, 82.8, 126.6, 127.6, 130.7, 139.9, 140.1, 140.8, 140.8, 142.4, 142.5, 142.6, 142.6, 143.0, 143.0, 143.3, 143.5, 143.5, 145.0, 145.0, 145.7, 145.7, 145.7, 145.8, 146.5, 146.5, 146.5, 147.2, 147.3, 147.8, 152.5, 153.3, 155.4, 156.4, 169.0 ppm. HRMS (MALDI+) $[M]^+$ Calc. for $C_{78}H_{24}O_2$: 992.1776; found: 992.1769.

1-(methoxycarbonylmethyl)-2-phenyl-1-cyclobuteno[3,4:1,2][60]fullerene (**8j**)

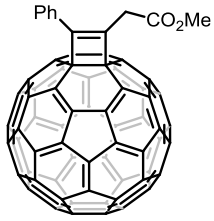

The adduct **8j** was prepared according to the general procedure by using methyl 4-phenylbuta-2,3-dienoate **3j** (2.9 mg, 0.016 mmol), [60]fullerene (6 mg, 0.008 mmol) and tetrabutylammonium hydroxide (6,7 mg, 0.008 mmol). Conversion: 48% (eluent CS_2, CS_2:CH_2Cl_2 100:1). ^{1}H NMR (700 MHz, $CDCl_3$) δ 3.84 (s, 3H), 4.32 (s, 2H), 7.54 (t, *J* = 7.4 Hz, 1H), 7.62 (t, *J* = 7.7 Hz, 2H), 8.22 (d, *J* = 7.2 Hz, 2H) ppm. ^{13}C NMR (175 MHz, $CDCl_3$) δ 34.9, 52.6, 77.7 (Csp^3-adduct), 127.4, 129.3, 129.7, 132.9, 139.4, 139.8, 140.4, 140.4, 142.0, 142.0, 142.2, 142.3, 142.6, 142.6, 142.9, 143.1, 143.2, 144.6, 144.6, 145.3, 145.3, 145.4, 145.4, 146.1, 146.1, 146.1, 146.8, 146.8, 146.8, 147.2, 152.5, 154.6, 155.4, 169.7 ppm. HRMS (MALDI+) $[M]^+$ Calc. for $C_{71}H_{10}O_2$: 894.0675; found: 894.0647.

1-(methoxycarbonylmethyl)-2-benzyl-1-cyclobuteno[3,4:1,2][60]fullerene (**8k**)

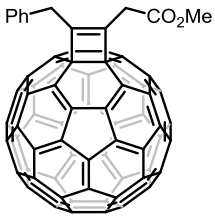

The adduct **8k** was prepared according to the general procedure by using methyl 5-phenylpenta-2,3-dienoate **3k** (3.1 mg, 0.016 mmol), [60]fullerene (6 mg, 0.008 mmo) and tetrabutylammonium hydroxide (6,7 mg, 0.008 mmol). Conversion: 31% (eluent CS_2, CS_2:CH_2Cl_2 100:1). ^{1}H NMR (700 MHz, $CDCl_3$) δ 3.80 (s, 3H), 3.87 (s, 2H), 4.35 (s, 2H), 7.30 (s, 1H), 7.39 (t, *J* = 7.6 Hz, 2H), 7.65 (d, *J* = 7.5 Hz, 2H) ppm. ^{13}C NMR (175 MHz, $CDCl_3$) δ 33.3, 33.8, 34.9, 52.4, 77.4 (Csp^3-adduct), 77.6 (Csp^3-adduct), 127.2, 127.2, 128.9 (br signal), 129.9, 137.0, 139.3, 139.4, 139.4, 140.0, 140.2, 141.9, 142.0, 142.1, 142.2, 142.4, 142.5, 142.8, 142.8, 144.5, 144.7, 144.9, 145.1, 145.2, 145.2, 145.3, 146.00, 146.0, 146.0, 146.7, 146.7, 146.9, 147.1, 155.4 ppm. HRMS (MALDI+) $[M]^+$ Calc. for $C_{72}H_{12}O_2$: 908.0832; found: 908.0800.

5.2.8. Synthesis of helicene-iminoesters 10

General procedure

Iminoesters **10** were synthesized following the procedure described in the literature by coupling of *tert*-butyl glycinate hydrochloride and 2-formylhexahelicene **9** in basic medium.

Racemic *tert*-butyl (E)-*N*-[(2-carbo[6]helicene)methylene]glycinate (**10**)

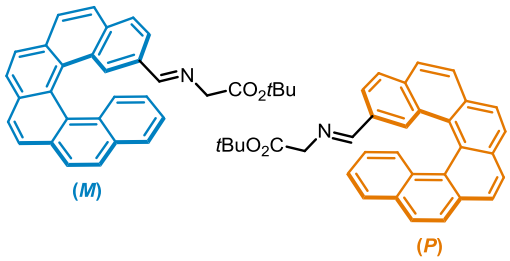

The racemic iminoester **10** was prepared according to the general procedure by using carbo[6]helicene-2-carbaldehyde **9**[157] (20 mg, 0.056 mmol,) *tert*-butyl glycinate hydrochloride (14 mg, 0.080 mmol), triethylamine (12 µL, 0.080

[157] Moussa, M. E. S.; Srebro, M.; Anger, E.; Vanthuyne, N.; Roussel, C.; Lescop, C.; Autschbach, J.; Crassous, J. *Chirality* **2013**, *25*, 455-465

mmol), and anhydrous sodium sulfate. Isolated yield: 99% (26 mg). ^{1}H NMR (300 MHz, $CDCl_3$) δ 8.04 – 7.78 (m, 11H), 7.68 (s, 1H), 7.58 (d, *J* = 8.5 Hz, 1H), 7.36 (s, 1H), 7.21 (t, *J* = 7.0 Hz, 1H), 6.69 (t, *J* = 7.7 Hz, 1H), δ 4.15 (d, *J* = 15.7 Hz, 1H), 4.03 (d, *J* = 16.0 Hz, 1H), 1.48 (s, 9H). ^{13}C NMR (75 MHz, $CDCl_3$) δ 165.2, 133.9, 133.8, 133.7, 132.9, 132.1, 131.9, 131.8, 130.1, 130.1, 129.9, 129.7, 128.9, 128.8, 128.6, 128.3, 128.2, 128.0, 127.9, 127.8, 127.7, 127.7, 127.4, 126.6, 126.3, 125.3, 123.3, 81.6, 77.9, 77.4, 77.0, 62.9, 28.5. HRMS (ESI+) $[M+H]^+$ Calc. for $C_{33}H_{28}NO_2$: 470,21200; found: 470,20835.

tert-Butyl (E)-*N*-[*M*-(2-carbo[6]helicene)methylene]glycinate **(*M*-10)**

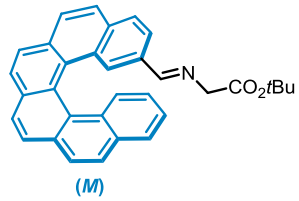

The iminoester ***M*-10** was prepared according to the general procedure by using *M*-carbo[6]helicene-2-carbaldehyde ***M*-9** (20 mg, 0.056 mmol,) *tert*-butyl glycinate hydrochloride (14 mg, 0.080 mmol), triethylamine (12 µL, 0.080 mmol), and anhydrous sodium sulfate. Isolated yield: 96% (25.5 mg). ^{1}H NMR (300 MHz, $CDCl_3$) δ 8.03 – 7.86 (m, 10H), 7.80 (d, *J* = 8.0 Hz, 1H), 7.68 (s, 1H), 7.58 (d, *J* = 8.5 Hz, 1H), 7.36 (s, 1H), 7.21 (ddd, *J* = 8.0, 6.9, 1.1 Hz, 1H), 6.69 (ddd, *J* = 8.4, 6.9, 1.4 Hz, 1H), δ 4.16 (dd, *J* = 16.0, 1.2 Hz, 1H), 4.03 (dd, *J* = 16.0, 1.1 Hz, 1H), 1.48 (s, 9H).

tert-Butyl (E)-*N*-[*P*-(2-carbo[6]helicene)methylene]glycinate **(*P*-10)**

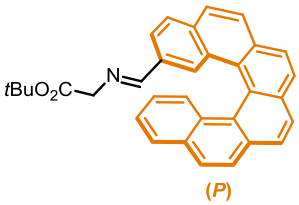

The iminoester ***P*-10** was prepared according to the general procedure by using *P*-carbo[6]helicene-2-carbaldehyde ***P*-9** (20 mg, 0.056 mmol,) *tert*-butyl glycinate hydrochloride (14 mg, 0.080 mmol), triethylamine (12 µL, 0.080 mmol), and anhydrous sodium sulfate. Isolated yield: 94% (25 mg). ^{1}H NMR (300 MHz, $CDCl_3$) δ 8.03 – 7.83 (m, 10H), 7.80 (d, *J* = 8.0 Hz, 1H), 7.68 (s, 1H), 7.58 (d, *J* = 8.5 Hz, 1H), 7.36 (s, 1H), 7.21 (ddd, *J* = 8.0, 7.0, 1.1 Hz, 1H), 6.69 (ddd, *J* = 8.4, 7.0, 1.3 Hz, 1H), δ 4.16 (dd, *J* = 16.0, 1.1 Hz, 1H), 4.03 (dd, *J* = 16.1, 1.0 Hz, 1H), 1.48 (s, 9H).

5.2.9. Synthesis of helicene-pyrrolidino[60]fullerenes 11-12

General procedure for catalytic 1,3-dipolar cycloaddition of helicene-azomethine ylides and [60]fullerene

Chiral ligand (0.0022 mmol) and metal salt (0.0022 mmol) were dissolved in toluene (3 mL). The solution was stirred for 1h at room temperature, and then, a solution of α-iminoester (0.0074 mmol). Finally, C_{60} (0.0149 mmol). The reaction mixture was stirred for 2.5 h, and afterwards, it was quenched with a saturated ammonium chloride solution (20 mL). The mixture was extracted with toluene (3 x 20mL), and the combined extracts were washed with brine (30 mL). The organic layer was dried over $MgSO_4$ and concentrated in vacuum. The crude product was purified by silica gel flash chromatography (1) CS_2/ 2) CS_2:DCM 100:1 to 10:1)).

(2*S*,5*S*)-2-*tert*-butoxycarbonyl-5-(*P*-2-carbo[6]helicene)pyrrolidino [3,4:1,2][60]fullerene (***P*,*S*,*S*-11**)

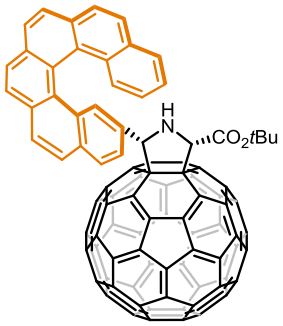

The adduct ***P*,*S*,*S*-11** was prepared according to the general procedure by using the catalytic system (R_p)-Fesulphos (1 mg, 0.0022 mmol) and $Cu(OAc)_2$ (4 mg, 0.0022 mmol), *tert*-butyl (E)-*N*-[*P*-(2-carbo[6]helicene)methylene]glycinate ***P*-10** (3.5 mg, 0.0074 mmol,) and C_{60} (11 mg, 0.0149 mmol). Isolated yield: 92% (9.8 mg). ^{1}H NMR (700 MHz, $CDCl_3$) δ 8.12 (s, 1H), 8.03 (d, *J* = 8.3 Hz, 2H), 8.01 – 7.92 (m, 8H), 7.86 (d, *J* = 7.3 Hz, 1H), 7.73 (d, *J* = 8.5 Hz, 1H), 7.49 – 7.46 (m, 1H), 6.86 – 6.83 (m, 1H), 5.31 (s, 1H), 4.93 (s, 1H), 1.54 (s, 9H). ^{13}C NMR (176 MHz, $CDCl_3$) δ 168.5, 153.2, 152.8, 151.8, 150.9, 147.1, 147.0, 146.9, 146.4, 146.3, 146.3, 146.1, 146.1, 146.0, 145.9, 145.8, 145.8, 145.7, 145.6, 145.5, 145.5, 145.3, 145.3, 145.1, 145.1, 145.0, 145.0, 144.3, 144.2, 144.2, 143.1, 143.0, 142.9, 142.6, 142.6, 142.5, 142.5, 142.3, 142.3, 142.1, 142.0, 142.0, 141.9, 141.9, 141.7, 141.6, 141.6, 141.2, 139.6, 139.4, 139.2, 138.8, 137.3, 136.3, 135.9, 135.1, 133.1, 132.8, 131.8, 131.6, 131.5, 130.0, 129.1, 128.8, 128.3, 127.9, 127.8, 127.7, 127.6, 127.5, 127.4, 127.3, 127.3, 127.2, 127.1, 126.9, 126.4, 126.2, 125.0, 124.0, 83.6, 78.6, 74.8,

72.9, 28.3. HRMS (ESI+) $[M+H]^+$ Calc. for $C_{93}H_{28}NO_2$: 1190,21200; found: 1190.21124.

(2*S*,5*S*)-2-*tert*-butoxycarbonyl-5-(*M*-2-carbo[6]helicene)pyrrolidino [3,4:1,2][60]fullerene (***M*,*S*,*S*-12**)

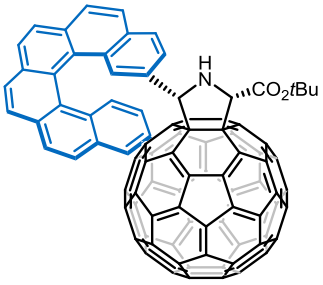

The adduct ***M*,*S*,*S*-12** was prepared according to the general procedure by using the catalytic system (R_p)-Fesulphos (1 mg, 0.0022 mmol) and $Cu(OAc)_2$ (4 mg, 0.0022 mmol), *tert*-butyl (E)-N-[*M*-(2-carbo[6]helicene)methylene]glycinate ***M*-10** (3.5 mg, 0.0074 mmol,) and C_{60} (11 mg, 0.0149 mmol). Isolated yield: 83% (7.2 mg). ^{1}H NMR (700 MHz, $CDCl_3$) δ 8.40 (s, 1H), 8.28 (d, *J* = 7.9 Hz, 1H), 8.22 (d, *J* = 8.4 Hz, 1H), 8.07 (d, *J* = 8.4 Hz, 1H), 8.00 – 7.94 (m, 6H), 7.90 (d, *J* = 8.1 Hz, 1H), 7.82 (d, *J* = 8.4 Hz, 1H), 7.60 (d, *J* = 8.0 Hz, 1H), 7.48 (t, *J* = 7.4 Hz, 1H), 6.92 (t, *J* = 7.5 Hz, 1H), 5.43 (s, 1H), 5.30 (s, 1H), 2.80 (s, 1H), 1.59 (s, 9H). ^{13}C NMR (176 MHz, $CDCl_3$) δ 167.6, 153.4, 153.1, 151.6, 150.9, 147.0, 146.9, 146.8, 146.3, 146.3, 146.2, 146.0, 146.0, 146.0, 145.9, 145.8, 145.7, 145.7, 145.4, 145.3, 145.3, 145.2, 145.1, 145.1, 145.1, 145.0, 144.5, 144.4, 144.3, 144.1, 144.1, 143.1, 142.8, 142.6, 142.6, 142.5, 142.5, 142.2, 142.2, 142.1, 142.0, 141.8, 141.7, 141.7, 141.6, 141.2, 139.8, 139.4, 139.3, 138.8, 137.3, 135.7, 135.5, 135.1, 133.1, 131.9, 131.8, 131.7, 131.3, 130.1, 129.5, 129.3, 129.1, 128.3, 128.2, 128.1, 128.0, 127.7, 127.5, 127.5, 127.5, 127.2, 127.1, 126.9, 126.3, 125.8, 125.3, 123.9, 83.1, 76.5, 73.7, 28.3. HRMS (ESI+) $[M+H]^+$ Calc. for $C_{93}H_{28}NO_2$: 1190,21200; found: 1190.21444.

5.2.10. Synthesis of iminoesters with EWD groups 13

General procedure

Iminoesters **13** was synthesized following the procedure described in the literature by coupling of *tert*-butyl glycinate hydrochloride and the corresponding benzaldehyde in basic medium.

tert-butyl (*E*)-2-((4-cyanobenzylidene)amino)acetate (**13a**)

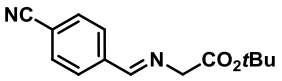

The iminoester **13a** was prepared according to the general procedure by using *p*-cyanobenzaldehyde (351.4 mg, 2.680 mmol, 0.9 eq.) *tert*-butyl glycinate hydrochloride (500.0 mg, 2.983 mmol, 1 eq.), triethylamine (0.4 mL, 2.983 mmol, 1 eq.) and anhydrous sodium sulfate. Quantitative isolated yield (835.6 mg). ^{1}H NMR (300 MHz, $CDCl_3$) δ 8.26 (s, 1H), 7.83 (d, *J* = 8.3 Hz, 2H), 7.64 (d, *J* = 8.2 Hz, 2H), 4.31 (s, 2H), 1.45 (s, 9H). ^{13}C NMR (75 MHz, $CDCl_3$) δ 169.2, 163.6, 139.9, 132.7, 129.2, 118.8, 114.6, 82.1, 62.8, 28.4.

tert-butyl (*E*)-2-((4-nitrobenzylidene)amino)acetate (**13b**)

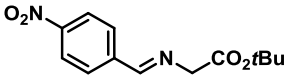

The iminoester **13b** was prepared according to the general procedure by using *p*-nitrobenzaldehyde (404.7 mg, 2.680 mmol, 0.9 eq.), *tert*-butyl glycinate hydrochloride (500.0 mg, 2.983 mmol, 1 eq.), triethylamine (0.4 mL, 2.983 mmol, 1 eq.) and anhydrous sodium sulfate. Isolated yield: 94% (666.3 mg). ^{1}H NMR (300 MHz, $CDCl_3$) δ 8.23 (s, 1H), 8.06 (d, *J* = 8.7 Hz, 2H), 7.79 (d, *J* = 8.7 Hz, 2H), 4.24 (s, 2H), 1.35 (s, 9H). ^{13}C NMR (75 MHz, $CDCl_3$) δ 169.1, 163.2, 149.5, 141.5, 129.5, 124.1, 82.1, 62.8, 28.4.

tert-butyl (*E*)-2-((2-fluorobenzylidene)amino)acetate (**13c**)

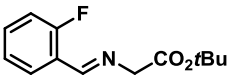

The iminoester **13c** was prepared according to the general procedure by using *o*-fluorobenzaldehyde (0.31 mL, 2.983 mmol, 1 eq.) *tert*-butyl glycinate hydrochloride (500.0 mg, 2.983 mmol, 1 eq.), triethylamine (0.4 mL, 2.983 mmol, 1 eq.) and anhydrous sodium sulfate. Isolated yield: 92% (650.7 mg). 1H NMR (300 MHz, CDCl3) δ 8.48 (s, 1H), 7.98 (dd, J = 10.7, 4.3 Hz, 1H), 7.31 (td, J = 7.5, 1.4 Hz, 1H), 7.08 (t, J = 7.5 Hz, 1H), 7.02 – 6.91 (m, 1H), 4.26 (s, 2H), 1.42 (s, 9H). 13C NMR (75 MHz, CDCl3) δ 169.5, 162.7 (d, J = 252.9 Hz), 158.7 (d, J = 4.8 Hz), 133.1 (d, J = 8.7 Hz), 128.2 (d, J = 2.6 Hz), 124.7 (d, J = 3.6 Hz), 123.7 (d, J = 9.1 Hz), 116.0 (d, J = 21.1 Hz), 81.7, 63.2, 28.4.

tert-butyl (*E*)-2-((3,5-difluorobenzylidene)amino)acetate (**13d**)

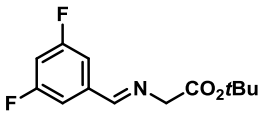

The iminoester **13d** was prepared according to the general procedure by using 3,5-difluorobenzaldehyde (423.5 mg, 2.983 mmol, 1 eq.) *tert*-butyl glycinate hydrochloride (500.0 mg, 2.983 mmol, 1 eq.), triethylamine (0.4 mL, 2.983 mmol, 1 eq.) and anhydrous sodium sulfate. Isolated yield: 95% (722.9 mg). ^{1}H NMR (300 MHz, $CDCl_3$) δ 8.19 (s, 1H), 7.35 – 7.28 (m, 2H), 6.88 (tt, *J* = 8.7, 2.4 Hz, 1H), 4.33 (s, 2H), 1.50 (s, 9H). ^{13}C NMR (75 MHz, $CDCl_3$) δ 169.0, 163.8 (dd, *J* = 148.4, 12.1 Hz), 162.7 (t, *J* = 3.0 Hz), 139.4 (t, *J* = 9.0 Hz), 111.2 (m), 106.3 (t, J = 25.6 Hz), 81.7, 62.3, 28.2. ^{19}F NMR (282 MHz, $CDCl_3$) δ -109.70.

tert-butyl (*E*)-2-((3,4,5-trifluorobenzylidene)amino)acetate (**13e**)

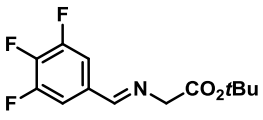

The iminoester **13e** was prepared according to the general procedure by using 3,4,5-trifluorobenzaldehyde (0.33 mL, 2.983 mmol, 1 eq.) *tert*-butyl glycinate hydrochloride (500.0 mg, 2.983 mmol, 1 eq.), triethylamine (0.4 mL, 2.983 mmol, 1 eq.) and anhydrous sodium sulfate. Isolated yield: 89% (725.01 mg). ^{1}H NMR (300 MHz, $CDCl_3$) δ 8.11 (s, 1H), 7.40 (dd, J = 8.1, 6.7 Hz, 2H), 4.28 (s, 2H), 1.46 (s, 9H). ^{13}C NMR (75 MHz, $CDCl_3$) δ 169.2, 161.9, 152.0 (m), 141.9 (dd, *J* = 238.9, 16.6 Hz), 132.2 (ddd, *J* = 5.8, 4.8, 2.1 Hz), 112.6 (m), 82.1 (s), 62.4 (s), 28.4 (s).

tert-butyl (*E*)-2-((perfluorobenzylidene)amino)acetate (**13f**)

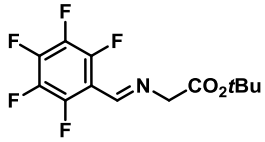

The iminoester **13f** was prepared according to the general procedure by using perfluorobenzaldehyde (476.4 mg, 2.429 mmol, 0.9 eq.) *tert*-butyl glycinate hydrochloride (500.0 mg, 2.983 mmol, 1 eq.), triethylamine (0.4 mL, 2.983 mmol, 1 eq.) and anhydrous sodium sulfate. Isolated yield: 79% (593.1 mg). ^{1}H NMR (300 MHz, $CDCl_3$) δ 8.34 (s, 1H), 4.34 (s, 1H), 1.44 (s, 9H).

5.2.11. Synthesis of pyrrolidino[60]fullerene with EWD groups 14

General procedure for catalytic 1,3-dipolar cycloaddition of phosphine-azomethine ylides and [60]fullerene

Ligand (0.028 mmol, 20% mol) and metal salt (0.028 mmol, 20% mol) were dissolved in anhydrous toluene (32.5 mL). The solution was stirred for 30 min at room temperature, under argon atmosphere, and then, a solution of the α-iminoester **13** (84.03 mg, 0.208 mmol, 1.5 eq.) in 5 mL of anh. toluene. Finally, C_{60} (100 mg, 0.139 mmol, 1 eq.). The reaction mixture was stirred for 15 h, and afterwards, it was quenched with a saturated ammonium chloride solution. The organic layer was dried over anh. $MgSO_4$ and concentrated in vacuum. The pyrrolidino[60]fullerene was isolated by silica gel chromatography (1) CS_2, 2) CS_2:DCM 7:3).

cis-2-*tert*-butoxycarbonyl-5-(4-cyanophenyl)pyrrolidino[3,4:1,2][60]fullerene (**14a**)

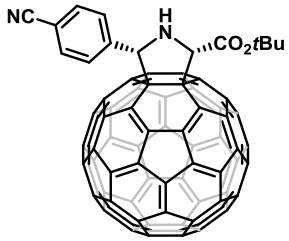

The adduct **14a** was prepared according to the general procedure by using the catalytic system (R_P)-FeSulPhos (**P-XIV**, 11.2 mg, 0.028 mmol) and $Cu(OAc)_2$ (4.7 mg, 0.028 mmol), iminoester **13a** (50.8 mg, 0.208 mmol), C_{60} (100.0 mg, 0.139 mmol). Isolated yield: 54% (96.5 mg). ^{1}H NMR (300 MHz, $CDCl_3$) δ 7.97 (d, *J* = 8.5 Hz, 2H), 7.77 (d, *J* = 7.9 Hz, 2H), 5.89 (s, 1H), 5.55 (s, 1H), 3.89 (br. s, 1H), 1.53 (s, 9H). HRMS (MALDI POS): $[M+H]^+$ Calc. for $C_{74}H_{17}N_2O_2$: 965,1290; found: 965,1282.

cis-2-*tert*-butoxycarbonyl-5-(4-nitrophenyl)pyrrolidino[3,4:1,2][60]fullerene (**14b**)

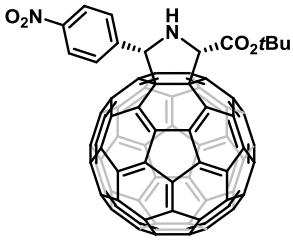

The adduct **14b** was prepared according to the general procedure by using the catalytic system (R_P)-FeSulPhos (**P-XIV**, 11.2 mg, 0.028 mmol) and $Cu(OAc)_2$ (4.7 mg, 0.028 mmol), iminoester **13b** (55.0 mg, 0.208 mmol), C_{60} (100.0 mg, 0.139 mmol). Isolated yield: 57% (78.0 mg). ^{1}H NMR (500 MHz, $CDCl_3$) δ 8.34 (d, *J* = 8.5 Hz, 2H), 8.05 (d, *J* = 8.5 Hz, 2H), 5.95 (s, 1H), 5.58 (s, 1H), 1.54 (s, 9H). ^{13}C NMR (126 MHz,

$CDCl_3$) δ 168.6, 168.6, 153.0, 153.0, 152.5, 151.4, 150.8, 148.5, 147.7, 147.6, 147.2, 146.9, 146.8, 146.8, 146.8, 146.7, 146.6, 146.5, 146.4, 146.4, 146.1, 146.1, 146.0, 145.9, 145.9, 145.9, 145.9, 145.8, 145.8, 145.7, 145.7, 145.5, 144.9, 144.8, 144.7, 144.7, 144.3, 143.6, 143.5, 143.2, 143.2, 143.2, 143.2, 143.1, 142.8, 142.7, 142.6, 142.6, 142.6, 142.6, 142.5, 142.5, 142.4, 142.4, 142.2, 142.1, 142.1, 140.5, 140.2, 140.1, 139.4, 137.5, 137.2, 136.3, 136.2, 129.4, 124.4, 84.4, 78.9, 77.7, 77.4, 77.2, 75.4, 74.8, 73.5, 28.6, 1.4. HRMS (MALDI POS): $[M+H]^+$ Calc. for $C_{73}H_{17}N_2O_4$: 985,1183; found: 985,1198.

cis-2-*tert*-butoxycarbonyl-5-(2-fluorophenyl)pyrrolidino[3,4:1,2][60]fullerene (**14c**)

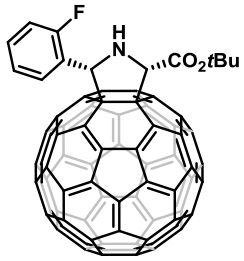

The adduct **14c** was prepared according to the general procedure by using the catalytic system (R_P)-FeSulPhos (**P-XIV**, 11.2 mg, 0.028 mmol) and $Cu(OAc)_2$ (4.7 mg, 0.028 mmol), iminoester **13b** (55.0 mg, 0.208 mmol), C_{60} (100.0 mg, 0.139 mmol). Isolated yield: 57% (78.0 mg).

cis-2-*tert*-butoxycarbonyl-5-(3,5-difluorophenyl)pyrrolidino[3,4:1,2][60]fullerene (**14d**)

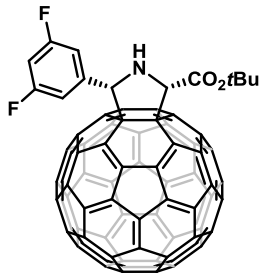

The adduct **14d** was prepared according to the general procedure by using the catalytic system (R_P)-FeSulPhos (**P-XIV**, 11.2 mg, 0.028 mmol) and $Cu(OAc)_2$ (4.7 mg, 0.028 mmol), iminoester **13d** (53.2 mg, 0.208 mmol), C_{60} (100.0 mg, 0.139 mmol). Isolated yield: 41% (56.2 mg). ^{1}H NMR (300 MHz, $CDCl_3$) δ 7.37 (dd, J = 7.7, 1.9 Hz, 2H), 6.83 (tt, J = 8.8, 2.4 Hz, 1H), 5.80 (s, 1H), 5.51 (s, 1H), 3.79 (br. s, 1H), 1.53 (s, 9H). ^{19}F NMR (282 MHz, $CDCl_3$) δ -107.75 (s).

cis-2-*tert*-butoxycarbonyl-5-(3,4,5-trifluorophenyl)pyrrolidino[3,4:1,2] [60]fullerene (**14e**)

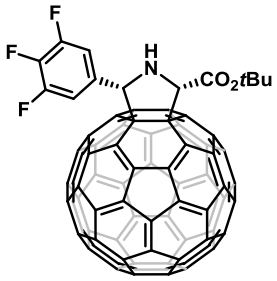

The adduct **14e** was prepared according to the general procedure by using the catalytic system (R_P)-FeSulPhos (**P-XIV**, 11.2 mg, 0.028 mmol) and $Cu(OAc)_2$ (4.7 mg, 0.028 mmol), iminoester **13e** (56.9 mg, 0.208 mmol), C_{60} (100.0 mg, 0.139 mmol). Isolated yield: 46% (62.2 mg). ^{1}H NMR (500 MHz, $CDCl_3$) δ 7.53 (dd, *J* = 7.5, 6.7 Hz, 2H), 5.76 (s, 1H), 5.52 (s, 1H), 3.69 (s, 1H), 1.53 (s, 9H). ^{13}C NMR (126 MHz, $CDCl_3$) δ 168.6, 152.9, 151.5, 150.8, 147.7, 147.6, 147.3, 146.9, 146.9, 146.8, 146.8, 146.7, 146.6, 146.5, 146.4, 146.4, 146.2, 146.1, 146.0, 145.9, 145.9, 145.9, 145.9, 145.8, 145.8, 145.7, 145.7, 145.6, 144.9, 144.9, 144.7, 144.7, 143.6, 143.5, 143.2, 143.2, 142.8, 142.6, 142.6, 142.6, 142.5, 142.5, 142.5, 142.4, 142.3, 142.1, 142.1, 140.6, 140.3, 140.1, 139.4, 137.7, 137.2, 136.3, 136.2, 129.5, 128.6, 112.9 (dd, *J* = 17.1, 5.2 Hz) , 84.4, 78.4, 74.8, 74.0, 73.1, 28.6.

cis-2-*tert*-butoxycarbonyl-5-(perfluorophenyl)pyrrolidino[3,4:1,2] [60]fullerene (**14f**)

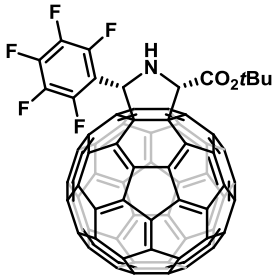

The adduct **14f** was prepared according to the general procedure by using the catalytic system (R_P)-FeSulPhos (**P-XIV**, 11.2 mg, 0.028 mmol) and $Cu(OAc)_2$ (4.7 mg, 0.028 mmol), iminoester **13f** (64.3 mg, 0.208 mmol), C_{60} (100.0 mg, 0.139 mmol). Isolated yield: 37% (52.9 mg).^{1}H NMR (300 MHz, $CDCl_3$) δ 6.21 (d, *J* = 14.2 Hz, 1H), 5.49 (dd, *J* = 13.0, 2.6 Hz, 1H), 4.97 (m, 1H), 1.53 (s, 9H). ^{13}C NMR (126 MHz, $CDCl_3$) δ 168.0, 152.8, 152.4, 150.7, 150.4, 147.6, 147.5, 146.9, 146.8, 146.8, 146.7, 146.7, 146.5, 146.4, 146.4, 146.4, 146.3, 146.0, 145.9, 145.9, 145.9, 145.9, 145.8, 145.8, 145.8, 145.7, 145.7, 145.4, 145.2, 144.8, 144.7, 144.7, 144.7, 143.6, 143.5, 143.2, 143.2, 143.1, 142.9, 142.8, 142.8, 142.6, 142.6, 142.5, 142.4, 142.2, 142.2, 142.2, 140.8, 140.4, 140.3, 139.6, 137.5, 137.1, 136.1, 135.8, 84.7, 80.0, 75.1, 68.6, 28.6. ^{19}F NMR (282 MHz, $CDCl_3$) δ -137.53 (d, *J* = 23.0 Hz), -139.86 (d, *J* = 21.4 Hz), -151.49 (t, *J* = 20.8 Hz), -159.64 (dd, *J* = 31.5, 14.4 Hz).

5.2.12. Synthesis of gold(I)-pyrrolidino[60]fullerene hybrid 17

tert-butyl (*E*)-2-((2-(diphenylphosphaneyl)benzylidene)amino)acetate (**16**)

General procedure

Iminoester **16** was synthesized following the procedure described in the literature by coupling of *tert*-butyl glycinate hydrochloride and 2-(diphenylphosphino)benzaldehyde in basic medium under argon atmosphere.

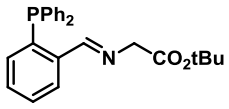

The iminoester **16** was prepared according to the general procedure by using 2-(diphenylphosphino)benzaldehyde (500 mg, 1.722 mmol) *tert*-butyl glycinate hydrochloride (360.8 mg, 2.153 mmol), triethylamine (0.3 mL, 2.153 mmol), and anhydrous sodium sulfate. Isolated yield: 83% (574.8 mg). ^{1}H NMR (300 MHz, $CDCl_3$) δ 9.02 (d, *J* = 5.3 Hz, 1H), 8.19 (dd, *J* = 7.2, 3.6 Hz, 1H), 7.40 (t, *J* = 7.5 Hz, 1H), 7.30 (dd, *J* = 11.5, 3.6 Hz, 12H), 6.97 – 6.91 (m, 1H), 4.22 (s, 2H), 1.47 (s, 9H). ^{13}C NMR (75 MHz, $CDCl_3$) δ 169.2, 163.4 (d, J = 25.1 Hz), 139.3 (d, J = 18.6 Hz), 137.5 (d, J = 18.6 Hz), 136.2 (d, J = 9.9 Hz), 133.9 (d, J = 20.3 Hz), 133.4, 130.8, 129.1 (d, J = 14.8 Hz), 128.6 (d, J = 7.8 Hz), 127.6 (d, J = 4.1 Hz), 81.3, 62.6, 28.1 ppm. ^{31}P{1H} NMR (122 MHz, $CDCl_3$) δ -15.49 ppm. HRMS (ESI+): $[M+H]^+$ Calc. for $C_{25}H_{26}NO_2P$: 403.1701; found: 403.1712. ATR-FTIR ν (C=O) = 1741 cm^{-1}.

General procedure for catalytic 1,3-dipolar cycloaddition of phosphine-azomethine ylides and [60]fullerene

Chiral ligand (0.028 mmol, 20% mol) and metal salt (0.028 mmol, 20% mol) were dissolved in anhydrous toluene (32.5 mL). The solution was stirred for 30 min at room temperature, under argon atmosphere, and then, a solution of the α-iminoester **16**(84.03 mg, 0.208 mmol, 1.5 equiv.). Finally, C_{60} (100 mg, 0.139 mmol, 1 equiv.) and Et_3N, when required (3.9 μL, 0.028 mmol). The reaction mixture was stirred for 2 h, and afterwards, it was quenched with a saturated ammonium chloride solution. The organic layer was dried over $MgSO_4$ and concentrated in vacuum. Firstly, the pyrrolidino[60]fullerene was isolated by silica gel chromatography (1) hexane:toluene 3:7 2) hexane:DCM 2:8). For separating the two pyrrolidino[60]fullerene diastereoisomers an additional purification by silica gel chromatography (hexane:CS_2:AcOEt 5:4,7:0,3).

trans-2-*tert*-butoxycarbonyl-5-(2-diphenylphosphine)phenylpyrrolidino [3,4:1,2][60]fullerene (*trans*-**17**).

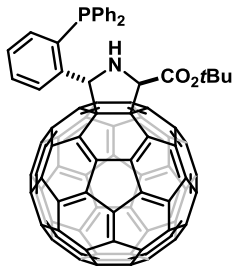

The adduct **17** was prepared according to the general procedure by using the catalytic system (±)-BINAP (**P-XVII**, 17.3 mg, 0.028 mmol) and $Cu(OTf)_2$ (10.0 mg, 0.028 mmol), iminoester **16** (84.0 mg, 0.208 mmol), C_{60} (100.0 mg, 0.139 mmol) and Et_3N (3.9 μL, 0.028 mmol). Isolated yield: 79% (122.6 mg). ^{1}H-RMN (700 MHz, $CDCl_3$) δ 8.36 (dd, *J* = 8.0, 4.1 Hz, 1H), 7.73 (d, *J* = 9.6 Hz, 1H), 7.52 (t, *J* = 7.4 Hz, 1H), 7.39 – 7.29 (m, 6H), 7.26 – 7.22 (m, 2H), 7.22 – 7.15 (m, 4H), 5.70 (s, 1H), 1.58 (s, 9H) ppm. ^{13}C NMR (176 MHz, $CDCl_3$) δ 171.2, 156.7, 154.3, 153.7, 152.1, 147.3, 147.2, 146.8, 146.4, 146.3, 146.2, 146.1, 146.1, 146.0, 145.9, 145.6, 145.6, 145.5, 145.4, 145.4, 145.2, 145.2, 145.1, 144.5, 144.5, 144.4, 144.3, 144.2, 143.1, 143.0, 143.0, 142.7, 142.5, 142.5, 142.3, 142.3, 142.2, 142.1, 142.1, 142.0, 142.0, 141.7, 141.6, 141.4, 140.0, 139.4, 139.1, 138.7, 138.7, 137.5, 137.4, 136.8, 136.4, 135.8, 135.5, 135.4, 134.1 (d, *J* = 19.8 Hz), 133.2 (d, *J* = 19.1 Hz), 130.0, 129.5, 128.8, 128.6 (d, *J* = 6.2 Hz), 128.5 (d, *J* = 5.8 Hz), 128.4, 83.3, 76.4, 73.8, 71.5, 28.3 ppm. ^{31}P{^{1}H} NMR (122 MHz, $CDCl_3$) δ -20.45 ppm. HRMS (ESI+): $[M+H]^+$ Calc. for $C_{85}H_{26}NO_2P$: 1124.1335; found: 1124.1090. ATR-FTIR ν (C=O) = 1735 cm^{-1}.

cis-2-*tert*-butoxycarbonyl-5-(2-diphenylphosphine)phenylpyrrolidino [3,4:1,2][60]fullerene (*cis*-**17**).

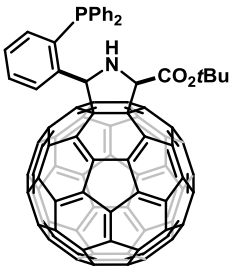

The adduct **17** was prepared according to the general procedure by using the catalytic system dppe (**P-XVI**, 11.1 mg, 0.028 mmol) and Ag(OAc) (4.6 mg, 0.028 mmol), iminoester **16** (84.0 mg, 0.208 mmol) and C_{60} (100.0 mg, 0.139 mmol). Isolated yield: 42% (65.2 mg). ^{1}H NMR (500 MHz, $CDCl_3$) δ 8.11 (dd, *J* = 7.7, 4.4 Hz, 1H), 7.66 (d, *J* = 7.9 Hz, 1H), 7.52 (t, *J* = 7.1 Hz, 1H), 7.34 (m, 4H), 7.26 – 7.16 (m, 8H), 5.58 (d, *J* = 9.8 Hz, 1H), 4.12 (br. s, 1H), 1.51 (s, 9H). ^{31}P{1H} NMR (122 MHz, $CDCl_3$) δ -20.45 ppm.

General procedure for the synthesis "one pot" of the gold(I)-pyrrolidino[60]fullerene hybrids **18**

In the first step, a solution of metallic salt (0.028 mmol, 20% mol) and ligand (0.028 mmol, 20% mol) in anhydrous toluene (32 mL) was stirred for 30 minutes under argon atmosphere. Subsequently α- iminoester **16** (56.0 mg, 0.139 mmol, 1 equiv.) and C_{60} (100 mg, 0.139 mmol, 1 equiv.) were added. The reaction has been maintained under argon atmosphere at the indicated temperature. The progress of the reaction was controlled by thin layer chromatography. When finished, the chloro(dimethyl sulfide)gold(I) (40.88 mg, 0.139 mmol, 1 eq.), dissolved in 13 mL of anhydrous DCM, was added. After 15 minutes, the reaction was stopped by washing the crude with a solution of 1 M ammonium chloride. The organic phase has been concentrated. The product is isolated by silica gel chromatography (1) toluene, 2) toluene:DCM 4:1 to 3:1).

[Chloro (*trans*-2-*tert*-butoxycarbonyl-5-(2-diphenylphosphine)phenyl pyrrolidino [3,4:1,2][60]-fullerene) gold (I) (*trans*-**18**).

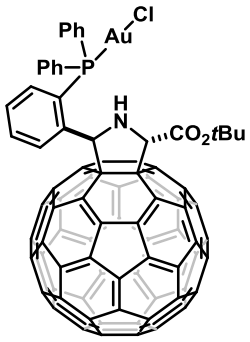

The adduct **18** was prepared according to the general procedure by using $Cu(OAc)_2$ (5.0 mg, 0.028 mmol), iminoester **16** (56.0 mg, 0.139 mmol), C_{60} (100.0 mg, 0.139 mmol) and $Au(SMe_2)Cl$ (40.9 mg, 0.139 mmol) at rt. Isolated yield: 41% (76.1 mg). ^{1}H NMR (500 MHz, $CDCl_3$) δ 8.63 (ddd, *J* = 7.8, 5.1, 0.9 Hz, 1H), 7.72 – 7.64 (m, 6H), 7.63 – 7.54 (m, 3H), 7.50 – 7.45 (m, 1H), 7.46 – 7.36 (m, 3H), 7.02 (ddd, *J* = 13.1, 7.3, 1.3 Hz, 1H), 5.63 (s, 1H), 1.51 (s, 9H) ppm. ^{13}C NMR (126 MHz, $CDCl_3$) δ 170.3, 155.8, 153.2, 153.0, 151.3, 147.3, 147.2, 146.5, 146.4, 146.3, 146.2, 146.1, 146.0, 146.0, 145.9, 145.7, 145.5, 145.5, 145.4, 145.4, 145.4, 145.3, 145.3, 145.2, 145.1, 144.5, 144.4, 144.3, 143.7, 143.6, 143.1, 143.0, 142.7, 142.6, 142.6, 142.5, 142.4, 142.3, 142.1, 142.1, 142.0, 142.0, 141.9, 141.9, 141.9, 141.7, 141.4, 140.1, 139.8, 139.3, 136.8, 136.7, 136.4, 135.6, 135.1 (d, *J* = 14.4 Hz), 134.6 (d, *J* = 14.1 Hz), 134.1 (d, *J* = 7.6 Hz), 133.2 (d, *J* = 8.3 Hz), 132.4 (d, *J* = 2.3 Hz), 132.0 (d, *J* = 2.4 Hz), 131.7 (d, *J* = 1.9 Hz), 129.8, 129.5 (d, *J* = 12.0 Hz), 129.3 (d, *J* = 11.9 Hz), 128.8 (d, *J* = 9.6 Hz), 128.4, 83.4, 75.9, 73.9, 71.1, 70.5 (d, *J* = 12.3 Hz), 28.3 ppm. ^{31}P{^{1}H}-NMR (122 MHz, $CDCl_3$) δ 25.33 ppm. HRMS (FAB+): [M-

Cl]$^+$ Calc. for $C_{85}H_{26}NO_2PAu$: 1321.1; found: 1321.5. ATR-FTIR ν (C=O) = 1731 cm^{-1}.

[Chloro (*cis*-2-*tert*-butoxycarbonyl-5-(2-diphenylphosphine)phenyl pyrrolidino[3,4:1,2][60]- fullerene) gold (I) (*cis*-**18**).

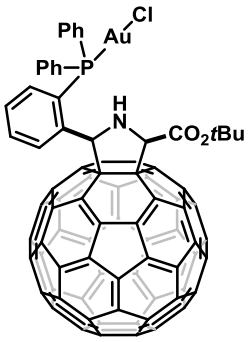

The adduct **18** was prepared according to the general procedure with a different order of reactives addition. The catalytic system is preformed in toluene and after that C_{60} is added. In another flask, the iminoester **16** and $Au(SMe_2)Cl$ are solved in anh. DCM. Finally, this last solution is slowly added to the toluene solution. $Cu(OAc)_2$ (5.0 mg, 0.028 mmol) and (R_P)-FeSulPhos **P-XV** (12.8 mg, 0.028 mmol), iminoester **16** (56.0 mg, 0.139 mmol), C_{60} (100.0 mg, 0.139 mmol) and $Au(SMe_2)Cl$ (40.9 mg, 0.139 mmol) at -18ºC. Isolated yield: 63% (115.7 mg). ^{1}H NMR (500 MHz, $CDCl_3$) δ 8.45 (ddd, *J* = 8.0, 5.1, 1.1 Hz, 1H), 7.72 – 7.65 (m, 3H), 7.63 – 7.53 (m, 5H), 7.50 – 7.45 (m, 1H), 7.42 (tt, *J* = 7.7, 1.2 Hz, 1H), 7.39 – 7.33 (m, 3H), 7.08 (ddd, *J* = 11.8, 7.3, 1.1 Hz, 1H), 5.53 (s, 1H), 1.51 (s, 9H) ppm. ^{13}C NMR (126 MHz, $CDCl_3$) δ 168.2, 152.9, 152.3, 151.8, 151.3, 147.1, 147.0, 146.8, 146.3, 146.2, 146.1, 146.1, 146.0, 145.7, 145.6, 145.5, 145.4, 145.3, 145.3, 145.2, 145.2, 145.2, 145.1, 144.5, 144.3, 144.0, 143.2, 142.8, 142.7, 142.6, 142.4, 142.3, 142.2, 142.1, 142.0, 142.0, 141.8, 141.7, 141.7, 141.0, 140.9, 139.6, 139.5, 139.4, 139.0, 137.2, 137.1, 136.8, 136.0, 134.9 (d, *J* = 14.0 Hz), 134.6 (d, *J* = 7.2 Hz), 134.4 (d, *J* = 14.1 Hz), 133.0, 132.8 (d, *J* = 7.9 Hz), 132.0, 129.5 (d, *J* = 12.1 Hz), 129.5 (d, *J* = 12.0 Hz), 129.2 (d, *J* = 9.8 Hz), 83.5, 77.6, 74.9, 72.4, 71.4 (d, *J* = 15.3 Hz), 28.2 ppm. ^{31}P{^{1}H} NMR (122 MHz, $CDCl_3$) δ 23.53 ppm. HRMS (FAB): [M-Cl]$^+$ Calc. for $C_{85}H_{26}NO_2PAu$: 1321.1; found: 1321.5. ATR-FTIR ν (C=O) = 1735 cm^{-1}.

5.2.13. Synthesis of [(η^n-ring)M(Pyrrolino[3,4:1,2][60] fullerene carboxylate)Cl] 20

Synthesis of 4-methyl-2-phenyloxazol-5(4H)-one (**19**)[158]

A solution of aniline (2g, 22 mmol) and NaOH (1.1 g, 28 mmol) in water (12 ml) is stirred for one hour at 25°C. Then, benzoic acid (372.1 mg, 3 mmol) is added and the mixture is stirred for 16 h. Later, the crude is washed with aqueous 1N HCl, extracted with EtOAc and finally washed with water. Organic phase is then dried over anhydrous Mg_2SO_4, filtered and solvent was removed under vacuum obtaining a white solid that is used without further purification.

A solution of the *N*- Benzoyl Alanine (592.7 mg, 3.07 mmol) in dry dichloromethane (30 ml) is cooled at 0°C. Then, 1- (3- Dimethylaminopropyl)- 3- ethylcarbodiimide hydrochloride (EDC·HCl; 646.0 mg, 3.37 mmol) is added and the mixture is stirred for 45 min. After this time, 30 ml of dichloromethane and 30 ml of water are added successively and the phases are separated. Organic phase is washed with 30 ml of aqueous saturated solution of $NaHCO_3$ and 30 ml of water. Then, combined organic phases are dried over anhydrous Mg_2SO_4, filtered and the organic solvent is evaporated under vacuum leading to the solid azlactone without further purification. White solid, isolated yield = 59% (317.1 mg).

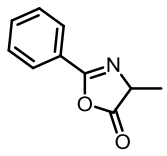

^{1}H NMR (300 MHz, $CDCl_3$) δ 8.01 (d, J = 7.7 Hz, 2H), 7.59 (t, *J* = 7.3 Hz, 1H), 7.50 (t, *J* = 7.6 Hz, 2H), 4.47 (q, *J* = 7.5 Hz, 1H), 1.61 (d, *J* = 7.6 Hz, 3H).

General procedure for the *in situ* [3+2] cycloaddition of azlactone **19** onto [60]fullerene and hybrid metallofullerene formation (**20Ir** and **20Rh**).

Starting pyrrolino[3,4:1,2][60]fullerene carboxylates were prepared "in situ" following a similar procedure described previously by our research group.[66]

A suspension of a mixture of AgOAc (24mg, 0.143 mmol, 1 eq.) and (+/-)-2,2'-Bis(diphenylphosphino)-1,1'-binaphthyl (BINAP; 89 mg, 0.143 mmol, 1 eq.) in 50 mL of anhydrous toluene is prepared in an 100 ml one-neck round bottom flask. After 5-10 min of stirring at 25°C, azlactone **19** (0.143 mmol, 1 eq.) is

[158] a) Peddibhotla, S.; Tepe, J. J. *J. Am. Chem. Soc.* **2004**, *126*, 12776-12777, b) Melhado, A. D.; Luparia, M.; Toste, F. D. *J. Am. Chem. Soc.* **2007**, *129*, 12638-12639

added to the solution. Later, [60]fullerene (100 mg, 0.143 mmol, 1 eq.) is added and the purple mixture is stirred overnight at 25°C. Thereafter, a solution of the corresponding metal dimer (Ir or Rh, 0.5 eq.) in DCM (5 mL) is added to the brown solution and stirred for 2 h. Finally, the solvent is evaporated under vacuum and the dark residue is purified by silica-gel column chromatography using CS_2 as eluent (recovering unreacted [60]fullerene). Then, DCM and mixtures of DCM/MeOH (indicated in each case) were employed to obtain the desired products. In all cases, dark brown solids were obtained and centrifuged in dry MeOH (2 x 2 mL, 15 min at 6000 rpm) and dried under vacuum.

[Cp*Ir(2-phenyl-5-methyl-5-carboxylatepyrrolino[3,4:1,2][60]fullerene)Cl] (**20Ir**).

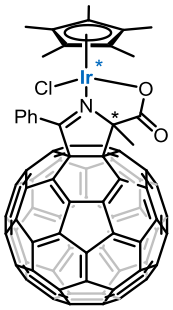

The product **20Ir** was obtained following the standard procedure as a brown solid after Flash Chromatography, eluent DCM and DCM/MeOH (100:1) in 40% isolated yield. ^{1}H NMR (700 MHz, $CDCl_3$): δ 7.51 (m, 5H, Ph), 2.61 (s, 3H, Me), 1.57 (s, 15H, Cp*) ppm. ^{13}C NMR (175MHz, $CDCl_3$): δ 179.9 (HMBC, C=N), 177.7 (HMBC, C=O), 151.6, 151.2, 148.6, 148.1, 147.4, 147.3, 147.2, 147.2, 146.7, 146.6, 146.3, 146.2, 146.2, 146.2, 146.1, 146.0, 146.0, 145.9, 145.7, 145.6, 145.5, 145.4, 145.3, 145.2, 144.9, 144.8, 144.7, 144.4, 143.6, 143.1, 142.9, 142.9, 142.8, 142.8, 142.7, 142.6, 142.6, 142.1, 141.9, 141.7, 141.6, 141.4, 141.3, 140.1, 140.0, 139.8, 139.2, 138.0, 137.4, 135.0, 134.7, 132.4, 130.5 (HSQC, CH-Ph), 90.8 (HMBC, C_3sp^3-adduct), 86.5 (C_5sp^3), 85.9 (HMBC, Cp*), 72.5 (HMBC, C_4sp^3-adduct), 33.5 (HSQC, Me), 9.3 (HSQC, Me-Cp*) ppm. HRMS (MALDI+) $[M+Na]^+$ Calc. for $C_{80}H_{23}ClNNaO_2Ir$: 1280.0939; found: 1280.0934. ATR-FTIR ν (C=O) = 1661 cm^{-1}.

[Cp*Rh(2-phenyl-5-methyl-5-carboxylatepyrrolino[3,4:1,2][60]fullerene)Cl] (**20Rh**).

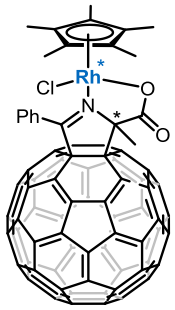

The product **20Rh** was obtained following the standard procedure as a brown solid after Flash Chromatography, eluent DCM and DCM/MeOH (100:1 to 40:1) in 38% isolated yield. ^{1}H NMR (700 MHz, $CDCl_3$): δ 7.53 (m, 5H, Ph), 2.61 (s, 3H, Me), 1.61 (s, 15H, Cp*) ppm. ^{13}C NMR (175MHz, $CDCl_3$): δ 180.3 (C=N), 176.4 (C=O), 152.0, 151.5, 148.7, 147.8, 147.5, 147.3, 147.2, 146.6, 146.6, 146.3, 146.2, 146.1, 146.1, 146.0, 146.0, 145.9, 145.8, 145.6, 145.4, 145.3, 145.2, 145.2, 145.1, 144.8, 144.7, 144.3, 143.5, 142.9, 142.9, 142.9, 142.7, 142.7, 142.6, 142.5, 142.0, 141.9, 141.9, 141.6, 141.4, 141.3, 140.1, 139.9, 139.7, 139.1, 137.9, 137.6, 134.8, 134.7, 132.6, 130.4 (CH-Ph), 94.3 (Cp*), 94.3 (Cp*), 91.6 (HMBC, C_3sp^3-adduct), 86.2 (C_5sp^3), 72.9 (HMBC, C_4sp^3-adduct), 33.9 (Me), 9.3 (Me-Cp*) ppm. HRMS (MALDI+) $[M+Na]^+$ Calc. for $C_{80}H_{23}ClNNaO_2Rh$: 1190.0365; found: 1190.0351. ATR-FTIR ν (C=O) = 1642 cm^{-1}.

5.2.14. Synthesis of cyclopenteno-H-[60]fullerenes 21a-c

General Procedure

We use the same described procedure for C_{60} (section 5.2.3) employing alkynoates with an additional nucleophilic group, such us a hydroxyl group.

1-ethoxycarbonyl-3-(1,1-dimethyl-2-oxacyclopentano[3,4:2,3])-1-cyclopenteno[4,5:1,2]-4H-[60]fullerene (**21a**)

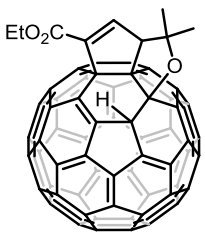

The adduct **21a** was prepared according to the general procedure using ethyl-5-hydroxy-5-methyl-3-hexynoate **1k** (11.1 mg, 0.065 mmol), [60]fullerene (50 mg, 0.069 mmol) and 1,2-bis(diphenylphosphino)ethane (5.2 mg, 0.0130 mmol). Conversion: 37% (eluent: hexane:CH_2Cl_2, 1:1). ^{1}H NMR (700 MHz, $CDCl_3$) δ 7.57 (s, 1H), 6.29 (s, 1H), 4.45 (d, *J* = 2.4 Hz, 1H), 4.45 – 4.37 (m, 2H), 1.96 (s, 3H), 1.85 (s, 3H), 1.41 (t, *J* = 7.1 Hz, 3H). ^{13}C NMR (176 MHz, $CDCl_3$) δ 163.4, 151.1, 150.1, 149.2, 148.9, 148.9, 148.2, 148.1, 147.9, 147.9, 147.1, 147.1, 146.9, 146.8, 146.7, 146.5, 146.4, 146.1, 145.7, 145.3, 145.3, 145.1, 145.1, 145.0,

144.9, 144.8, 144.8, 144.8, 144.6, 144.4, 144.3, 144.3, 144.2, 144.2, 144.1, 143.9, 143.9, 143.8, 143.4, 143.1, 143.1, 142.9, 142.9, 142.7, 142.5, 142.5, 142.2, 141.6, 141.4, 140.9, 140.4, 139.1, 138.1, 138.0, 136.2, 136.1, 134.6, 97.2, 87.0, 77.2, 77.0, 76.8, 76.1, 73.3, 70.6, 61.4, 59.6, 32.0, 28.4, 14.3 ppm. HRMS (MALDI+): $[M+Na]^+$ Calc. for $C_{69}H_{14}NaO_3$: 913.0841; found: 913.0821.

1-*tert*-butoxycarbonyl-3-(1,1-dimethyl-2-oxacyclopentano[3,4:2,3])-1-cyclopenteno[4,5:1,2]-4H-[60]fullerene (**21b**)

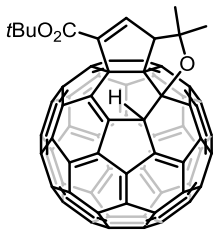

The adduct **21b** was prepared according to the general procedure using *tert*-butyl-5-hydroxy-5-methyl-3-hexynoate **1l** (12.9 mg, 0.065 mmol), [60]fullerene (50 mg, 0.069 mmol) and 1,2-bis(diphenylphosphino)ethane (5.2 mg, 0.0130 mmol). Conversion: 35% (eluent: hexane:CH_2Cl_2, 1:1). ^{1}H NMR (700 MHz, CDCl3) δ 7.47 (s, 1H), 6.29 (s, 1H), 4.40 (s, 1H), 1.95 (s, 3H), 1.83 (s, 3H), 1.58 (s, 9H). ^{13}C NMR (176 MHz, CDCl3) δ 162.7, 151.2, 150.3, 149.2, 148.9, 148.8, 148.2, 148.1, 148.1, 147.1, 147.1, 147.0, 146.9, 146.7, 146.5, 146.4, 146.0, 145.7, 145.4, 145.3, 145.2, 145.1, 145.1, 144.9, 144.8, 144.8, 144.6, 144.4, 144.3, 144.2, 144.1, 143.9, 143.9, 143.7, 143.1, 143.0, 142.9, 142.7, 142.7, 142.5, 142.5, 142.2, 141.5, 141.5, 140.9, 140.2, 139.6, 139.0, 138.0, 136.2, 136.1, 134.5, 97.2, 87.0, 82.8, 77.2, 77.0, 76.8, 76.3, 73.3, 70.3, 59.6, 32.0, 28.4, 28.3 ppm. HRMS (MALDI+): $[M]^+$ Calc. for $C_{71}H_{18}O_3$: 918.1256; found: 918.1234.

3-(1,1-dimethyl-2-oxacyclopentano[3,4:2,3])-1-cyclopenteno[4,5:1,2]-4H-[60]fullerene-1-carboxylic acid (**21c**)

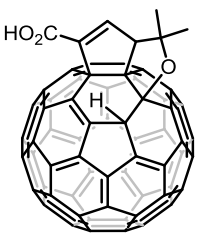

The adduct **21c** was prepared treating **21b** (30 mg, 0.033 mmol) with 0.3 mL of TFA in 1.2 mL of DCM. Yield: 77%. ^{1}H NMR (700 MHz, THF-d_8) δ 7.61 (s, 1H), 6.38 (s, 1H), 4.57 (s, 1H), 1.92 (s, 3H), 1.80 (s, 3H). ^{13}C NMR (176 MHz, THF-d_8) δ 161.9, 149.9, 149.0, 147.1, 147.1, 146.9, 146.8, 146.8, 146.3, 146.1, 145.8, 145.5, 145.1, 145.0, 144.9, 144.7, 144.4, 144.3, 144.2, 143.9, 143.9, 143.6, 143.4, 143.4, 143.3, 143.0, 142.8, 142.7, 142.7, 142.6, 142.4, 142.4, 142.3, 142.2, 142.2, 142.1, 142.1, 141.8, 141.8, 141.3, 140.9, 140.8, 140.8, 140.8, 140.4, 140.3, 139.6, 139.2, 138.7, 138.0, 136.8, 136.0, 135.6, 134.1, 133.9, 132.7, 95.2, 85.4, 74.5, 71.8, 68.9, 65.0, 64.9, 64.8, 64.7, 64.7, 64.6, 64.6, 64.4, 64.3, 57.8,

29.2, 25.6, 23.0, 22.9, 22.8, 22.7, 22.6, 22.5, 22.4, 22.3 ppm. HRMS (ESI): [M-H]$^-$ Calc. for $C_{67}H_9O_3$: 861.0557; found: 861.0375.

5.2.15. Synthesis of $[(C6H5)_3P]_2Pt(\eta^2\text{-}C_{60})$ 22

General Procedure

This platinum-C_{60} complex was prepared following the procedure previously described by addition of $[(C_6H_5)_3P]_2Pt(\eta^2\text{-}C_2H_4)$ to C_{60} in toluene under a dinitrogen atmosphere resulted in formation of an emerald-green solution from which black microcrystals precipitated over the course of 2 hours.[81a]

[μ-(1,2-η)[60]fullerene]bis(triphenylphosphane)platinum (**22**)

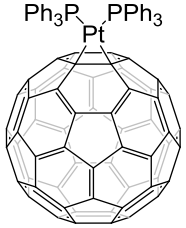

This product is already described and it showed identical spectroscopic properties.

^{31}P NMR (202 MHz, $CDCl_3$) δ 29.3 (s) ppm with satellites due to coupling of ^{31}P to the spin-1/2 isotope ^{195}Pt (33.8% abundance) ($J_{P\text{-}Pt}$ = 3939 Hz).

5.3. Representative NMR spectra of compounds

Triethyl oct-7-en-2-yne-1,5,5-tricarboxylate (**1c**)

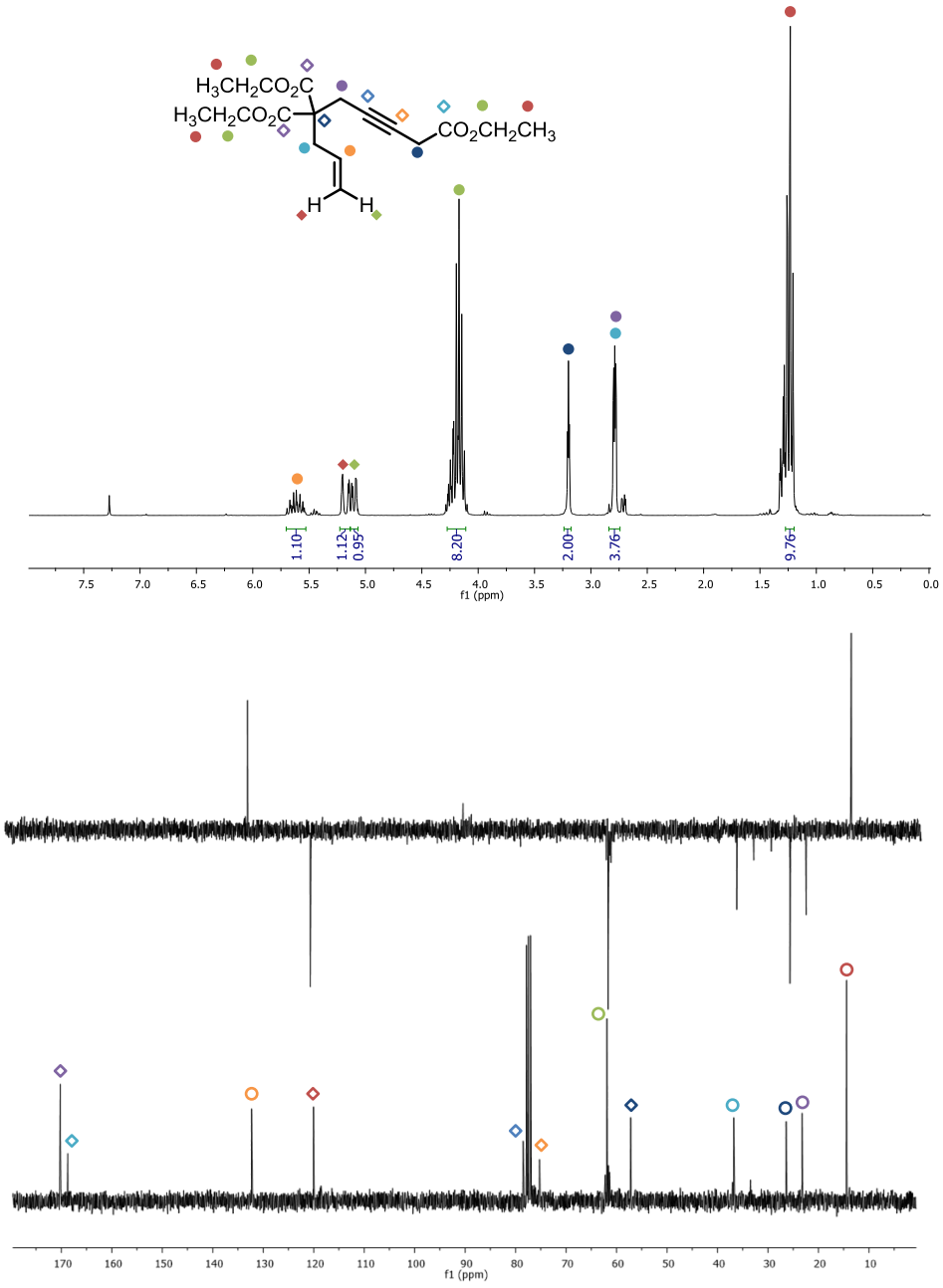

Tetraethyl nona-2,7-diyne-1,5,5,9-tetracarboxylate (**1d**)

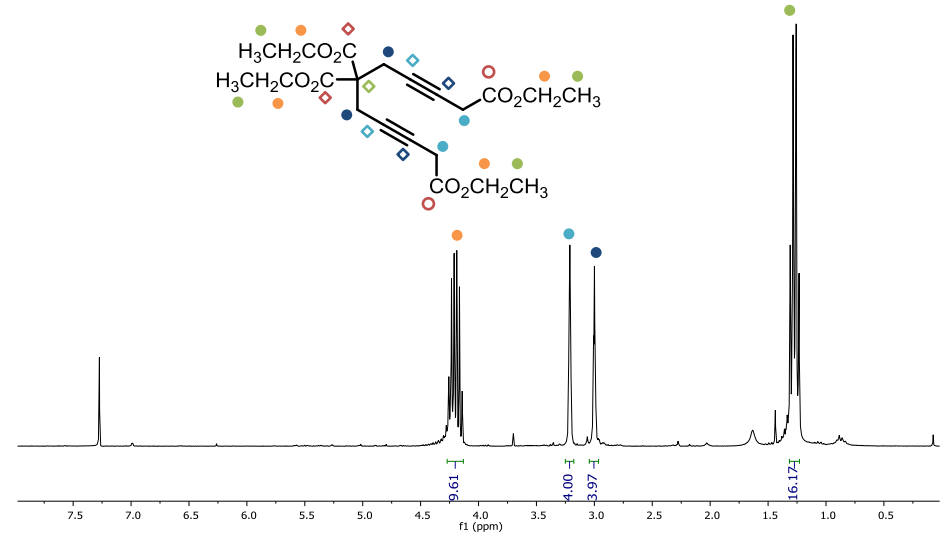

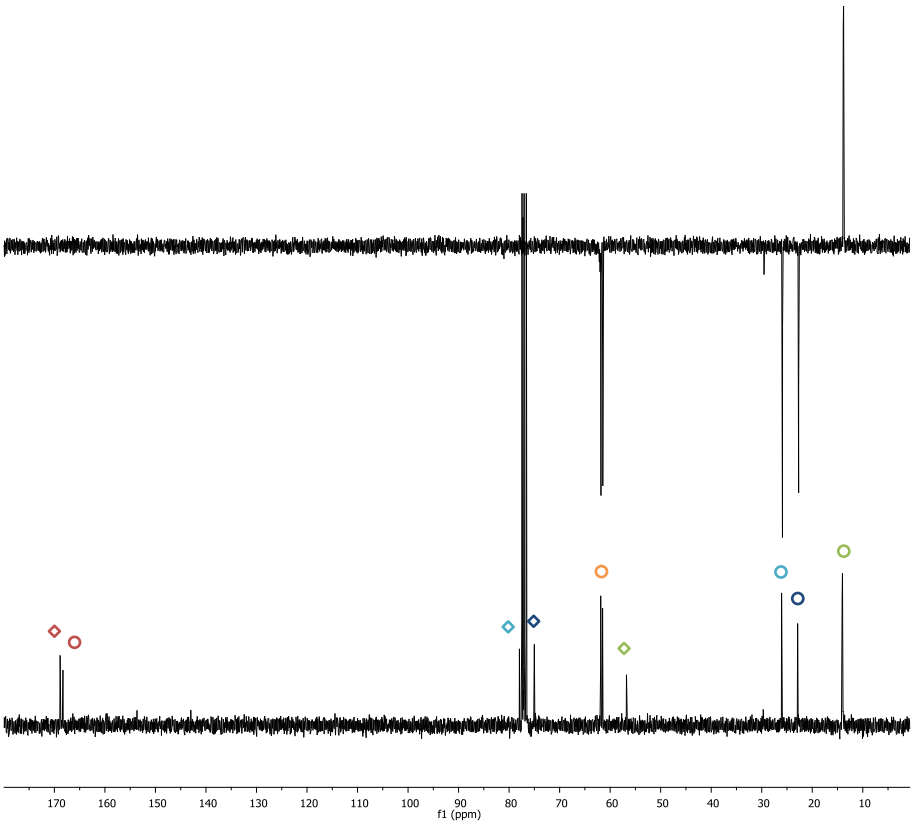

Ethyl 4-(4-chlorophenyl)but-3-ynoate (**1g**)

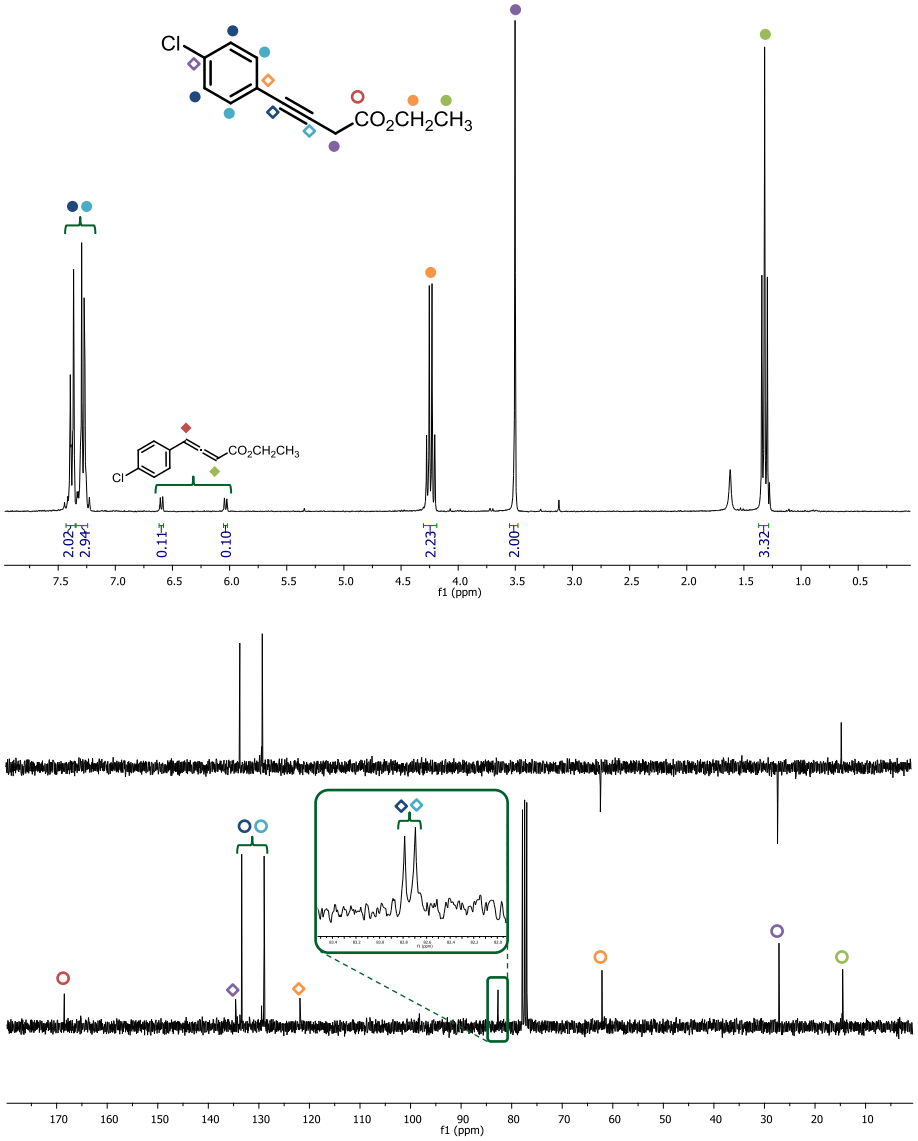

tert-Butyl 4-(4-bromophenyl)but-3-ynoate (**1h**)

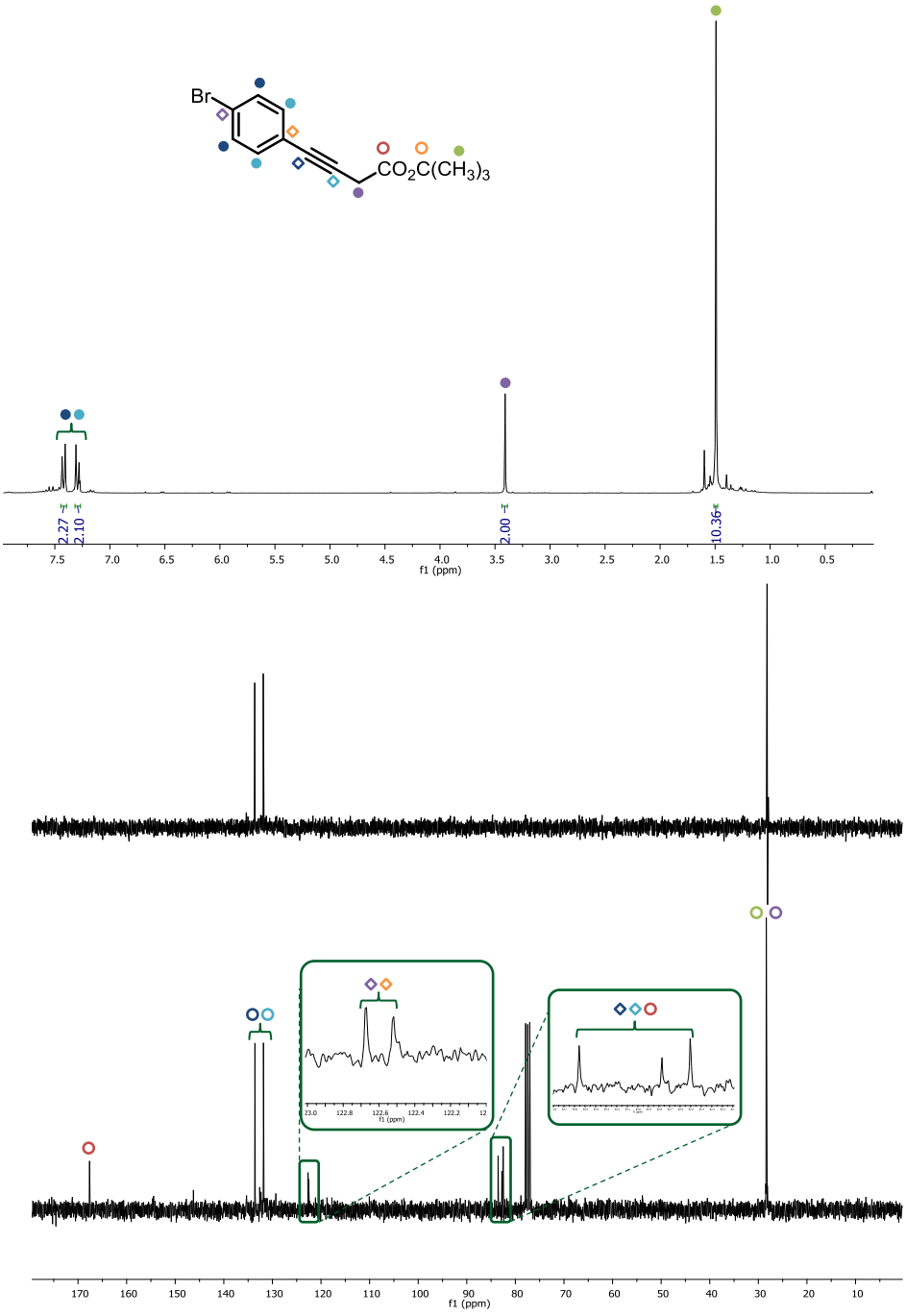

tert-Butyl 4-(3,4-dichlorophenyl)but-3-ynoate (**1i**)

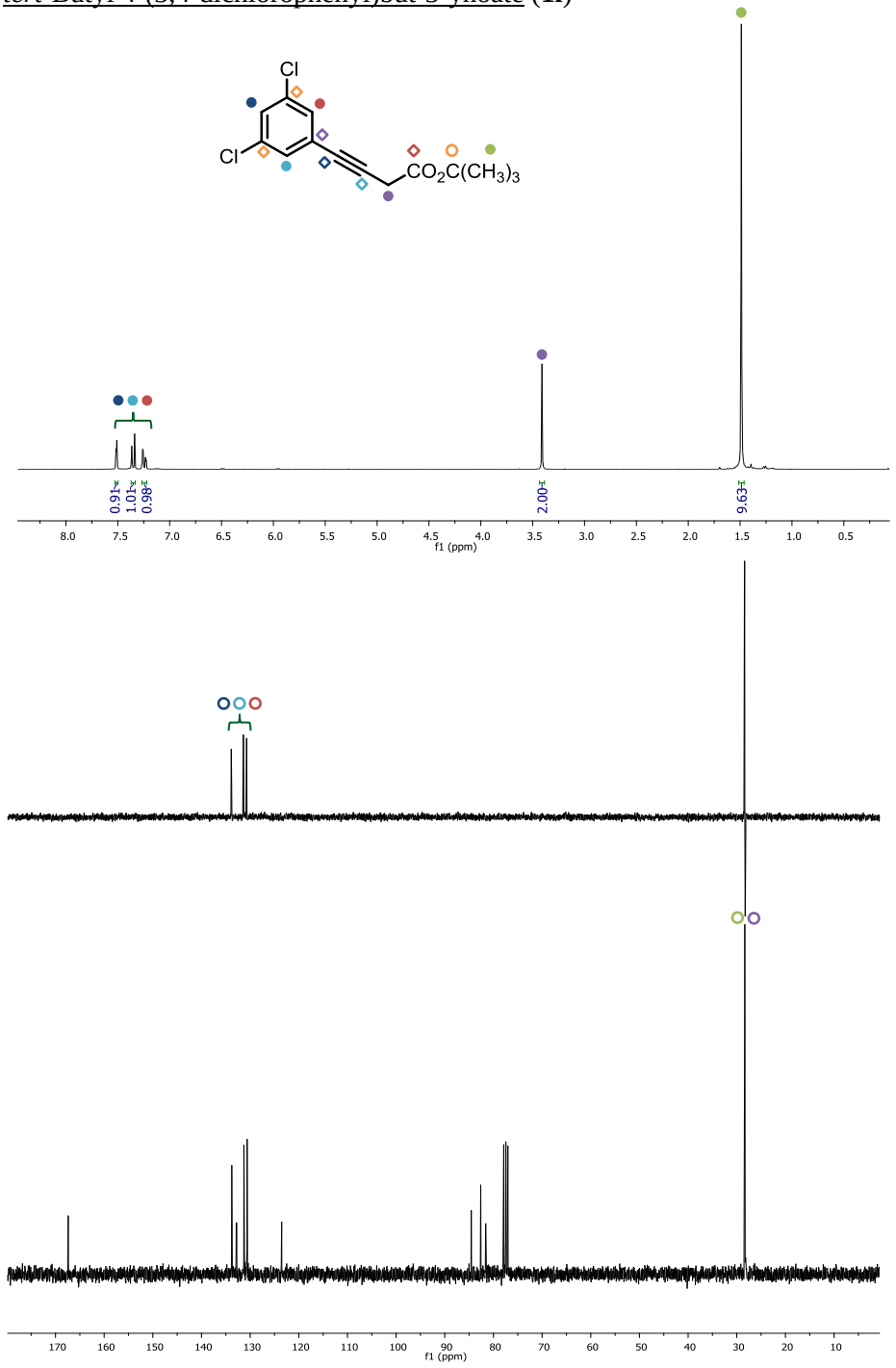

1-ethoxycarbonyl-3-(2,2-diethoxycarbonyl-4-pentenyl)-1-cyclopenteno[4,5:1,2][60]fullerene (**2b**)

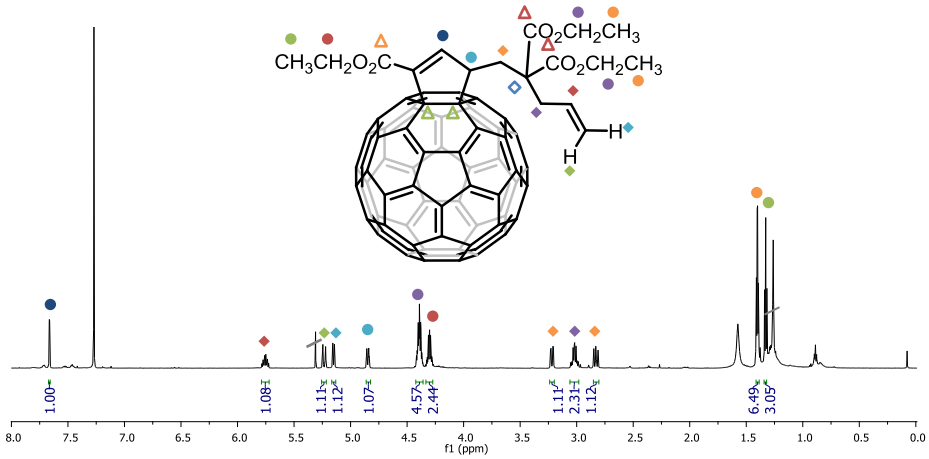

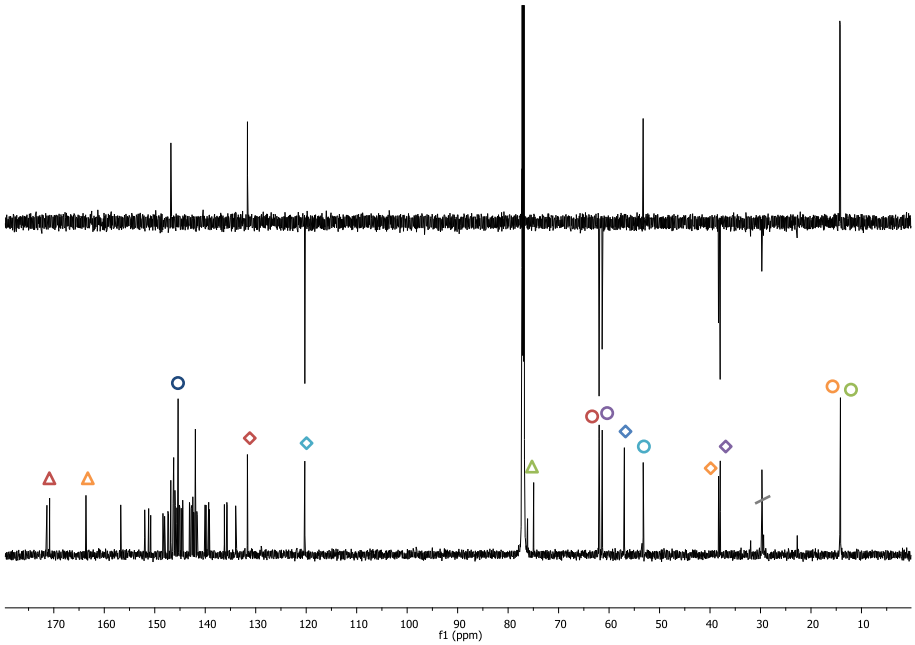

(3*R*)-1-*tert*-butoxycarbonyl-3-phenyl-1-cyclopenteno[4,5:1,2][60]fullerene (**2c**)

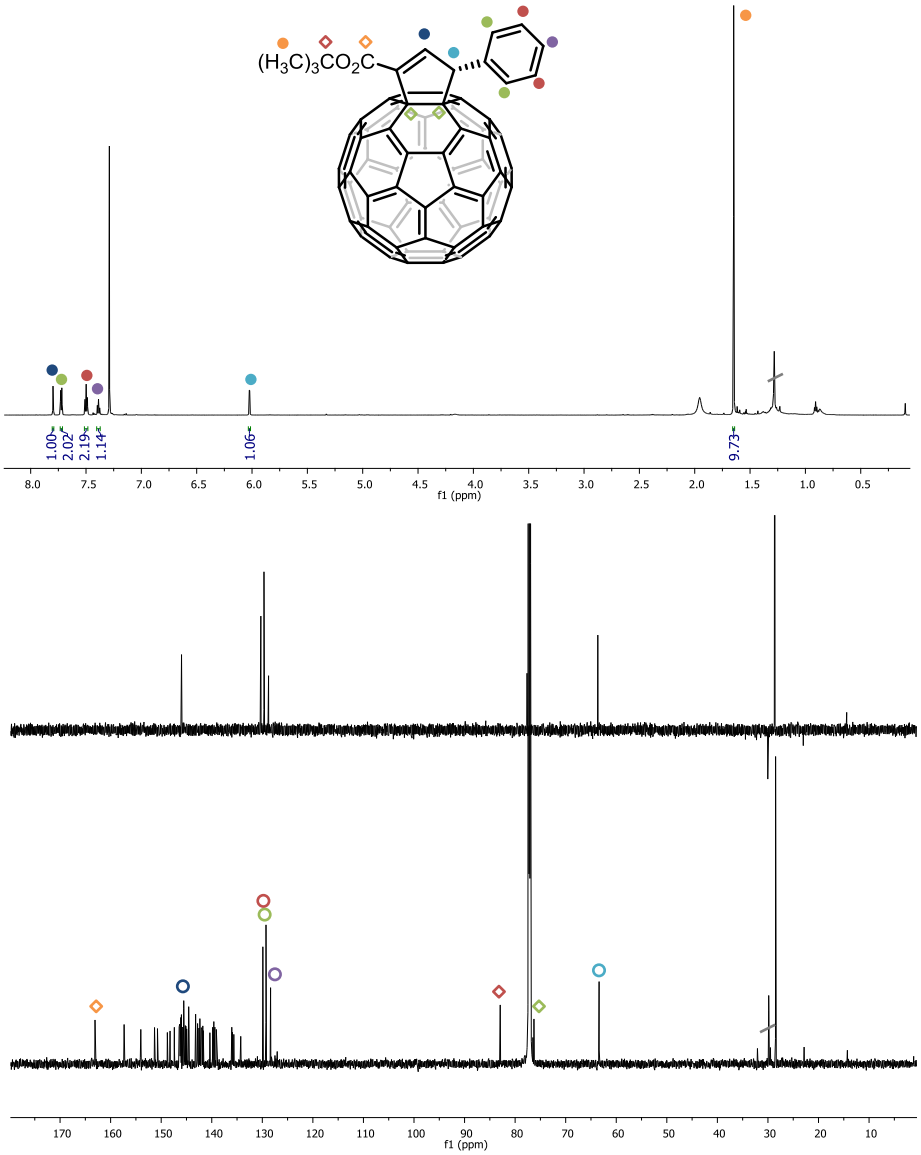

(3*S*)-1-ethoxycarbonyl-3-benzyl-1-cyclopenteno[4,5:1,2][60]fullerene (**2d**)

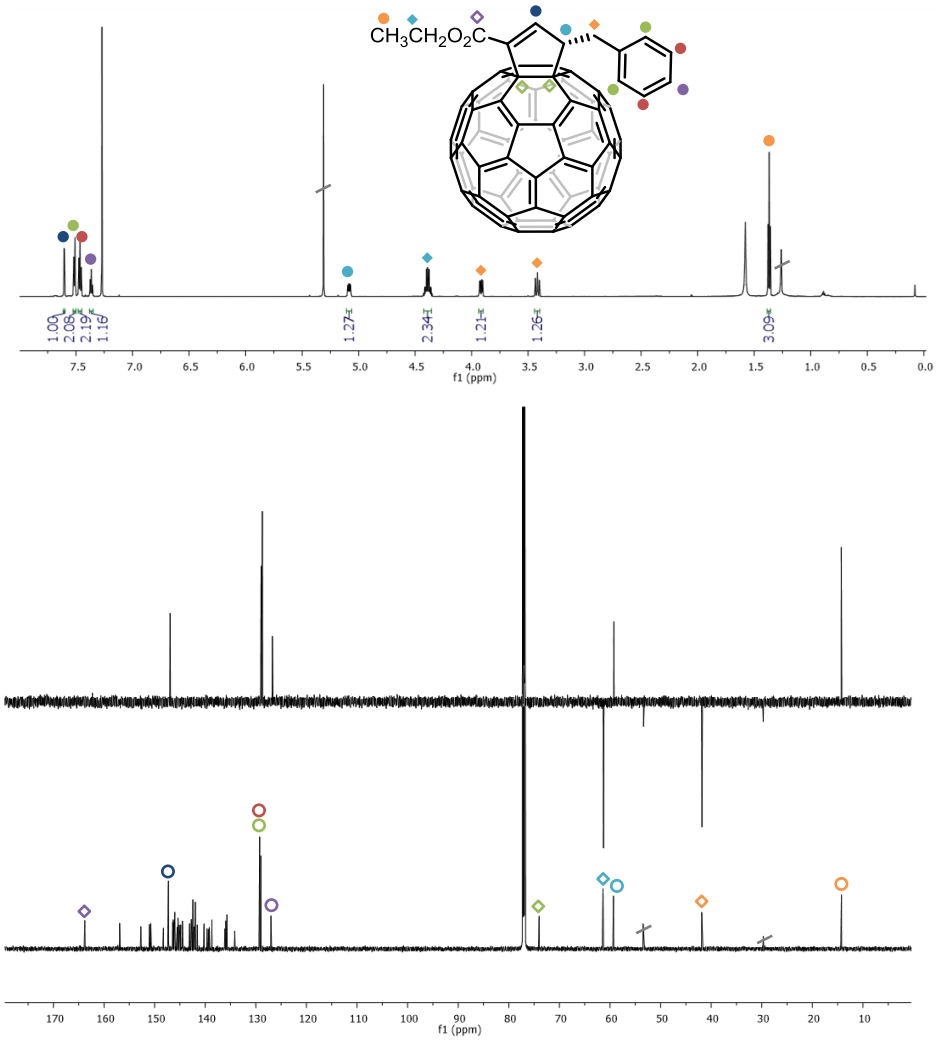

(3*S*)-1-*tert*-*but*oxycarbonyl-3-benzyl-1-cyclopenteno[4,5:1,2][60]fullerene (**2i**)

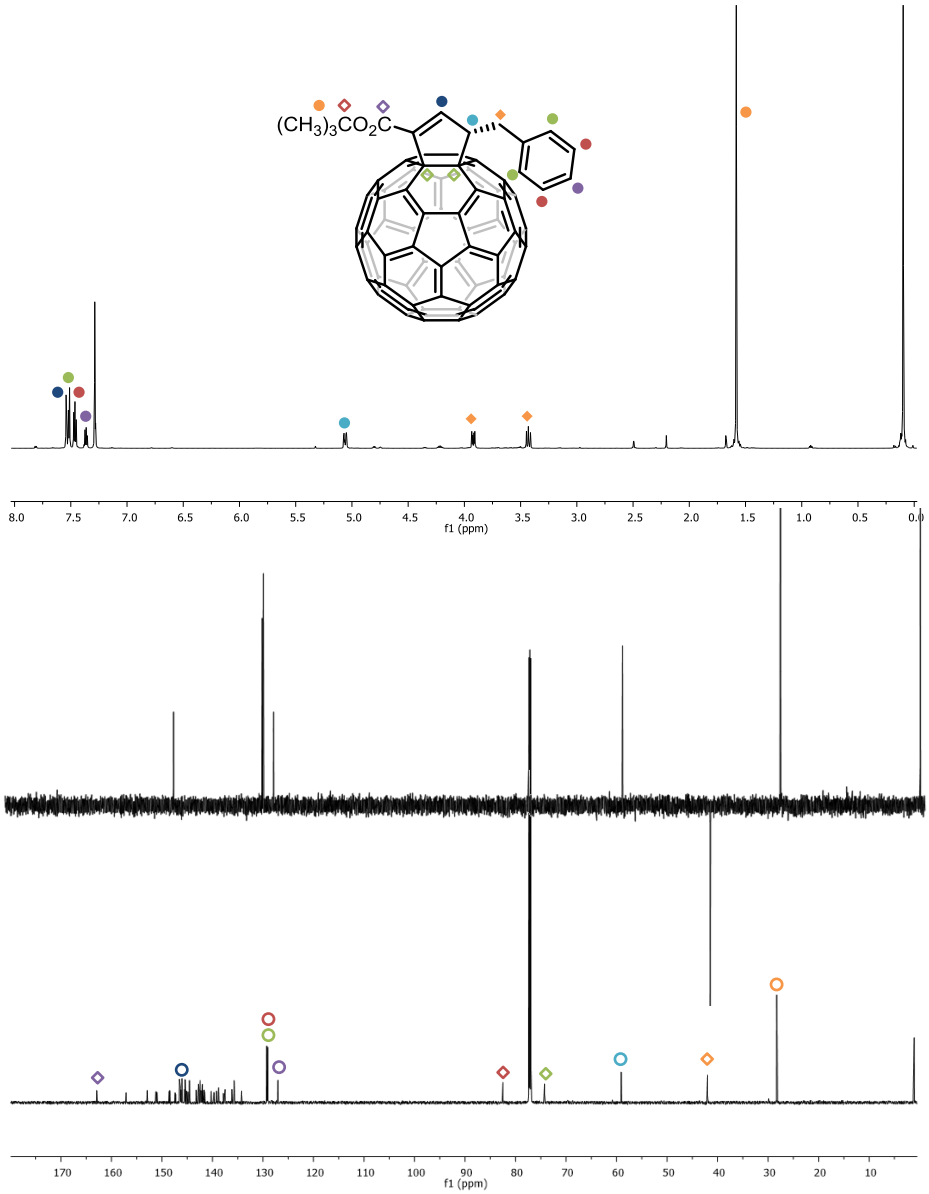

(3*S*)-2-methoxycarbonyl-3-phenyl-1-cyclopenteno[4,5:1,2][60]fullerene (**6**)

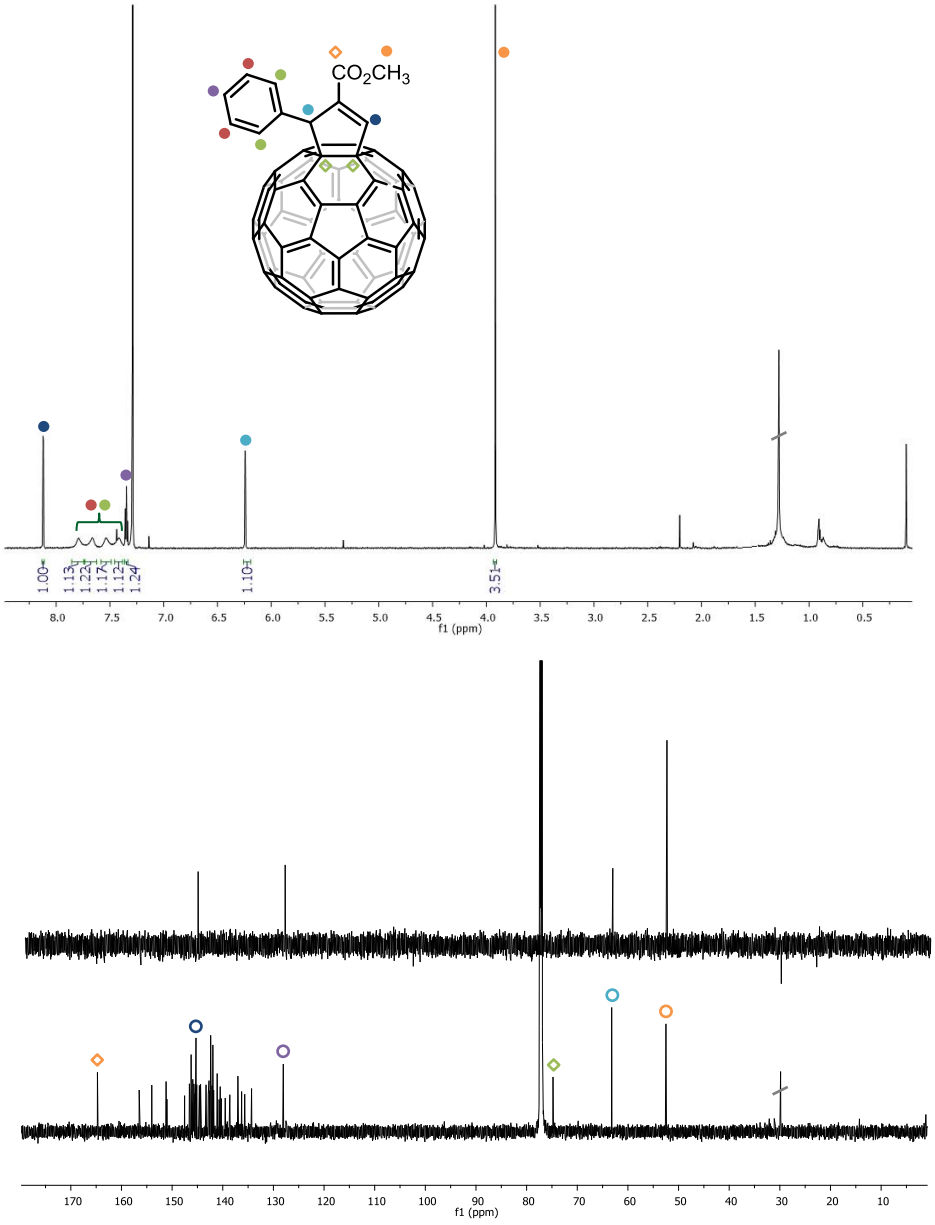

1-ethoxycarbonyl-3-methyl-1-cyclopenteno[4,5:25',8'][70]fullerene (**7a**)

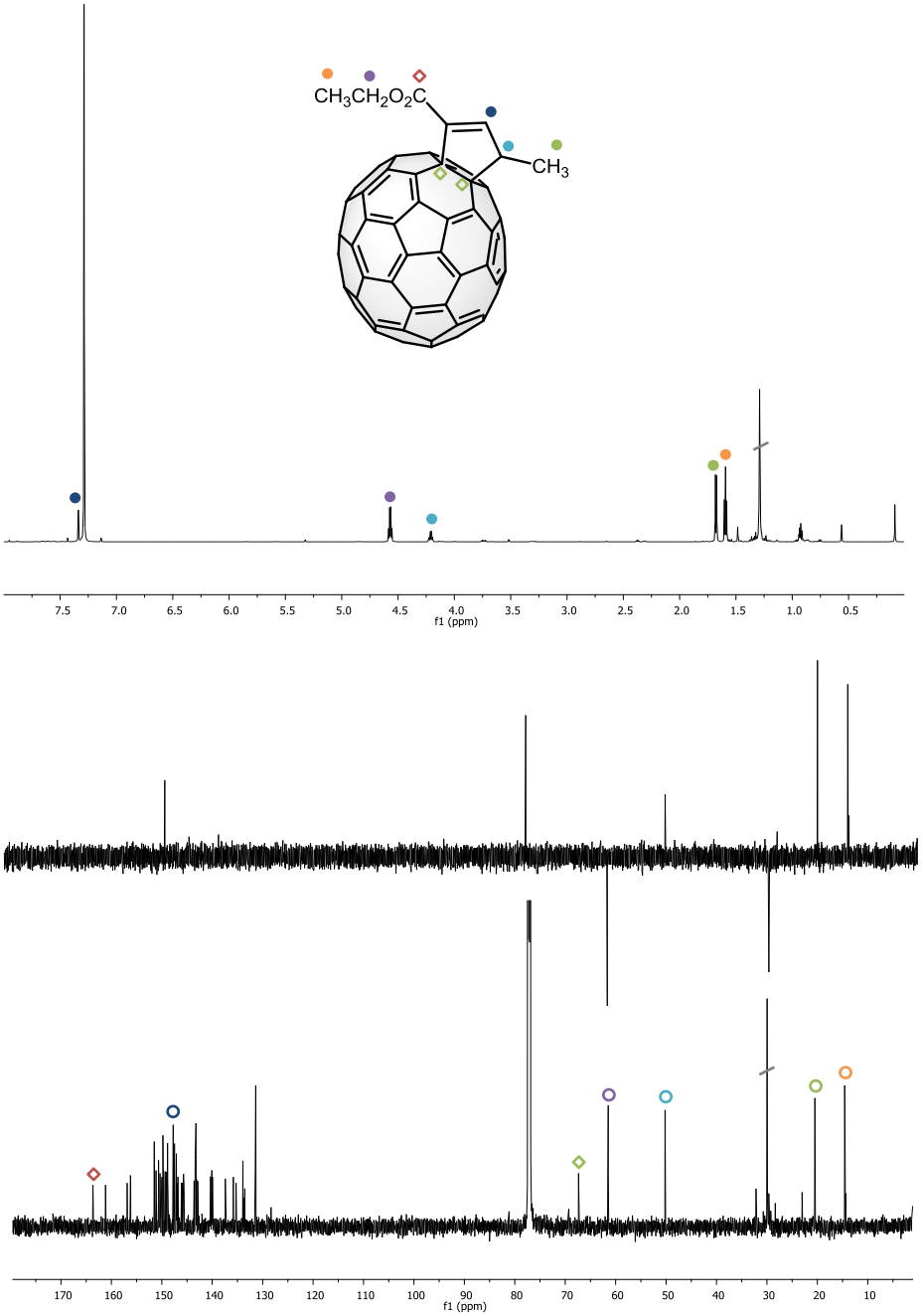

1-ethoxycarbonyl-3-phenyl-1-cyclopenteno[4,5:25',8'][70]fullerene (**7b**)

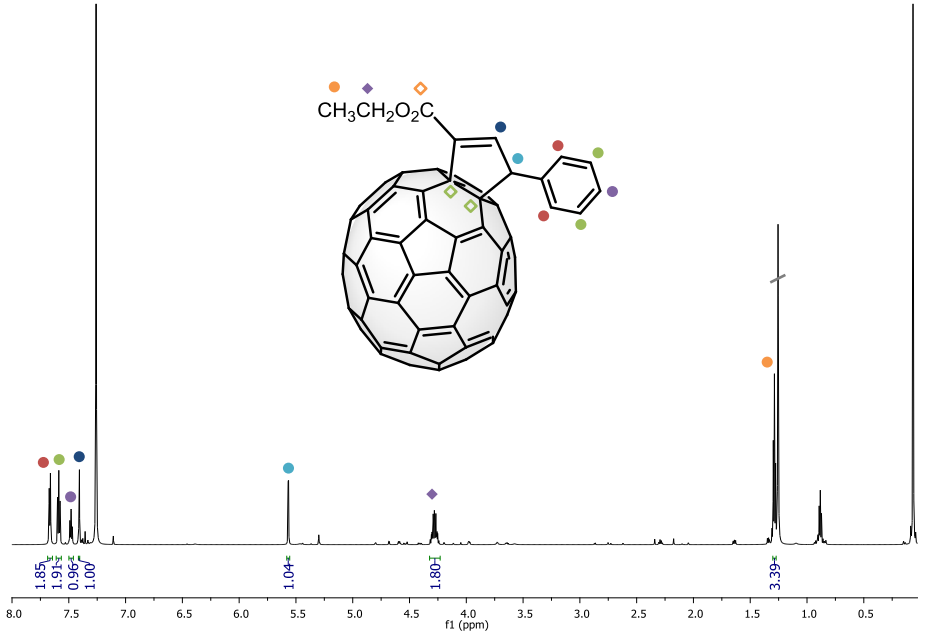

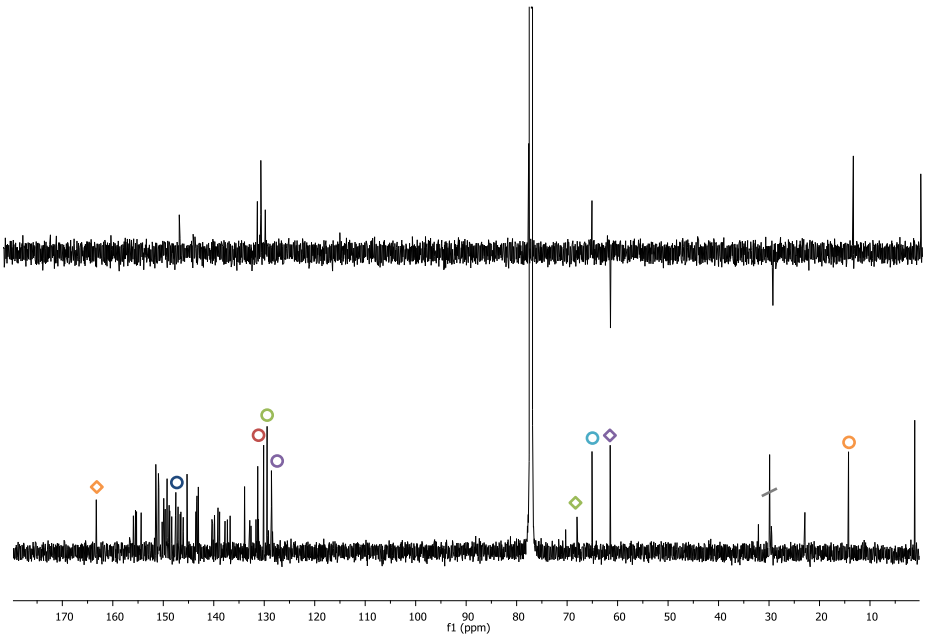

1-ethoxycarbonyl-3-phenyl-1-cyclopenteno[4,5:,8':25'][70]fullerene (**7b´**)

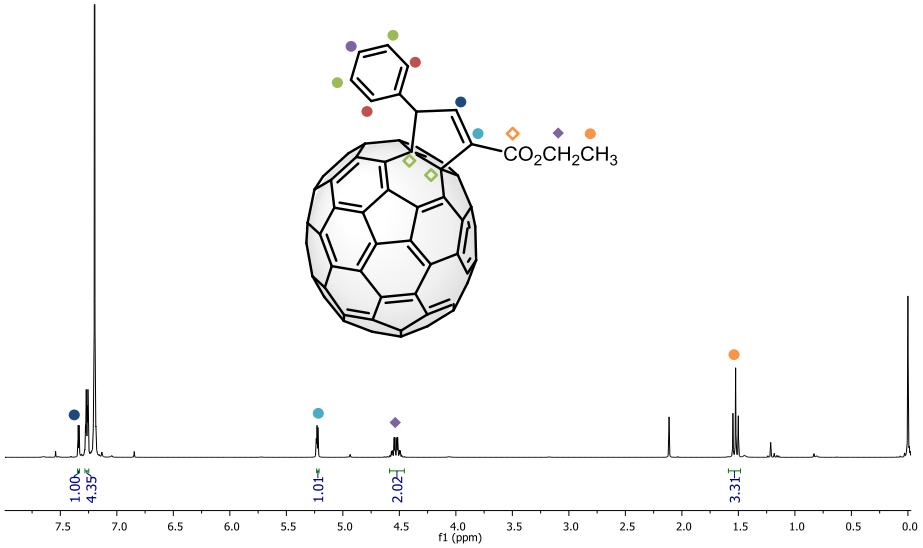

1-(ethoxycarbonylmethyl)-2-phenyl-1-cyclobuteno[3,4:1,2][60]fullerene (**8a**)

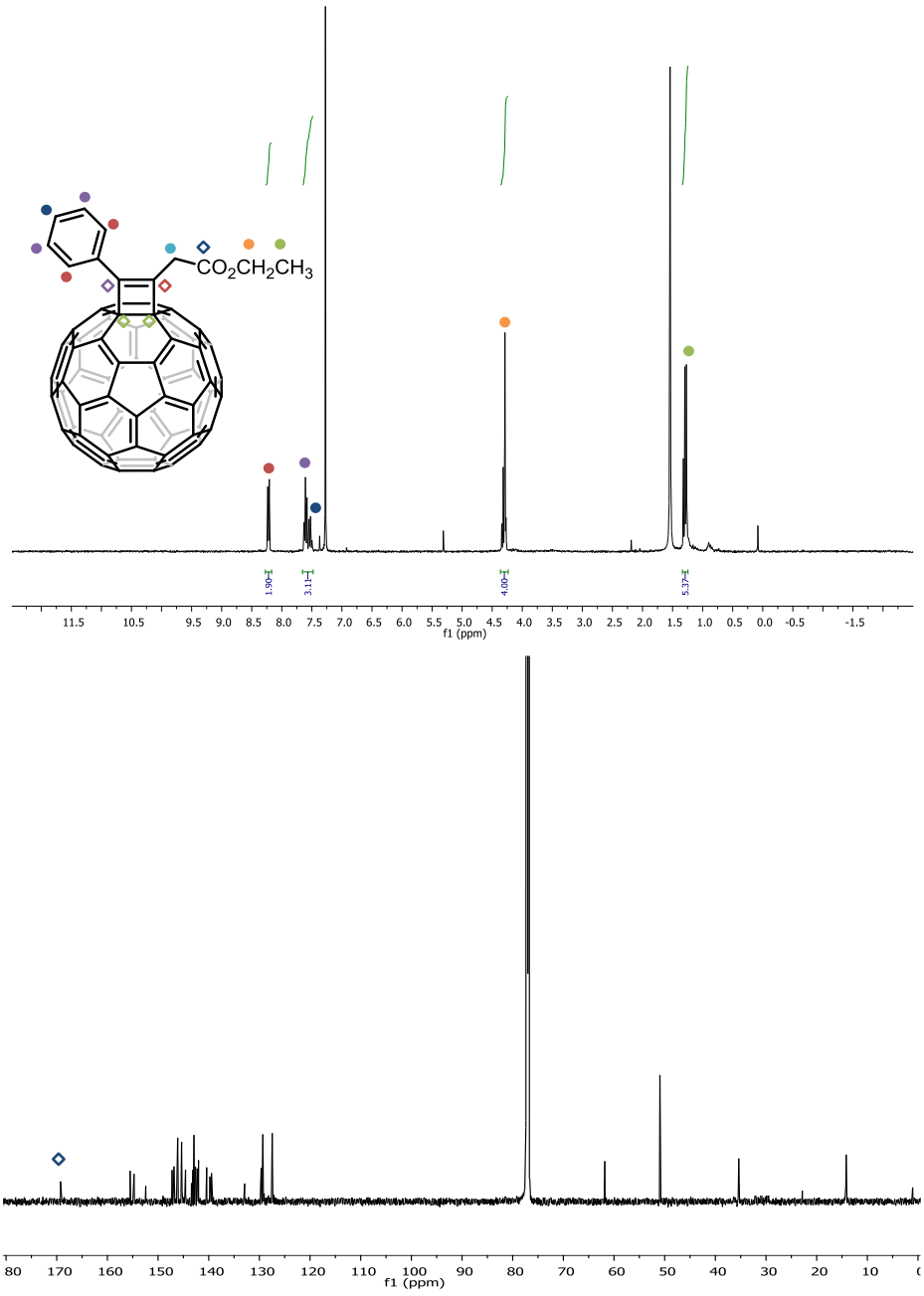

1-(ethoxycarbonylmethyl)-2-ethyl-1-cyclobuteno[3,4:1,2][60]fullerene (**8b**)

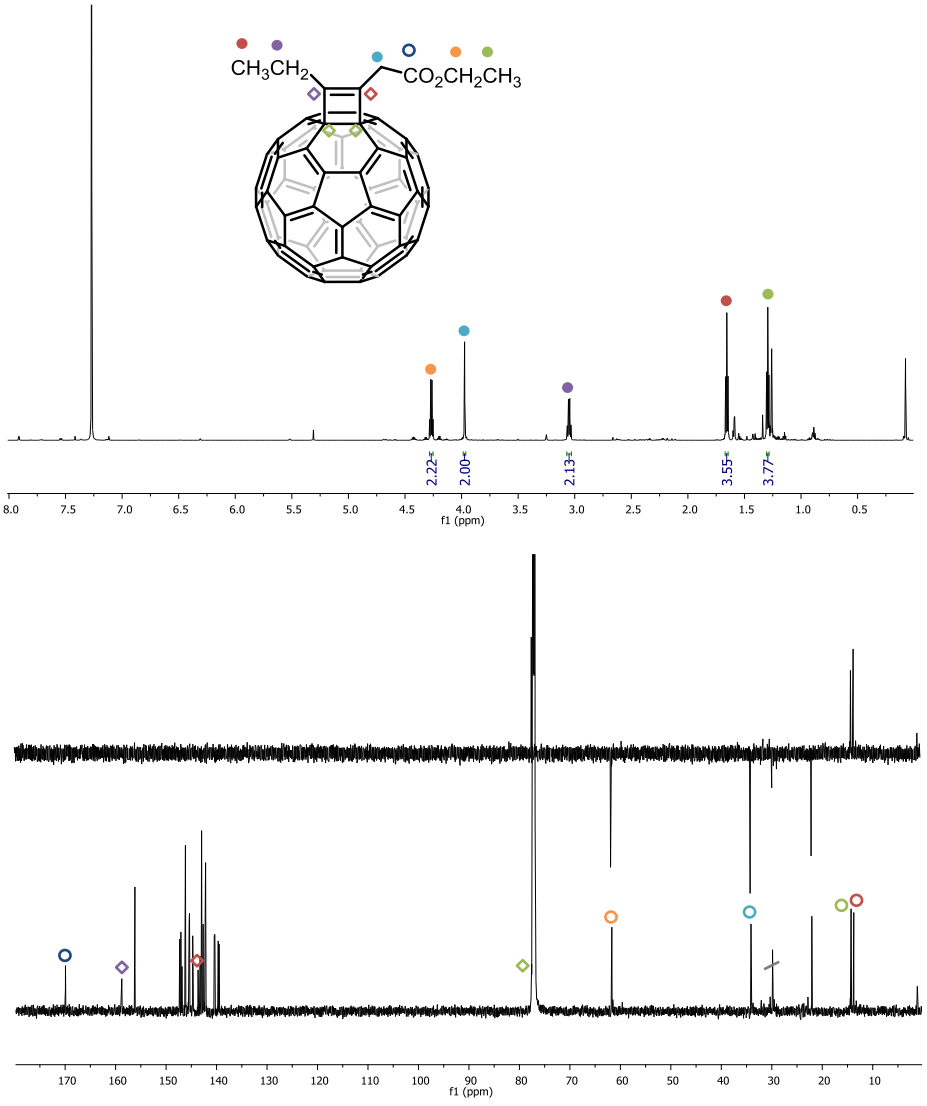

1-(ethoxycarbonylmethyl)-2-methyl-1-cyclobuteno[3,4:1,2][60]fullerene (**8c**)

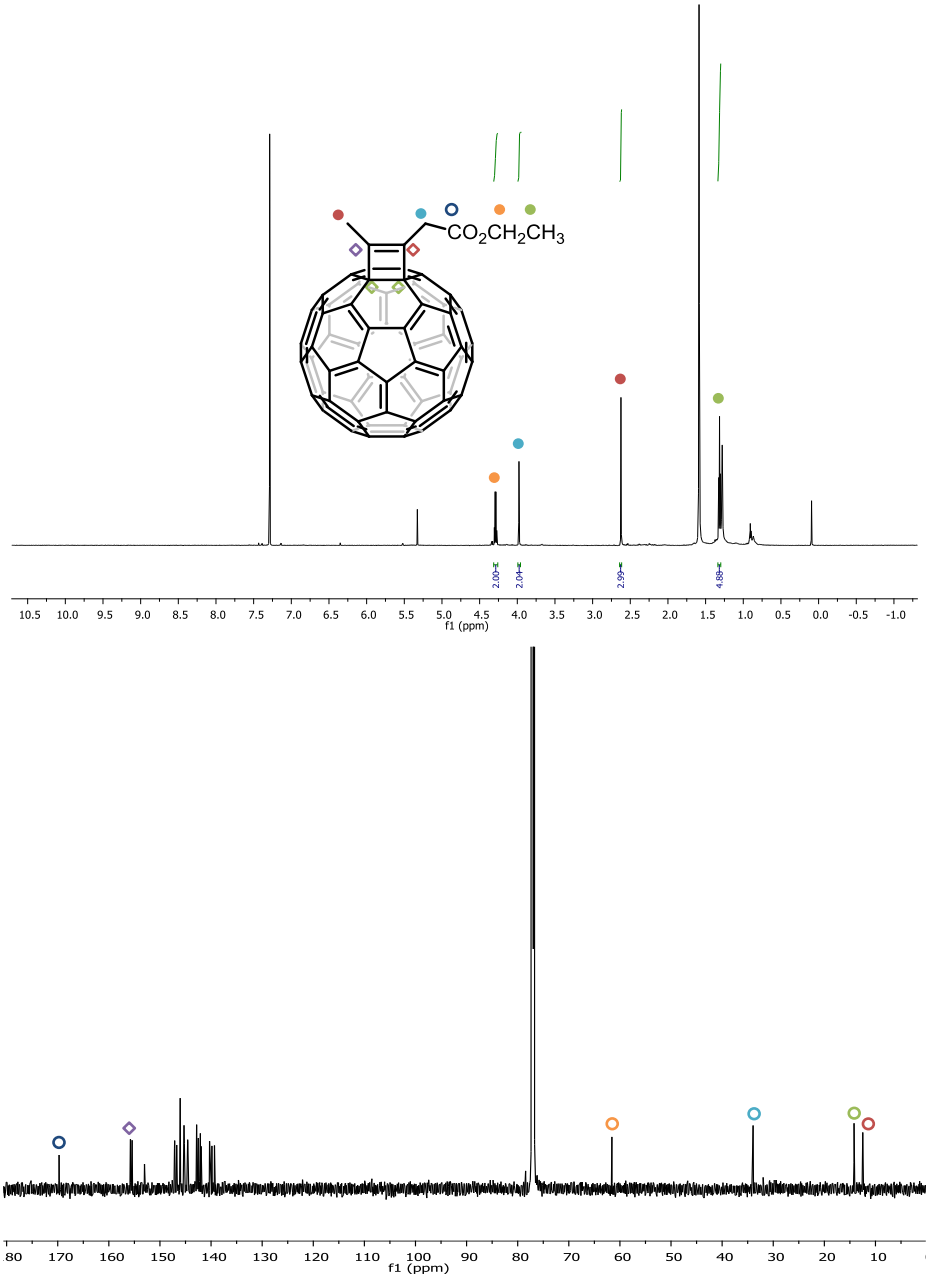

1-(ethoxycarbonylmethyl)-2-benzyl-1-cyclobuteno[3,4:1,2][60]fullerene (**8d**)

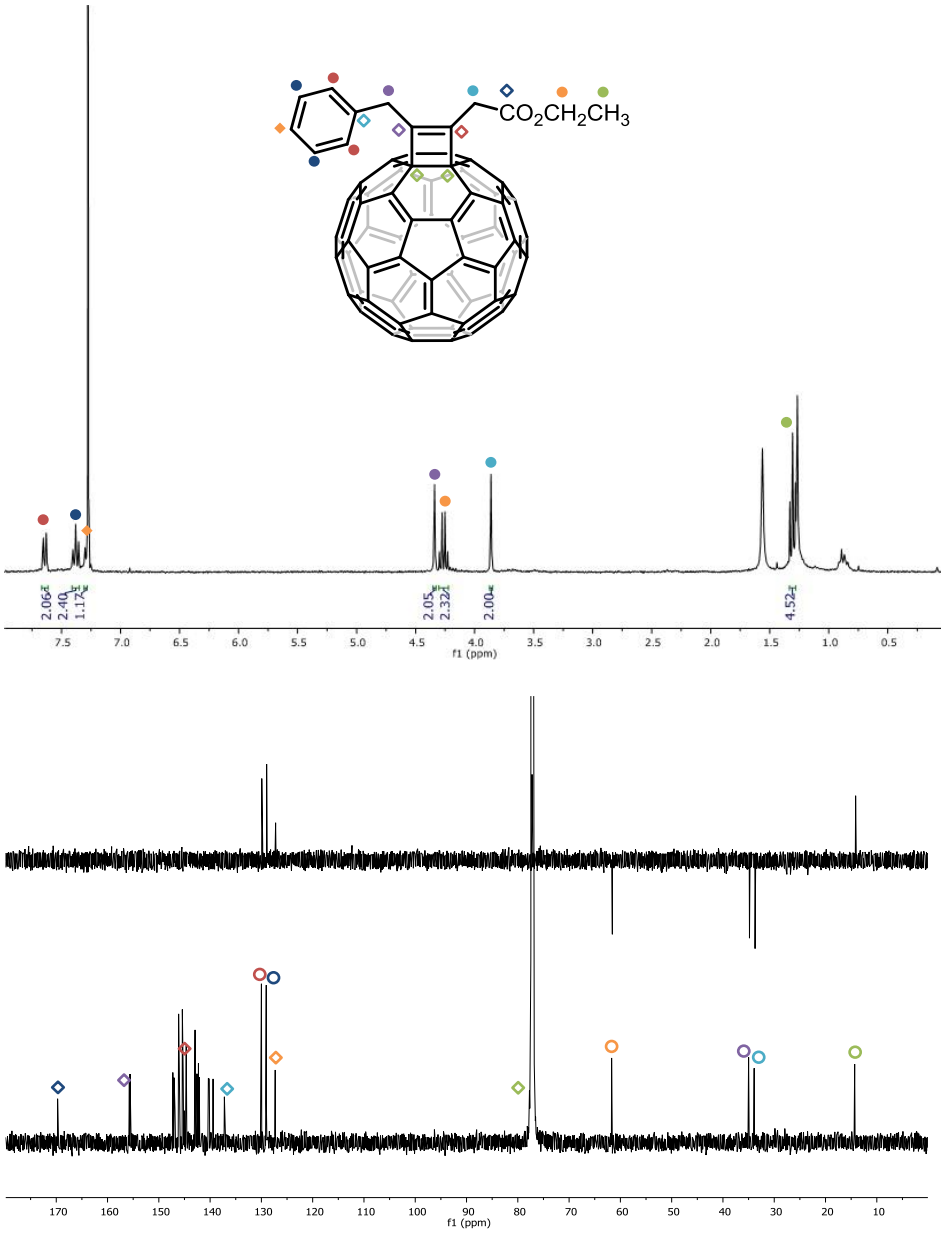

1-(benzyloxycarbonylmethyl)-2-phenyl-1-cyclobuteno[3,4:1,2][60]fullerene (**8e**)

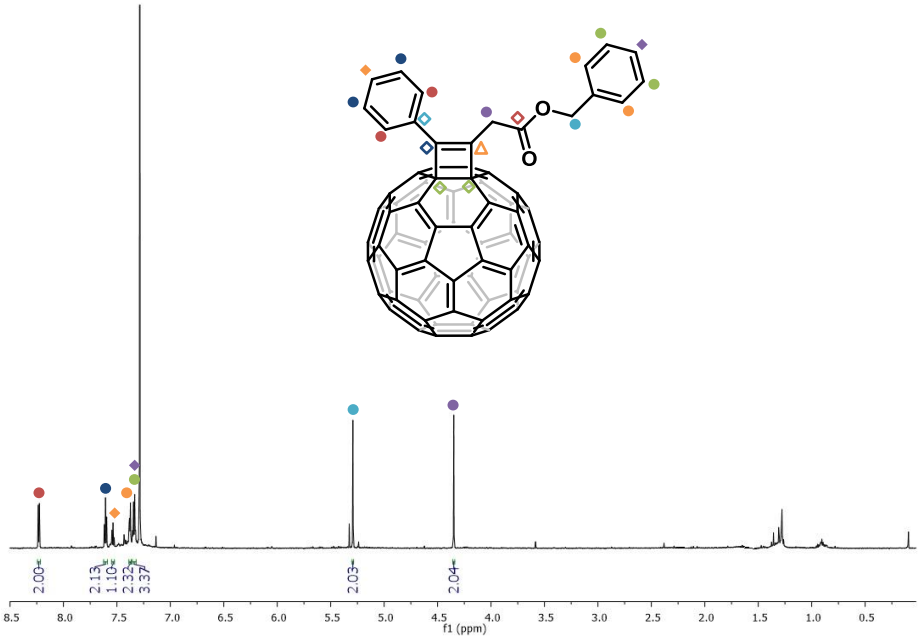

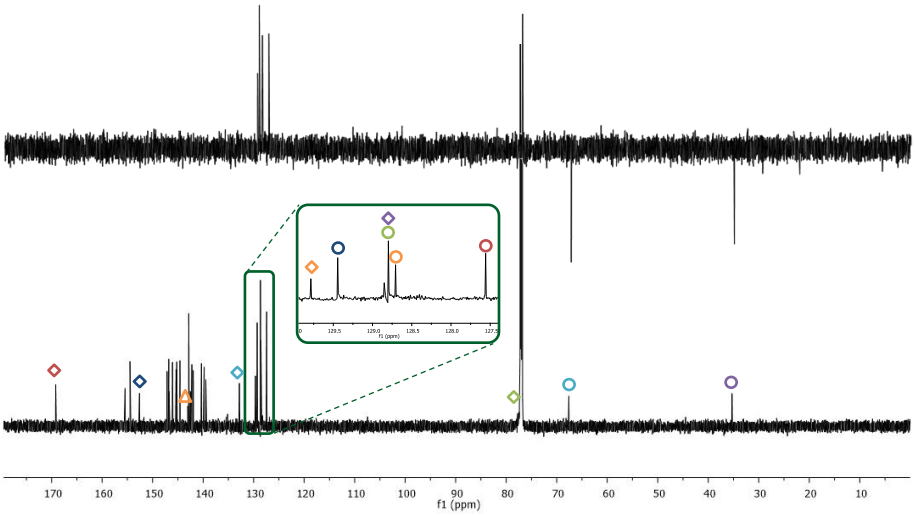

1-(ethoxycarbonylmethyl)-2-(4-chlorophenyl)-1-cyclobuteno[3,4:1,2][60]fullerene (**8f**)

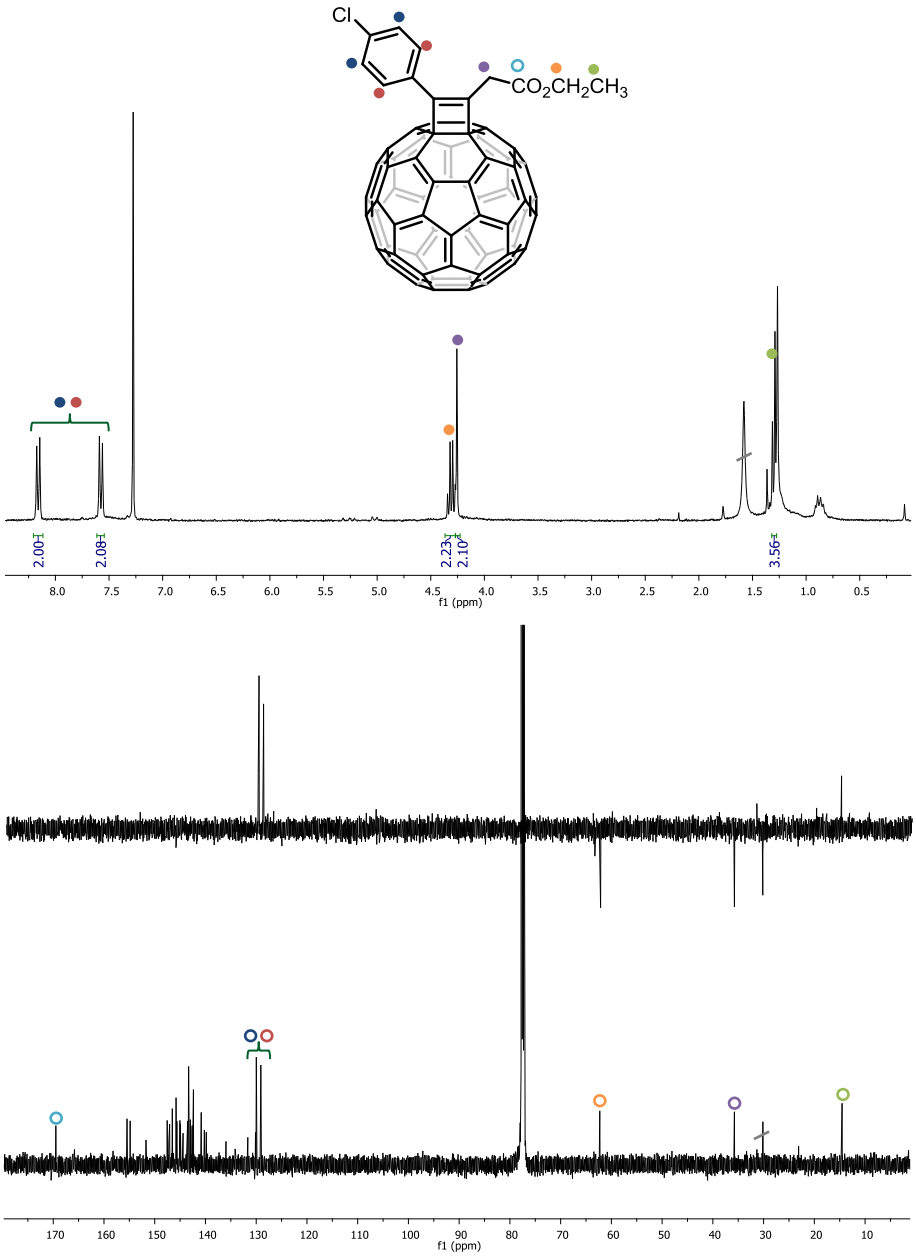

1-(*tert*-butoxycarbonylmethyl)-2-(4-bromophenyl)-1-cyclobuteno[3,4:1,2][60]fullerene (**8g**)

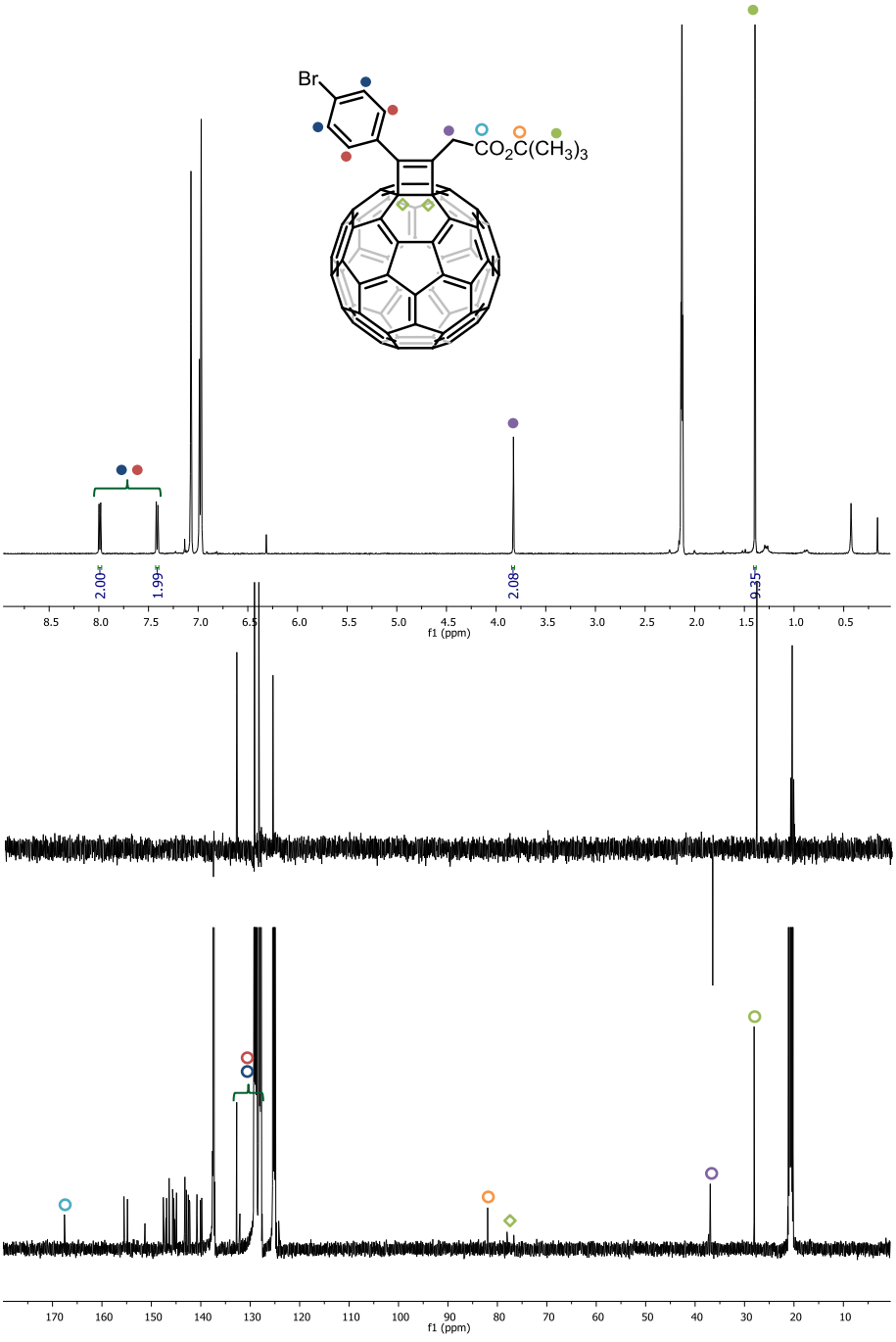

1-(*tert*-butoxycarbonylmethyl)-2-(3,5-dichlorophenyl)-1-cyclobuteno[3,4:1,2][60]fullerene (**8h**)

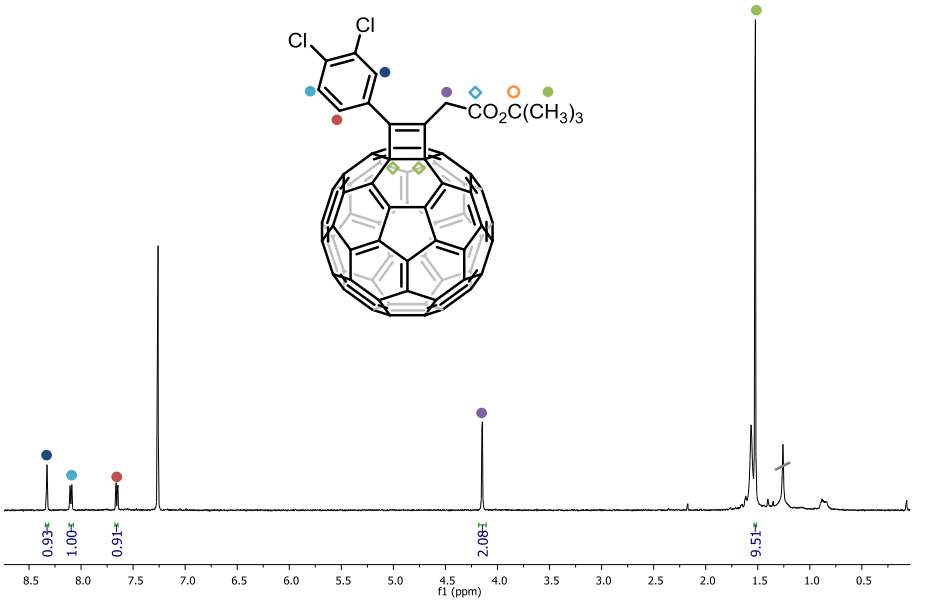

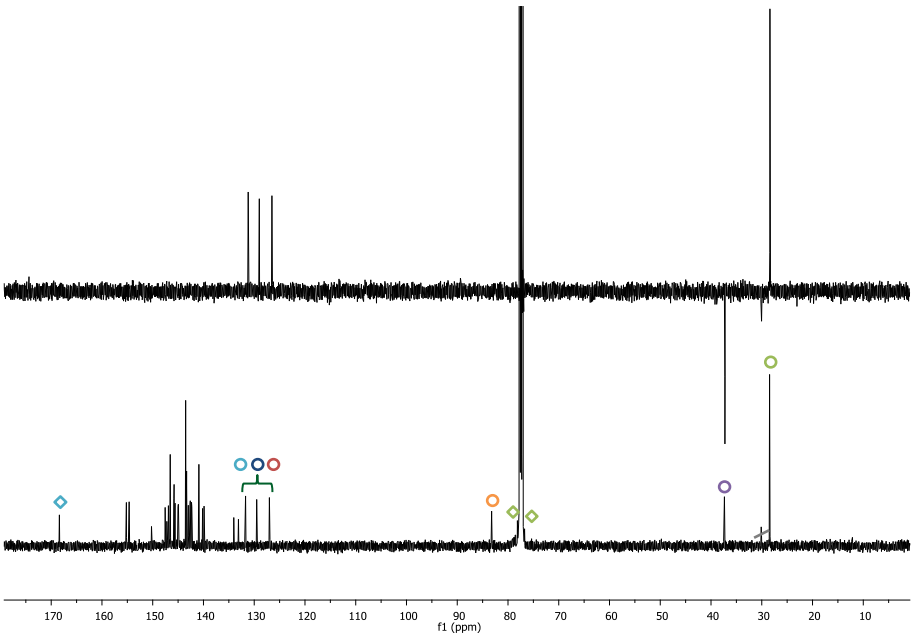

1-(*tert*-butoxycarbonylmethyl)-2-(4-*tert*-butylphenyl)-1-cyclobuteno[3,4:1,2][60]fullerene (**8i**)

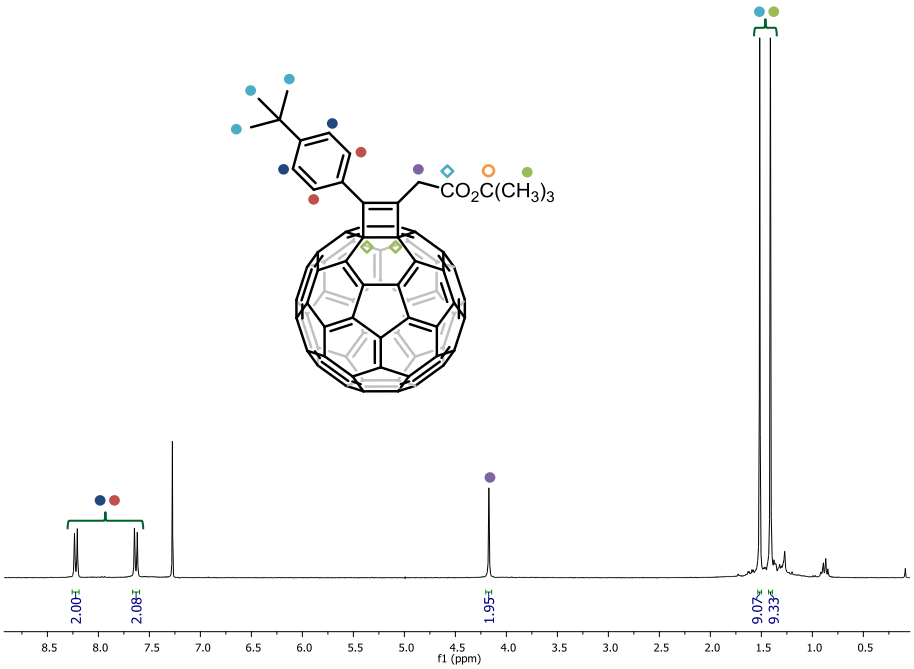

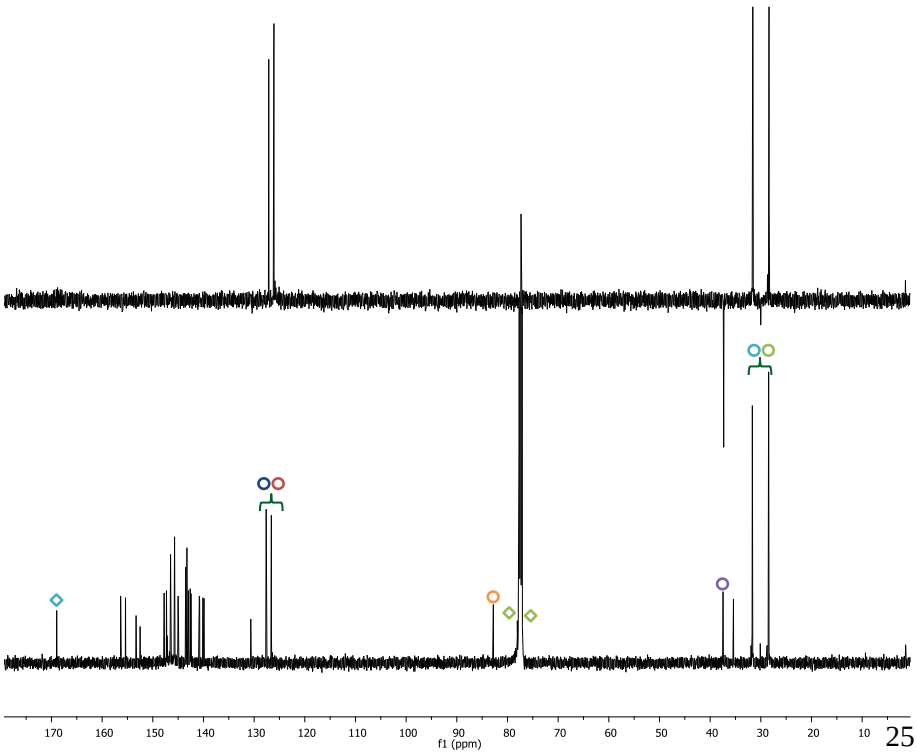

1-(methoxycarbonylmethyl)-2-phenyl-1-cyclobuteno[3,4:1,2][60]fullerene (**8j**)

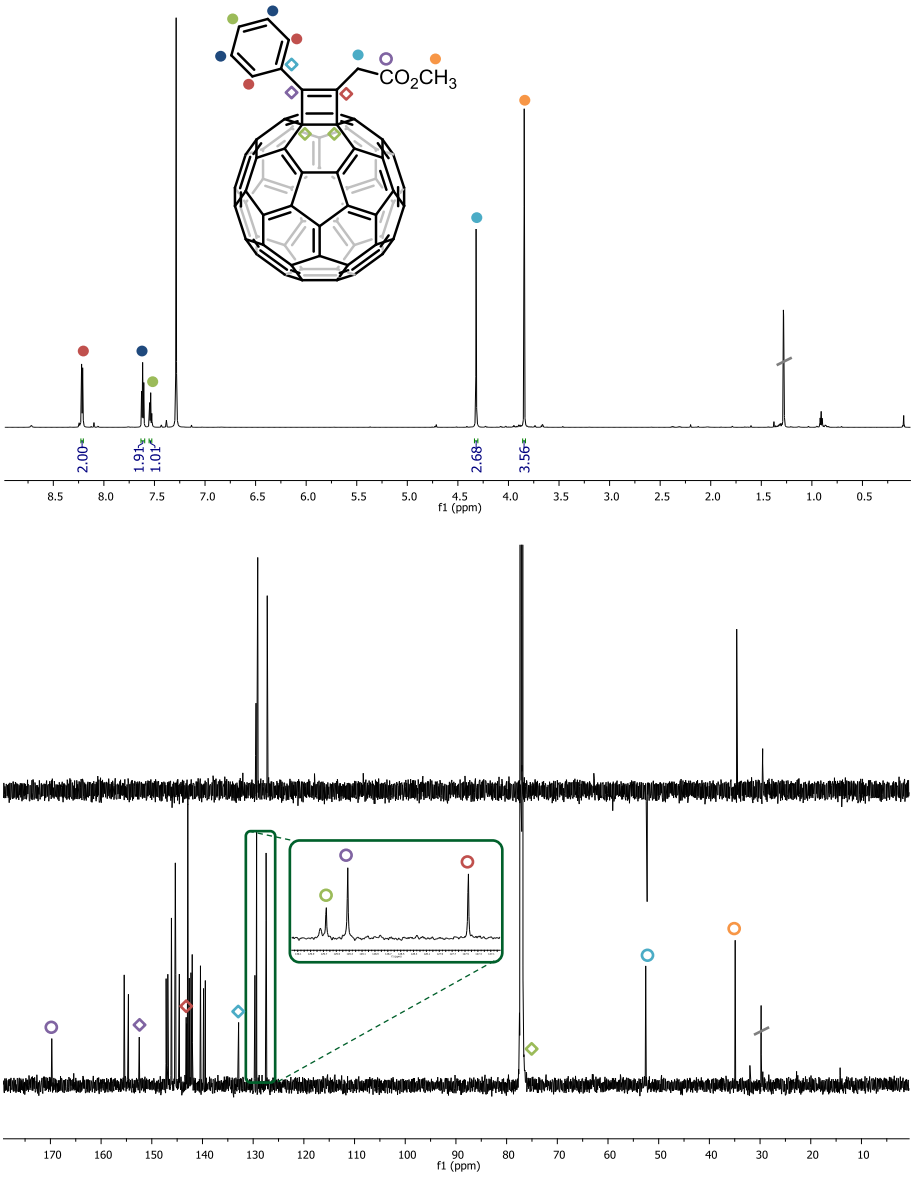

1-(methoxycarbonylmethyl)-2-benzyl-1-cyclobuteno[3,4:1,2][60]fullerene (**8k**)

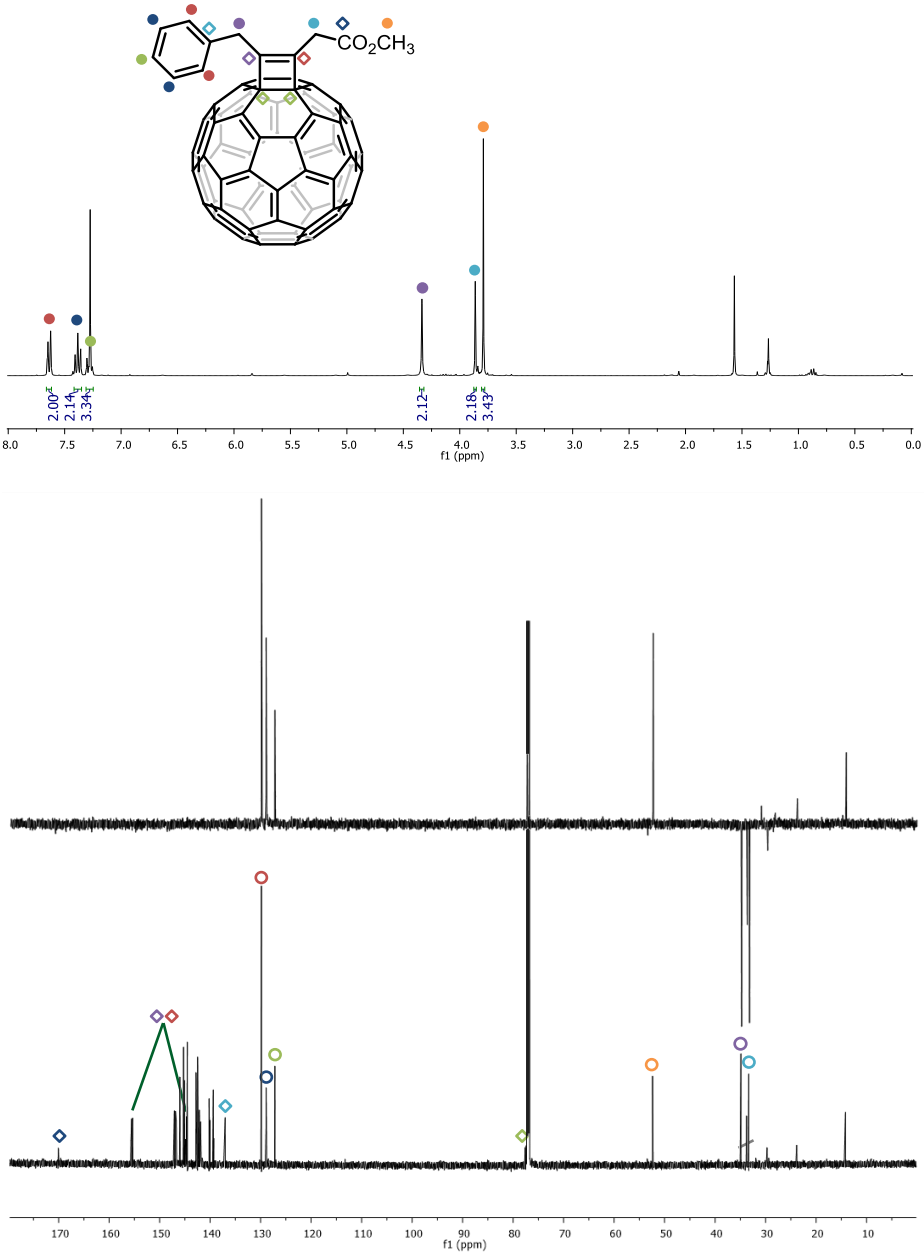

Racemic *tert*-butyl (E)-*N*-[(2-carbo[6]helicene)methylene]glycinate (**10**)

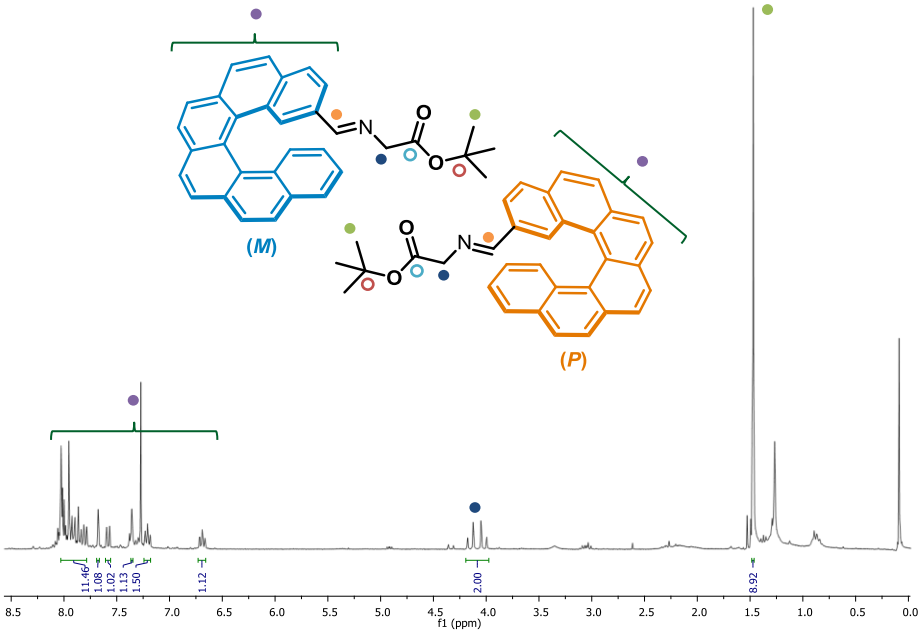

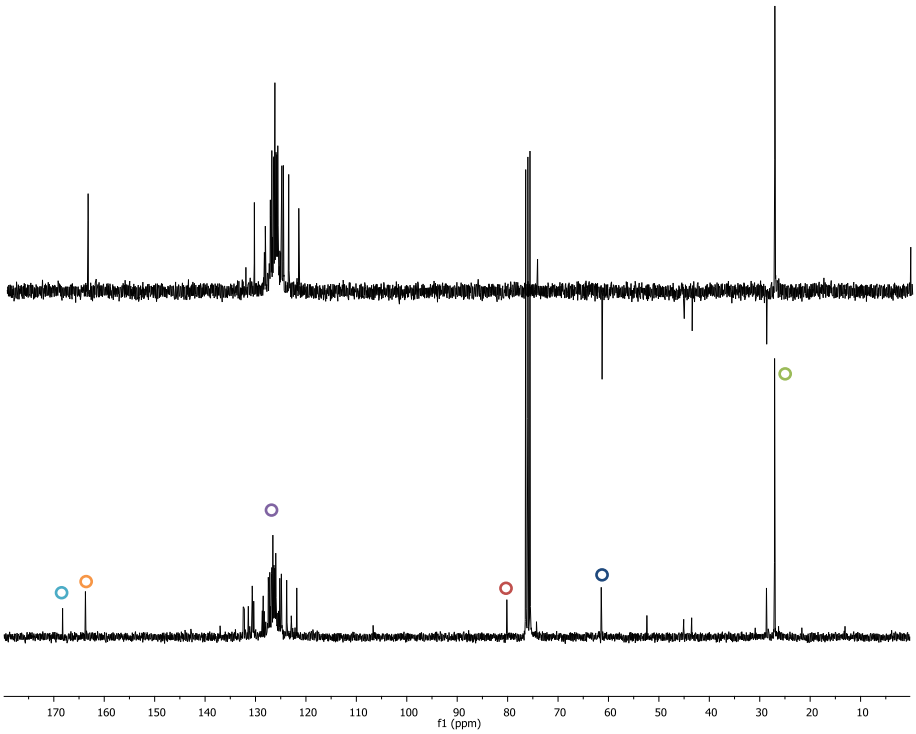

(2*S*,5*S*)-2-*tert*-butoxycarbonyl-5-(*P*-2-carbo[6]helicene)pyrrolidino [3,4:1,2][60]fullerene (***P*,*S*,*S*-11**)

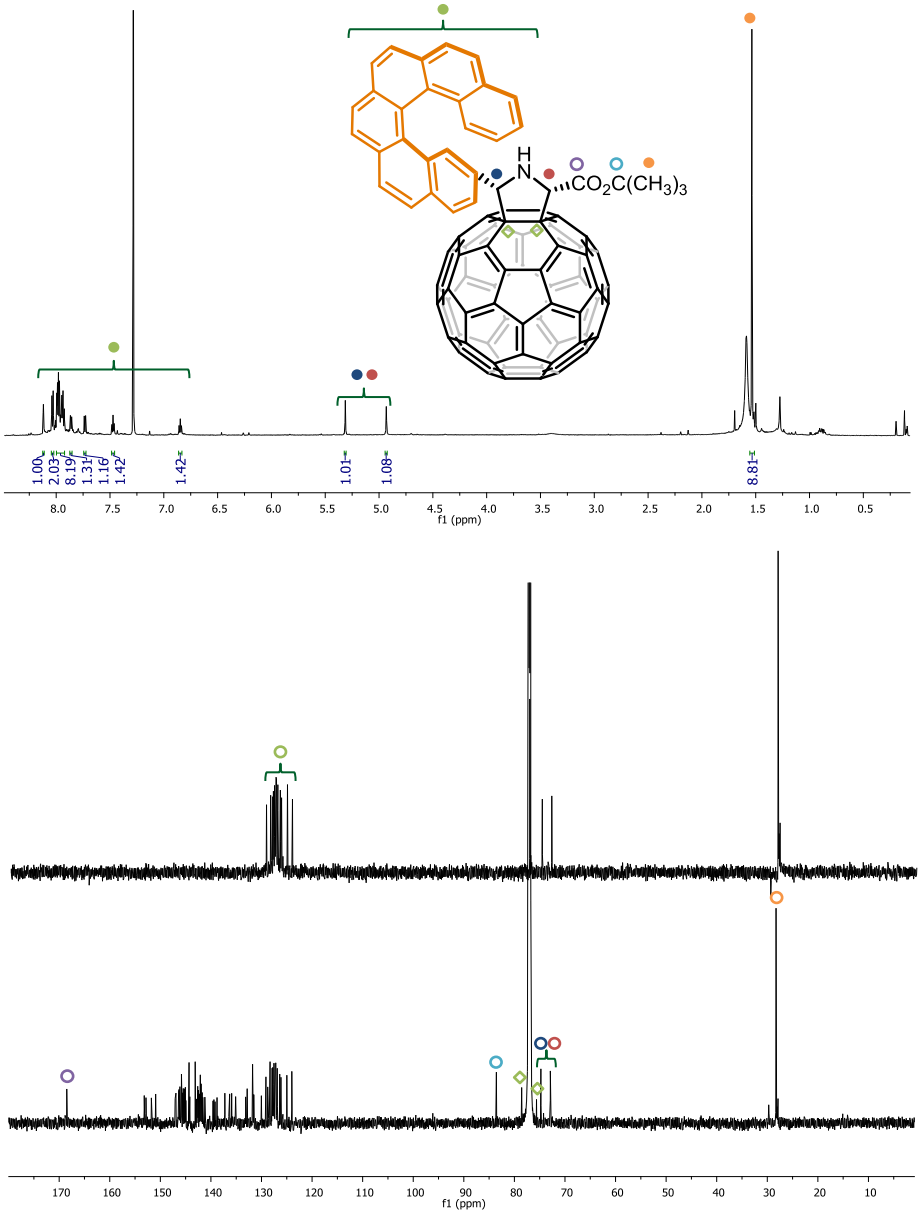

(2*S*,5*S*)-2-*tert*-butoxycarbonyl-5-(*M*-2-carbo[6]helicene)pyrrolidino [3,4:1,2][60]fullerene (***M*,*S*,*S*-12**)

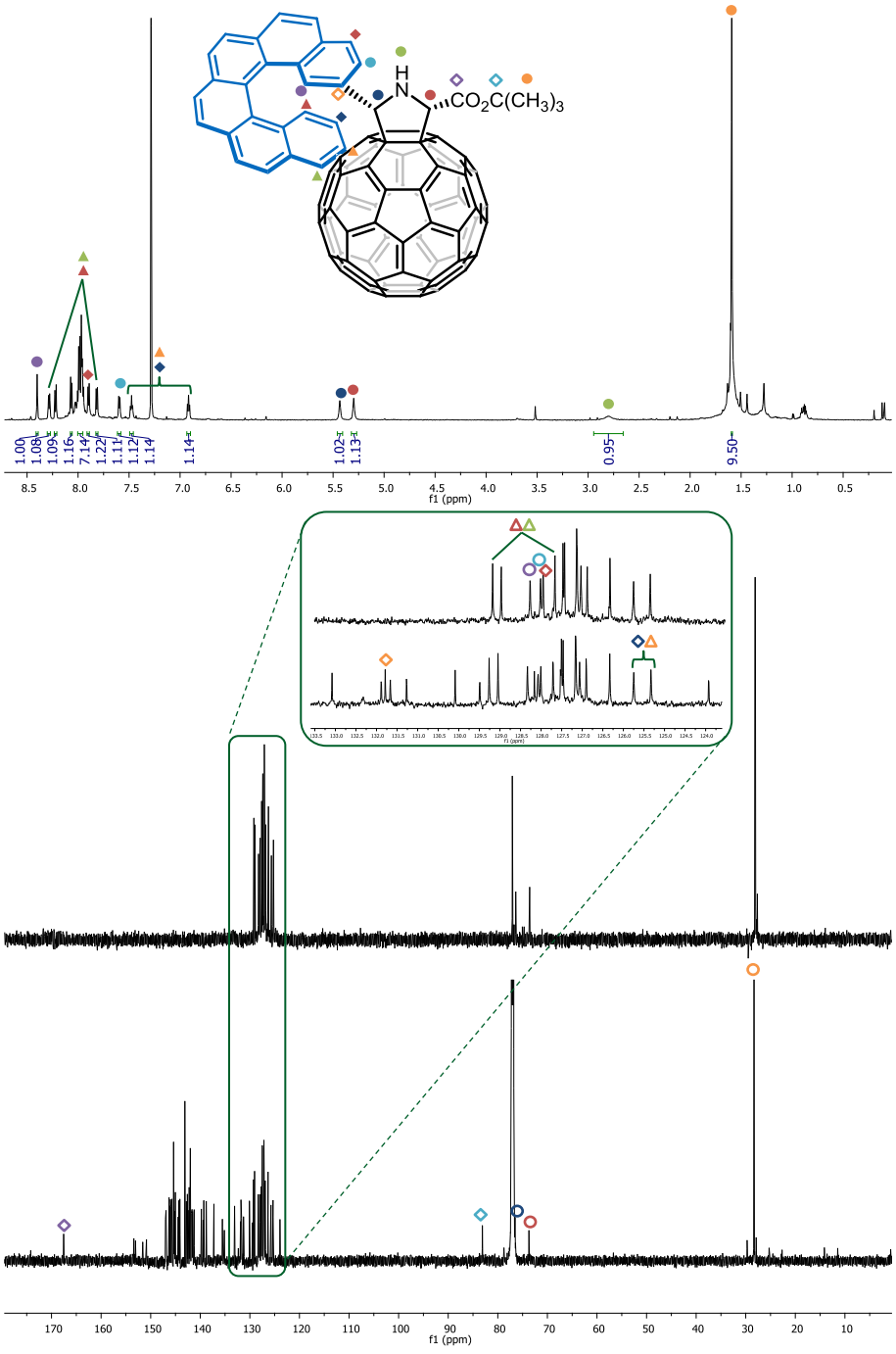

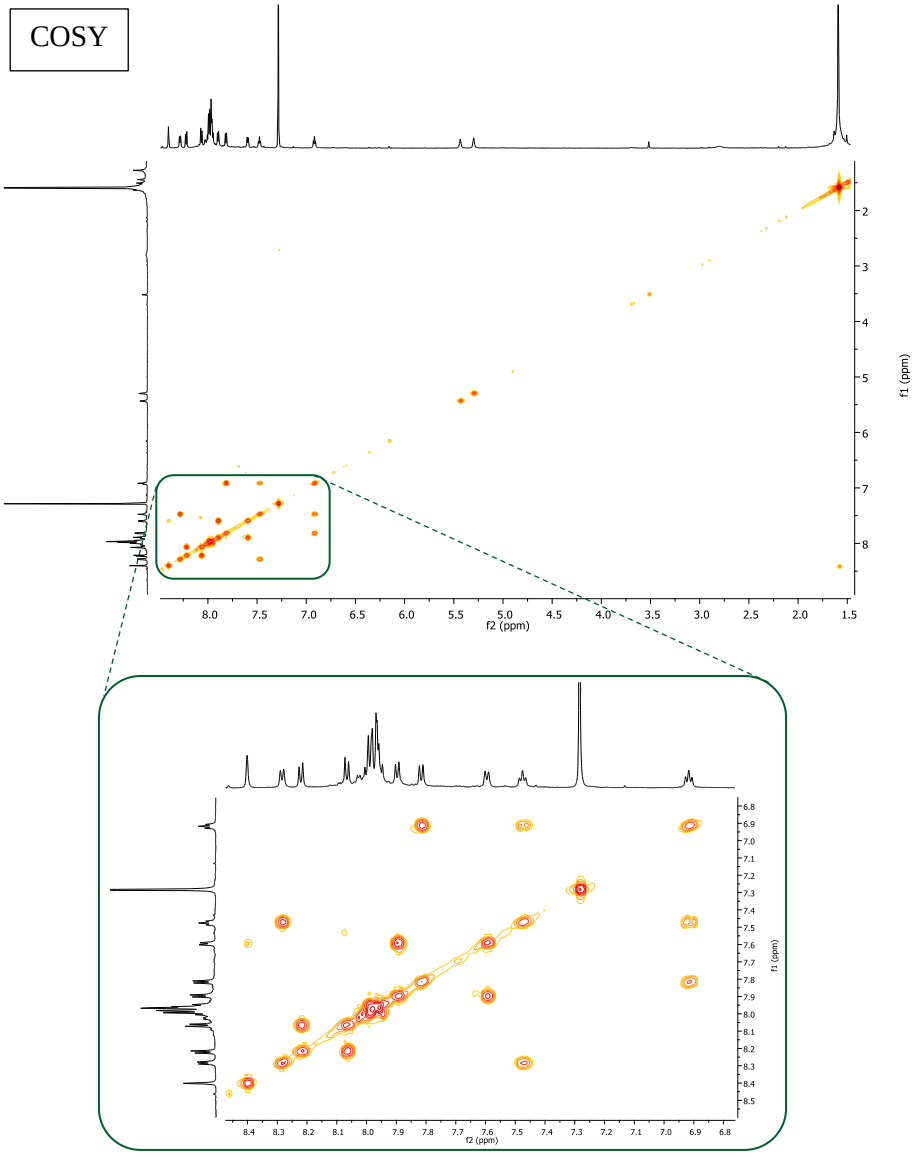
COSY
f2 (ppm)
f1 (ppm)

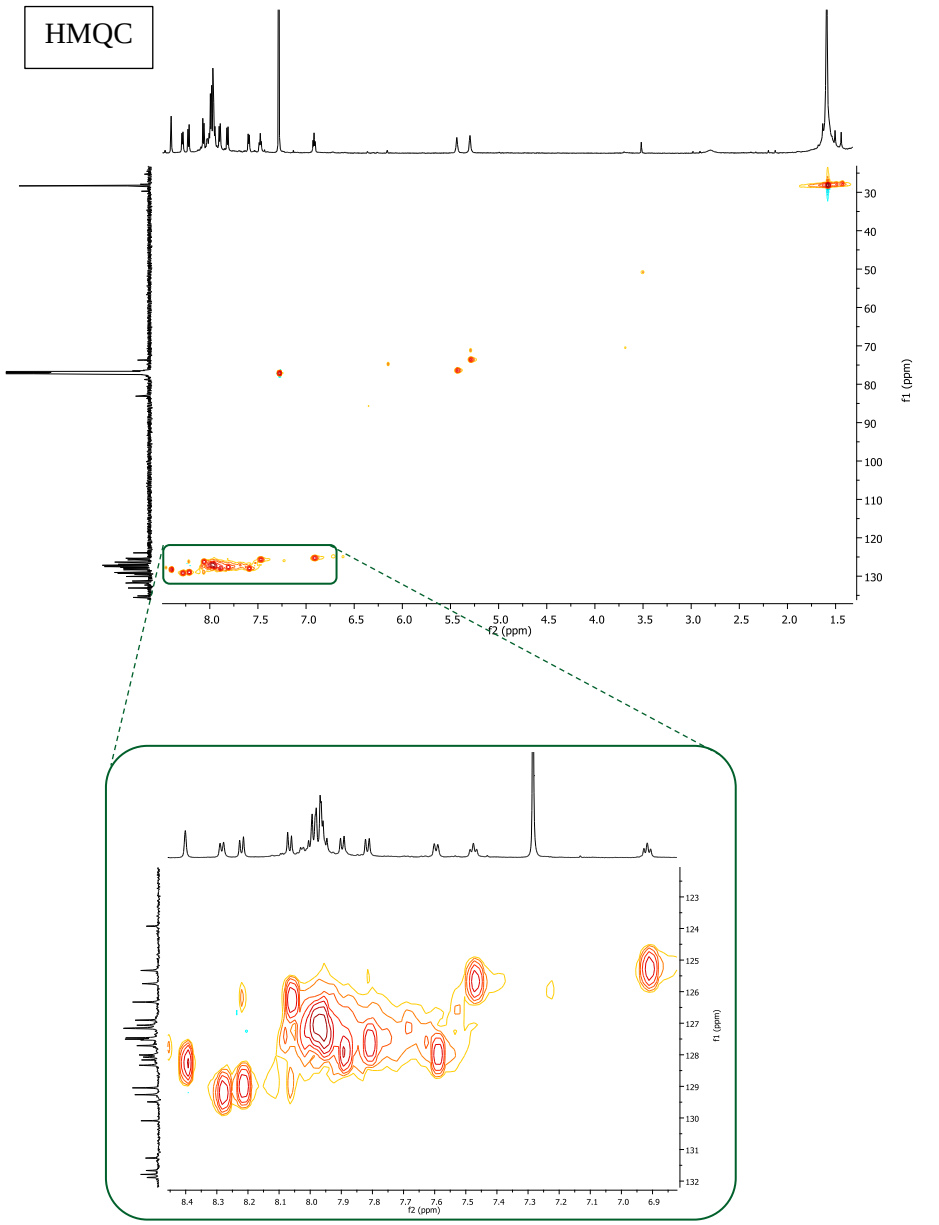
HMQC
f1 (ppm)
f2 (ppm)

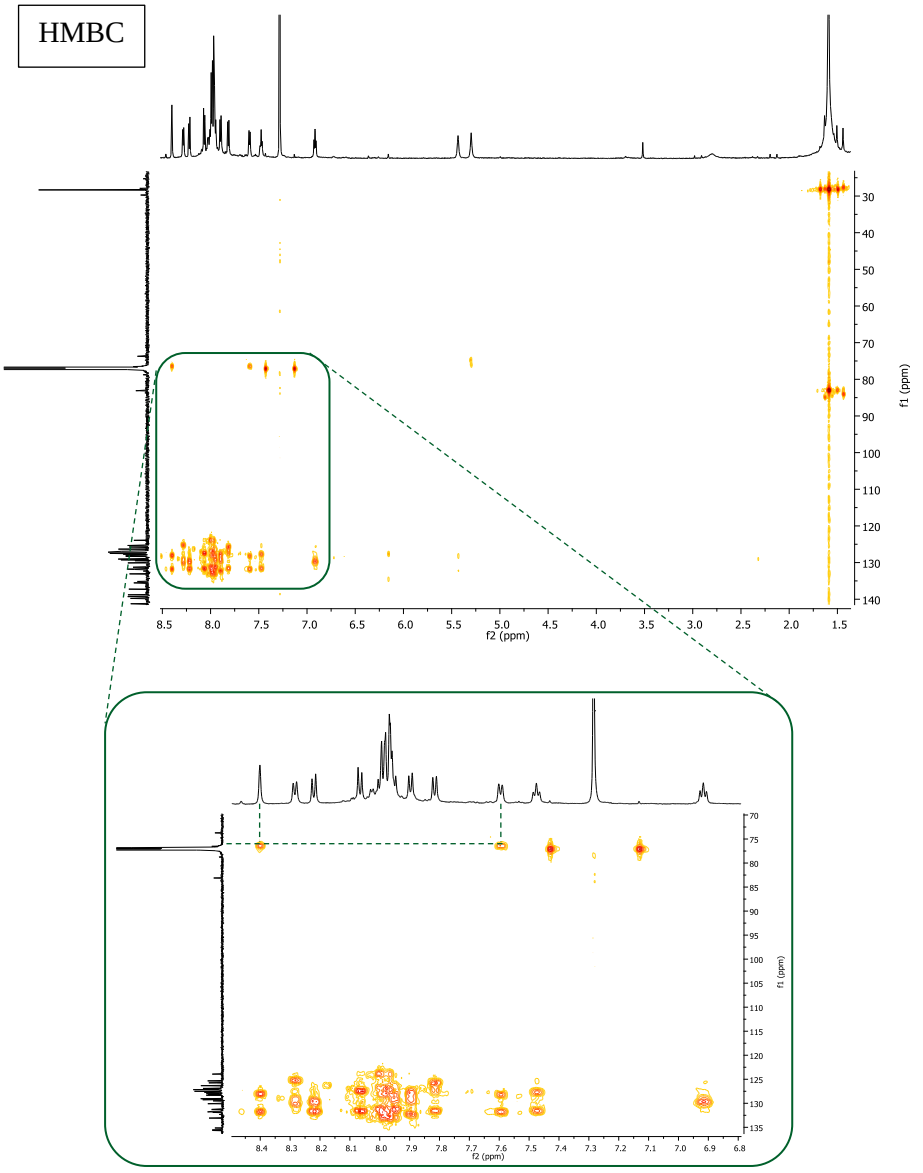
HMBC
f2 (ppm)
f1 (ppm)

tert-butyl (*E*)-2-((4-cyanobenzylidene)amino)acetate (**13a**)

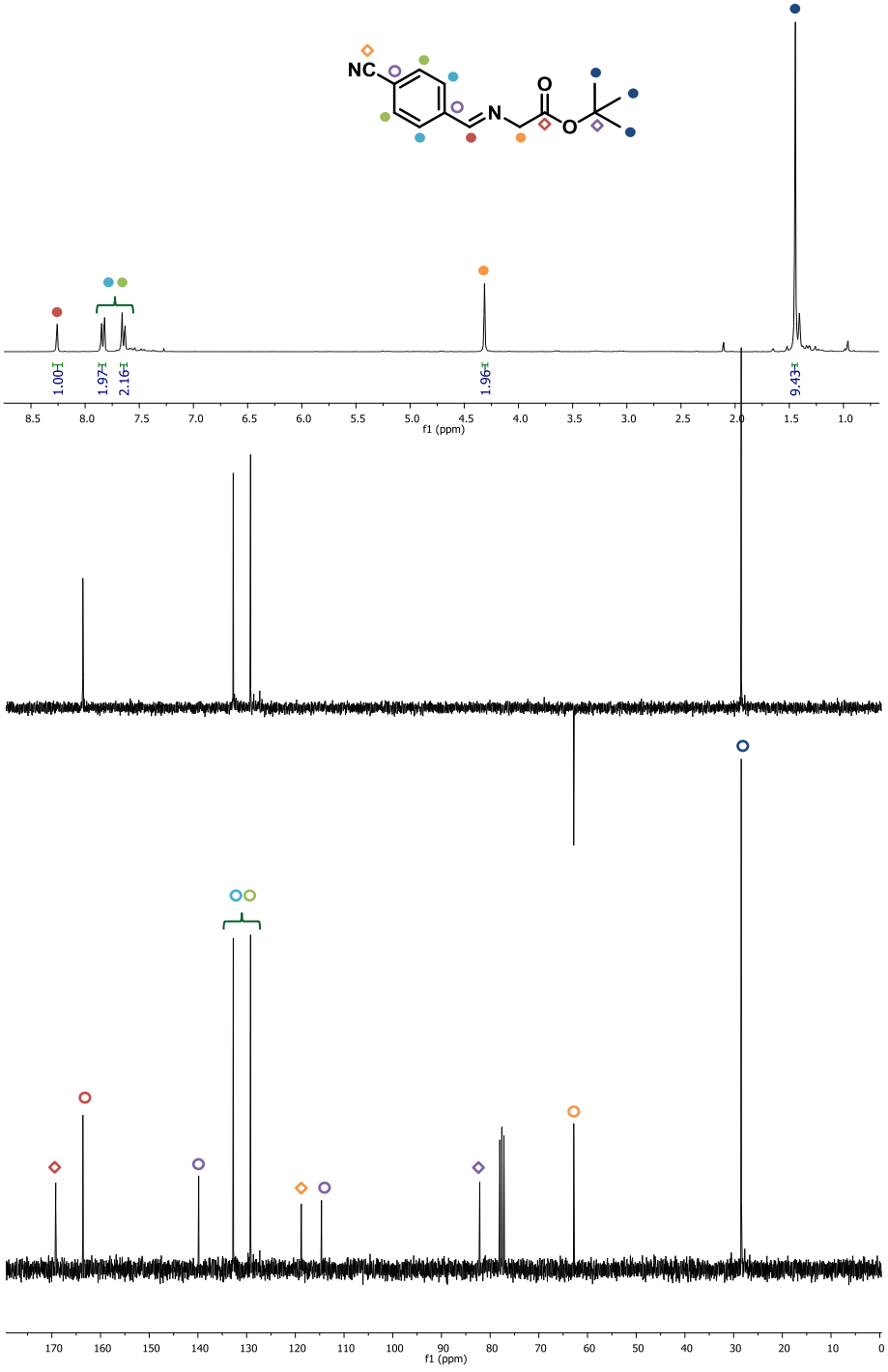

tert-butyl (E)-2-((4-nitrobenzylidene)amino)acetate (**13b**)

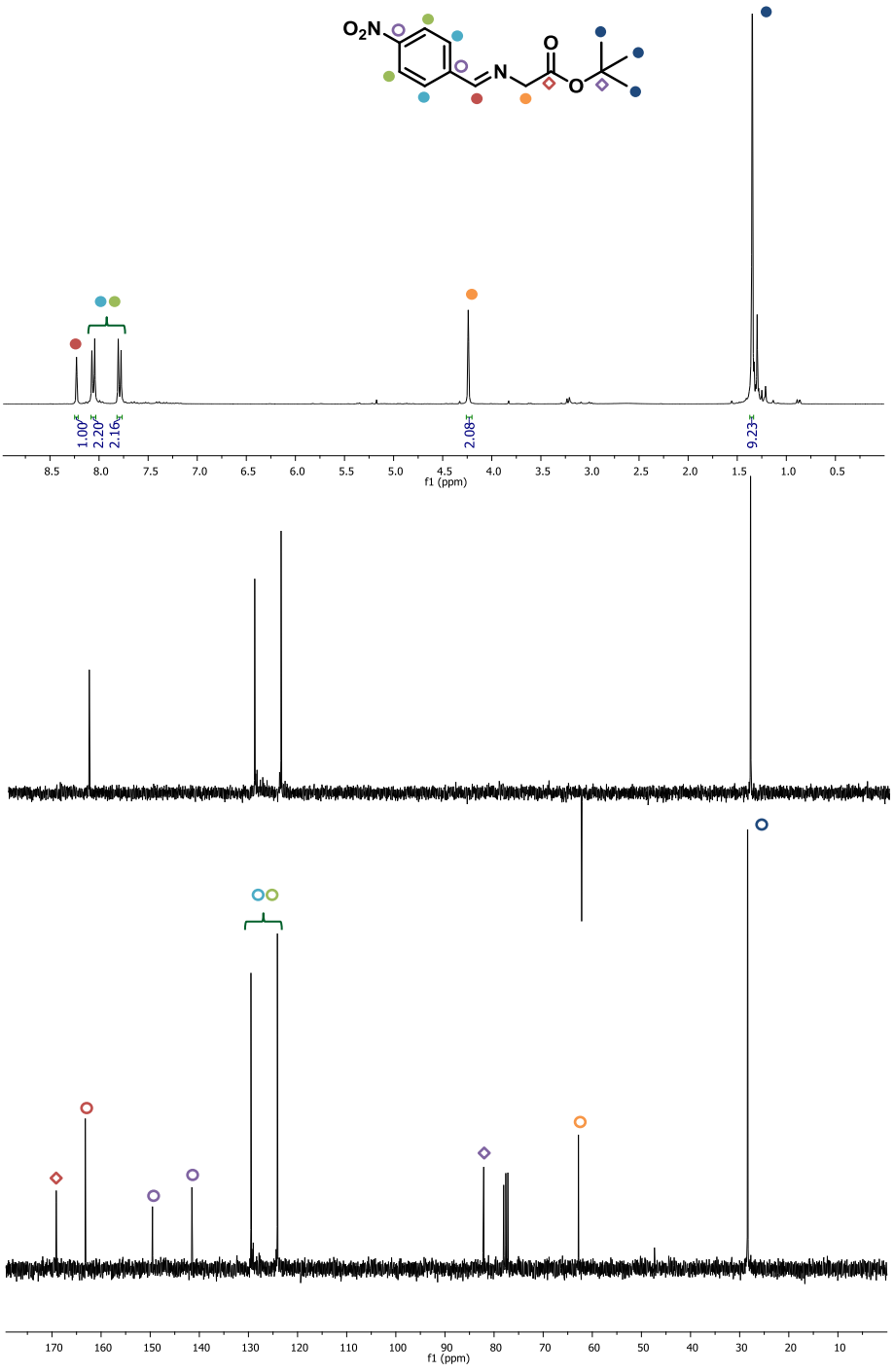

tert-butyl (*E*)-2-((2-(diphenylphosphaneyl)benzylidene)amino)acetate (**16**)

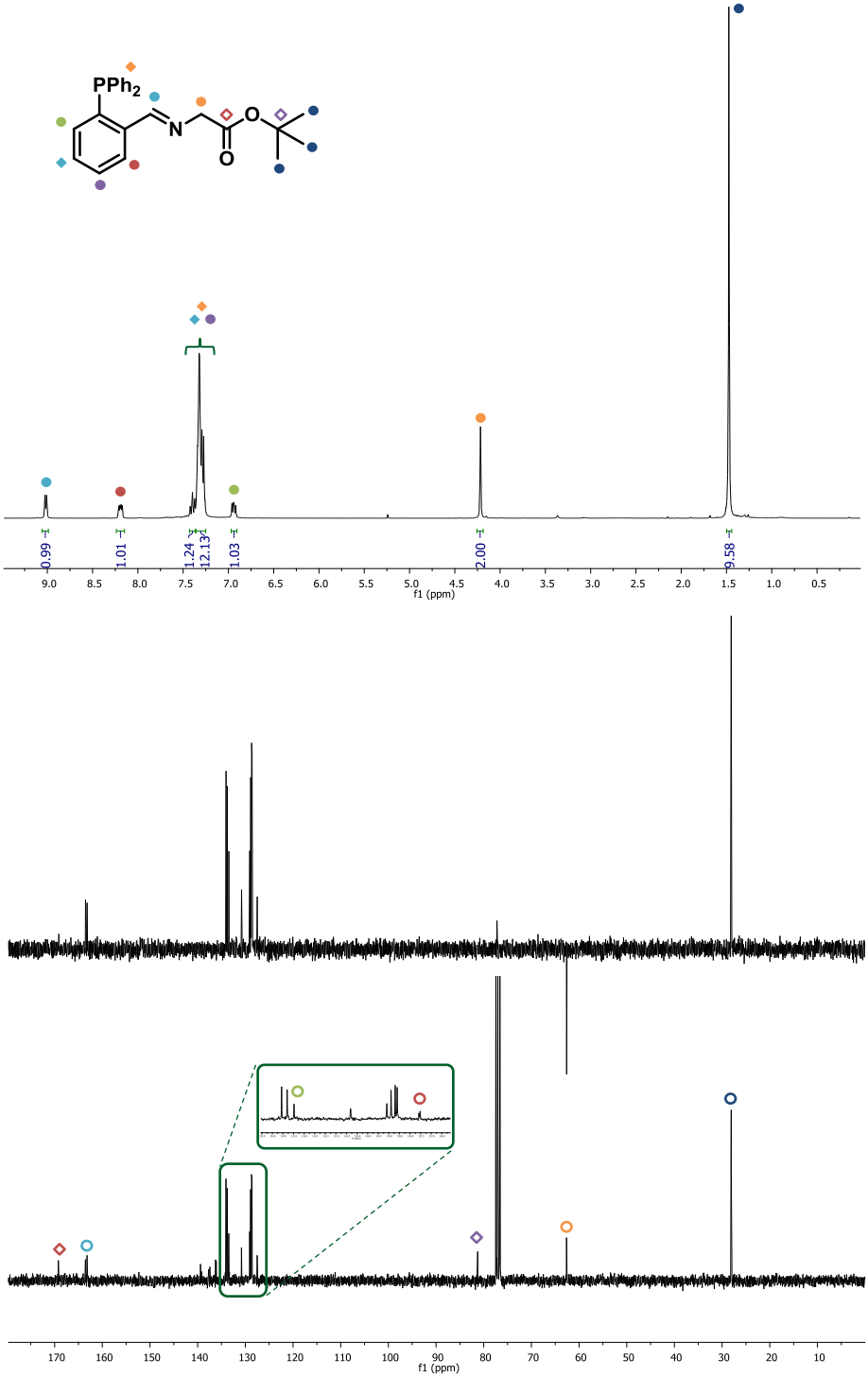

trans-2-*tert*-butoxycarbonyl-5-(2-diphenylphosphine)phenylpyrrolidino[3,4:1,2][60]fullerene (*trans*-**17**)

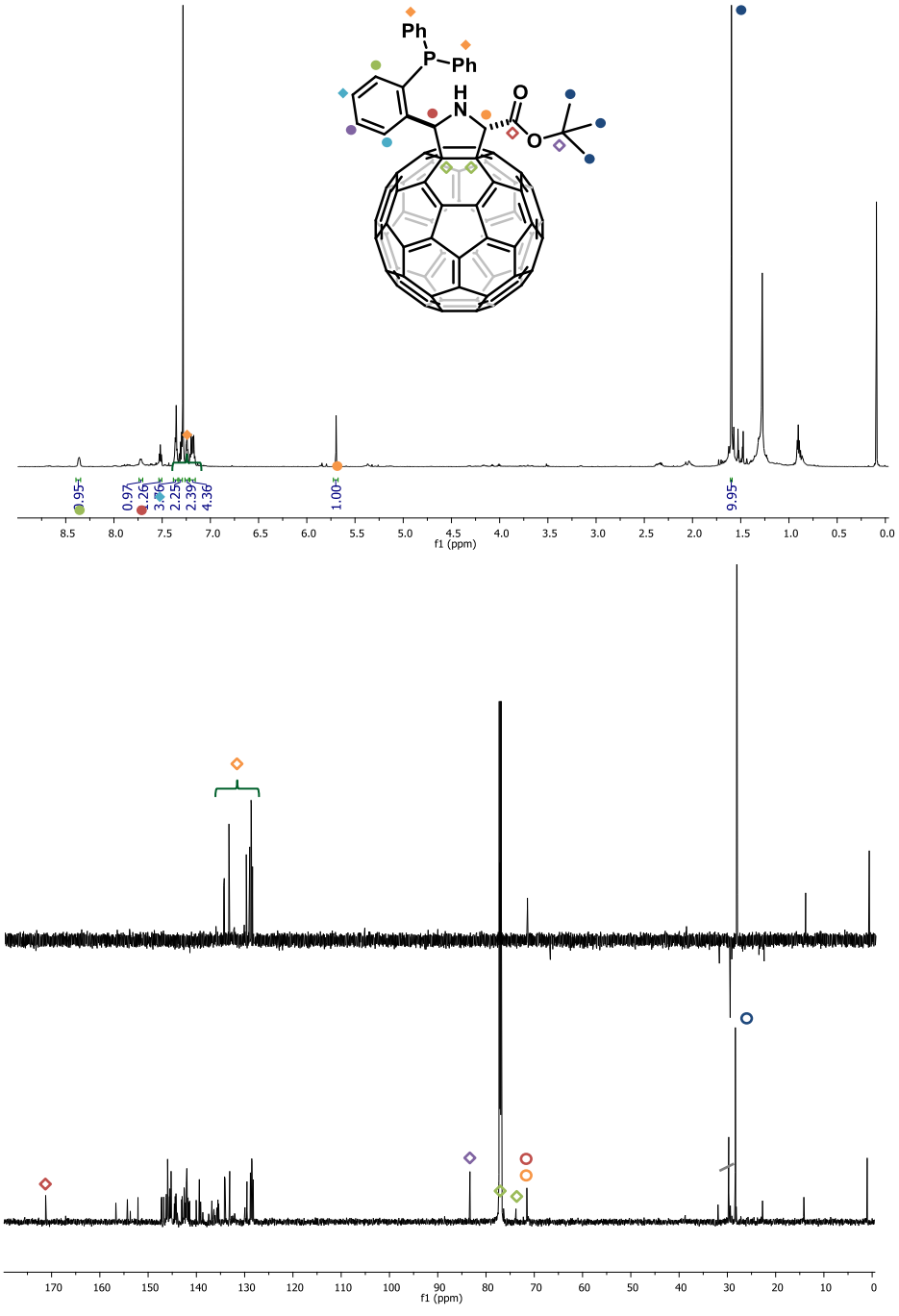

[Chloro(*trans*-2-*tert*-butoxycarbonyl-5-(2-diphenylphosphine)phenyl pyrrolidino[3,4:1,2][60]-fullerene) gold (I) (*trans*-**18**)

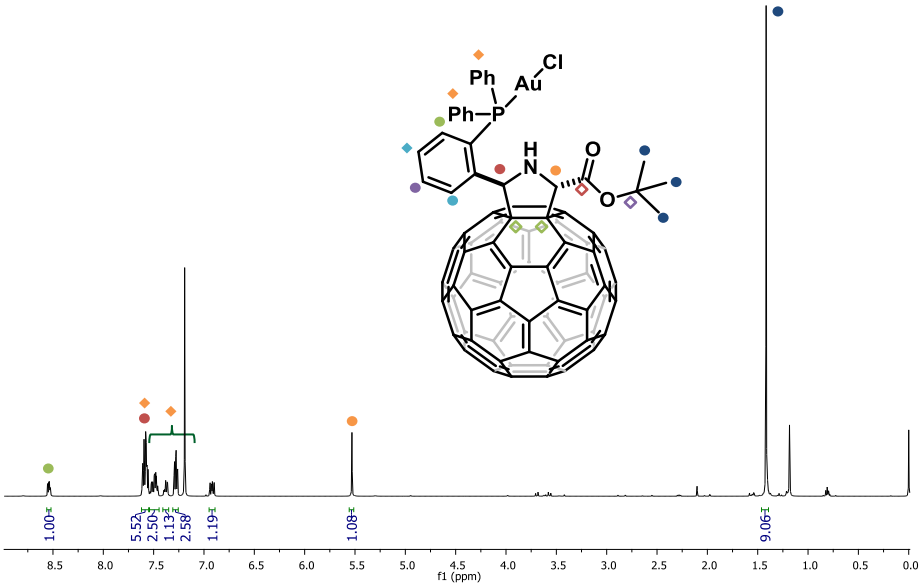

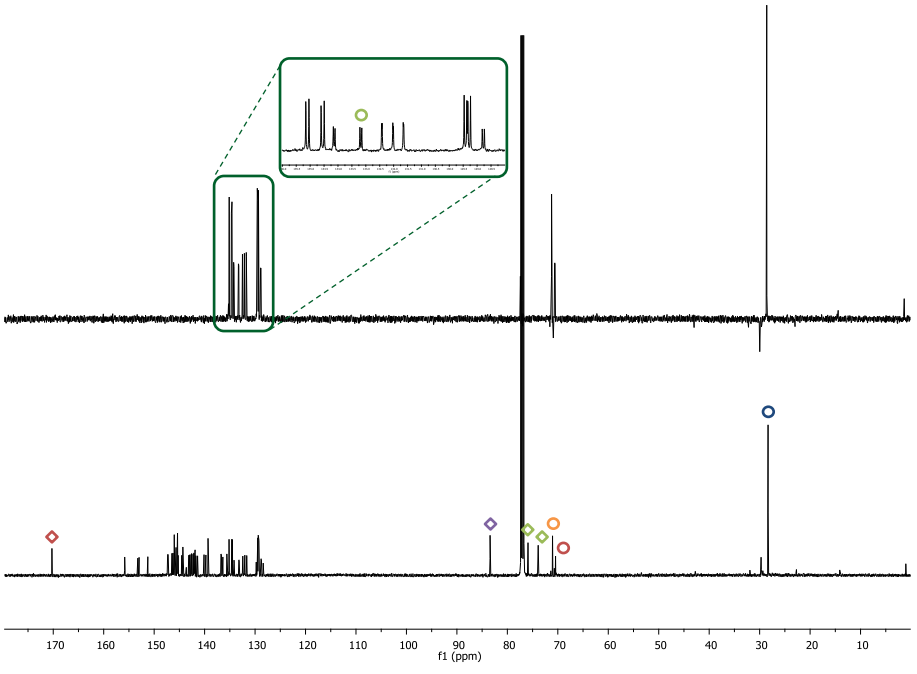

[Chloro (*cis*-2-*tert*-butoxycarbonyl-5-(2-diphenylphosphine)phenylpyrrolidino [3,4:1,2][60]- fullerene) gold (I) (*cis*-**18**).

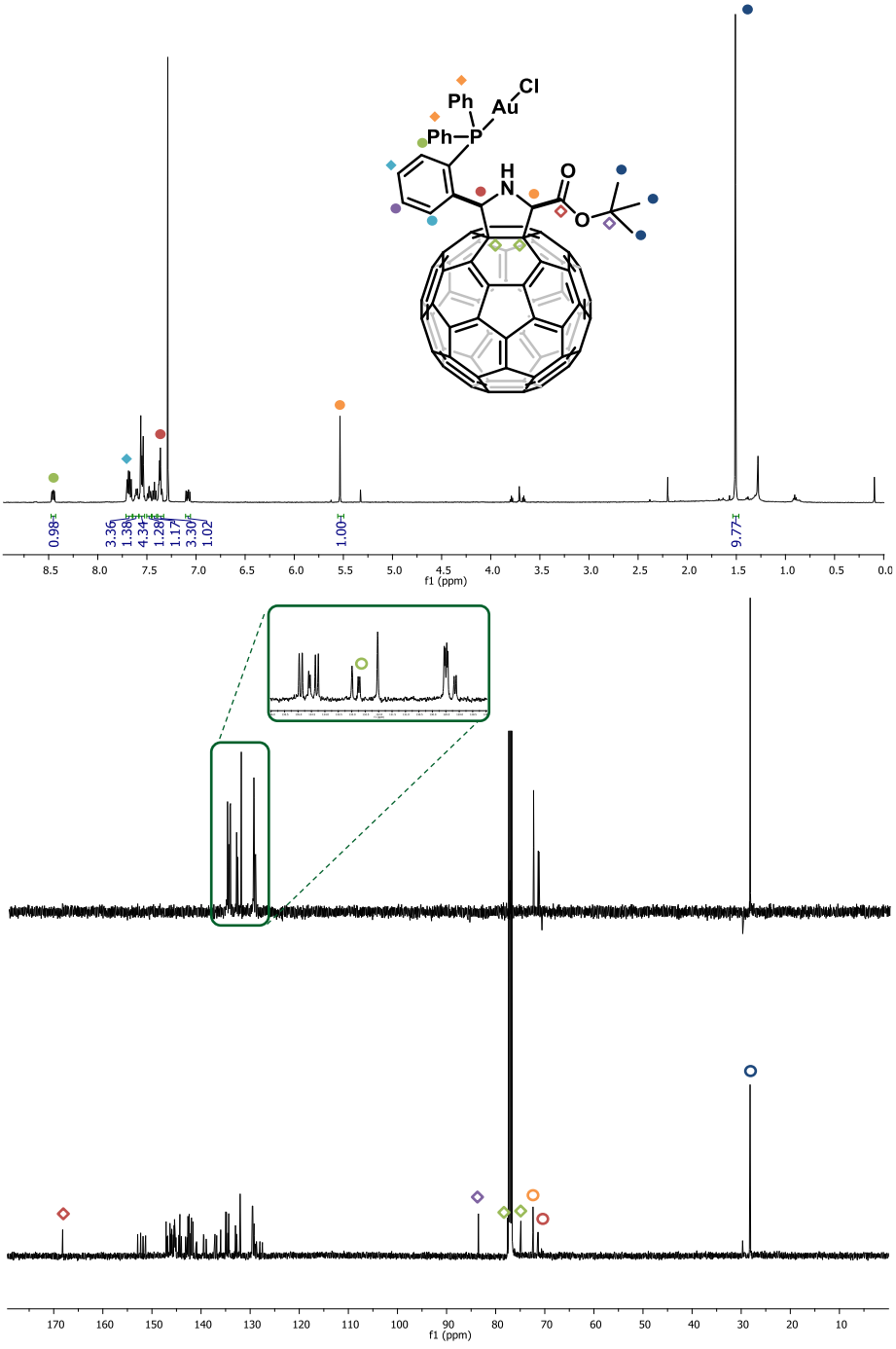

[Cp*Ir(2-phenyl-5-methyl-5-carboxylatepyrrolino[3,4:1,2][60]fullerene)Cl] (**20Ir**).

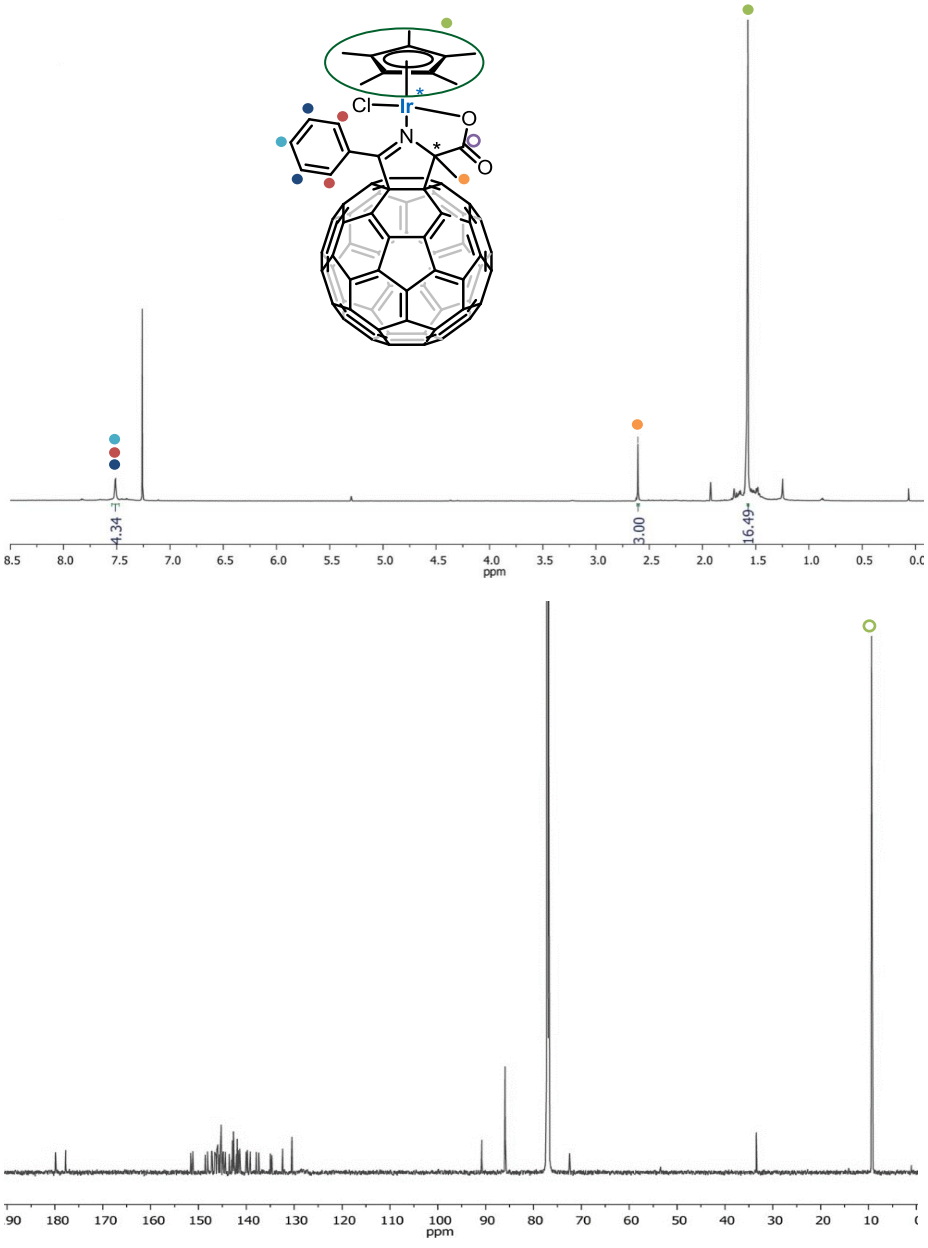

[Cp*Rh(2-phenyl-5-methyl-5-carboxylatepyrrolino[3,4:1,2][60]fullerene)Cl] (**20Rh**).

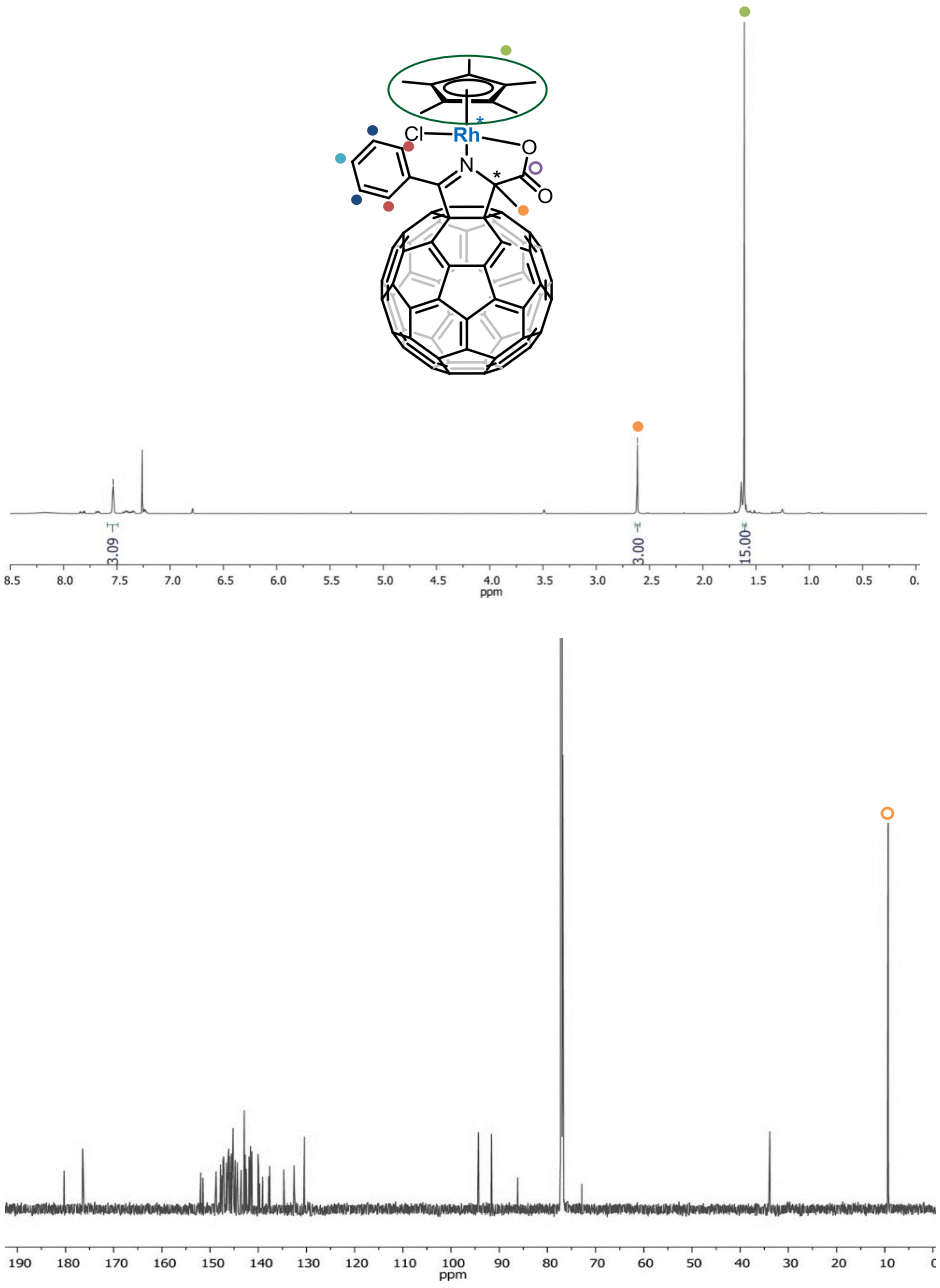

[μ-(1,2-η)[60]fullerene]bis(triphenylphosphane)platinum (**22**)

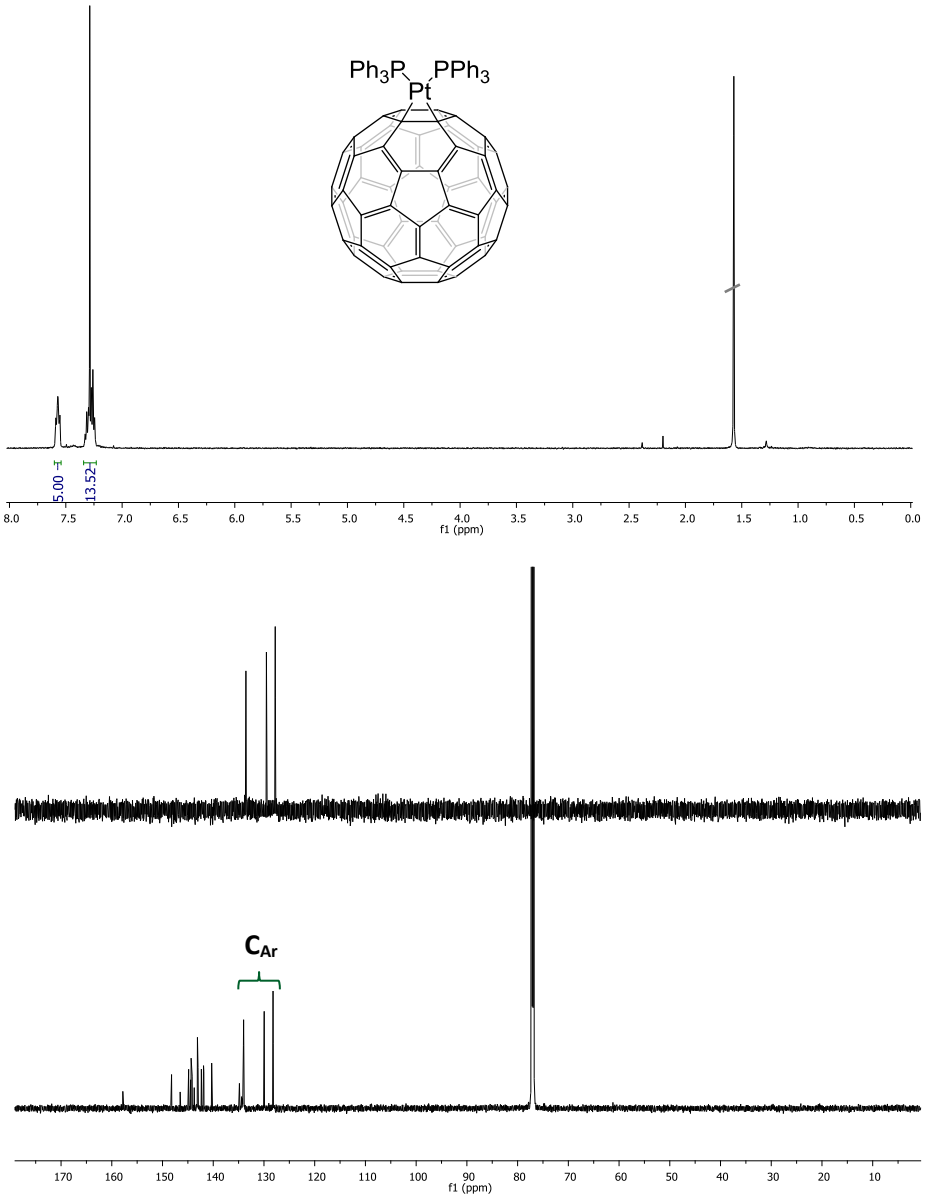

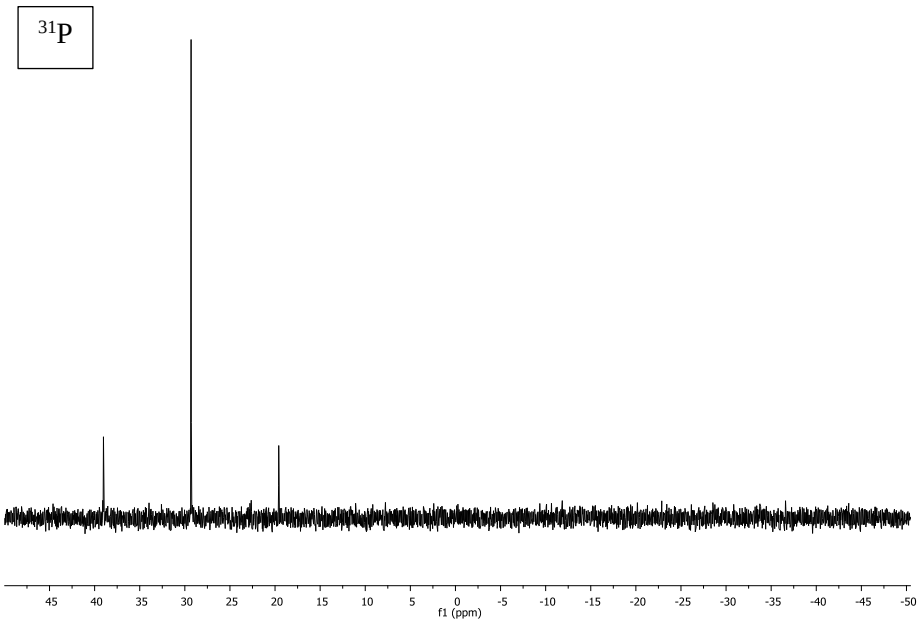
^{31}P
45
40
35
30
25
20
15
10
5
0
-5
-10
-15
-20
-25
-30
-35
-40
-45
-50
f1 (ppm)

1-ethoxycarbonyl-3-(1,1-dimethyl-2-oxacyclopentano[3,4:2,3])-1-cyclopenteno[4,5:1,2]-4H-[60]fullerene (**21a**)

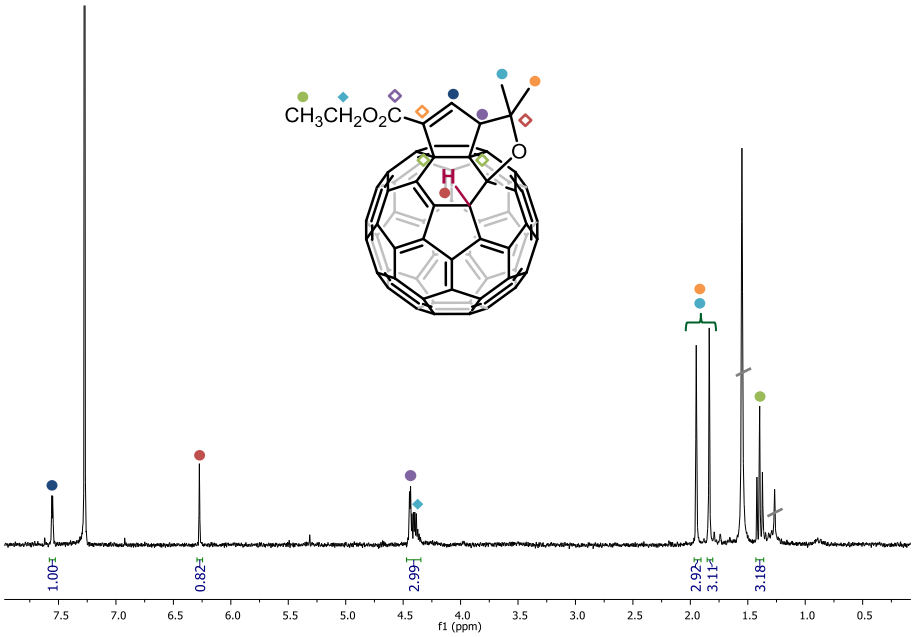

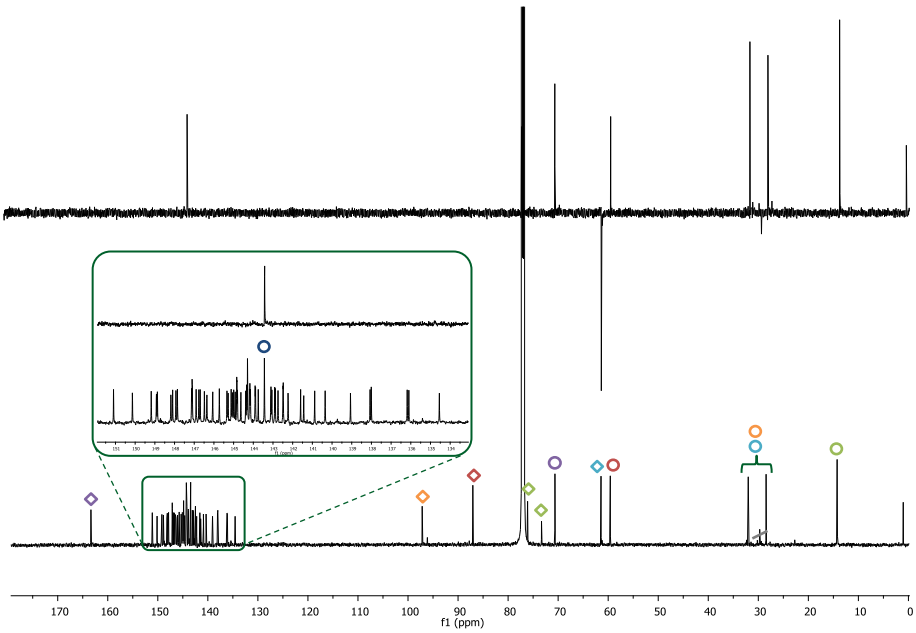

1-*tert*-butoxycarbonyl-3-(1,1-dimethyl-2-oxacyclopentano[3,4:2,3])-1-cyclopenteno[4,5:1,2]-4H-[60]fullerene (**21b**)

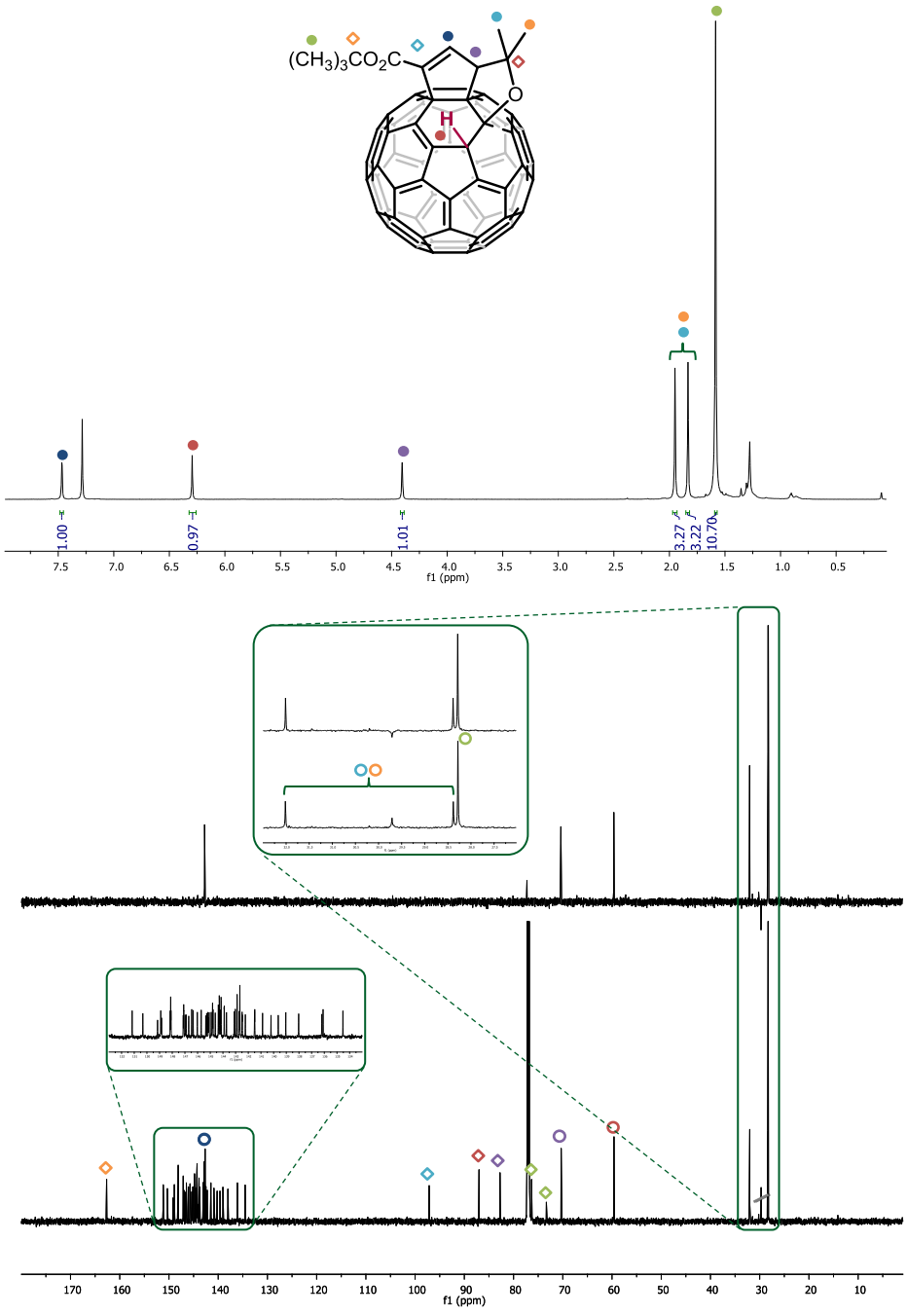

3-(1,1-dimethyl-2-oxacyclopentano[3,4:2,3])-1-cyclopenteno[4,5:1,2]-4H-[60]fullerene-1-carboxylic acid (**21c**)

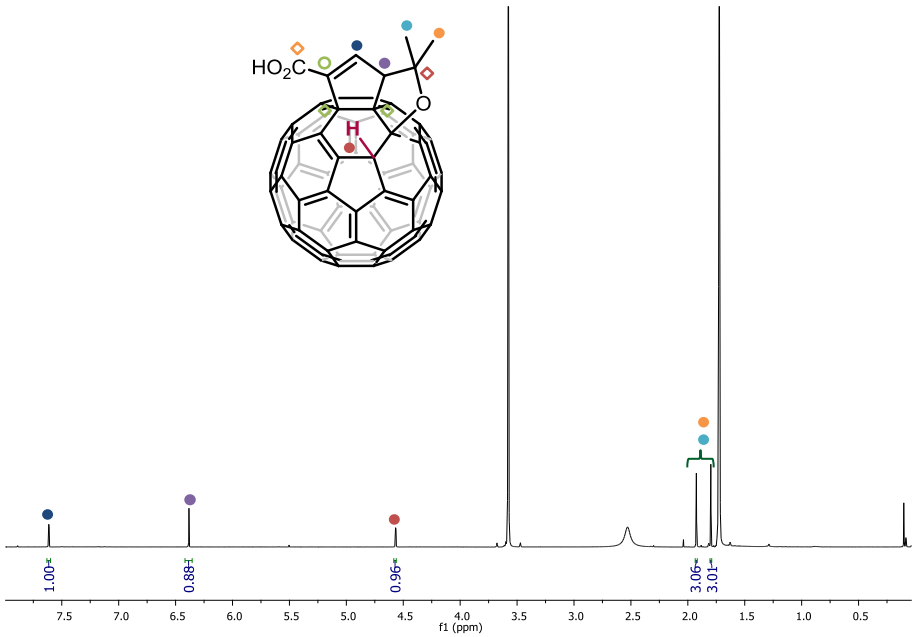

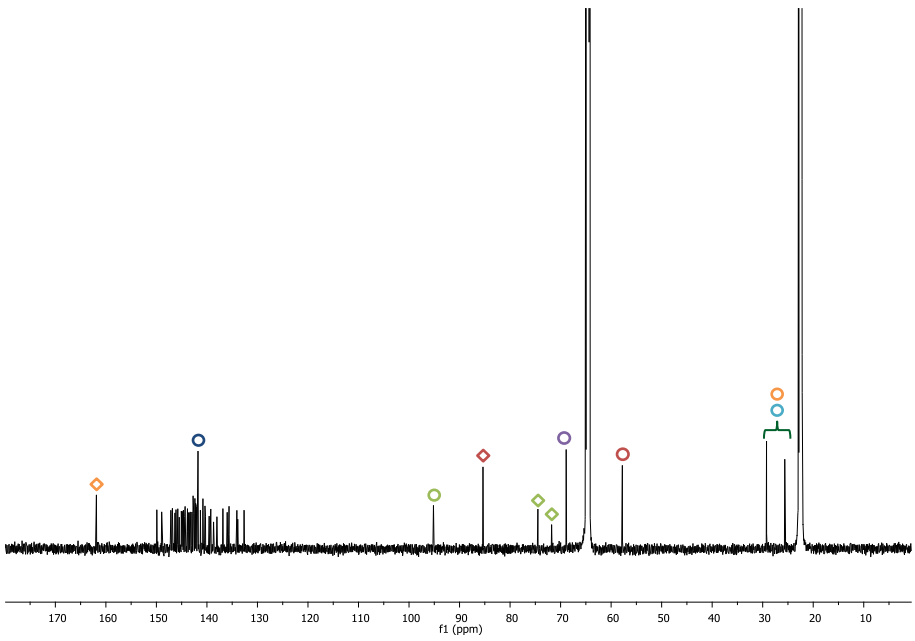

5.4. Photocurrent *vs.* time graphics

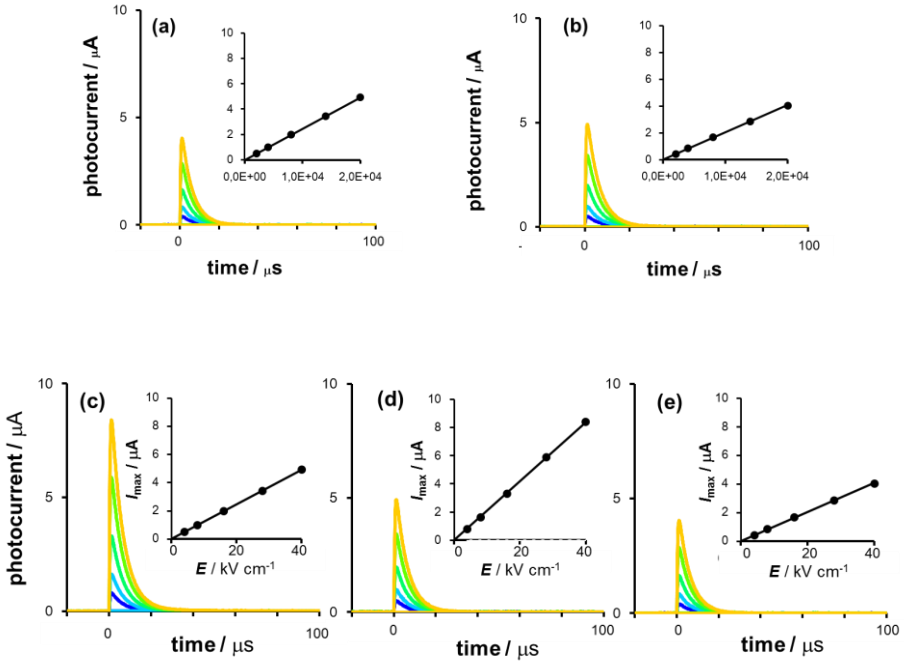

Figure 80. Current transients upon photoexcitation at 355 nm of (a) **8b**, (b) **8a**, (c) **8j**, (d) **8k**, and (e) PCBM on comb-type Au electrodes upon excitation at 355 nm with the power of 10 mW. The applied bias was increased from blue to orange. The insets show the maximum values of current as a function of the electric field strength.

CONCLUSIONS

6. CONCLUSIONS

Synthesis and electronic properties of fullerenes-fused unsaturated carbocycles

We have reported the synthesis of chiral cyclopent-1-enecarboxylate[60]fullerene by phosphine-catalyzed [3+2] cycloaddition. Thus, more accessible alkynoates as precursor of allenoates have been used. Furthermore, the reaction has been optimized with the use of chiral phosphine **P-XIV**, which presents an amine group in its structure, providing good yields and excellent *ee* with both, allenoates and alkynoates. This methodology has been extended to suitable substituted acrylate as dipole (Boc-protected Morita-Baylis-Hillman adduct) affording the different regioisomer 1-ethoxycarbonyl-2-phenylcyclopent-1-eno[3,4:1,2][60]fullerene, and to C_{70} as dipolarophile with high site-, regio-, and good sterereoselective results.

On the other hand, we have carried out the synthesis of new fullerene derivatives endowed with a less-explored fused cyclobutene ring by using allenoates or their *in situ* precursor alkynoates and a simple organic base under mild conditions. Furthermore, a plausible mechanism for the formation of the cyclobuteno[3,4:1,2][60]fullerenes has been provided. The chemical structure of the new cycloadducts has been thoroughly established by spectroscopic techniques, and unambiguously confirmed by X-ray diffraction analysis.

FP-TRMC measurements revealed that the new family of cyclobuteno[60]fullerenes exhibits higher electron mobility than PCBM, thus, confirming their interest as appealing n-type organic semiconductors. Furthemore, we have confirmed the relevance of chirality in an important electronic property of fullerenes such as charge carrier mobility, which proves the importance of asymmetric synthesis for the preparation of chiral carbon nanostructures.

Reversible stereodivergent cycloaddition of a helicene derivative onto [60]fullerene: a chiral resolution strategy

We report for the first time the use of the less-explored “reversible” covalent chemistry of [60]fullerene as a useful alternative to carry out the resolution of racemic species. In the representative studied example, the resolution of the racemate of a pyrrolidino[3,4:1,2][60]fullerene endowed with helicenes is

described. It involves the reversible stereodivergent 1,3-dipolar cycloaddition reaction of racemic helicene-iminoeters onto [60]fullerene employing only catalytic amounts of chiral agents, which affords two diastereomeric helicene-pyrrolidino[3,4:1,2][60]fullerenes in excellent enantiomeric excesses. Subsequent conventional silica-gel chromatography diastereoisomers separation and metal-catalyzed retro-cycloaddition reaction yields the starting 1,3-dipoles whose hydrolyses lead to the starting 2-formylhelicene enantiomers in good yields and excellent optical purity. This protocol represents a general and efficient method which validates fullerenes for racemates resolution and, in particular, for their efficiency in the resolution of these singular helicene systems.

Metallofullerene hybrids

New chiral fullerenes derivatives endowed with metal centers have been prepared. Along with new stereogenic at iridium complexes, we have achieved the first stereoselective synthesis of gold(I)-fullerene hybrids.

Furthermore, we have been able to control the diastereoselectivity of this compound carrying out the reaction in "one pot" process and, thus, achieving *trans*- and *cis*-gold(I)-pyrrolidino[60]fullerene with a complete diastereoselectivity.

Fullerenes derivatives for photoelectrocatalytic devices

We have reported the highly stereoselective catalytic synthesis of two series of fullerene-based molecular catalysts for ORR. Iridium and rhodium pyrrolino[60]fullerene complexes were prepared with a complete diastereoselectivity (d.e. >99%) and the structure of the iridium-fullerene complex was confirmed by X-ray analysis. On the other hand, metal-free fullerene catalysts, endowed with a highly active C-H bond, have been obtained by a regioselective *cis*-1 addition to the C_{60} cage.

The electrocatalytic activity on the oxygen reduction reactions has been tested in bulk heterojunction photo-electrochemical cells, affording current values up to ten fold higher than widely used PCBM, which confirms an enhanced photocatalytic property of the novel compounds. Remarkably, metal-free fullerene derivatives proved to give photocurrents comparable to related hybrids, thanks to the highly active C-H bond on the fullerene cage.

REFERENCES

7. REFERENCES

1. a) Levi, P. *The Periodic Table*, Ed. Schocken Books, New York, 1995, b) Carey, F. A. *Organic Chemistry,* Ed. McGraw-Hill Companies, New York, 1996.

2. Kroto, H. W.; Heath, J. R.; O'Brien, S. C.; Curl, R. F.; Smalley, R. E. C_{60}: Buckminsterfullerene. *Nature* **1985**, *318*, 162-163.

3. Kraetschmer, W.; Lamb, L. D.; Fostiropoulos, K.; Huffman, D. R. Solid C_{60}: A New Form of Carbon. *Nature* **1990**, *347*, 354-358.

4. a) Iijima, S. Helical Microtubules of Graphitic Carbon. *Nature* **1991**, *354*, 56-58, b) Iijima, S.; Ichihashi, T. Single-shell Carbon Nanotubes of 1nm Diameter. *Nature* **1993**, *363*, 603-605, c) Bethune, D. S.; Kiang, C. H.; de Vries, M. S.; Gorman, G.; Savoy, R.; Vázquez, J.; Beyers, R. Cobalt-catalyzed Growth of Carbon Nanotubes with Single-atomic-layer Walls. *Nature* **1993**, *363*, 605-607.

5. a) Novoselov, K. S.; Geim, A. K.; Morozov, S. V.; Jiang, D.; Zhang, Y.; Dubonos, S. V.; Grigorieva, I. V.; Firsov, A. A. Electric Field Effect in Atomically Thin Carbon Films. *Science* **2004**, *306*, 666-669, b) Geim, A. K.; Novoselov, K. S. The Rise of Graphene. *Nat. Mater.* **2007**, *6*, 183-191.

6. a) Akasaka, T.; Nagase, S. *Endofullerenes: A New Family of Carbon Clusters,* Ed. Kluver Academic Publishers, Dordrecht (The Netherlands), 2002, b) Dunsch, L.; Yang, S. Metal Nitride Cluster Fullerenes: Their Current State and Future Prospects. *Small* **2007**, *3*, 1298-1320, c) Chaur, M.; Melin, F.; Ortiz, A.; Echegoyen, L. Chemical, Electrochemical, and Structural Properties of Endohedral Metallofullerenes. *Angew. Chem. Int. Ed.* **2009**, *48*, 7514-7538.

7. Iijima, S.; Yudasaka, M.; Yamada, R.; Bandow, S.; Suenaga, K.; Kokai, F.; Takahashi, K. Nano-aggregates of Single-walled Graphitic Carbon Nano-horns. *Chem. Phys. Lett.* **1999**, *309*, 165-170.

8. Ugarte, D. Curling and Closure of Graphitic Networks under Electron-beam Irradiation. *Nature* **1992**, *359*, 707-709.

9. a) Delgado, J. L.; Herranz, M. Á; Martín, N. The Nano-forms of Carbon. *J. Mater. Chem.* **2008**, *18*, 1417-1426, b) Pinzón, R.; Villalta-Cerdas, A.;

Echegoyen, L. *Unimolecular and Supramolecular Electronics I: Chemistry and Physics Meet at Metal-Molecule Interfaces*, Ed. Springer Berlin Heidelberg, Berlín, 2012, c) Choudhary, N.; Hwang, S.; Choi, W. *Handbook of Nanomaterials Properties*, Ed. Springer Berlin Heidelberg, Berlín, 2014, d) Marcaccio, M.; Paolucci, F. *Making and Exploiting Fullerenes, Graphene, and Carbon Nanotubes*, Topics in current chemistry, Ed. Springer, Berlin, 2014, e) Martín, N. Carbon Nanoforms for Photovoltaics: Myth or Reality? *Adv. Energy Mater.* **2017**, *7*, 1601102.

10. a) Schmalz, T. G.; Seitz, W. A.; Klein, D. J.; Hite, G. E. Sixty-carbon-atom Carbon Cages. *Chem. Phys. Lett.* **1986**, *130*, 203-207, b) Kroto, H. W. The Stability of the Fullerenes C_n, with n = 24, 28, 32, 36, 50, 60 and 70. *Nature* **1987**, *329*, 529-531.

11. Taylor, R.; Hare, J. P.; Abdul-Sada, A.; Kroto, H. W. Isolation, separation and characterisation of the fullerenes C_{60} and C_{70}: the third form of carbon. *J. Chem. Soc., Chem. Commun.* **1990**, 1423-1425.

12. a) Echegoyen, L.; Echegoyen, L. E. Electrochemistry of Fullerenes and Their Derivatives. *Acc. Chem. Res.* **1998**, *31*, 593-601, b) Guldi, D. M. Fullerenes: Three Dimensional Electron Acceptor Materials. *Chem. Commun.* **2000**, 321-327.

13. Xie, Q.; Perez-Cordero, E.; Echegoyen, L. Electrochemical Detection of C_{60}^{6-} and C_{70}^{6-}: Enhanced Stability of Fullerides in Solution. *J. Am. Chem. Soc.* **1992**, *114*, 3978-3980.

14. Martín, N.; Sánchez, L.; Illescas, B.; Pérez, I. C_{60}-Based Electroactive Organofullerenes. *Chem. Rev.* **1998**, *98*, 2527-2547.

15. Delgado, J. L.; Bouit, P.; Filippone, S.; Herranz, M. A.; Martín, N. Organic Photovoltaics: A Chemical Approach. *Chem. Commun.* **2010**, *46*, 4853-4865.

16. a) Hare, J. P.; Kroto, H. W.; Taylor, R. Preparation and UV / visible spectra of fullerenes C_{60} and C_{70}. *Chem. Phys. Lett.* **1991**, *177*, 394-398, b) Harigaya, K.; Abe, S. Optical Absorption Spectra and Geometric Effects in Higher Fullerenes. *J. Phys.: Condens. Matter.* **1996**, *8*, 8057-8066.

17. a) Kronholm, D.; Hummelen, J. C. Organic Electronics. *Material Matters* **2007**, *2*, 16, b) Anthony, J. E.; Facchetti, A.; Heeney, M.; Marder, S. R.; Zhan, X. n-Type Organic Semiconductors in Organic Electronics. *Adv. Mater.* **2010**, *22*, 3876-3892.

18. a) Hummelen, J. C.; Knight, B. W.; LePeq, F.; Wudl, F.; Yao, J.; Wilkins, C. L. Preparation and Characterization of Fulleroid and Methanofullerene Derivatives. *J. Org. Chem.* **1995**, *60*, 532-538, b) Yu, G.; Gao, J.; Hummelen, J. C.; Wudl, F.; Heeger, A. J. Polymer Photovoltaic Cells: Enhanced Efficiencies via a Network of Internal Donor-acceptor Heterojunctions. *Science* **1995**, *270*, 1789-1791.

19. Leary, E.; Gonzalez, M. T.; van der Pol, C.; Bryce, M. R.; Filippone, S.; Martín, N.; Rubio-Bollinger, G.; Agrait, N. Unambiguous One-Molecule Conductance Measurements under Ambient Conditions. *Nano Lett.* **2011**, *11*, 2236-2241.

20. Wang, Y.; Xu, J.; Wang, Y.; Chen, H. Emerging Chirality in Nanoscience. *Chem. Soc. Rev.* **2013**, *42*, 2930-2962.

21. Kitaev, V. Chiral Nanoscale Building Blocks-from Understanding to Applications. *J. Mater. Chem.* **2008**, *18*, 4745-4749.

22. Henson, Z. B.; Müllen, K.; Bazan, G. C. Design Strategies for Organic Semiconductors Beyond the Molecular Formula. *Nat. Chem.* **2012**, *4*, 699-704.

23. a) Taylor, R.; Walton, D. R. The Chemistry of Fullerenes. *Nature* **1993**, *363*, 685-693, b) Hirsch, A.; Brettreich, M. *Fullerenes: Chemistry and Reactions,* Ed. Wiley-VCH, Weinheim (Germany), 2005.

24. Maroto, E. E.; Izquierdo, M.; Reboredo, S.; Marco-Martínez, J.; Filippone, S.; Martín, N. Chiral Fullerenes from Asymmetric Catalysis. *Acc. Chem. Res.* **2014**, *47*, 2660-2670.

25. a) Maggini, M.; Scorrano, G.; Prato, M. Addition of Azomethine Ylides to C_{60}: Synthesis, Characterization, and Functionalization of Fullerene Pyrrolidines. *J. Am. Chem. Soc.* **1993**, *115*, 9798-9799, b) Prato, M.; Maggini, M. Fulleropyrrolidines: A Family of Full-Fledged Fullerene Derivatives. *Acc. Chem. Res.* **1998**, *31*, 519-526, c) Tagmatarchis, N.;

Prato, M. The Addition of Azomethine Ylides to [60]Fullerene Leading to Fulleropyrrolidines. *Synlett* **2003**, 768-779.

26. a) Martín, N.; Altable, M.; Filippone, S.; Martín- Domenech, A.; Echegoyen, L.; Cardona, C. M. Retro- Cycloaddition Reaction of Pyrrolidinofullerenes. *Angew. Chem. Int. Ed.* **2006**, *45*, 110-114, b) Lukoyanova, O.; Cardona, C. M.; Altable, M.; Filippone, S.; Martín-Domenech, Á; Martín, N.; Echegoyen, L. Selective Electrochemical Retro- Cycloaddition Reaction of Pyrrolidinofullerenes. *Angew. Chem. Int. Ed.* **2006**, *45*, 7430-7433, c) Filippone, S.; Izquierdo, M.; Martín-Domenech, A.; Osuna, S.; Solà, M.; Martín, N. On the Mechanism of the Thermal Retrocycloaddition of Pyrrolidinofullerenes (Retro-Prato Reaction). *Chem. Eur. J.* **2008**, *14*, 5198-5206.

27. Brunetti, F. G.; Herrero, M. A.; Muñoz, J. M.; Giordani, S.; Díaz-Ortiz, A.; Filippone, S.; Ruaro, G.; Meneghetti, M.; Prato, M.; Vázquez, E. Reversible Microwave-assisted Cycloaddition of Aziridines to Carbon Nanotubes. *J. Am. Chem. Soc.* **2007**, *129*, 14580-14581.

28. Guryanov, I.; Montellano Lopez, A.; Carraro, M.; Da Ros, T.; Scorrano, G.; Maggini, M.; Prato, M.; Bonchio, M. Metal-free, Retro-cycloaddition of Fulleropyrrolidines in Ionic Liquids under Microwave Irradiation. *Chem. Commun.* **2009**, 3940-3942.

29. Martín, N.; Segura, J. L.; Wudl, F. In *New Concepts in Diels-Alder Cycloadditions to Fullerenes;* Guldi, D. M., Martin, N., Eds.; Fullerenes: From Synthesis to Optoelectronic Properties; Springer: Dordrecht (Netherlands), 2002; pp 81-120.

30. Segura, J. L.; Martín, N. o-Quinodimethanes: Efficient Intermediates in Organic Synthesis. *Chem. Rev.* **1999**, *99*, 3199-3246.

31. Chikama, A.; Fueno, H.; Fujimoto, H. Theoretical Study of the Diels-Alder Reaction of C_{60}. Transition-state Structures and Reactivities of C-C Bonds. *J. Phys. Chem.* **1995**, *99*, 8541-8549.

32. a) Hoke II, S. H.; Molstad, J.; Dilettato, D.; Jay, M. J.; Carlson, D.; Kahr, B.; Cooks, R. G. Reaction of Fullerenes and Benzyne. *J. Org. Chem.* **1992**, *57*, 5069-5071, b) Tsuda, M.; Ishida, T.; Nogami, T.; Kurono, S.; Ohashi, M.

Addition Reaction of Benzyne to Fullerene C_{60}. *Chem. Lett.* **1992**, 2333-2334.

33. Vassilikogiannakis, G.; Orfanopoulos, M. Regio- and Stereoselectivity of the [2+2] Photocycloaddition of Acyclic Enones to C_{60}. *J. Org. Chem.* **1999**, *64*, 3392-3393.

34. Zhang, X.; Romero, A.; Foote, C. S. Photochemical [2+2] Cycloaddition of *N*,*N*-Diethylpropynylamine to C_{60}. *J. Am. Chem. Soc.* **1993**, *115*, 11024-11025.

35. a) Zhang, X.; Foote, C. S. [2+2] Cycloadditions of Fullerenes: Synthesis and Characterization of $C_{62}O_3$ and $C_{72}O_3$, the First Fullerene Anhydrides. *J. Am. Chem. Soc.* **1995**, *117*, 4271-4275, b) Zhang, X.; Fan, A.; Foote, C. S. [2+2] Cycloaddition of Fullerenes with Electron-Rich Alkenes and Alkynes. *J. Org. Chem.* **1996**, *61*, 5456-5461, c) Matsui, S.; Kinbara, K.; Saigo, K. A Novel Reaction of [60]Fullerene. A Formal [2+2] Cycloaddition with Aryloxy- and Alkoxyketenes. *Tetrahedron Lett.* **1999**, *40*, 899-902, d) Nair, V.; Sethumadhavan, D.; Nair, S. M.; Shanmugam, P.; Treesa, P. M.; Eigendorf, G. K. Reaction of Allenamides with [60]Fullerene: Formation of Novel Cyclobutane Annulated Fullerene Derivatives. *Synthesis* **2002**, *2002*, 1655-1657.

36. a) Martín, N.; Altable, M.; Filippone, S.; Martín- Domenech, A.; Güell, M.; Solà, M. Thermal [2+2] Intramolecular Cycloadditions of Fuller- 1,6-enynes. *Angew. Chem. Int. Ed.* **2006**, *45*, 1439-1442, b) Xiao, Z.; Matsuo, Y.; Maruyama, M.; Nakamura, E. Regioselective [2+2] Cycloaddition of a Fullerene Dimer with an Alkyne Triggered by Thermolysis of an Interfullerene C–C Bond. *Org. Lett.* **2013**, *15*, 2176-2178.

37. Wudl, F. The Chemical Properties of Buckminsterfullerene (C_{60}) and the Birth and Infancy of Fulleroids. *Acc. Chem. Res.* **1992**, *25*, 157-161.

38. a) Smith, A. B.; Strongin, R. M.; Brard, L.; Furst, G. T.; Romanow, W. J.; Owens, K. G.; King, R. C. 1,2-Methanobuckminsterfullerene ($C_{61}H_2$), the parent fullerene cyclopropane: synthesis and structure. *J. Am. Chem. Soc.* **1993**, *115*, 5829-5830, b) Smith, A. B.; Strongin, R. M.; Brard, L.; Furst, G. T.; Romanow, W. J.; Owens, K. G.; Goldschmidt, R. J. $C_{71}H_2$ cyclopropanes and annulenes: synthesis and characterization. *J. Chem. Soc., Chem. Commun.* **1994**, 2187-2188, c) Smith, A. B.; Strongin,

R. M.; Brard, L.; Furst, G. T.; Romanow, W. J.; Owens, K. G.; Goldschmidt, R. J.; King, R. C. Synthesis of prototypical fullerene cyclopropanes and annulenes. isomer differentiation via NMR and UV spectroscopy. *J. Am. Chem. Soc*. **1995**, *117*, 5492-5502, d) Haldimann, R.,F.; Klarner, F.; Diederich, F. Reactions of C2v-Symmetrical C_{60} Pentakis-adducts with Diazomethane: Regioselective Formation of Hexakis- to Octakis-adducts and Mechanism of Methanofullerene Formation by Addition of Diazomethane Followed by Dinitrogen Extrusion. *Chem.Commun.* **1997**, 237-238.

39. Suzuki, T.; Li, Q.; Khemani, K. C.; Wudl, F. Dihydrofulleroid H_3C_{61}: synthesis and properties of the parent fulleroid. *J. Am. Chem. Soc.* **1992**, *114*, 7301-7302.

40. Bingel, C. Cyclopropanierung von fullerenen. *Chem. Ber*. **1993**, *126*, 1957-1959.

41. a) Figueira-Duarte, T.; Clifford, J.; Amendola, V.; Gégout, A.; Olivier, J.; Cardinali, F.; Meneghetti, M.; Armaroli, N.; Nierengarten, J. F. Synthesis and excited state properties of a [60]fullerene derivative bearing a star-shaped multi-photon absorption chromophore. *Chem. Commun.* **2006**, *0* 2054-2056, b) Yan, W.; Seifermann, S. M.; Pierrat, P.; Bräse, S. Synthesis of highly functionalized C_{60} fullerene derivatives and their applications in material and life sciences. *Org. Biomol. Chem.* **2015**, *13*, 25-54.

42. Muñoz, A.; Sigwalt, D.; Illescas, B. M.; Luczkowiak, J.; Rodríguez-Pérez, L.; Nierengarten, I.; Holler, M.; Remy, J.; Buffet, K.; Vincent, S. P.; Rojo, J.; Delgado, R.; Nierengarten, J.; Martín, N. Synthesis of giant globular multivalent glycofullerenes as potent inhibitors in a model of Ebola virus infection. *Nat. Chem.* **2016**, *8*, 50-57.

43. a) Nossal, J.; Saini, R. K.; Alemany, L.; Meier, M.; Billups, W. E. The Synthesis and Characterization of Fullerene Hydrides. *Eur. J. Org. Chem.* **2001**, *2001*, 4167-4180, b) 38. Cataldo, F.; Iglesias-Grothh, S. *Fulleranes: the Hydrogenated Fullerenes*, Ed. Springer, Dordrecht, 2010.

44. Taylor, R. $C_{70}H_{36}$ is Probably an Aromatic Compound. *J. Chem. Soc., Perkin Trans. 2* **1994**, 2497-2498.

45. Haufler, R. E.; Conceicao, J.; Chibante, L. P. F.; Chai, Y.; Byrne, N. E.; Flanagan, S.; Haley, M. M.; O'Brien, S. C.; Pan, C.; et al Efficient Production of C_{60} (Buckminsterfullerene), $C_{60}H_{36}$, and the Solvated Buckide Ion *J. Phys. Chem.* **1990**, *94*, 8634-8636.

46. Talyzin, A. V.; Tsybin, Y. O.; Purcell, J. M.; Schaub, T. M.; Shulga, Y. M.; Noreus, D.; Sato, T.; Dzwilewski, A.; Sundqvist, B.; Marshall, A. G. Reaction of Hydrogen Gas with C_{60} at Elevated Pressure and Temperature: Hydrogenation and Cage Fragmentation. *J. Phys. Chem. A* **2006**, *110*, 8528-8534.

47. Wang, G. W.; Li, Y. J.; Li, F. B.; Liu, Y. C. A Simple Preparation of Dihydrofullerene and its Reversion to Fullerene (C_{60}). *Lett. Org. Chem.* **2005**, *2*, 595-598.

48. a) Thilgen, C.; Gosse, I.; Diederich, F. Chirality in Fullerene Chemistry. *Top. Stereochem.* **2003**, *23*, 1-124, b) Thilgen, C.; Diederich, F. Structural Aspects of Fullerene ChemistryA Journey through Fullerene Chirality. *Chem. Rev.* **2006**, *106*, 5049-5135.

49. Ettl, R.; Chao, I.; Diederich, F.; Whetten, R. L. Isolation of C_{76}, a Chiral (D_2) Allotrope of Carbon. *Nature* **1991**, *353*, 149-153.

50. Vasella, A.; Uhlmann, P.; Waldraff, C. A. A.; Diederich, F.; Thilgen, C. Fullerene Sugars: Preparation of Enantiomerically Pure, Spiro-linked *C*-Glycosides of C_{60}. *Angew. Chem. Int. Ed. Engl.* **1992**, *31*, 1388-1390.

51. Kusukawa, T.; Ando, W. Substituents Effects on the Addition of Silyllithium and Germyllithium to C_{60}. *J. Organomet. Chem.* **1998**, *561*, 109-120.

52. Hawkins, J. M.; Meyer, A.; Solow, M. A. Osmylation of C_{70}: Reactivity versus Local Curvature of the Fullerene Spheroid. *J. Am. Chem. Soc.* **1993**, *115*, 7499-7500.

53. Kraszewska, A.; Rivera-Fuentes, P.; Thilgen, C.; Diederich, F. First Enantiomerically Pure C_{70}-adducts with a non-Inherently Chiral Addition Pattern. *New J. Chem.* **2009**, *33*, 386-396.

54. a) Hirsch, A.; Lamparth, I.; Karfunkel, H. R. Fullerene Chemistry in Three Dimensions: Isolation of Seven Regioisomeric Bisadducts and Chiral Trisadducts of C_{60} and Di(ethoxycarbonyl)methylene. *Angew. Chem. Int.*

Ed. Engl. **1994**, *33*, 437-438, b) Nishimura, T.; Tsuchiya, K.; Ohsawa, S.; Maeda, K.; Yashima, E.; Nakamura, Y.; Nishimura, J. Macromolecular Helicity Induction on a Poly(phenylacetylene) with C_2-Symmetric Chiral [60]Fullerene-bisadducts. *J. Am. Chem. Soc.* **2004**, *126*, 11711-11717.

55. Gross, B.; Schurig, V.; Lamparth, I.; Herzog, A.; Djojo, F.; Hirsch, A. Enantiomeric separation of [60]fullerene derivatives with an inherent chiral addition pattern. *Chem. Commun.* **1997**, *0*, 1117-1118.

56. a) Bianco, A.; Maggini, M.; Scorrano, G.; Toniolo, C.; Marconi, G.; Villani, C.; Prato, M. Synthesis, Chiroptical Properties, and Configurational Assignment of Fulleroproline Derivatives and Peptides. *J. Am. Chem. Soc.* **1996**, *118*, 4072-4080, b) Nierengarten, J. F.; Gramlich, V.; Cardullo, F.; Diederich, F. Regio- and Diastereoselective Bisfunctionalization of C_{60} and Enantioselective Synthesis of a C_{60} Derivative with a Chiral Addition Pattern. *Angew. Chem. Int. Ed. Engl.* **1996**, *35*, 2101-2103, c) Guerra, S.; Schillinger, F.; Sigwalt, D.; Holler, M.; Nierengarten, J. Synthesis of Optically pure [60]fullerene *e*,*e*,*e*-Tris adducts. *Chem. Commun.* **2013**, *49*, 4752-4754.

57. Novello, F.; Prato, M.; Da Ros, T.; De Amici, M.; Bianco, A.; Toniolo, C.; Maggini, M. Stereoselective Additions to [60]Fullerene. *Chem. Commun.* **1996**, *0*, 903-904.

58. Illescas, B. M.; Martín, N.; Poater, J.; Solà, M.; Aguado, G. P.; Ortuno, R. M. Diastereoselective Synthesis of Fulleropyrrolidines from Suitably Functionalized Chiral Cyclobutanes. *J. Org. Chem.* **2005**, *70*, 6929-6932.

59. Djojo, F.; Hirsch, A. Synthesis and Chiroptical Properties of Enantiomerically Pure Bis- and Trisadducts of C_{60} with an Inherent Chiral Addition Pattern. *Chem. Eur. J.* **1998**, *4*, 344-356.

60. Filippone, S.; Maroto, E. E.; Martín-Domenech, Á; Suárez, M.; Martín, N. An Efficient Approach to Chiral Fullerene Derivatives by Catalytic Enantioselective 1,3-Dipolar Cycloadditions. *Nat. Chem.* **2009**, *1*, 578-582.

61. Maroto, E. E.; Filippone, S.; Martín-Domenech, Á; Suárez, M.; Martín, N. Switching the Stereoselectivity: (Fullero)pyrrolidines "a la Carte". *J. Am. Chem. Soc.* **2012**, *134*, 12936-12938.

62. Sawai, K.; Takano, Y.; Izquierdo, M.; Filippone, S.; Martín, N.; Slanina, Z.; Mizorogi, N.; Waelchli, M.; Tsuchiya, T.; Akasaka, T.; Nagase, S. Enantioselective Synthesis of Endohedral Metallofullerenes. *J. Am. Chem. Soc.* **2011**, *133*, 17746-17752.

63. Maroto, E. E.; Izquierdo, M.; Murata, M.; Filippone, S.; Komatsu, K.; Murata, Y.; Martín, N. Catalytic stereodivergent functionalization of $H_2@C_{60}$. *Chem. Commun.* **2014**, *50*, 740-742.

64. Maroto, E. E.; Mateos, J.; García-Borràs, M.; Osuna, S.; Filippone, S.; Herranz, M. Á; Murata, Y.; Solà, M.; Martín, N. Enantiospecific cis–trans Isomerization in Chiral Fulleropyrrolidines: Hydrogen-Bonding Assistance in the Carbanion Stabilization in $H_2O@C_{60}$. *J. Am. Chem. Soc.* **2015**, *137*, 1190-1197.

65. Vidal, S.; Izquierdo, M.; Alom, S.; Garcia-Borràs, M.; Filippone, S.; Osuna, S.; Solà, M.; Whitby, R. J.; Martín, N. Effect of incarcerated HF on the exohedral chemical reactivity of $HF@C_{60}$. *Chem. Commun.* **2017**, *53*, 10993-10996.

66. Marco-Martínez, J.; Reboredo, S.; Izquierdo, M.; Marcos, V.; López, J. L.; Filippone, S.; Martín, N. Enantioselective Cycloaddition of Münchnones onto [60]Fullerene: Organocatalysis versus Metal Catalysis. *J. Am. Chem. Soc.* **2014**, *136*, 2897-2904.

67. Marco-Martínez, J.; Marcos, V.; Reboredo, S.; Filippone, S.; Martín, N. Asymmetric Organocatalysis in Fullerenes Chemistry: Enantioselective Phosphine-catalyzed Cycloaddition of Allenoates onto C_{60}. *Angew. Chem. Int. Ed.* **2013**, *52*, 5115-5119.

68. O'Donovan, B. F.; Hitchcock, P. B.; Meidine, M. F.; Kroto, H. W.; Taylor, R.; Walton, D. R. M. Phosphine-catalysed Cycloaddition of Buta-2,3-dienoates and But-2-ynoates to [60]Fullerene. *Chem. Commun.* **1997**, *0*, 81-82.

69. Zhang, C.; Lu, X. Phosphine-Catalyzed Cycloaddition of 2,3-Butadienoates or 2-Butynoates with Electron-Deficient Olefins. A Novel [3 + 2] Annulation Approach to Cyclopentenes. *J. Org. Chem.* **1995**, *60*, 2906-2908.

70. Wilson, S. R.; Lu, Q.; Cao, J.; Wu, Y.; Welch, C. J.; Schuster, D. I. Chiral Non-racemic C_{60} Derivatives: A Proposed Sector Rule for Fullerene Absolute Configuration. *Tetrahedron* **1996**, *52*, 5131-5142.

71. Zhu, Y.; Gergel, N.; Majumdar, N.; Harriott, L. R.; Bean, J. C.; Pu, L. First Optically Active Molecular Electronic Wires. *Org. Lett.* **2006**, *8*, 355-358.

72. a) Réthoré, C.; Avarvari, N.; Canadell, E.; Auban-Senzier, P.; Fourmigué, M. Chiral Molecular Metals: Syntheses, Structures, and Properties of the AsF_6^- Salts of Racemic (±)-, (*R*)-, and (*S*)-Tetrathiafulvalene−oxazoline Derivatives. *J. Am. Chem. Soc.* **2005**, *127*, 5748-5749, b) Pop, F.; Auban-Senzier, P.; Frąckowiak, A.; Ptaszyński, K.; Olejniczak, I.; Wallis, J. D.; Canadell, E.; Avarvari, N. Chirality Driven Metallic versus Semiconducting Behavior in a Complete Series of Radical Cation Salts Based on Dimethyl-Ethylenedithio-Tetrathiafulvalene (DM-EDT-TTF). *J. Am. Chem. Soc.* **2013**, *135*, 17176-17186.

73. Hatakeyama, T.; Hashimoto, S.; Oba, T.; Nakamura, M. Azaboradibenzo[6]helicene: Carrier Inversion Induced by Helical Homochirality. *J. Am. Chem. Soc.* **2012**, *134*, 19600-19603.

74. Yang, Y.; Rice, B.; Shi, X.; Brandt, J. R.; Correa, d. C.; Hedley, G. J.; Smilgies, D.; Frost, J. M.; Samuel, I. D. W.; Otero-de-la-Roza, A.; Johnson, E. R.; Jelfs, K. E.; Nelson, J.; Campbell, A. J.; Fuchter, M. J. Emergent Properties of an Organic Semiconductor Driven by its Molecular Chirality. *ACS Nano* **2017**, *11*, 8329-8338.

75. Josse, P.; Favereau, L.; Shen, C.; Dabos-Seignon, S.; Blanchard, P.; Cabanetos, C.; Crassous, J. Enantiopure versus Racemic Naphthalimide End-capped Helicenic Non-fullerene Electron Acceptors: Impact on Organic Photovoltaics Performance. *Chem. Eur. J.* **2017**, *23*, 6277-6281.

76. Xiaobo, S.; Inho, S.; Hiroyoshi, O.; Lee, Y. H.; Tianming, Z.; Tatsuhiro, K.; Hyung, J. J.; Masaki, K.; Oh, J. H. Supramolecular Nanostructures of Chiral Perylene Diimides with Amplified Chirality for High-Performance Chiroptical Sensing. *Adv. Mater.* **2017**, *29*, 1605828.

77. Ohsawa, S.; Maeda, K.; Yashima, E. Syntheses and Chiroptical Properties of Optically Active Helical Poly(phenylacetylene)s Bearing [60]Fullerene Pendants. *Macromolecules* **2007**, *40*, 9244-9251.

78. Hizume, Y.; Tashiro, K.; Charvet, R.; Yamamoto, Y.; Saeki, A.; Seki, S.; Aida, T. Chiroselective Assembly of a Chiral Porphyrin-fullerene Dyad: Photoconductive Nanofiber with a Top-class Ambipolar Charge-Carrier Mobility. *J. Am. Chem. Soc.* **2010**, *132*, 6628-6629.

79. a) Friedman, S. H.; Ganapathi, P. S.; Rubin, Y.; Kenyon, G. L. Optimizing the Binding of Fullerene Inhibitors of the HIV-1 Protease through Predicted Increases in Hydrophobic Desolvation. *J. Med. Chem.* **1998**, *41*, 2424-2429, b) Zhu, Z.; Schuster, D. I.; Tuckerman, M. E. Molecular Dynamics Study of the Connection between Flap Closing and Binding of Fullerene-Based Inhibitors of the HIV-1 Protease. *Biochemistry* **2003**, *42*, 1326-1333.

80. Balch, A. L.; Olmstead, M. M. Reactions of Transition Metal Complexes with Fullerenes (C_{60}, C_{70}, etc.) and Related Materials. *Chem. Rev.* **1998**, *98*, 2123-2166.

81. a) Fagan, P. J.; Calabrese, J. C.; Malone, B. The Chemical Nature of Buckminsterfullerene (C_{60}) and the Characterization of a Platinum Derivative. *Science* **1991**, *252*, 1160-1161, b) Song, L.; Wang, G.; Liu, P.; Hu, Q. Synthetic and Structural Studies on Transition Metal Fullerene Complexes Containing Phosphorus and Arsenic Ligands: Crystal and Molecular Structures of (η^2-C_{60})M(dppf) (dppf = 1,1‘-Bis(diphenylphosphino)ferrocene; M = Pt, Pd), (η^2-C_{60})Pt($AsPh_3$)$_2$, (η^2-C_{60})Pt(dpaf) (dpaf = 1,1‘-Bis(diphenylarsino)ferrocene), and (η^2-C_{70})Pt(dpaf). *Organometallics* **2003**, *22*, 4593-4598, c) Song, L.; Yu, G.; Su, F.; Hu, Q. Synthetic and Structural Studies on the Transition-Metal Fullerene Complexes (η^2-C_{60})M(η^5-$Ph_2PC_5H_4$)$_2$Ru] and (η^2-C_{60})M(η^5-$Ph_2PC_5H_4$)$_2$Co]$^+$(PF_6)$^-$ (M=Pd, Pt) and the Related Compound {η^5-$Ph_2P(O)C_5H_4$]$_2$Co}$^+$(PF_6)$^-$. *Organometallics* **2004**, *23*, 4192-4198.

82. a) Nagashima, H.; Nakaoka, A.; Saito, Y.; Kato, M.; Kawanishi, T.; Itoh, K. C_{60}Pd: The First Organometallic Polymer of Buckminsterfullerene. *J. Chem. Soc., Chem. Commun.* **1992**, *0*, 377-379, b) Song, L.; Yu, G.; Wang, H.; Su, F.; Hu, Q.; Song, Y.; Gao, Y. Synthesis, Characterization and Properties of Transition Metal Pd/Pt [60]Fullerene Complexes Containing Phosphane Ligands − Crystal Structure of Pd(η^2-C_{60}){$Ph_2PCH_2(CH_2OCH_2)_2CH_2PPh_2$}]. *Eur. J. Inorg. Chem.* **2004**, *2004*, 866-871, c) Song, L.; Su, F.; Hu, Q.; Grigiotti, E.; Zanello, P. Synthesis, Characterization, and Electrochemical Properties of Novel Transition

Metal–Fullerene Complexes Containing Di- and Tetraphosphane Ligands. *Eur. J. Inorg. Chem.* **2006**, *2006*, 422-429.

83. a) Balch, A. L.; Lee, J. W.; Noll, B. C.; Olmstead, M. M. Structural Characterization of {(η^2-C_{60})RhH(CO)(PPh_3)$_2$}: Product of the Reaction of Fullerene C_{60} with the Hydrogenation Catalyst Carbonylhydridotris(triphenylphosphine)rhodium. *Inorg. Chem.* **1993**, *32*, 3577-3578, b) Usatov, A. V.; Kudin, K. N.; Vorontsov, E. V.; Vinogradova, L. E.; Novikov, Y. N. Organometallic Hydrides as Reactants in Fullerene Chemistry. Interaction of the Fullerenes C_{60} and C_{70} with HM(CO)(PPh_3)$_3$ (M=Rh and Ir) and HIr(C_8H_{12})(PPh_3)$_2$. *J. Organomet. Chem* **1996**, *522*, 147-153.

84. a) Balch, A. L.; Catalano, V. J.; Lee, J. W. Accumulating Evidence for the Selective Reactivity of the 6-6 Ring Fusion of Fullerene, C_{60}. Preparation and Structure of (η^2-C_{60})Ir(CO)Cl(PPh_3)$_2$·5C_6H_6. *Inorg. Chem.* **1991**, *30*, 3980-3981, b) Balch, A. L.; Catalano, V. J.; Lee, J. W.; Olmstead, M. M.; Parkin, S. R. (η^2-C_{70})Ir(CO)Cl(PPh_3)$_2$: The Synthesis and Structure of an Iridium Organometallic Derivative of a Higher Fullerene. *J. Am. Chem. Soc.* **1991**, *113*, 8953-8955, c) Balch, A. L.; Ginwalla, A. S.; Lee, J. W.; Noll, B. C.; Olmstead, M. M. Partial Separation and Structural Characterization of C_{84} Isomers by Crystallization of (η^2-C_{84})Ir(CO)Cl(P(C_6H_5)$_3$)$_2$. *J. Am. Chem. Soc.* **1994**, *116*, 2227-2228, d) Usatov, A.; Martynova, E.; Dolgushin, F.; Peregudov, A.; Antipin, M.; Novikov, Y. Fullerene and Carborane in One Coordination Sphere: Synthesis and Structure of a Mixed η^2-C_{60} and σ-Carboranyl Complex of Iridium. *Eur. J. Inorg. Chem.* **2002**, *2002*, 2565-2567.

85. Thompson, D.; Jones, M.; Baird, M. Anionic Cyclopentadienyl C_{60} Complexes of Molybdenum and Tungsten; The Strange Case of Iron. *Eur. J. Inorg. Chem.* **2003**, *2003*, 175-180.

86. Song, H.; Lee, K.; Park, J. T.; Choi, M. Synthesis, Structure, and Electrochemical Studies of μ_3-η^2,η^2,η^2-C_{60} Triosmium Complexes. *Organometallics* **1998**, *17*, 4477-4483.

87. a) Lee, K.; Hsu, H.; Shapley, J. R. Coordination of C_{60} to Penta- and Hexaruthenium Cluster Frames. *Organometallics* **1997**, *16*, 3876-3877, b) Guldi, D. M.; Rahman, G. M. A.; Marczak, R.; Matsuo, Y.; Yamanaka, M.;

Nakamura, E. Sharing Orbitals: Ultrafast Excited State Deactivations with Different Outcomes in Bucky Ferrocenes and Ruthenocenes. *J. Am. Chem. Soc.* **2006**, *128*, 9420-9427.

88. Sawamura, M.; Kuninobu, Y.; Toganoh, M.; Matsuo, Y.; Yamanaka, M.; Nakamura, E. Hybrid of Ferrocene and Fullerene. *J. Am. Chem. Soc.* **2002**, *124*, 9354-9355.

89. Song, L.; Liu, J.; Hu, Q.; Weng, L. Synthesis and Crystal Structures of Two Isomerically Pure Organotransition-Metal [60]Fullerene Derivatives Containing dppb Ligands: mer-$M(CO)_3(dppb)(\eta^2\text{-}C_{60})$ (M = Mo, W). *Organometallics* **2000**, *19*, 1643-1647.

90. a) Maggini, M.; Karlsson, A.; Scorrano, G.; Sandonà, G.; Farnia, G.; Prato, M. Ferrocenyl Fulleropyrrolidines: A Cyclic Voltammetry Study. *J. Chem. Soc., Chem. Commun.* **1994**, *0*, 589-590, b) Iyoda, M.; Sultana, F.; Sasaki, S.; Butenschön, H. Synthesis of Novel Fullerene Complex: The [4+2] Cycloadduct of (Bicyclo[3.2.0]hepta-1,3-dienyl)cobalt(I) Complex with C_{60}. *Tetrahedron Lett.* **1995**, *36*, 579-582, c) 21. Guldi, D. M.; Maggini, M.; Scorrano, G.; Prato, M. Intramolecular Electron Transfer in Fullerene/Ferrocene Based Donor−bridge−acceptor Dyads. *J. Am. Chem. Soc.* **1997**, *119*, 974-980, d) Herranz, M. Á; Illescas, B.; Martín, N.; Luo, C.; Guldi, D. M. Donor/Acceptor Fulleropyrrolidine Triads. *J. Org. Chem.* **2000**, *65*, 5728-5738.

91. a) Crane, J. D.; Hitchcock, P. B.; Kroto, H. W.; Taylor, R.; Walton, D. R. M. Preparation and Characterisation of $C_{60}(ferrocene)_2$. *J. Chem. Soc., Chem. Commun.* **1992**, *0*, 1764-1765, b) Crane, J. D.; Hitchcock, P. B. Crystallographic Characterisation of the Lattice Structure $C_{60}\cdot Fe_4(CO)_4(\eta^5\text{-}C_5H_5)_4]$ as the 1/3 Benzene Solvate. *J. Chem. Soc., Dalton Trans.* **1993**, *0*, 2537-2538, c) Olmstead, M. M.; Costa, D. A.; Maitra, K.; Noll, B. C.; Phillips, S. L.; Van Calcar, P. M.; Balch, A. L. Interaction of Curved and Flat Molecular Surfaces. The Structures of Crystalline Compounds Composed of Fullerene (C_{60}, $C_{60}O$, C_{70}, and $C_{120}O$) and Metal Octaethylporphyrin Units. *J. Am. Chem. Soc.* **1999**, *121*, 7090-7097, d) Boyd, P. D. W.; Reed, C. A. Fullerene−Porphyrin Constructs. *Acc. Chem. Res.* **2005**, *38*, 235-242.

92. Marco-Martínez, J.; Vidal, S.; Fernández, I.; Filippone, S.; Martín, N. Stereodivergent-at-Metal Synthesis of [60]Fullerene Hybrids. *Angew. Chem. Int. Ed.* **2017**, *56*, 2136-2139.

93. a) Carmona, D.; Pilar Lamata, M.; Viguri, F.; San José, E.; Mendoza, A.; Lahoz, F. J.; García-Orduña, P.; Atencio, R.; Oro, L. A. Half-sandwich Organometallic Complexes with Stereogenic Metal Centres: Synthesis and Characterization of Diastereomeric (η^n-ring)M(Aa)X] (Aa=α-Amino Carboxylate) Compounds. *J. Organomet. Chem.* **2012**, *717*, 152-163, b) Bauer, W.; Prem, M.; Polborn, K.; Karlheinz, S.; Steglich, W.; Beck, W. Organometallic Complexes of Iridium, Palladium, Chromium and Iron from 2-Phenyl-5(4H)-oxazolones − Organometallic Labelled Dipeptides. *Eur. J. Inorg. Chem.* **1998**, *1998*, 485-493.

94. Rispens, M. T.; Meetsma, A.; Rittberger, R.; Brabec, C. J.; Sariciftci, N. S.; Hummelen, J. C. Influence of the Solvent on the Crystal Structure of PCBM and the Efficiency of MDMO-PPV:PCBM 'Plastic' Solar Cells. *Chem. Commun.* **2003**, *0*, 2116-2118.

95. Hoppe, H.; Sariciftci, N. S. Organic Solar Cells: An Overview. *J. Mater. Res.* **2004**, *19*, 1924-1945.

96. a) Gustafson, M. P.; Clark, N.; Winther-Jensen, B.; MacFarlane, D. R. Organic Photovoltaic Structures as Photo-active Electrodes. *Electrochim. Acta* **2014**, *140*, 309-313, b) Bourgeteau, T.; Tondelier, D.; Geffroy, B.; Brisse, R.; Cornut, R.; Artero, V.; Jousselme, B. Enhancing the Performances of P3HT:PCBM–MoS_3-based H_2-Evolving Photocathodes with Interfacial Layers. *ACS Appl. Mater. Interfaces* **2015**, *7*, 16395-16403, c) Haro, M.; Solis, C.; Molina, G.; Otero, L.; Bisquert, J.; Gimenez, S.; Guerrero, A. Toward Stable Solar Hydrogen Generation Using Organic Photoelectrochemical Cells. *J. Phys. Chem. C* **2015**, *119*, 6488-6494, d) Suppes, G. M.; Fortin, P. J.; Holdcroft, S. Photoelectrochemical Hydrogen Evolution: Single-Layer, Conjugated Polymer Films Bearing Surface-Deposited Pt Nanoparticles. *J. Electrochem. Soc.* **2015**, *162*, H551-H556, e) Fumagalli, F.; Bellani, S.; Schreier, M.; Leonardi, S.; Rojas, H. C.; Ghadirzadeh, A.; Tullii, G.; Savoini, A.; Marra, G.; Meda, L.; Gratzel, M.; Lanzani, G.; Mayer, M. T.; Antognazza, M. R.; Di Fonzo, F. Hybrid

Organic-inorganic H_2-evolving Photocathodes: Understanding the Route towards High Performance Organic Photoelectrochemical Water Splitting. *J. Mater. Chem. A* **2016**, *4*, 2178-2187.

97. Bellani, S.; Ghadirzadeh, A.; Meda, L.; Savoini, A.; Tacca, A.; Marra, G.; Meira, R.; Morgado, J.; Di Fonzo, F.; Antognazza, M. R. Hybrid Organic/Inorganic Nanostructures for Highly Sensitive Photoelectrochemical Detection of Dissolved Oxygen in Aqueous Media. *Adv. Funct. Mater.* **2015**, *25*, 4531-4538.

98. Guerrero, A.; Haro, M.; Bellani, S.; Antognazza, M. R.; Meda, L.; Gimenez, S.; Bisquert, J. Organic Photoelectrochemical Cells with Quantitative Photocarrier Conversion. *Energy Environ. Sci.* **2014**, *7*, 3666-3673.

99. a) Steele, B. C. H.; Heinzel, A. Materials for Fuel-cell Technologies. *Nature* **2001**, *414*, 345-352, b) Cheng, F.; Chen, J. Metal-air Batteries: From Oxygen Reduction Electrochemistry to Cathode Catalysts. *Chem. Soc. Rev.* **2012**, *41*, 2172-2192.

100. Chen, Z.; Higgins, D.; Yu, A.; Zhang, L.; Zhang, J. A Review on Non-precious Metal Electrocatalysts for PEM Fuel Cells. *Energy Environ. Sci.* **2011**, *4*, 3167-3192.

101. a) Wang, D.; Su, D. Heterogeneous Nanocarbon Materials for Oxygen Reduction Reaction. *Energy Environ. Sci.* **2014**, *7*, 576-591, b) Dai, L.; Xue, Y.; Qu, L.; Choi, H.; Baek, J. Metal-Free Catalysts for Oxygen Reduction Reaction. *Chem. Rev.* **2015**, *115*, 4823-4892.

102. Gong, K.; Du, F.; Xia, Z.; Durstock, M.; Dai, L. Nitrogen-Doped Carbon Nanotube Arrays with High Electrocatalytic Activity for Oxygen Reduction. *Science* **2009**, *323*, 760-763.

103. a) Guan, J.; Chen, X.; Wei, T.; Liu, F.; Wang, S.; Yang, Q.; Lu, Y.; Yang, S. Directly Bonded Hybrid of Graphene Nanoplatelets and Fullerene: Facile Solid-state Mechanochemical Synthesis and Application as Carbon-based Electrocatalyst for Oxygen Reduction Reaction. *J. Mater. Chem. A* **2015**, *3*, 4139-4146, b) Higgins, D.; Zamani, P.; Yu, A.; Chen, Z. The Application of Graphene and its Composites in Oxygen Reduction Electrocatalysis: A Perspective and Review of Recent Progress. *Energy Environ. Sci.* **2016**, *9*, 357-390.

104. a) Langa, F.; Nierengarten, J. F. *Fullerenes: Principles and Applications*, Ed. RSC: Cambridge, UK, 2007, b) Martín, N.; Nierengarten, J. F. *Supramolecular Chemistry of Fullerenes and Carbon Nanotubes*, Ed. Wiley-VCH, Weinheim (Germany), 2012.

105. MacMillan, D. W. C. The Advent and Development of Organocatalysis. *Nature* **2008**, *455*, 304-308.

106. Suárez, A.; Fu, G. C. A Straightforward and Mild Synthesis of Functionalized 3-Alkynoates. *Angew. Chem. Int. Ed.* **2004**, *43*, 3580-3582.

107. a) Liu, H.; Leow, D.; Huang, K.; Tan, C. Enantioselective Synthesis of Chiral Allenoates by Guanidine-Catalyzed Isomerization of 3-Alkynoates. *J. Am. Chem. Soc.* **2009**, *131*, 7212-7213, b) Tang, Y.; Chen, Q.; Liu, X.; Wang, G.; Lin, L.; Feng, X. Direct Synthesis of Chiral Allenoates from the Asymmetric C-H Insertion of α-Diazoesters into Terminal Alkynes. *Angew. Chem. Int. Ed.* **2015**, *54*, 9512-9516, c) Qian, D.; Wu, L.; Lin, Z.; Sun, J. Organocatalytic Synthesis of Chiral Tetrasubstituted Allenes from Racemic Propargylic Alcohols. *Nat. Commun.* **2017**, *8*, 567.

108. a) Marinetti, A.; Kruger, V.; Buzin, F. Synthesis of Chiral Phosphetanes. *Tetrahedron Lett.* **1997**, *38*, 2947-2950, b) Ostermeier, M.; Prieß, J.; Helmchen, G. Mono- and Bidentate Phosphinanes—New Chiral Ligands and Their Application in Catalytic Asymmetric Hydrogenations. *Angew. Chem. Int. Ed.* **2002**, *41*, 612-614.

109. Yang, H.; Ren, W.; Miao, C.; Dong, C.; Yang, Y.; Xi, H.; Meng, Q.; Jiang, Y.; Sun, X. DMAP-Catalyzed [3+2] and [4+2] Cycloaddition Reactions between [60]Fullerene and Unmodified Morita–Baylis–Hillman Adducts in the Presence of Ac_2O. *J. Org. Chem.* **2013**, *78*, 1163-1170.

110. Meier, M. S.; Wang, G.; Haddon, R. C.; Brock, C. P.; Lloyd, M. A.; Selegue, J. P. Benzyne Adds Across a Closed 5−6 Ring Fusion in C_{70}: Evidence for Bond Delocalization in Fullerenes. *J. Am. Chem. Soc.* **1998**, *120*, 2337-2342.

111. Maroto, E. E.; de Cózar, A.; Filippone, S.; Martín-Domenech, Á; Suarez, M.; Cossío, F. P.; Martín, N. Hierarchical Selectivity in Fullerenes: Site-,

Regio-, Diastereo-, and Enantiocontrol of the 1,3-Dipolar Cycloaddition to C_{70}. *Angew. Chem. Int. Ed.* **2011**, *50*, 6060-6064.

112. a) Li, H.; Risko, C.; Seo, J. H.; Campbell, C.; Wu, G.; Brédas, J.; Bazan, G. C. Fullerene–Carbene Lewis Acid–Base Adducts. *J. Am. Chem. Soc.* **2011**, *133*, 12410-12413, b) Yamada, M.; Akasaka, T.; Nagase, S. Carbene Additions to Fullerenes. *Chem. Rev.* **2013**, *113*, 7209-7264, c) Lorbach, A.; Maverick, E.; Carreras, A.; Alemany, P.; Wu, G.; García-Garibay, M.; Bazán, G. C. A Fullerene-carbene Adduct as a Crystalline Molecular Rotor: Remarkable Behavior of a Spherically-shaped Rotator. *Phys. Chem. Chem. Phys.* **2014**, *16*, 12980-12986.

113. Bantreil, X.; Nolan, S. P. Synthesis of *N*-Heterocyclic Carbene Ligands and Derived Ruthenium Olefin Metathesis Catalysts. *Nature Protocols* **2011**, *6*, 69-77.

115. Sampath, M.; Loh, T. Highly Enantio-, Regio- and Diastereo-selective One-pot [2+3]-Cycloaddition Reaction via Isomerization of 3-Butynoates to Allenoates. *Chem. Sci.* **2010**, *1*, 739-742.

116. a) Xu, B.; Hammond G. Thermodynamically Favored Aldol Reaction of Propargyl or Allenyl Esters: Regioselective Synthesis of Carbinol Allenoates. *Angew. Chem. Int. Ed.* **2008**, *47*, 689-692, b) Liu, L.; Xu, B.; Hammond, G. B. Michael Addition of Allenoates to Electron-Deficient Olefins: Facile Synthesis of 2-Alkynyl-Substituted Glutaric Acid Derivatives. *Org. Lett.* **2008**, *10*, 3887-3890, c) Wang, W.; Xu, B.; Hammond, G. B. Synthesis of Functionalized α,α-Disubstituted β-Alkynyl Esters from Allenoates through an Alkynylenolate Intermediate. *Org. Lett.* **2008**, *10*, 3713-3716.

117. a) Liang Po-Wei; Chueh Chu-Chen; Williams, S. T.; Jen, A. K. Roles of Fullerene-Based Interlayers in Enhancing the Performance of Organometal Perovskite Thin-Film Solar Cells. *Adv. Energy Mater.* **2015**, *5*, 1402321, b) Stranks, S. D.; Nayak, P. K.; Wei, Z.; Thomas, S.; Snaith, H. J. Formation of Thin Films of Organic–Inorganic Perovskites for High-Efficiency Solar Cells. *Angew. Chem. Int. Ed.* **2015**, *54*, 3240-3248.

118. a) de Meijere, A. Bonding Properties of Cyclopropane and their Chemical Consequences. *Angew. Chem. Int. Ed Engl.* **1979**, *18*, 809-826, b) La Rosa, A.; Gillemot, K.; Leary, E.; Evangeli, C.; González, M. T.; Filippone, S.;

Rubio-Bollinger, G.; Agraït, N.; Lambert, C. J.; Martín, N. Does a Cyclopropane Ring Enhance the Electronic Communication in Dumbbell-Type C_{60} Dimers? *J. Org. Chem.* **2014**, *79*, 4871-4877.

119. a) Honsho, Y.; Miyakai, T.; Sakurai, T.; Saeki, A.; Seki, S. Evaluation of Intrinsic Charge Carrier Transport at Insulator-Semiconductor Interfaces Probed by a Non-Contact Microwave-Based Technique. *Sci. Rep.* **2013**, *3*, 3182, b) Mitsui, C.; Okamoto, T.; Yamagishi, M.; Tsurumi, J.; Yoshimoto, K.; Nakahara, K.; Soeda, J.; Hirose, Y.; Sato, H.; Yamano, A.; Uemura, T.; Takeya, J. High-Performance Solution-Processable N-Shaped Organic Semiconducting Materials with Stabilized Crystal Phase. *Adv. Mater.* **2014**, *26*, 4546-4551.

121. a) Seki, S.; Saeki, A.; Sakurai, T.; Sakamaki, D. Charge Carrier Mobility in Organic Molecular Materials Probed by Electromagnetic Waves. *Phys. Chem. Chem. Phys.* **2014**, *16*, 11093-11113, b) Saeki, A.; Koizumi, Y.; Aida, T.; Seki, S. Comprehensive Approach to Intrinsic Charge Carrier Mobility in Conjugated Organic Molecules, Macromolecules, and Supramolecular Architectures. *Acc. Chem. Res.* **2012**, *45*, 1193-1202.

122. a) Russell, T. A.; Vedejs, E. *Enantiodivergent Reactions: Divergent Reactions on a Racemic Mixture and Parallel Kinetic Resolution*, Ed. Wiley-VCH Verlag GmbH & Co. KGaA, Weinheim, Germany, 2014, b) Miller, L. C.; Sarpong, R. Divergent Reactions on Racemic Mixtures. *Chem. Soc. Rev.* **2011**, *40*, 4550-4562.

123. Gingras, M. One Hundred Years of Helicene Chemistry. Part 3: Applications and Properties of Carbohelicenes. *Chem. Soc. Rev.* **2013**, *42*, 1051-1095.

124. a) Rickhaus, M.; Mayor, M.; Juricek, M. Chirality in Curved Polyaromatic Systems. *Chem. Soc. Rev.* **2017**, *46*, 1643-1660, b) Rickhaus, M.; Mayor, M.; Juricek, M. Strain-induced Helical Chirality in Polyaromatic Systems. *Chem. Soc. Rev.* **2016**, *45*, 1542-1556.

125. Gingras, M.; Felix, G.; Peresutti, R. One Hundred Years of Helicene Chemistry. Part 2: Stereoselective Syntheses and Chiral Separations of Carbohelicenes. *Chem. Soc. Rev.* **2013**, *42*, 1007-1050.

126. a) Giacalone, F.; Segura, J. L.; Martín, N. Synthesis of 1,1'-Binaphthyl-Based Enantiopure C_{60} Dimers. *J. Org. Chem.* **2002**, *67*, 3529-3532, b) Illescas, B.; Rifé, J.; Ortuño, R. M.; Martín, N. Stereoselective Synthesis of C_{60}-based Cyclopropane Amino Acids. *J. Org. Chem.* **2000**, *65*, 6246-6248, c) Maggini, M.; Scorrano, G.; Bianco, A.; Toniolo, C.; Prato, M. Synthesis and Characterization of Both Enantiomers of a Chiral C_{60} Derivative with C_2 Symmetry. *Tetrahedron Lett.* **1995**, *36*, 2845-2846.

127. a) Crassous, J.; Rivera, J.; Fender, N. S.; Lianhe, S.; Echegoyen, L.; Thilgen, C.; Herrmann, A.; Diederich, F. Chemistry of C_{84}: Separation of three constitutional isomers and optical resolution of D_2-C_{84} by using the "Bingel–Retro-Bingel" strategy. *Angew. Chem. Int. Ed.* **1999**, *38*, 1613-1617, b) Kessinger, R.; Crassous, J.; Herrmann, A.; Rüttimann, M.; Echegoyen, L.; Diederich, F. Preparation of enantiomerically pure C_{76} with a general electrochemical method for the removal of di(alkoxycarbonyl)methano bridges from methanofullerenes: The retro-Bingel reaction. *Angew. Chem. Int. Ed.* **1998**, *37*, 1919-1922.

128. Maroto, E. E.; Filippone, S.; Suárez, M.; Martínez-Álvarez, R.; de Cózar, A.; Cossío, F. P.; Martín, N. Stereodivergent Synthesis of Chiral Fullerenes by [3 + 2] Cycloadditions to C_{60}. *J. Am. Chem. Soc.* **2014**, *136*, 705-712.

129. a) Martín, N.; Altable, M.; Filippone, S.; Martín-Domenech, Á New Reactions in Fullerene Chemistry. *Synlett* **2007**, *2007*, 3077-3095, b) Martín, N.; Altable, M.; Filippone, S.; Martín-Domenech, Á; Martínez-Álvarez, R.; Suárez, M.; Plonska-Brzezinska, M.; Lukoyanova, O.; Echegoyen, L. Highly Efficient Retro-cycloaddition Reaction of Isoxazolino[4,5:1,2][60]- and [70]Fullerenes. *J. Org. Chem.* **2007**, *72*, 3840-3846.

130. Saleh, N.; Shen, C.; Crassous, J. Helicene-based transition metal complexes: synthesis, properties and applications. *Chem. Sci.* **2014**, *5*, 3680-3694.

131. Isla, H.; Crassous, J. Helicene-based chiroptical switches. *Compt. Rend. Chim.* **2016**, *19*, 39-49.

132. Shen, Y.; Chen, C. F. *Helicenes Chemistry: From Synthesis to Applications*, Ed. Springer, Berlin, 2017.

133. Ying, Y.; da Costa, R. C.; Smilgies Detlef-M.; Campbell, A. J.; Fuchter, M. J. Induction of Circularly Polarized Electroluminescence from an Achiral Light-Emitting Polymer via a Chiral Small-Molecule Dopant. *Adv. Mater.* **2013**, *25*, 2624-2628.

134. Brandt, J. R.; Wang, X.; Yang, Y.; Campbell, A. J.; Fuchter, M. J. Circularly Polarized Phosphorescent Electroluminescence with a High Dissymmetry Factor from PHOLEDs Based on a Platinahelicene. *J.Am.Chem.Soc.* **2016**, *138*, 9743-9746.

135. Yang, Y.; da Costa, R. C.; Fuchter, M. J.; Campbell, A. J. Circularly polarized light detection by a chiral organic semiconductor transistor. *Nat. Photon.* **2013**, *7*, 634-638.

136. Schweinfurth, D.; Zalibera, M.; Kathan, M.; Shen, C.; Mazzolini, M.; Trapp, N.; Crassous, J.; Gescheidt, G.; Diederich, F. Helicene Quinones: Redox-Triggered Chiroptical Switching and Chiral Recognition of the Semiquinone Radical Anion Lithium Salt by Electron Nuclear Double Resonance Spectroscopy. *J. Am. Chem. Soc.* **2014**, *136*, 13045-13052.

137. Shen, C.; Loas, G.; Srebro-Hooper, M.; Vanthuyne, N.; Toupet, L.; Cador, O.; Paul, F.; López Navarrete, J. T.; Ramírez, F. J.; Nieto-Ortega, B.; Casado, J.; Autschbach, J.; Vallet, M.; Crassous, J. Iron Alkynyl Helicenes: Redox-Triggered Chiroptical Tuning in the IR and Near-IR Spectral Regions and Suitable for Telecommunications Applications. *Angew. Chem. Int. Ed.* **2016**, *55*, 8062-8066.

138. Verbiest, T.; Elshocht, S. V.; Kauranen, M.; Hellemans, L.; Snauwaert, J.; Nuckolls, C.; Katz, T. J.; Persoons, A. Strong Enhancement of Nonlinear Optical Properties Through Supramolecular Chirality. *Science* **1998**, *282*, 913-915.

139. Kiran, V.; Mathew, S. P.; Cohen, S. R.; Hernández Delgado, I.; Lacour, J.; Naaman, R. Helicenes—A New Class of Organic Spin Filter. *Adv. Mater.* **2016**, *28*, 1957-1962.

140. Bouvier, R.; Durand, R.; Favereau, L.; Srebro-Hooper, M.; Dorcet, V.; Roisnel, T.; Vanthuyne, N.; Vesga, Y.; Donnelly, J.; Hernandez, F.; Autschbach, J.; Trolez, Y.; Crassous, J. Helicenes Grafted with 1,1,4,4-Tetracyanobutadiene Moieties: π-Helical Push–Pull Systems with Strong

Electronic Circular Dichroism and Two-Photon Absorption. *Chem. Eur. J.* **2018**, *24*, 14484-14494.

141. a) Ajamaa, F.; Figueira Duarte, T. M.; Bourgogne, C.; Holler, M.; Fowler, P. W.; Nierengarten, J. Restricted Rotation in (Phenylpyrrolidino)fullerene Derivatives. *Eur. J. Org. Chem.* **2005**, *2005*, 3766-3774, b) Suárez, M.; Verdecia, Y.; Illescas, B.; Martínez-Alvarez, R.; Alvarez, A.; Ochoa, E.; Seoane, C.; Kayali, N.; Martín, N. Synthesis and Study of Novel Fulleropyrrolidines Bearing Biologically Active 1,4-Dihydropyridines. *Tetrahedron* **2003**, *59*, 9179-9186, c) Illescas, B.; Martínez-Grau, M. A.; Torres, M. L.; Fernández-Gadea, J.; Martín, N. Synthesis of New C_{60} Derivatives Containing Biologically Active 4-aryl-1,4-dihydropyridines. *Tetrahedron Lett.* **2002**, *43*, 4133-4136, d) De la Torre, M. D. L.; Marcorin, G. L.; Pirri, G.; Tomé, A. C.; Silva, A. M. S.; Cavaleiro, J. A. S. Synthesis of Novel [60]Fullerene–Flavonoid Dyads. *Tetrahedron Lett.* **2002**, *43*, 1689-1691, e) Eckert, J.; Nicoud, J.; Nierengarten, J.; Liu, S.; Echegoyen, L.; Barigelletti, F.; Armaroli, N.; Ouali, L.; Krasnikov, V.; Hadziioannou, G. Fullerene−Oligophenylenevinylene Hybrids: Synthesis, Electronic Properties, and Incorporation in Photovoltaic Devices. *J. Am. Chem. Soc.* **2000**, *122*, 7467-7479, f) De la Cruz, P.; De la Hoz, A.; Font, L. M.; Langa, F.; Pérez-Rodríguez, M. C. Solvent-free Phase Transfer Catalysis Under Microwaves in Fullerene Chemistry. A Convenient Preparation of *N*-Alkylpyrrolidino[60]fullerenes. *Tetrahedron Lett.* **1998**, *39*, 6053-6056.

142. Chen, C.; Yeh, W. Synthesis and Characterization of Fullerophosphine–Au(I) Complexes. *J. Organomet. Chem.* **2015**, *784*, 41-45.

143. Stasyuk, A. J.; Stasyuk, O. A.; Filippone, S.; Martín, N.; Solà, M.; Voityuk, A. A. Stereocontrolled Photoinduced Electron Transfer in Metal-Fullerene Hybrids. *Chem. Eur. J.* **2018**, *24*, 13020-13025.

144. a) Laurie, S. H. *Comprehensive Coordination Chemistry, vol. 2*, Ed. Pergamon, Oxford, 1987, b) Nakamoto, K. *Infrared and Raman Spectra of Inorganic and Coordination Compounds*, Ed. Wiley, New York, 1986.

145. a) Cheng, Y.; Liao, M.; Chang, C.; Kao, W.; Wu, C.; Hsu, C. Di(4-methylphenyl)methano-C_{60} Bis-adduct for Efficient and Stable Organic

Photovoltaics with Enhanced Open-Circuit Voltage. *Chem. Mater.* **2011**, *23*, 4056-4062, b) Sánchez-Díaz, A.; Izquierdo, M.; Filippone, S.; Martín, N.; Palomares, E. The Origin of the High Voltage in DPM12/P3HT Organic Solar Cells. *Adv. Funct. Mater.* **2010**, *20*, 2695-2700, c) García-Belmonte, G.; Boix, P. P.; Bisquert, J.; Lenes, M.; Bolink, H. J.; La Rosa, A.; Filippone, S.; Martín, N. Influence of the Intermediate Density-of-States Occupancy on Open-Circuit Voltage of Bulk Heterojunction Solar Cells with Different Fullerene Acceptors. *J. Phys. Chem. Lett.* **2010**, *1*, 2566-2571.

146. a) Nie, Y.; Li, L.; Wei, Z. Recent Advancements in Pt and Pt-free Catalysts for Oxygen Reduction Reaction. *Chem. Soc. Rev.* **2015**, *44*, 2168-2201, b) Qiao, J.; Lin, R.; Li, B.; Ma, J.; Liu, J. Kinetics and Electrocatalytic Activity of Nanostructured Ir–V/C for Oxygen Reduction Reaction. *Electrochim. Acta* **2010**, *55*, 8490-8497, c) Cao, D.; Wieckowski, A.; Inukai, J.; Alonso-Vante, N. Oxygen Reduction Reaction on Ruthenium and Rhodium Nanoparticles Modified with Selenium and Sulfur. *J. Electrochem. Soc.* **2006**, *153*, A874.

147. Perrin, D. D.; Amariego, I. F.; Perrin, D. R. *Purification of laboratory Chemicals*, Ed. Pergamon Press, Oxford, 1980.

148. Lang, R. W.; Hansen, H. α-Allenic Esters from α-Phosphoranylidene Esters and Acid Chlorides. *Org. Syn.* **1984**, *62*, 202-207.

149. Li, C.; Wang, X.; Sun, X.; Tang, Y.; Zheng, J.; Xu, Z.; Zhou, Y.; Dai, L. Iron Porphyrin-Catalyzed Olefination of Ketenes with Diazoacetate for the Enantioselective Synthesis of Allenes. *J. Am. Chem. Soc.* **2007**, *129*, 1494-1495.

150. Laxmidhar, R.; Harned Andrew M. Allene Carboxylates as Dipolarophiles in Rh-Catalyzed Carbonyl Ylide Cycloadditions. *Chem. Eur. J.* **2009**, *15*, 12926-12928.

151. Wang, G.; Liu, X.; Chen, Y.; Yang, J.; Li, J.; Lin, L.; Feng, X. Diastereoselective and Enantioselective Alleno-aldol Reaction of Allenoates with Isatins to Synthesis of Carbinol Allenoates Catalyzed by Gold. *ACS Catal.* **2016**, *6*, 2482-2486.

152. Hashmi, A. S.; Döpp, R.; Lothschütz, C.; Rudolph, M.; Riedel, D.; Rominger, F. Scope and Limitations of Palladium-Catalyzed Cross-Coupling Reactions with Organogold Compounds. *Adv. Synth. Catal.* **2010**, *352*, 1307-1314.

153. Hopkinson, M. ; Tessier, A.; Salisbury, A.; Giuffredi, G. ; Combettes, L. ; Gee, A. ; Gouverneur, V. Gold-Catalyzed Intramolecular Oxidative Cross-Coupling of Nonactivated Arenes. *Chem. Eur. J.* **2010**, *16*, 4739-4743.

154. Sano, S.; Matsumoto, T.; Yano, T.; Toguchi, M.; Nakao, M. Synthesis of Allenyl Esters by Horner–Wadsworth–Emmons Reactions of Ketenes Mediated by Isopropylmagnesium Bromide. *Synlett* **2015**, *26*, 2135-2138.

155. Marinetti, A.; Jus, S.; Labrue, F.; Lemarchand, A.; Genêt, J.; Ricard, L. Synthesis and Characterisation of Monophosphines and Aminophosphines Bearing Chiral Phosphetane Units. *Synthesis* **2001**, *14*, 2095-2104.

156. Zhang, T.; Dai, L.; Hou, X. Enantioselective Allylic Substitution of Morita–Baylis–Hillman Adducts Catalyzed by Planar Chiral [2.2]paracyclophane Monophosphines. *Tetrahedron: Asymmetry* **2007**, *18*, 1990-1994.

157. Moussa, M. E. S.; Srebro, M.; Anger, E.; Vanthuyne, N.; Roussel, C.; Lescop, C.; Autschbach, J.; Crassous, J. Chiroptical Properties of Carbo[6]Helicene Derivatives Bearing Extended π-Conjugated Cyano Substituents. *Chirality* **2013**, *25*, 455-465.

158. a) Peddibhotla, S.; Tepe, J. J. Stereoselective Synthesis of Highly Substituted Δ-Pyrrolines: exo-Selective 1,3-Dipolar Cycloaddition Reactions with Azlactones. *J. Am. Chem. Soc.* **2004**, *126*, 12776-12777, b) Melhado, A. D.; Luparia, M.; Toste, F. D. Au(I)-Catalyzed Enantioselective 1,3-Dipolar Cycloadditions of Münchnones with Electron-Deficient Alkenes. *J. Am. Chem. Soc.* **2007**, *129*, 12638-12639.